

# **Genetic and biological analysis of root lesion nematode (*Pratylenchus thornei*) resistance loci in wheat**

A thesis submitted for the degree of  
Doctor of Philosophy

By  
**Muhammad Shefatur Rahman**

Discipline of Plant Breeding and Genetics  
School of Agriculture, Food and Wine  
Faculty of Sciences  
The University of Adelaide, Australia



December 2019

## **Table of Contents**

Table of Contents .....	i
List of Tables .....	viii
List of Figures .....	x
List of Appendices .....	xvi
List of movie clip .....	xvii
Abstract .....	xviii
Thesis Declaration .....	xx
Acknowledgements .....	xxi
<b>Chapter 1: General introduction .....</b>	<b>1</b>
1.1 Introduction .....	1
1.2 References .....	3
<b>Chapter 2: Resistance against root lesion nematode in wheat: A review .....</b>	<b>4</b>
2.1 Statement of authorship .....	4
2.2 Introduction .....	6
2.3 Root lesion nematodes .....	8
2.4 Life cycle .....	8
2.5 Mechanism of pathogenesis .....	9
2.6 The plant's response .....	11
2.7 Impact on wheat crop production .....	11
2.8 <i>P. thornei</i> disease management .....	12
2.9 Sources of resistant and tolerant wheat lines .....	13
2.10 Genetic analysis of <i>P. thornei</i> and <i>P. neglectus</i> resistance in wheat.....	14

2.11 Nematode resistance genes.....	15
2.12 Physical and chemical basis of plant defence against parasitic nematodes.....	18
2.12.1 Physical resistance.....	18
2.12.2 Chemical resistance.....	20
2.13 Conclusion .....	26
2.14 References .....	27
<b>Chapter 3: Fine mapping of root lesion nematode (<i>Pratylenchus thornei</i>)</b>	
<b>resistance loci on chromosomes 6D and 2B of wheat .....</b>	<b>36</b>
3.1 Statement of authorship .....	36
3.2 Abstract .....	38
3.3 Keywords .....	38
3.4 Author contribution statement .....	39
3.5 Key message .....	39
3.6 Introduction .....	40
3.7 Materials and methods .....	45
3.7.1 Plant Material .....	45
3.7.2 <i>P. thornei</i> resistance experimental design and assessment .....	47
3.7.3 90K SNP genotyping .....	50
3.7.4 KASP assays .....	50
3.7.5 Initial identification and mapping of linked SNPs using Sokoll/Krichauff DH lines .....	50
3.7.6 QTL re-analysis in Sokoll/Krichauff DH lines using revised genetic maps	52
3.7.7 Reference genome sequence and gene annotation .....	52
3.8 Results .....	54

3.8.1 Identification of SNPs .....	54
3.8.2 90K maps .....	54
3.8.3 QTL re-mapping <i>QRlnt.sk-6D</i> using the whole DH population .....	54
3.8.4 Fine mapping of <i>QRlnt.sk-6D</i> by graphical genotyping using DH and RIL recombinants .....	57
3.8.5 Identification of candidate nematode resistance genes in the <i>QRlnt.sk-6D</i> interval .....	60
3.8.6 QTL re-mapping <i>QRlnt.sk-2B</i> using the whole DH population .....	62
3.8.7 Fine mapping of <i>QRlnt.sk-2B</i> by graphical genotyping using DH and RIL recombinants .....	64
3.8.8 Identification of candidate nematode resistance genes in the <i>QRlnt.sk-2B</i> interval .....	64
3.9 Discussion .....	69
3.9.1 Candidate genes for <i>P. thornei</i> resistance .....	71
<i>Isoflavone reductase (IFR) and Flavonoid 3'-hydroxylases</i> .....	71
<i>Chalcone synthase</i> .....	72
<i>Phenylalanine ammonia-lyases</i> .....	72
<i>NBS-LRR proteins</i> .....	75
<i>Receptor-like protein kinases</i> .....	75
<i>Ribosome-inactivating proteins</i> .....	76
3.10 Acknowledgments .....	77
3.11 Conflict of interest .....	77
3.12 References .....	78
<b>Chapter 4: Detection and quantification of <i>Pratylenchus thornei</i> in wheat root using quantitative real-time PCR</b> .....	<b>85</b>



4.1 Statement of authorship.....	85
4.2 Introduction .....	87
4.3 Materials and methods .....	89
4.3.1 Nematode DNA extraction from pure culture .....	89
4.3.2 Nematode DNA extraction from plant root .....	89
4.3.3 Real-time PCR .....	91
4.3.4 Generation of standard curves .....	92
4.3.5 Quantification of <i>P. thornei</i> in root samples.....	92
4.4 Results .....	94
4.4.1 <i>P. thornei</i> DNA extraction from pure culture and wheat root .....	94
4.4.2 Real-time qPCR assay .....	94
4.4.3 Linear regression analysis from DNA of pure <i>P. thornei</i> culture and identification of PCR inhibitors .....	96
4.4.4 Generation of a Standard Regression using DNA extracted from mixtures of <i>P. thornei</i> and root powder .....	99
4.4.5 Quantification of <i>P. thornei</i> grown on RIL lines of varying resistance levels .....	103
4.5 Discussion .....	105
4.6 References .....	109
<b>Chapter 5: Metabolomic analysis of root tissues and root exudates from wheat         lines contrasting for <i>Pratylenchus thornei</i> resistance .....</b>	<b>112</b>
5.1 Statement of authorship .....	112
5.2 Introduction .....	114
5.3 Materials and methods .....	117
5.3.1 Plant Materials .....	117

5.3.2 Collection of root exudates .....	117
5.3.3 Sampling roots challenged with <i>P. thornei</i> .....	120
5.3.4 Nematode samples .....	120
5.3.5 Preparation of root exudates for metabolomic analysis .....	120
5.3.6 Preparation of root tissues for metabolomic analysis .....	121
5.3.7 Preparation of nematode samples for metabolomic analysis .....	121
5.3.8 Sample derivatisation .....	122
5.3.9 GC-MS analysis .....	123
5.3.10 Data processing and statistical analysis .....	123
5.4 Results .....	125
5.4.1 Metabolomic analysis of root exudates .....	125
5.4.1.1 Metabolites in wheat root exudates associated with <i>P. thornei</i> resistance QTL	125
<i>Exudate metabolites associated with both the 6D and 2B QTL</i> <i>(Table 5.1, section A)</i> .....	125
<i>Exudate metabolites associated only with the 6D QTL (Table 5.1,</i> <i>section B)</i> .....	126
<i>Exudate metabolites associated only with the 2B QTL (Table 5.1,</i> <i>section C)</i> .....	126
5.4.2 Metabolomic analysis of root tissues .....	129
5.4.2.1 Principal Component Analysis (PCA) .....	129
5.4.2.2 Root tissue metabolite differences between Sokoll and Krichauff	132
<i>Amino acids</i> .....	132
<i>Organic acids</i> .....	132
<i>Sugars</i> .....	133

<i>Miscellaneous</i> .....	134
5.4.2.3 Differences in metabolites of <i>P. thornei</i> challenged roots associated with resistance QTL .....	137
5.4.2.4 Metabolic analysis of nematode samples .....	138
5.5 Discussion .....	140
5.5.1 Analysis of root exudates .....	140
<i>Amino acids</i> .....	142
<i>Organic acids</i> .....	142
<i>Sugars</i> .....	143
5.5.2 Metabolic profiling of wheat roots challenged by <i>P. thornei</i> .....	144
5.5.2.1 Constitutively synthesized metabolites .....	144
5.5.2.2 Changes in wheat metabolites after <i>P. thornei</i> challenge .....	145
<i>Amino acids</i> .....	145
<i>Organic acids</i> .....	146
<i>Sugars</i> .....	146
5.6 References .....	148
<b>Chapter 6: Histochemical and histopathological responses of wheat roots     infected by <i>Pratylenchus thornei</i></b> .....	153
6.1 Statement of authorship .....	153
6.2 Introduction .....	155
6.3 Materials and methods .....	158
6.3.1 PKH26 labelling of nematodes .....	158
6.3.2 Plant materials and nematode inoculation .....	158
6.3.3 Root sample embedding and sectioning .....	159

6.3.4 Staining .....	159
6.3.5 Whole-mount confocal imaging .....	160
6.3.6 Confocal microscopy .....	160
6.4 Results .....	162
6.4.1 Histological responses of wheat roots to <i>P. thornei</i> inoculation .....	162
6.4.2 Histochemical staining .....	168
6.5 Discussion .....	176
6.6 Acknowledgement .....	180
6.7 References .....	181
<b>Chapter 7: General discussion, contribution to the knowledge and future research direction .....</b>	<b>185</b>
7.1 Introduction .....	185
7.2 Fine mapping of root lesion nematode ( <i>Pratylenchus thornei</i> ) resistance loci on chromosomes 6D and 2B of wheat .....	186
7.3 Detection and quantification of <i>P. thornei</i> in wheat root using quantitative real- time PCR .....	188
7.4 Metabolomic analysis of root tissues and root exudates from wheat lines contrasting for <i>Pratylenchus thornei</i> resistance .....	190
7.5 Histochemical and histopathological responses of wheat roots infected by <i>P.</i> <i>thornei</i> .....	192
7.6 Wheat <i>P. thornei</i> resistance genes may contribute to biochemical and physical resistance at the metabolic and cellular level .....	194
7.7 Limitations and future research directions .....	196
7.8 Conclusion .....	199
7.9 References .....	201

## List of Tables

	Title	Page number
<b>Table 2.1</b>	Features of cloned nematode resistance genes (adapted from Fuller et al. 2008)	16
<b>Table 3.1</b>	Six bi-parental recombinant inbred line (RIL) populations used for high resolution mapping of <i>Pratylenchus thornei</i> resistance loci in wheat	46
<b>Table 3.2</b>	Candidate nematode resistance genes in the <i>QRlnt.sk-6D</i> QTL interval, in genomic sequence annotations of Chinese Spring IWGSC RefSeq v1.0 and <i>Aegilops tauschii</i> , Aet v4.0. Homologous genes between two species are aligned in the same line and homologous group of genes are segmented with the horizontal lines	61
<b>Table 3.3</b>	Candidate resistance genes in the <i>QRlnt.sk-2B</i> QTL interval on chromosome 2B, in the Chinese Spring IWGSC RefSeq v1.0 gene annotations	68
<b>Table 4.1</b>	Cycle threshold (Ct) values of quantitative real-time PCR reactions with a <i>Pratylenchus thornei</i> specific primer pair, using as template <i>Pratylenchus thornei</i> DNA serially diluted in either water or uninoculated root DNA extract	97
<b>Table 4.2</b>	Ct values of the individual data points used for the development of the standard curve using the <i>Pratylenchus thornei</i> DNA samples extracted from wheat root powder	100
<b>Table 4.3</b>	Quantification of <i>Pratylenchus thornei</i> in sixteen wheat lines (with various levels of <i>Pratylenchus thornei</i> resistance) using qPCR assay. The results (total nematode number and level of resistance) were compared with PreDicta B test conducted in a commercial laboratory (SARDI)	104
<b>Table 4.4</b>	Estimated cost for QPCR based <i>Pratylenchus thornei</i> quantification from wheat root samples	106

## List of Tables (Continued)

	Title	Page number
<b>Table 5.1</b>	Analysis of metabolites in root exudates associated with <i>Pratylenchus thornei</i> resistance. The level of metabolites (fold-difference) were compared between resistant (Sk-R, 6D-R and 2B-R) and susceptible (Kr-S and Null-S) lines to identify metabolites associated with 6D+2B (Section A), 6D (Section B) or 2B (Section C) resistance QTL. 1: Fold-differences were calculated based on average values from four replicates. 2: Highlights show compounds that were significantly (t-test, $P < 0.05$ ) higher ( <i>green</i> colour) or lower ( <i>blue</i> colour) in resistant line compared to the susceptible line. AA, OA, S and M refers to amino acids, organic acids, sugars and miscellaneous biochemical groups, respectively	128
<b>Table 5.2</b>	Fold- differences of metaboliltes between root samples of <i>Pratylenchus thornei</i> resistant (R) and susceptible (S) cultivars Sokoll (Sk) and Krichauff (Kr), respectively. Control (without nematode inoculation) and nematode inoculated are denoted by C and I, respectively. Values that are highlighted in <i>cyan</i> have a t-test value (fold- difference between the two samples in the heading of each column) significant at $P < 0.05$ but not for the Bonferroni-corrected P value. Values that are highlighted in <i>green</i> also have a t-test value significant for the Bonferroni-corrected P value (0.05 divided by the number of metabolites)	135
<b>Table 5.3</b>	Analysis of metabolites in root tissues associated with <i>Pratylenchus thornei</i> resistance. The level of metabolites (fold-difference) were compared between resistant (Sk-R-I, 6D-R-I and 2B-R-I) and susceptible (Kr-S-I and Null-S-I) lines to identify metabolites associated with 6D+2B (Section A), 6D (Section B) or 2B (Section C) QTL. 1: Fold-differences were calculated based on average values from four replicates. 2: Highlights shows where compounds were significantly (t-test, $P < 0.05$ ) higher ( <i>green</i> colour) or lower ( <i>blue</i> colour) in resistant line compared to the susceptible line. AA, OA, S and M refers to amino acids, organic acids, sugars and miscellaneous biochemical groups	139

## List of Figures

	Title	Page number
<b>Fig. 2.1</b>	The major groups of plant secondary metabolites and their precursors from primary metabolism. 1. Shikimate pathway 2. Amino acid pathway 3. Acetate-mevalonate pathway 4. Acetate-malonate pathway (modified from Mohr and Schopfer 1995)	21
<b>Fig. 3.1</b>	Recombinant inbred lines (RILs) were evaluated for resistance to <i>Pratylenchus thornei</i> in a growth room. Plants were grown in steam-pasteurized sand-filled plastic pots fitted into baskets, which were in turn placed in plastic tubs. Water was supplied periodically from reservoirs to the tubs	49
<b>Fig. 3.2</b>	Genetic linkage map of part of the 6DS chromosome arm made using the Sokoll/Krichauff doubled haploid population (a) and its alignment to the physical map of Chinese spring (b) and <i>Aegilops tauschii</i> (c). The interval of the <i>Pratylenchus thornei</i> resistance QTL <i>QRlnt.sk-6D</i> is shown as shaded bars and the physical locations of the markers defining the QTL interval are boxed	56
<b>Fig. 3.3</b>	Graphical genotyping of the <i>QRlnt.sk-6D</i> QTL region in Sokoll/Krichauff doubled haploid (DH) lines (a) and recombinant inbred lines (RILs) from six crosses (b). Marker positions are given, as genetic locations (cM) in the Sokoll/Krichauff DH map and as physical locations in the Chinese Spring and <i>Aegilops tauschii</i> genome sequences. Marker alleles from the resistant parent Sokoll are denoted by ‘A’ and alleles from the susceptible lines Krichauff, Correll, Mace and Scout are denoted by ‘B’	59

## List of Figures (Continued)

<b>Fig. 3.4</b>	Genetic linkage map of part of the 2BS chromosome arm made using the Sokoll/Krichauff DH population (a), aligned with the sequence in durum wheat (Svevo) (b) and Chinese Spring (c). The interval of the <i>QRInt.sk-6D Pratylenchus thornei</i> resistance QTL is shown as shaded bars and the physical locations of the markers defining the QTL interval are boxed	63
<b>Fig. 3.5</b>	Graphical genotypes of Sokoll/ Krichauff (S/K) doubled haploid (DH) lines in the <i>QRInt.sk-2B</i> QTL region. The lines are grouped into two classes, ‘a’ and ‘b’ based on the presence of either the susceptibility (Krichauff) or resistance (Sokoll) allele at the stronger <i>QRInt.sk-6D</i> QTL. Marker positions are shown as the genetic location (cM) in the S/K DH map, and the physical positions in the genome sequences of emmer wheat, bread wheat cv. Chinese Spring, and durum wheat cv. Svevo. Marker alleles from the resistant parent Sokoll are denoted by ‘A’ and alleles from the susceptible parent Krichauff are denoted by ‘B’	66
<b>Fig. 3.6</b>	Graphical genotypes of recombinant RILs derived from six crosses, for the <i>QRInt.sk-2B</i> QTL region. The lines were grouped into two classes, ‘a’ and ‘b’ based on the presence of either the susceptible (Corell, Mace and Scout) or resistance (Sokoll) allele at the 6DS QTL. Marker positions are shown as the genetic location (cM) in the Sokoll/Krichauff DH map, and the physical positions in the genome sequences of emmer wheat, bread wheat cv. Chinese Spring, and durum wheat cv. Svevo. Alleles from Sokoll are denoted by ‘A’ and alleles from the susceptible parents are denoted by ‘B’	67



## List of Figures (Continued)

<b>Fig. 3.7</b>	The flavonoid and isoflavonoid biosynthetic pathway (Dixon et al. 2002, Naoumkina et al. 2010). The enzymes are as follows: PAL: L-phenylalanine ammonia-lyase; CHS: Chalcone synthase; IFR: Isoflavone reductase; F3'H: Flavonoid 3'-hydroxylase; I2'H: Isoflavone 2'-hydroxylase; VR: Vestitone reductase. The products of the candidate resistance genes for <i>QRInt.sk-6D</i> and <i>QRInt.sk-2B</i> QTL are boxed	74
<b>Fig. 4.1</b>	(A) Amplification curves of each quantitative real-time PCR reaction used in the development of the standard curve. Y-axis is the relative fluorescence unit (RFU), which rises in each cycle (x-axis). The baseline threshold is 1107 RFU which is auto calculated by the BioRad CFX manager software. Control reaction without <i>Pratylenchus thornei</i> DNA template did not produced any amplification. (B) Melting curve profiles of amplicons amplified by a <i>P. thornei</i> -specific primer pair, with melting temperature at 86.7°C. Y-axis is the changes in florescence level (-d(RFU)/dT) with respect to per unit change (increase) in temperature (x-axis)	95
<b>Fig. 4.2</b>	(A) Linear regressions created from qPCR assays of <i>Pratylenchus thornei</i> DNA diluted with nano pure water or (B) uninoculated wheat root DNA. (C) Plot showing correlation between the regression curves in terms of Ct values of these qPCR assays	98
<b>Fig. 4.3</b>	Standard regression based on <i>Pratylenchus thornei</i> DNA extracted from a series of <i>Pratylenchus thornei</i> (25 to 10,000 nematodes mixed with 30 mg root powder. Data also shown in Table 4.2	101
<b>Fig. 4.4</b>	Numbers of <i>Pratylenchus thornei</i> (Pt) determined by real-time PCR plotted against the numbers of <i>Pratylenchus thornei</i> added to the root powder. Pure <i>Pratylenchus thornei</i> (25, 50, 100, 500, 1000, 2500, 5000, 7500, 10000) were added to 30 mg of root powder	102

## List of Figures (Continued)

<b>Fig. 5.1</b>	Collection of root exudates from wheat seedlings. A. Experimental setup B. Checking for contamination in root exudate solution	119
<b>Fig. 5.2</b>	Principal Component Analysis (PCA) of the root tissue metabolic profiles of Sokoll, Krichauff and three doubled haploid lines. <i>Pratylenchus thornei</i> resistance and susceptible lines are referred as R and S, respectively. <i>Pratylenchus thornei</i> inoculated and control samples are referred as I and C, respectively. The first and second principal components explained 51.1% of the variance	130
<b>Fig. 5.3</b>	Dendrogram of root tissue metabolite samples (replicates of genotype treatment combinations) generated using the method of Ward as the algorithm method and the Spearman distance as the dissimilarity coefficient	131
<b>Fig. 6.1</b>	Confocal imaging of <i>Pratylenchus thornei</i> outside of plant roots. <i>Pratylenchus thornei</i> was stained with PKH26 for 24h and stored at 4°C until imaging. A. Intense fluorescence of intestinal lipids (arrow). B. An entire PKH26 labelled <i>Pratylenchus thornei</i> . Morphological features such as the lip region (L) was visible in the labelled nematode. The anterior and posterior regions of <i>Pratylenchus thornei</i> are labelled AR and PR, respectively. Scale bars= 50µm	164
<b>Fig. 6.2</b>	PKH26 labelled <i>Pratylenchus thornei</i> inside Sokoll root tissues. Images were taken 10 days after inoculation. Still images were taken of live nematodes inside root tissue using a confocal microscope. A. Nematode searching for suitable place to thrust at the cell wall. B and C. <i>Pratylenchus thornei</i> stylet thrusting (arrow) at the corner of the cell. I, Intestine; M, metacarpus; S, stylet. Scale bars= 50µm	165
<b>Fig. 6.3</b>	PKH26 labelled <i>Pratylenchus thornei</i> inside Krichauff root tissues. Images were captured four weeks after inoculation. Nematodes (N) occupied multiple cells by breaking the cell walls, resulting in an empty layer (EL) in the cortical tissues. Deposition of eggs (E) in empty layers were also observed	166

## List of Figures (Continued)

- |                 |   |     |
|-----------------|---|-----|
| <b>Fig. 6.4</b> | Comparative anatomies of <i>Pratylenchus thornei</i> uninfected (A) and infected (B) Sokoll root. Calcofluor-white and propidium iodide stained (simultaneous) transverse sections. Sequential excitation at 404, 488 and 561 nm with corresponding emission at 450 (blue), 525 (green) and 595 (red) nm resulted the confocal image a, b and c, respectively. The blue channel might show the presence of cellulose and other $\beta$ -1,4-linked carbohydrates. The red channel shows the propidium iodide stained cell wall. The composite image of blue, red and green channels is shown in d. Co, cortical cells; Xy, Xylem; En, endodermis; Ep, epidermis; Ph, Phloem | 170 |
| <b>Fig. 6.5</b> | Comparative anatomies of <i>Pratylenchus thornei</i> uninfected (A) and infected (B) Krichauff root. Calcofluor-white and propidium iodide stained transverse sections. Sequential excitation at 404, 488 and 561 nm with corresponding emission at 450 (blue), 525 (green) and 595 (red) nm resulted the confocal image a, b and c, respectively. The blue channel might show the presence of cellulose and other $\beta$ -1,4-linked carbohydrates. The red channel shows the propidium iodide stained cell wall. The composite image of blue, red and green channels is represented in image d   | 171 |
| <b>Fig. 6.6</b> | Transverse section of calcofluor-white stained Sokoll root. Confocal images were taken 10 days after <i>Pratylenchus thornei</i> infection. Sequential excitation at 404 and 561 nm with corresponding emission at 450 (blue) and 595 (red) nm resulted the confocal image a and b, respectively. The composite image of blue and red channels is represented by image c. PKH26 stained <i>Pratylenchus thornei</i> (N) was observed damaging the cortical cell layer. Scale bars represent 50 $\mu$ m  | 172 |

## List of Figures (Continued)

- 
- |                 |  |     |
|-----------------|--|-----|
| <b>Fig. 6.7</b> | Deposition of callose or callose-like substances in <i>Pratylenchus thornei</i> infected (10 days after inoculation) Sokoll root section. Root tissues were treated with aniline blue and images were taken using a confocal microscope. Sequential excitation at 404, 488 and 561 nm with corresponding emission at 450 (blue), 525 (green) and 595 (red) nm resulted the confocal image a, b and c, respectively. The composite image of blue, red and green channels is represented by image d. Both green and red color shows the presence of callose and callose-like substances. N, nematode   | 173 |
| <b>Fig. 6.8</b> | Observation of lignin or lignin-like substances in <i>Pratylenchus thornei</i> infected (10 days after inoculation) Sokoll root section. Root tissues were treated with phloroglucinol and images were taken using confocal microscope. Sequential excitation at 404, 488 and 561 nm with corresponding emission at 450 (blue), 525 (green) and 595 (red) nm resulted the confocal image a, b and c, respectively. Lignin was shown in red and green channel. The composite image of blue, red and green channels represented by image d. Cell layer damaged due to <i>Pratylenchus thornei</i> infection (arrow). N, nematode. Scale bars represent 50 $\mu$ m  | 174 |
| <b>Fig. 6.9</b> | <i>Pratylenchus thornei</i> infected (10 days after inoculation) Sokoll root section, treated with calcoflour white and phloroglucinol. Images were taken using confocal microscope. Sequential excitation at 404 and 561 nm with corresponding emission at 450 (blue) and 595 (red) nm resulted the confocal image a and b, respectively. Confocal image from transmitted light channel shown in image c and a combination of blue, red and transmitted light channel shown in image d. Necrosis occurred in the cell due to <i>Pratylenchus thornei</i> infection (Nc). Strong fluorescence observed in proximity to nematode infected cell indicating lignin or lignin-like substances deposition (L). N, nematode. Scale bars represent 50 $\mu$ m | 175 |
-

## **List of Appendices**

<b>Title</b>		<b>Page number</b>
<b>Appendix 1</b>	Supplementary tables of chapter 3	204
<b>Appendix 2</b>	Supplementary tables of chapter 5	206

### List of movie clip

	<b>Title</b>	<b>Page number</b>
<b>Movie clip 1</b>	<i>Pratylenchus thornei</i> in Sokoll root (10 days after inoculation). <i>Pratylenchus thornei</i> was labelled with PKH26. The movie of the live nematode was recorded using a Nikon A1 confocal microscope. Movie speed is 10x faster than real time	167

## **Abstract**

The root lesion nematode *Pratylenchus thornei* feeds on roots of wheat (*Triticum aestivum*) plants, causing significant damage to the roots at the cellular level, resulting in yield reduction. In a previous study, *P. thornei* resistance QTL, *QRInt.sk-6D* and *QRInt.sk-2B* were identified in a Sokoll/Krichauff wheat DH population. The current project was undertaken with the aim to dissect the genetic and biological basis of this resistance. To better define the genetic basis of resistance, both resistance loci were fine mapped using the Sokoll/Krichauff DH population and six newly developed RIL populations. Bulk segregant analysis with the 90K Wheat SNP array identified linked SNPs, which were subsequently converted to KASP assays for mapping in the DH and RIL populations. *QRInt.sk-6D* was delimited to a 3.5 cM interval, representing 1.77 Mbp in the bread wheat cv. Chinese Spring reference genome sequence and 2.29 Mbp in the *Ae. tauschii* genome sequence. These intervals contained 42 and 43 gene models in the respective annotated genome sequences. *QRInt.sk-2B* was delimited to 1.4 cM, corresponding 3.14 Mbp in the durum wheat cv. Svevo reference sequence and 2.19 Mbp in Chinese Spring. The interval in Chinese Spring contained 56 high confidence gene models. Intervals for both QTL contained genes with similarity to those previously reported to be involved in disease resistance, namely genes for phenylpropanoid-biosynthetic-pathway-related enzymes, NBS-LRR proteins and protein kinases. The potential roles of these candidate genes in *P. thornei* resistance are discussed. The KASP markers reported in this study could potentially be used for marker assisted breeding of *P. thornei* resistant wheat cultivars.

To quantify *P. thornei* from wheat root, a qPCR-based assay was developed. A standard curve was produced to quantify *P. thornei* from wheat root samples. The standard curve was validated by estimating *P. thornei* from sixteen wheat lines with known levels of resistance. Overall, the assay was 2.4-fold less expensive compared to the commercial service (PreDicta B test,

SARDI). The DNA extraction protocol was inexpensive as it works without using a commercial DNA extraction kit.

In order to identify metabolites associated with resistance loci, the GC-MS based metabolic profiles of root exudates and root tissues from the resistant lines were compared with the susceptible lines. In root exudates, 21 metabolites were found to be associated with resistance QTL. Likewise, from root tissue, 15 metabolites were found to be associated with the resistance QTL. These metabolites were derived from diverse biochemical groups, including amino acids and amines, organic acids, sugars, sugar alcohols and sugar phosphates. The possible roles of these resistance compounds in *P. thornei* resistance is largely unknown. However, their nematotoxic properties against other plant parasitic nematodes were discussed.

In response to *P. thornei* infection, the histological and histochemical responses of wheat roots were investigated. The use of the fluorescent dye PKH26 (for *P. thornei* labelling) and confocal microscopy enabled visualisation of live *P. thornei* both out and inside wheat root tissue. In response to *P. thornei* infection, secondary cell wall thickening (deposition of cellulose, callose, lignin and suberin) was observed in the *P. thornei* resistant cultivar, Sokoll. Secondary cell wall thickening might result in physical reinforcement of the cell wall restricting *P. thornei* migration in the resistant root tissues.



## **Thesis Declaration**

I certify that this work contains no material which has been accepted for the award of any other degree or diploma in my name, in any university or other tertiary institution and, to the best of my knowledge and belief, contains no material previously published or written by another person, except where due reference has been made in the text. In addition, I certify that no part of this work will, in the future, be used in a submission in my name, for any other degree or diploma in any university or other tertiary institution without the prior approval of the University of Adelaide and where applicable, any partner institution responsible for the joint-award of this degree.

I acknowledge that copyright of published works contained within this thesis resides with the copyright holder(s) of those works.

I also give permission for the digital version of my thesis to be made available on the web, via the University's digital research repository, the Library Search and also through web search engines, unless permission has been granted by the University to restrict access for a period of time.

I acknowledge the support I have received for my research through the provision of an Australian Government Research Training Program Scholarship.

  
.....

**Muhammad Shefatur Rahman**

13/12/2019

## **Acknowledgements**

First and foremost, I would like to acknowledge my academic supervisors, Dr. Klaus Oldach, Dr. Nick Collins and Dr. Katherine Linsell for their excellent guidance and immense support throughout my PhD.

Klaus, thank you for being patient with me. You have always lifted me up and encouraged me during my hard times. I appreciate the massive contribution of time, ideas and expertise that you gave to my project. Thank you for showing this pathway to become a scientist. Thank you for being supportive to me throughout this long journey.

Nick, I feel extremely lucky to have had you as one of my supervisors. This work simply would not be possible without your suggestions, constructive criticisms and immense support in writing the thesis. Thank you for being helpful whenever needed. Thank you for sharing your knowledge and time with me.

Katherine, it all started from your PhD, and now we were able to extend the work from where you have ended. Simply this work would not be possible without your guidance. Thank you for being supportive to me throughout my PhD.

I gratefully acknowledge the financial support of The University of Adelaide, Australian Centre for Plant Functional Genomics (ACPFG) and South Australian Research and Development Institute (SARDI) for conducting the research. I am grateful to receive the Adelaide Graduate Research Scholarship (AGRS) and ACPFG research scholarship for the PhD. I am grateful to SARDI and The University of Adelaide for providing research facilities, laboratory and office space throughout the period of the PhD. I also acknowledge Grains Research and Development Corporation (GRDC) for their financial assistance.

I would like to extend my gratitude to Dr. Julian Taylor for helping in statistical analysis, Dr. Matthew Hayden for the 90K Wheat SNP array analysis, Dr. Ute Roessner for the Metabolomic analysis, Dr. Gwenda Mayo for microscopy study and Danuta Pounsett for the nematode experiments. Thank you all for your contributions for the completion of these PhD projects. Thanks also to my independent advisor, Professor Peter Langridge for his valuable suggestions and advice. I would also like to express my gratitude to the post-graduate coordinator, Professor Eileen Scott, for her advice and support.

I am thankful to different laboratories for providing me the support in conducting the research. I am thankful to the molecular marker laboratory of the University of Adelaide for providing me the

laboratory support for the genetic analysis experiments; the nematology laboratory in SARDI for their support in nematode assay and the Waite microscopy of the University of Adelaide for their support in microscopic studies.

I would like to acknowledge all the members of the SARDI molecular genetics laboratory, particularly, Dr. Tim Sutton, Dr. John Harris, Dr. Yusuf Genc, Dr. Judy Cheong, Dr. Yongle Li, and Simon Micheltore for their constant support throughout my PhD. My gratitude extends to John and Tim for providing me the financial support during my hard time. Special thanks to John for all those conversations that we had regarding the PhD projects. Thank you for sharing your knowledge and talking about the future research aspects. My sincere thanks to Yusuf, Judy, Leo and Simon for encouraging me for the successful completion of the thesis. Thank you all for being friends with me both within and outside the lab.

I must express my very profound gratitude to my friends and family for their unfailing support and continuous encouragement throughout my years of study and through the process of researching and writing this thesis. This accomplishment would not have been possible without them. I would like to acknowledge Roa Alhelly for her immense support during this time. You have been always supportive towards reaching my goals. Without you, this work would not have been possible to accomplish.

Special thanks to my friends who have been supportive throughout this long journey. Special thanks to Dali, Anwar, Emon, Grisham, Rezwan, Nasir and Jamil for all your support and encouragement. I remember all my friends playing cricket and soccer in Adelaide; you all gave me moral support throughout this long period of time. Thank you all.

I would like to express my gratitude to my lovely daughter, Sasmeeen. I am truly indebted to you for your sacrifice that I could not be with you while pursuing my studies. Thinking of you is always encouraging to accomplish my goals. Last but not least, I would like to express my gratitude to my parents and my brother for their support and encouragement in all aspects of my career and life. My deepest gratitude to my father A.S. Wazed Ali. This work would not have been possible without his encouragement. Thank you, dad, for being supportive to me throughout my life. This is only possible because of you!!

**Muhammad Shefatur Rahman (Shefat)**

December 2019

## **Chapter 1**

### **General introduction**

# **Chapter 1**

## **General introduction**

### **1.1 Introduction**

Root lesion nematode (*Pratylenchus thornei*) is one of the most important plant parasitic nematodes, causing significant damage in global wheat production (Smiley and Nicol 2009), including the Australian grain belt (Thompson et al. 2008; Vanstone et al. 2008). They feed on roots of wheat plants, causing significant damage to the roots at the cellular level, resulting in yield reduction. Genetic resistance is believed to be the most effective and sustainable way to minimise the losses caused by this nematode species (Mokrini et al. 2019). In a previous study, a doubled haploid (DH) wheat population of 150 lines, developed from a cross between a synthetic derived wheat cultivar Sokoll (*P. thornei* resistant) and the cultivar Krichauff (*P. thornei* susceptible) was investigated to identify quantitative trait loci (QTL) for resistance (Linsell et al. 2014a). Two highly significant QTL for *P. thornei* resistance were identified, on chromosomes 6D (*QRlnt.sk-6D*) and 2B (*QRlnt.sk-2B*). In another study, the resistant and susceptible lines from the Sokoll/ Krichauff DH population were investigated to determine the stage at which resistance occur (Linsell et al. 2014b). *P. thornei* migration and multiplication was suppressed in roots and root exudates of resistant wheat lines, suggesting the presence of chemical compounds in resistant wheat lines acting against *P. thornei*. The genes underlying the QTL might involve in synthesising these resistance compounds.

The present research project was undertaken to make progress towards identifying the resistance genes underlying the QTL, to identify candidate root or root-exudate compounds with potential resistance activity, to use microscopy to identify potential nematode resistance

mechanisms, and to develop markers and methods to reliably and cheaply select for nematode resistance in breeding. To this end, the specific aims of this research were to:

1. Fine map the *P. thornei* resistance loci on chromosome 6D and 2B of wheat (Chapter 3)
2. Develop a cost-effective *P. thornei* quantification method using quantitative real-time PCR (Chapter 4)
3. Analyse metabolites of root exudates and root tissues from wheat lines contrasting for *P. thornei* resistance (Chapter 5)
4. Characterize histochemical and histological responses of wheat roots infected by *P. thornei* (Chapter 6)

The literature relevant to this research project are reviewed in Chapter 2 and the major findings of these studies, limitations and potential areas of future research are discussed in Chapter 7.

## 1.2 References

- Linsell KJ, Rahman MS, Taylor JD, Davey RS, Gogel BJ, Wallwork H, Forrest KL, Hayden MJ, Taylor SP, Oldach KH (2014a) QTL for resistance to root lesion nematode (*Pratylenchus thornei*) from a synthetic hexaploid wheat source. *Theoretical and Applied Genetics* 127:1409-1421
- Linsell KJ, Riley IT, Davies KA, Oldach KH (2014b) Characterization of resistance to *Pratylenchus thornei* (nematoda) in wheat (*Triticum aestivum*): attraction, penetration, motility, and reproduction. *Phytopathology* 104:174-187
- Mokrini F, Viaene N, Waeyenberge L, Dababat AA, Moens M (2019) Root-lesion nematodes in cereal fields: importance, distribution, identification, and management strategies. *Journal of Plant Diseases and Protection* 126:1-11
- Smiley RW, Nicol JM (2009) Nematodes which challenge global wheat production. In: Carver BF(ed) *Wheat Science and Trade*. Wiley-Blackwell, Ames, IA pp 171-187
- Thompson JP, Owen KJ, Stirling GR, Bell MJ (2008) Root-lesion nematodes (*Pratylenchus thornei* and *P. neglectus*): a review of recent progress in managing a significant pest of grain crops in northern Australia. *Australasian Plant Pathology* 37:235-242
- Vanstone VA, Hollaway GJ, Stirling GR (2008) Managing nematode pests in the southern and western regions of the Australian cereal industry: continuing progress in a challenging environment. *Australasian Plant Pathology* 37:220-234

## **Chapter 2**

### **Resistance against root lesion nematode in wheat: A review**



## **Chapter 2**

### **Resistance against root lesion nematode in wheat: A review**

#### **2.1 Statement of authorship**

## Statement of Authorship

Title of the paper	Resistance against root lesion nematode in wheat: A review
Publication Status	Unpublished and unsubmitted work written in manuscript style
Publication details	This chapter will be prepared as a manuscript for submission to a refereed journal

#### **Principal Author**

Name of Principal Author (Candidate)	Muhammad Shefatur Rahman		
Contribution to the paper	Critically reviewed the relevant published articles, prepared the first draft of the manuscript and took primary responsibility for manuscript revision.		
Overall percentage (%)	70		
Certification	This paper reports on original research I conducted during the period of my Higher Degree by Research candidature and is not subject to any obligations or contractual agreements with a third party that would constrain its inclusion in this thesis. I am the primary author of this paper.		
Signature		Date	4.12.2019

#### **Co-Author Contributions**

By signing the Statement of Authorship, each author certifies that:

- I. the candidate's stated contribution to the publication is accurate (as detailed above);
- II. permission is granted for the candidate to include the publication in the thesis; and
- III. the sum of all co-author contributions is equal to 100% less the candidate's stated contribution.

Name of Co- Author	Katherine J. Linsell		
Contribution to the paper	Suggested the overall structure of the review topics, read the manuscript and suggested revisions.		
Signature		Date	5/12/19

Name of Co- Author	Nicholas C. Collins		
Contribution to the paper	Read the manuscript and suggested revisions.		
Signature		Date	9/12/19

Name of Co- Author	Klaus H. Oldach		
Contribution to the paper	Provided overall supervision and helped writing the manuscript		
Signature		Date	4. 12. 2019

## 2.2 Introduction

Plant parasitic nematodes of the genus *Pratylenchus* feed on roots of crop plants, causing significant damage to the roots, resulting in yield reduction. Two of the most important species, *Pratylenchus thornei* and *Pratylenchus neglectus* are associated with yield loss in wheat throughout the world, particularly in dryland agriculture, as in the Australian wheatbelt (Vanstone et al. 2008), and the Pacific Northwest of the United States of America (USA) (Smiley et al. 2014). *P. thornei* has reduced yields by as much as 85% in Australia, 37% in Mexico, 70% in Israel, and 50% in the USA (Smiley and Nicol 2009). *P. neglectus* has caused losses of up to 37% in the USA and 30% in Australia (Vanstone et al. 2008). In controlling the damage, crop rotation or application of nematicides do not offer sustainable and economic control measures. Consequently, over the last 20 years, research has focused on genetic improvement in wheat cultivars for resistance and tolerance to root lesion nematodes. With the aim of genetic improvement, significant research progress has been made in finding natural sources of resistance and corresponding quantitative trait loci (QTLs). From this available genetic information, development of suitable markers that are useful for marker assisted breeding programs is still underway (Jayatilake et al. 2013; Linsell et al. 2014a; Mokrini et al. 2019). Further, molecular dissection of resistance and tolerance loci aims to identify the underlying genes and their function in the plant's defence mechanism. Knowledge of the defence mechanism controlled by specific QTL represents additional information for breeders that aim to combine different mechanisms for a longer lasting resistance or tolerance against nematodes. In comparison to sedentary endoparasitic nematode species, such as *Meloidogyne* and *Heterodera*, not much research progress has been presented (since the late 1980s) in *Pratylenchus* in terms of dissecting the molecular and biochemical basis of the plant's resistance mechanisms. Host-plant biochemistry and the nature of plant resistance to nematode species were reviewed by Giebel (1982), Bell (1981) and Trudgill (1991). A review on root

lesion nematodes has recently been published by Fosu-Nyarko and Jones (2016) which described the current status of molecular research in *Pratylenchus* spp., with a major focus on host-pathogen interaction and molecular diagnostics were discussed. The following review will report on research progress on the topic of root lesion nematode resistance in wheat, with a focus on the nematode's mode of infection and the plant's resistance mechanism. Progress in breeding of resistant wheat cultivars will also be discussed here.

## 2.3 Root lesion nematodes

Plant parasitic nematodes of the genus *Pratylenchus* are predominantly parasitic to plant roots and are known as root lesion nematodes (Castillo and Vovlas 2007). They are vermiform in shape and microscopic in size (about 0.5 mm long and 0.02 mm in diameter) (Smiley and Nicol 2009). They damage the roots by puncturing the root cells and predispose plants to root-infecting fungi such as *Pythium*, *Rhizoctonia* and *Fusarium* (Kurppa and Vrain 1985). Root lesion nematodes are important parasitic nematodes for cereals including wheat (Smiley 2009), barley (Sharma et al. 2011) and grain legumes (chickpea, faba beans and beans) (Luc et al. 2005; McDonald and Nicol 2005). Their symptoms are non-specific and often confused with other stresses such as nitrogen deficiency, drought, and the above-mentioned fungal root rots. Although root lesion nematodes feed on living root tissues, they may also survive between the cropping seasons in dead root debris and in soil (Smiley and Nicol 2009). They can survive over dry periods in a dehydrated form until favourable conditions return.

There are nearly 70 species in the genus *Pratylenchus* and eight of them are parasitic to wheat. Four species (*P. neglectus*, *P. thornei*, *P. crenatus*, and *P. penetrans*) occur throughout the world in temperate cereal producing areas (Smiley and Nicol 2009). *P. neglectus* and *P. thornei* are the most prevalent and associated with the greatest wheat yield losses (Vanstone et al. 1998)

## 2.4 Life cycle

Males are rare in *Pratylenchus* populations and thus females reproduce by mitotic parthenogenesis (De Waele and Elsen 2002). *Pratylenchus* penetrates and feeds within the root cortex, and eggs are deposited singly in the cavities created by migration (Acedo and Rhode 1971; Bridge and Starr 2007). Females can also deposit eggs in the soil (Pudasaini et al. 2008).

The life cycle of root lesion nematode consists of six life stages, *i.e.*, the egg, four juvenile (J1, J2, J3 and J4) and the adult stage. The first stage juvenile (J1) develops inside the egg, then moults to the second stage juvenile (J2). The J2 hatches from the egg and emerges into soil or root of the plant. With two additional moults, nematodes develop to third (J3) and fourth (J4) stage juveniles. Finally, the J4 moults to become a fully developed adult. The entire life cycle of root lesion nematode may require 45 to 65 days to complete (Castillo and Vovlas 2007). Motile *Pratylenchus* life stages (J2 to adult) are parasitic to plants as adults and juveniles can penetrate, migrate and feed within roots (Bridge and Starr 2007).

## **2.5 Mechanism of pathogenesis**

Invasion mechanisms of *P. thornei* and *P. neglectus* in wheat are less studied. However, related *Pratylenchus* species, such as *P. penetrans*, which affect legume and fruit crops, have been investigated in more detail (Castillo et al. 1995; Castillo et al. 1998; Townshend 1963a, b, 1978, 1984; Townshend et al. 1989). The proposed general invasion mechanisms (penetration and feeding) are based on histopathological models of closely related and well documented *Pratylenchus* species. Feeding behaviour of *Pratylenchus* nematodes broadly can be separated into four phases; probing and root exploration, penetration, ectoparasitic and endoparasitic feeding (Linsell et al. 2014a; Zunke 1990).

*Pratylenchus* are attracted towards the plant's root region most probably due to the stimulative properties of root exudates (Baxter and Blake 1967; Wallace 1974, 1989). Once reached the root hair zone, they search the surface of the root for an acceptable site to penetrate (Zunke 1990). They explore the root by touching the epidermal layer with their lips and protracting their stylet enough to touch but not to pierce the cell wall (Kurppa and Vrain 1985). There appears to be no site preference for *P. thornei* in penetrating the roots (Castillo et al. 1998).

However, few studies have demonstrated that *P. penetrans* prefer the root hair zone (Townshend 1978; Zunke 1990). This preference may have a biochemical basis for attraction or a physical basis allowing easier entry (Townshend 1978).

Following cell surface exploration, *Pratylenchus* insert their stylet several times into the chosen cellular site (Kurppa and Vrain 1985; Zunke 1990). They thrust their stylet repeatedly to penetrate the elastic epidermal cell wall. Once the stylet is inserted to a length of approximately 2  $\mu\text{m}$ , salivation commenced (Kurppa and Vrain 1985). During salivation, the median bulb of the oesophagus pulsed several times and secretions passed from the stylet into the root cell. The saliva predigests the cytoplasmic contents to be ingested. During salivation, the cellular content does not appear to be changed, but the cytoplasmic streaming rates increased (Zunke 1990).

After entering the root, *Pratylenchus* migrate intra-cellularly and feed on cortical cells. They puncture the cells by tearing a hole at the pierced site and then force root entry by waving their bodies vigorously (Kurppa and Vrain 1985; Zunke 1990). During migration at every new cell, the nematodes puncture all corners of the cell with stylet thrusts and then pierce a row of holes over the entire end wall. By pressing its anterior end against the weakened cell, it pushed through into the adjacent cells. Castillo et al. (1998) observed that within the cortical cells, *Pratylenchus* stretch out or coil, and depending on the cell size, they occupy a single cell or several layers of tissue.

*Pratylenchus* activity (feeding and migration) is confined predominantly in cortical parenchyma. Both physical and biochemical factors result in cellular damage to cells in which they fed. Damaged cells contain cytoplasmic debris composed of degenerated organelles and condensed

cytoplasm. Common ultrastructural changes in cortical parenchyma cells include condensed necrotic cytoplasm, loss of membrane integrity in the plasmalemma, tonoplast and nuclear membrane as well as degradation of mitochondria, dictyosomes and endoplasmic reticula (Castillo et al. 1998; Townshend et al. 1989).

## **2.6 The plant's response**

The formation of root lesions is the ultimate symptom of the plants infected with *Pratylenchus*. Initially, a water-soaked lesion develops on the root which turns olive green and ultimately reddish brown (Townshend and Stobbs 1981; Waele and Elsen 2002). The initial lesions are 1-2 mm in length and over time, the lesions increase and merge together to form large sections of discoloured tissue. As *Pratylenchus* infection impairs root function, above ground symptoms usually resemble nutrient and water deficiencies (Whitehead 1997). For instance, higher *P. thornei* populations reduced the water extraction rate in an intolerant wheat cultivar, QT8447 compared to a tolerant cultivar Strzelecki, resulting in a 34% yield loss of the intolerant cultivar (Whish et al. 2014).

## **2.7 Impact on wheat crop production**

*P. thornei* are widely distributed in the Australian wheat belt (Hollaway et al. 2008; Thompson et al. 2008; Vanstone et al. 2008) and is associated with yield reductions in northern (Thompson et al. 2010; Thompson et al. 2008), southern (Nicol et al. 1999; Vanstone et al. 1998) and western wheat growing regions (Vanstone et al. 2008) of Australia. It was estimated that *P. thornei* causes up to 62% wheat yield loss in the northern grain region of Australia (Owen et al. 2014). The extent of yield loss is related to the nematode density in the soil (Taylor and Evans 1998; Thompson et al. 1995). It was estimated that the damage caused by *P. thornei*



costs Australian wheat growers AU\$50 M per year (wheat priced at AU\$239/t) (Murray and Brennan 2010).

## **2.8 *P. thornei* disease management**

A number of management practices have been followed to reduce the damage caused by *P. thornei* (reviewed in Mokrini et al. 2019). Cultural practices, such as crop rotation, field sanitation, conservation tillage and fertilization with inorganic sources of nitrogen were found to be less effective in managing *P. thornei* population (Mokrini et al. 2019; Thompson et al. 2008). Application of nematicides to *P. thornei* infested field offered yield advantage to some extent (Taylor et al. 1999), but due to the toxic effects (on humans and environment), nematicides are not recommended (Taylor et al. 1999; Vanstone et al. 2008). Moreover, *P. thornei* can occur in large numbers throughout the soil profile, making it uneconomical to apply nematicides at an effective rate (Vanstone et al. 1998).

Genetic resistance can reduce the reliance on pesticides and requires limited-technological management and hence is considered as the preferred means of controlling many diseases (Ogbonnaya et al. 2008). Incorporation of resistance into wheat cultivars results in yield advantages. For instance, incorporating partial *P. thornei* resistance into wheat cultivar increased yields by up to 17% compared to intolerant commercial cultivars (Thompson et al. 2008). However, a high-level resistant wheat cultivar has not yet been found and current breeding activities are using different levels of partial resistance (Thompson et al. 2008). In order to achieve superior resistance against *P. thornei*, it is necessary to identify alternate sources of resistance genes which can be introduced into wheat cultivars through breeding activities.

## 2.9 Sources of resistant and tolerant wheat lines

Reduced yield losses are observed in wheat cultivars which are tolerant or resistant to the presence of pathogenic nematode species. Tolerance describes the ability of the plant to withstand nematode infection and to yield well when grown in nematode infested soil (Cook 1974). Resistance refers to the host gene effects that restrict or retard nematode multiplication in the host species (Rohde 1972). Resistance and tolerance have been shown to be under separate genetic control in some plant-nematode interactions (Roberts 2002; Thompson et al. 1999). Consequently, the breeding objective would be the development of wheat varieties with both, tolerance and resistance, to root lesion nematodes.

Modern hexaploid wheat cultivars are generally susceptible to root lesion nematodes. In order to improve resistance in wheat varieties by breeding, wheat germplasm has been screened for sources of resistance. Initially, a bread wheat line, GS50a, was selected as a source of partial resistance to *P. thornei* from a severely infested field of a susceptible wheat variety, Gatcher (Thompson and Clewett 1986). Since, GS50a has been used in breeding programs to improve *P. thornei* resistance in modern wheat cultivars. However, due to the only partial resistance offered by GS50a, additional germplasm such as Middle Eastern landraces, wild wheat progenitors and synthetic wheats have been evaluated for resistance.

*Pratylenchus thornei* is likely to be native to the Middle Eastern region where modern wheat and its progenitors have developed (Feldman and Sears 1981). Host and pathogen co-evolved in this region. For instance, 25 wheat accessions were identified as having more superior resistance than GS50a in a screen of 274 Iranian landraces (Sheedy and Thompson 2009).

Diploid and tetraploid wheat accessions of wild progenitors were also evaluated for *P. thornei* resistance. For instance, a collection of 251 accessions were tested for *P. thornei* resistance and greater resistance than GS50a was found in 11 *Aegilops speltoides* (S-[B]-genome), 10 *Triticum monococcum* (A<sup>m</sup>-genome), and 5 *Triticum urartu* (A<sup>u</sup>-genome) accessions (Sheedy et al. 2012). Moreover, 39 *Aegilops tauschii* (D-genome) *P. thornei* resistant accessions were reported from a screening experiment of 244 accessions (Thompson and Haak 1997). Gene transfer from these wild diploid and tetraploid wheat progenitors could be achieved by direct hybridisation with adapted durum and bread wheat cultivars, homologous recombination, backcrossing and selection (Friebe et al. 1996).

Resistance found in diploid relatives, such as *Ae. tauschii* ( $2n=2x=14$ , DD), can be transferred to bread wheat by developing synthetic hexaploid wheat ( $2n=6x=42$ , AABBDD) through hybridising with tetraploid durum wheat ( $2n=4x=28$ , AABB) (Lagudah et al. 1993). By exploiting root lesion nematode resistance in a synthetic hexaploid wheat collection, 59 of 186 wheat accessions were reported to possess higher resistance than GS50a (Thompson 2008). In another report, an additional 53 synthetic hexaploid wheat accessions were found to be resistant to *P. thornei* (Ogbonnaya et al. 2008).

## **2.10 Genetic analysis of *P. thornei* and *P. neglectus* resistance in wheat**

In the majority of root lesion nematode resistance screening experiments, traditional phenotyping methods were applied. Nematodes were quantified from soil and roots through extraction of live nematodes and direct counting by microscopic assessment. However, high variation between replicates occurs with these traditional techniques due to variable nematode extraction efficiencies, taxonomic misidentification and sub-sampling errors (Hollaway et al. 2003; Taylor and Evans 1998). In contrast to these lengthy, and thus expensive phenotypic

screening methods, molecular markers closely linked to resistance genes offer an alternative method to select for resistance or tolerance in a practical breeding program.

In search of suitable markers for marker assisted selection and to identify genomic locations of resistance, genetic analyses were conducted in mapping populations segregating for resistance using large sets of molecular markers covering all chromosomes. Middle Eastern and synthetic wheat germplasm were utilised as sources of resistance in developing doubled haploid and recombinant inbred line populations. Molecular markers like Diversity Array Technology (DArT), Simple Sequence Repeats (SSRs) and Single Nucleotide Polymorphisms (SNPs) were utilised to construct linkage maps and to locate quantitative trait loci (QTLs) in wheat populations. A number of *P. thornei* and *P. neglectus* resistance QTLs have been reported and have been summarised in Table 2 by Linsell et al. (2014a). In the majority of these experiments, QTLs were repeatedly identified on chromosome 2B and 6D. Detailed fine mapping of these QTLs with the aim of identifying genes responsible for resistance and closely linked markers that are suitable for selection in a breeding program are underway.

## **2.11 Nematode resistance genes**

Until now, eight nematode resistance genes have been cloned from plants (reviewed in Fuller et al. 2008; Kandoth and Mitchum 2013; Williamson and Kumar 2006). All of these genes confer resistance against sedentary endoparasites. Apart from *HS1<sup>pro-1</sup>*, all of the nematode resistance proteins resemble the most common class of plant R proteins in their domain structure. The nature of resistance responses of these genes were characterised by the prevention or breakdown of the specific nematode feeding structure (syncytium). Features of these resistance genes are summarised in Table 2.1.

**Table 2.1** Features of cloned nematode resistance genes (adapted from Fuller et al. 2008)

Gene	Host plant (Source of resistance)	Nematodes and other pathogens	Protein structure	Nature of resistance response	References
<i>HS1<sup>Pro-1</sup></i>	Wild relative of sugar beet ( <i>Beta procumbens</i> )	Sugarbeet cyst nematode ( <i>Heterodera schachtii</i> )	Amino-terminal leucine-rich region	Syncytium is initiated but develops abnormally and nematode development is restricted at J2 stage	Cai et al. (1997); Murray et al. (2007)
<i>Rhg1</i> and <i>Rhg4</i>	Soybean ( <i>Glycine max</i> )	Soybean cyst nematode ( <i>Heterodera glycines</i> )	LRR, transmembrane region and kinase	HR initiated following formation of syncytium, which subsequently breaks down. Surrounding cells become necrotic, isolating the syncytium.	Hauge et al. (2006); Lightfoot and Meksem (2002)
<i>Mi-1.2</i>	Wild relative of cultivated tomato ( <i>Solanum peruvianum</i> )	<i>Meloidogyne incognita</i> , <i>Meloidogyne javanica</i> , <i>Meloidogyne arenaria</i> Potato aphid White Fly	CC-NBS-LRR	HR initiated before feeding site develops.	Liu et al. (2012); Milligan et al. (1998); Vos et al. (1998)
<i>Mi9</i>	Wild relative of cultivated tomato ( <i>Solanum peruvianum</i> )	Root knot nematode ( <i>Meloidogyne</i> spp.)	CC-NBS-LRR	Not described in detail	Jablonska et al. (2007)
<i>Hero A</i>	Wild relative of cultivated tomato ( <i>Solanum pimpinellifolium</i> )	<i>Globodera rostochiensis</i> , <i>Globodera pallida</i>	CC-NBS-LRR	HR initiated after the formation of syncytium. Development is abnormal and surrounding cells degenerate and become necrotic, isolating the syncytium.	Ernst et al. (2002); Sobczak et al. (2005)
<i>Gpa2</i>	Potato ( <i>S. tuberosum</i> )	<i>Globodera pallida</i>	CC-NBS-LRR	Not described in detail	Van der Vossen et al. (2000)
<i>Gro1-4</i>	Potato ( <i>S. tuberosum</i> )	<i>Globodera rostochiensis</i>	TIR-NBS-LRR	Not described in detail	Paal et al. (2004)

The nematode resistance gene *HSI<sup>pro-1</sup>* was isolated from a wild relative of sugar beet and acts against the cyst nematode *H. schachtii* (Cai et al. 1997). The encoded protein does not have obvious similarities with other known resistance proteins. The protein contains a putative N-terminal extracellular imperfect LR region and a transmembrane domain. The *HSI<sup>pro-1</sup>* encoded protein confers resistance on the basis of a gene-for-gene relationship (Thurau et al. 2003). *HSI<sup>pro-1</sup>* is specifically expressed in syncytia of *H. schachtii* and is up-regulated transcriptionally in resistant sugar beet roots upon nematode infection.

The tomato gene *Mi-1.2* confers resistance against several root knot nematode species (Milligan et al. 1998; Vos et al. 1998). The *Mi-1.2* gene also confers resistance against potato aphid (Rossi et al. 1998) and white fly (Nombela et al. 2003). The encoded protein belongs to the CC-NBS-LRR class of resistance genes. *Mi-1.2* is constitutively expressed throughout the whole plant and this expression was not found to be altered by inoculation with the target pathogen (de Ilarduya et al. 2001). Resistance to the root-knot nematode involves induction of HR following nematode invasion. Generation of reactive oxygen species in the early stage of infection is thought to be one of the reasons for rapid induction of HR in the *Mi-1,2* – mediated resistance response (Melillo et al. 2006).

The potato cyst nematode (*Globodera pallida*) resistance gene *Gpa-2* was isolated from potato and belongs also to the CC-NBS-LRR class of resistance genes (Van der Vossen et al. 2000). *Gpa-2* is highly similar in its predicted amino acid sequence to the protein encoded by Potato Virus X (PVX) resistance gene *Rx*.

The *Hero A* gene has been identified in a wild tomato (*Lycopersicon pimpinellifolium*) and confers broad spectrum resistance against the potato cyst nematode (PCN) species *G.*

*rostochiensis* and *G. pallida*. It belongs to the CC-NBS-LRR class of resistance genes (Ernst et al. 2002). *Hero A* gene- mediated resistance responses to PCN were characterised at the cellular and molecular level using the tomato breeding line (LA1792) (possessing the *Hero* multigene family) and a transgenic line (L10) (with the *Hero A* gene, driven by native promoter) (Sobczak et al. 2005). The *Hero A* gene was found to be expressed constitutively in all tissues and was up-regulated in root tissues in response to PCN infection. In both the breeding and transgenic lines, the syncytia degenerated a few days after infection. Only a few surviving syncytia were able to support the development of males and consequently, the nematode population decreased.

## **2.12 Physical and chemical basis of plant defence against parasitic nematodes**

Biochemical and histopathological studies have suggested a number of physical and chemical mechanisms of defence responses against nematode species including migratory nematodes. These physical and chemical barriers affect nematode migration, development and reproduction and might lead to resistance. In the following section, the biochemical basis of disease resistance in plants against plant parasitic nematodes will be discussed. Emphasis will be given on migratory endoparasites, particularly the root lesion nematodes, *Pratylenchus* spp.

### **2.12.1 Physical resistance**

The plant cell wall forms a rigid barrier to ectoparasitic nematodes that feed on the outer plant tissue and to endoparasitic nematodes that must penetrate to feed on cytoplasm or to move through roots and initiate a feeding structure. Plant cell walls consist of cellulose cross-linked with hemicelluloses embedded in a gel-like matrix composed of pectin and glycoproteins (Carpita and Gibeaut 1993). The invading nematode uses its stylet for mechanical disruption of the host plant cell wall (Wyss and Zunke 1986; Zunke 1990). Nematodes also secrete

hydrolytic cell wall-degrading enzymes to assist penetration (reviewed in Davis et al. 2011; Haegeman et al. 2012). For instance, beta-1,4-endoglucanase has been isolated from sedentary nematodes, and is capable of degrading cellulose (Smant et al. 1998). Based on transcriptome analysis, this endoglucanase has also been found in the migratory nematode species *P. penetrans* (Yoji et al. 2001), *Radopholus similis* (Haegeman et al. 2008) and *P. zae* (Fosu-Nyarko et al. 2016). It has also been found in sedentary nematode species from the genera *Meloidogyne* (Béra-Maillet et al. 2000), *Globodera* (Goellner et al. 2000) and *Heterodera* (de Boer et al. 1999). In addition to cellulose degrading enzymes, plant parasitic nematodes also secrete pectin-degrading enzymes. For instance, pectate lyase and polygalaturonases were identified by sequence analysis of the transcriptome of *P. coffeae* (Haegeman et al. 2011) and *P. zae* (Fosu-Nyarko et al. 2016).

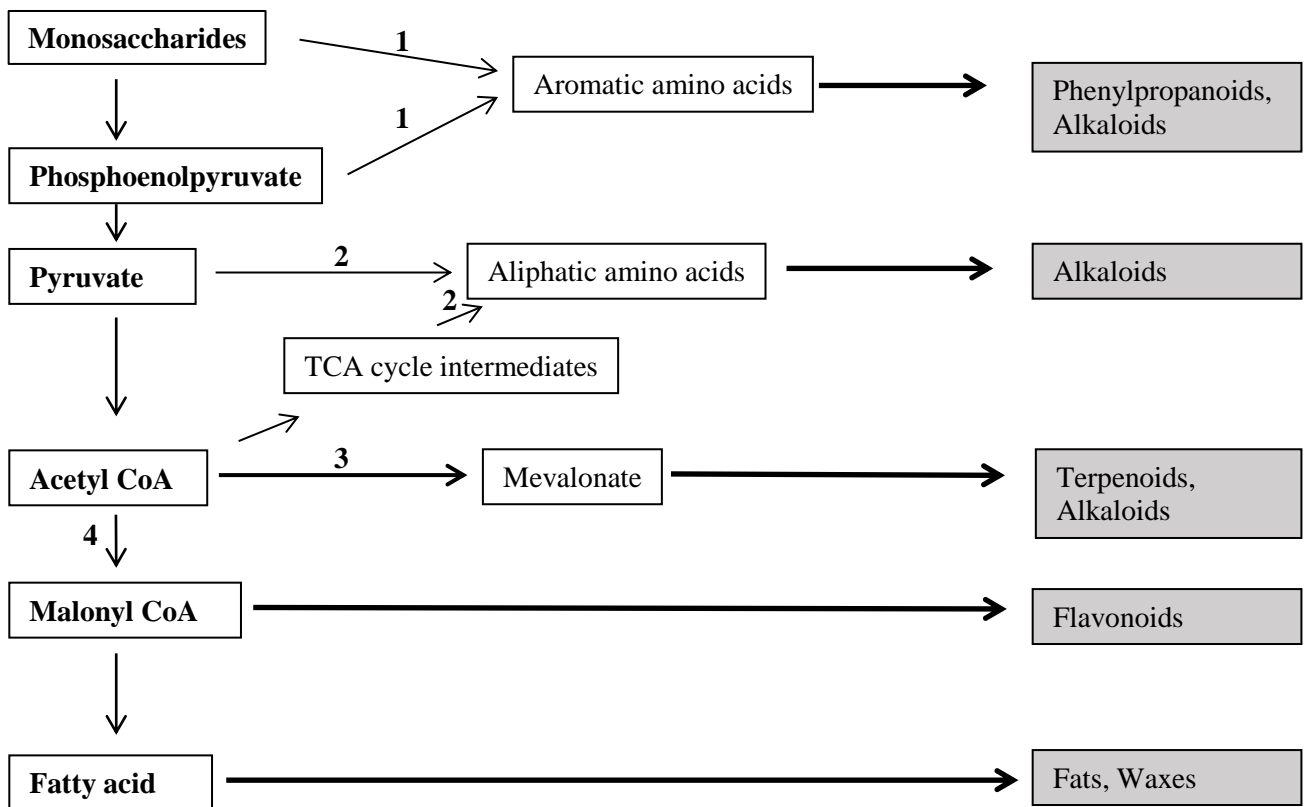
Impregnation of cell walls with lignin (Ride 1978) or suberin (Vance et al. 1980), or cross-linking of cell walls by hydroxycinnamic acids (Hartley and Jones 1977), may reduce substrate availability for these hydrolytic enzymes, and decrease nematode feeding or slow down migration. For instance, the presence of higher levels of lignin and suberin in endodermal cells of resistant banana roots (compared to the susceptible banana root) was thought to be associated with *R. similis* resistance (Valette et al. 1998; Wuyts et al. 2007). Moreover, a higher level of hydroxycinnamic acid (ferulic acid) might prevent *R. similis* feeding and migration in the cortex of banana roots by covalently binding with cell-wall polysaccharides (Wuyts et al. 2007).



### **2.12.2 Chemical resistance**

Plant chemical compounds can be classified into two major groups; primary and secondary metabolites. Primary plant metabolites (e.g. sugars, amino acids and fatty acids) are produced by, and are involved in fundamental metabolic processes of the plant's growth and development, such as photosynthesis and respiration. Secondary metabolites include all remaining plant chemicals, which are derived from primary metabolites (Seigler 1998) (Fig. 2.1). A number of secondary metabolites are known to have a role in defence against plant parasitic nematodes (Giebel 1982; Zinov'eva et al. 2004) and other phytopathogens such as fungi and bacteria (Bednarek and Schulze-Lefert 2009). These chemical compounds may contribute to defence by creating a toxic environment, suppressing the development and reproduction of the nematodes. Defence compounds are divided into phytoanticipins and phytoalexins. The first group comprises low-molecular-weight antimicrobial compounds that are either preformed or generated from constitutively generated precursors following microbial invasion. The second group consists of low-molecular-weight antimicrobial metabolites that are both synthesized by and accumulated in plants after exposure to pathogens (VanEtten et al. 1994).

**Fig. 2.1** The major groups of plant secondary metabolites and their precursors from primary metabolism. 1. Shikimate pathway 2. Amino acid pathway 3. Acetate-mevalonate pathway 4. Acetate-malonate pathway (modified from Mohr and Schopfer 1995)



So far, few chemical compounds have been found to be active against migratory endoparasitic nematodes, including *P. penetrans* and *R. similis*. The majority of these compounds represent end products of the phenylpropanoid pathway with a few other chemicals from terpenoid and alkaloid groups.

In banana roots, histochemical observations revealed that higher level of flavonoids, dopamine, caffeic esters and ferulic acid constitutively produced in resistance root compared to the susceptible root. These phenolic compounds inhibit penetration of the nematodes in the root, contributing to *R. similis* resistance (Valette et al. 1998).

The phenolic compounds were investigated for nematicidal activities *in vitro* (Wuyts et al. 2006). Flavonoids were found as a repellent for *R. similis* and *M. incognita*. By contrast, dopamine was found as an attractant to *R. similis*, while ferulic acid acted as a motility inhibitor. By creating a toxic environment for nematode ingress and multiplication, these phenolic compounds might contribute to nematode resistance.

In soybean, the isoflavonoid phytoalexin, glyceollin has been found to be active against *M. incognita* (Edens et al. 1995). Glyceollin inhibits oxidative respiration and motility of *M. incognita in vitro*, which is thought to be the possible reason behind limited nematode development in resistant soybean roots (Kaplan et al. 1980a, b). In response to *P. scribneri* invasion, two isoflavonoid phytoalexins, coumestrol and psoralidin, accumulated in resistant lima bean root (Rich et al. 1977). Coumestrol showed motility inhibitive activity in *in vitro* assays. In resistant alfalfa, a higher level of medicarpin may be involved in resistance to *P. penetrans* as it exhibited motility inhibitive activity *in vitro* (Baldridge et al. 1999).

In cotton, production of a terpenoid aldehyde, gossypol, has been implicated in resistance against *M. incognita* (Veech and McClure 1977). *M. incognita* larvae were inactivated when exposed to gossypol *in vitro* (Veech 1979).

Genome-wide transcriptional changes revealed that, in ramie (*Boehmeria nivea* L. Gaud), three metabolic pathways, phenylalanine metabolism, carotenoid biosynthesis and phenylpropanoid biosynthesis were strongly influenced by root lesion nematode infection (Liu et al. 2015). In that study, six and seven genes in the phenylpropanoid biosynthesis pathway and the phenylalanine metabolism pathway were found to be enriched, respectively. It was hypothesised that the changes in the expression of genes in phenylpropanoid metabolism pathways lead to the change in phenylpropanoid production, which can increase resistance to RLN in ramie.

Tissue browning and necrosis, or lesion formation, is often observed as a host response to nematode infection. In plants resistant to sedentary endoparasites, necrosis is sometimes localised around the nematode head or its feeding structure and is regarded as a defence response (Bleve-Zacheo et al. 1990; Paulson and Webster 1972). For migratory endoparasitic nematodes, lesion formation results from the disruption of cortical cell integrity. However, the extent and speed of lesion formation differs according to the host plant (Rohde 1972). Infected tissue is characterized by an accumulation of phenolic compounds (Giebel 1982). Phenolics accumulate either from direct synthesis through the phenylpropanoid pathway or by release from conjugates (Rohde 1972). Along with phenylpropanoids, oxidative enzymes, such as peroxidase and polyphenol oxidase, are released from cellular compartments or are newly synthesized after nematode infection. These enzymes catalyse the oxidation of phenylpropanoids to quinones, which polymerize into polyphenols, e.g. tannins and melanins.

These pigments give necrotic tissue its characteristic brown colour (Rohde 1972). For instance, invasion of tomato roots by *M. incognita* resulted in the accumulation of a phenolic compound, chlorogenic acid, which was subsequently oxidised by polyphenol oxidase (either from the host or the nematode). This in turn resulted in the formation of brown-coloured melanins in injured areas (Hung and Rohde 1973). Oxidation products of chlorogenic acid inhibit nematode activity and prevent penetration of endodermal cells (Hung and Rohde 1973) by impairing the nematodes' respiration process (Chang and Rohde 1969).

In a compatible interaction between a host and a migratory nematode, tissue browning, and necrosis occurs at a slow rate as a consequence of cellular damage (Giebel 1982). Consequently, nematodes move away to healthy cells and spread necrosis or leave the root. In the case of an incompatible interaction with a migratory nematode, necrosis is believed to occur in a hypersensitive manner, i.e. rapid, highly localized and intensive (Giebel 1982; Rohde 1972). Due to these hypersensitive-like reactions, nematodes may leave the root tissue or die.

Until now, physical and biochemical mechanisms of resistance in wheat against *P. thornei* and *P. neglectus* have not been reported. The attraction and penetration behaviour of *P. thornei* were investigated in resistant and susceptible wheat lines (Linsell et al. 2014b). In that experiment, along with the parental lines, a sub-sample of doubled haploid lines with contrasting resistance phenotypes to *P. thornei* (3 most resistant and 3 most susceptible DH lines) were investigated to determine whether attraction and penetration of roots, and maturation within roots were involved in this resistance. At different time points (6 to 48 hours after inoculation), the number of nematodes attracted towards the roots was not significantly different between resistant and susceptible lines. This result suggested attractant or repellent compounds may not be a factor in determining resistance. Neither was a significant difference

found in *P. thornei* penetration rates between the resistant and susceptible genotypes, suggesting that resistance in the Sokoll x Krichauff population involved post-infectious mechanisms. However, crushed root suspensions from unchallenged plants of the resistant cultivar reduced nematode motility and development more than those of the susceptible cultivar *in vitro*. These results suggest the possibility of preformed plant metabolites in *P. thornei* resistance in wheat.

It will be worthwhile to investigate chemical compounds inhibiting *Pratylenchus* migration and reproduction that are constitutively synthesised in wheat. Either this synthesis is specific to the resistant genotypes or the compound(s) accumulate to higher concentrations than in the susceptible genotypes. Due to the role phytoalexins have played in plant resistance to other *Pratylenchus* species, the synthesis of phytoalexins, and whether they are involved in post penetration resistance also needs to be investigated in the *Pratylenchus*-wheat interaction. Resistance may also depend on location and rate of synthesis of these toxic chemical compounds (Veech 1982). Histochemical observations need to be conducted in order to localise potential toxic compounds in plant tissues. The role of these compounds in defence can be determined through *in vitro* assays. Such a study may address the question, whether physical (such as cell wall lignification) or chemical (such as rapid accumulation of toxic phenolic compounds) or both defence mechanisms are leading to the resistance responses in resistant wheat genotypes against *P. thornei* and *P. neglectus*. In practical breeding, genetic sources of these different components of resistance could then be used alternatively or in combination to improve resistance.

## 2.13 Conclusion

Histopathological changes in wheat to root lesion nematode invasion and during resistance responses have not been extensively analysed. Research so far suggested that in wheat, root lesion nematode resistance may suppress several stages of nematode invasion, migration and development, and may involve several biochemical pathways. While several *P. thornei* and *P. neglectus* resistance QTLs have been identified, there is currently no (commercial) completely resistant bread wheat cultivar available. Thus, there is a need to identify genes underlying QTLs and develop gene-based markers that can be utilised by plant breeders in order to incorporate this resistance into commercial wheat cultivars.

## 2.14 References

- Acedo JR, Rohde RA (1971) Histochemical root pathology of *Brassica oleracea capitata* L. infected by *Pratylenchus penetrans* (Cobb) Filipjev and Schuurmans Stekhoyen (Nematoda:Tylenchidae). *Journal of Nematology* 3:62-68
- Baldrige GD, O'Neill NR, Samac DA (1998) Alfalfa (*Medicago sativa* L.) resistance to the root-lesion nematode, *Pratylenchus penetrans*: defense-response gene mRNA and isoflavonoid phytoalexin levels in roots. *Plant molecular biology* 38:999-1010
- Baxter RI, Blake CD (1967) Invasion of wheat roots by *Pratylenchus thornei*. *Nature* 215:1168-1169
- Bednarek P, Schulze-Lefert P (2009) Role of plant secondary metabolites at the host-pathogen interface. In: Roberts JA (ed) *Annual Plant Reviews, Volume 34: Molecular Aspects of Plant Disease Resistance*, Wiley-Blackwell, pp 220-260
- Bell AA (1981) Biochemical mechanisms of disease resistance. *Annual Review of Plant Physiology* 32:21-81
- Béra-Maillet C, Arthaud L, Abad P, Rosso M-N (2000) Biochemical characterization of MI-ENG1, a family 5 endoglucanase secreted by the root-knot nematode *Meloidogyne incognita*. *European Journal of Biochemistry* 267:3255-3263
- Bleve-Zacheo T, Melillo MT, Zacheo G (1990) Ultrastructural response of potato roots resistant to cyst nematode *Globodera rostochiensis* pathotype Ro1. *Revue de Nématologie* 13:29-36
- Bridge J, Starr JL (2007) *Plant nematodes of agricultural importance: A color handbook*. Academic Press, Boston
- Cai D, Kleine M, Kifle S, Harloff H-J, Sandal NN, Marcker KA, Klein-Lankhorst RM, Salentijn EMJ, Lange W, Stiekema WJ, Wyss U, Grundler FMW, Jung C (1997) Positional cloning of a gene for nematode resistance in sugar beet. *Science* 275:832-834
- Carpita NC, Gibeaut DM (1993) Structural models of primary cell walls in flowering plants: consistency of molecular structure with the physical properties of the walls during growth. *Plant Journal* 3:1-30
- Castillo P, Trapero-Casas JL, Jimenez-Diaz RM (1995) Effect of time, temperature, and inoculum density on reproduction of *Pratylenchus thornei* in carrot disk cultures. *Journal of Nematology* 27:120-124
- Castillo P, Vovlas N (2007) *Pratylenchus* (Nematoda: Pratylenchidae): diagnosis, biology, pathogenicity and management. Brill Academic Publishers, Leiden, Netherlands
- Castillo P, Vovlas N, Jiménez-Díaz RM (1998) Pathogenicity and histopathology of *Pratylenchus thornei* populations on selected chickpea genotypes. *Plant Pathology* 47:370-376



Chang LM, Rohde RA (1969) The repellent effect of necrotic tissues on the nematode *Pratylenchus penetrans*. *Phytopathology* 59:398

Cook R (1974) Nature and inheritance of nematode resistance in cereals. *Journal of Nematology* 6:165-174

Davis EL, Haegeman A, Kikuchi T (2011) Degradation of the plant cell wall by nematodes. In: Jones J, Gheysen G, Fenoll C (eds) *Genomics and Molecular Genetics of Plant-Nematode Interactions*. Springer Netherlands, Dordrecht, pp 255-272

de Boer JM, Yan Y, Wang X, Smant G, Hussey RS, Davis EL, Baum TJ (1999) Developmental expression of secretory  $\beta$ -1,4-endoglucanases in the subventral esophageal glands of *Heterodera glycines*. *Molecular Plant-Microbe Interactions* 12:663-669

de Ilarduya OM, Moore AE, Kaloshian I (2001) The tomato *Rme1* locus is required for Mi-1-mediated resistance to root-knot nematodes and the potato aphid. *The Plant Journal* 27:417-425

De Waele D, Elsen A (2002) Migratory endoparasites: *Pratylenchus* and *Radopholus* spp. In: Starr JL, Cook R, Bridge J (eds) *Plant Resistance to Parasitic Nematodes*. CABI publishing, Wallingford, UK, pp 175-206

Edens RM, Anand SC, Bolla RI (1995) Enzymes of the phenylpropanoid pathway in soybean infected with *Meloidogyne incognita* or *Heterodera glycines*. *Journal of Nematology* 27:292-303

Ernst K, Kumar A, Kriseleit D, Kloos D-U, Phillips MS, Ganai MW (2002) The broad-spectrum potato cyst nematode resistance gene (*Hero*) from tomato is the only member of a large gene family of NBS-LRR genes with an unusual amino acid repeat in the LRR region. *Plant Journal* 31:127-136

Feldman M, Sears ER (1981) The wild gene resources of wheat. *Scientific American* 244:102-113

Fosu-Nyarko J, Jones MGK (2016) Advances in understanding the molecular mechanisms of root lesion nematode host interactions. *Annual Review of Phytopathology* 54:253-278

Fosu-Nyarko J, Tan J-ACH, Gill R, Agrez VG, Rao U, Jones MGK (2016) *De novo* analysis of the transcriptome of *Pratylenchus zeae* to identify transcripts for proteins required for structural integrity, sensation, locomotion and parasitism. *Molecular Plant Pathology* 17:532-552

Friebe B, Jiang J, Raupp WJ, McIntosh RA, Gill BS (1996) Characterization of wheat-alien translocations conferring resistance to diseases and pests: current status. *Euphytica* 91:59-87

Fuller VL, Lilley CJ, Urwin PE (2008) Nematode resistance. *New Phytologist* 180:27-44

Giebel J (1982) Mechanism of resistance to plant nematodes. *Annual Review of Phytopathology* 20:257-279

- Goellner M, Smant G, De Boer JM, Baum TJ, Davis EL (2000) Isolation of Beta-1,4-endoglucanase genes from *Globodera tabacum* and their expression during parasitism. *Journal of nematology* 32:154-165
- Haegeman A, Jacob J, Vanholme B, Kyndt T, Gheysen G (2008) A family of GHF5 endo-1,4-beta-glucanases in the migratory plant-parasitic nematode *Radopholus similis*. *Plant Pathology* 57:581-590
- Haegeman A, Joseph S, Gheysen G (2011) Analysis of the transcriptome of the root lesion nematode *Pratylenchus coffeae* generated by 454 sequencing technology. *Molecular and Biochemical Parasitology* 178:7-14
- Haegeman A, Mantelin S, Jones JT, Gheysen G (2012) Functional roles of effectors of plant-parasitic nematodes. *Gene* 492:19-31
- Hartley RD, Jones EC (1977) Phenolic components and degradability of cell walls of grass and legume species. *Phytochemistry* 16:1531-1534
- Hauge BM, Wang MLI, Parsons JD, Parnell LD (2006) Nucleic acid molecules and other molecules associated with soybean cyst nematode resistance. WO 01/51627 PCT/US01/00552 Patent # 20030005491
- Hollaway GJ, Ophel-Keller K, Taylor S, Burns R, McKay A (2003) Effect of soil water content, sampling method and sample storage on the quantification of root lesion nematodes (*Pratylenchus* spp.) by different methods. *Australasian Plant Pathology* 32:73-79
- Hollaway GJ, Vanstone VA, Nobbs J, Smith JG, Brown JS (2008) Pathogenic nematodes of cereal crops in south-west Victoria, Australia. *Australasian Plant Pathology* 37:505-510
- Hung CL, Rohde RA (1973) Phenol accumulation related to resistance in tomato to infection by root-knot and lesion nematodes. *Journal of Nematology* 5:253-258
- Jablonska B, Ammiraju JSS, Bhattarai KK, Mantelin S, de Ilarduya OM, Roberts PA, Kaloshian I (2007) The *Solanum arcanum* conferring heat-stable resistance to root-knot nematodes is a homolog of *Mi-1*. *Plant Physiology* 143:1044
- Jayatilake DV, Tucker EJ, Bariana H, Kuchel H, Edwards J, McKay AC, Chalmers K, Mather DE (2013) Genetic mapping and marker development for resistance of wheat against the root lesion nematode *Pratylenchus neglectus*. *BMC Plant Biology* 13:230. <https://doi.org/10.1186/1471-2229-13-230>
- Kandoth PK, Mitchum MG (2013) War of the worms: how plants fight underground attacks. *Current Opinion in Plant Biology* 16:457-463
- Kaplan DT, Keen NT, Thomason IJ (1980a) Association of glyceollin with the incompatible response of soybean roots to *Meloidogyne-incognita*. *Physiological Plant Pathology* 16:309-318

Kaplan DT, Keen NT, Thomason IJ (1980b) Studies on the mode of action of glyceollin in soybean - incompatibility to the root-knot nematode, *Meloidogyne incognita*. *Physiological Plant Pathology* 16:319-325

Kurppa S, Vrain TC (1985) Penetration and feeding behaviour of *Pratylenchus penetrans* in strawberry roots. *Revue de Nematologie* 8:273-276

Lagudah ES, Appels R, McNeil D, Schachtman DP (1993) Exploiting the diploid 'D' genome chromatin for wheat improvement. In: Gustafson JP, Appels R, Raven P (eds) *Gene Conservation and Exploitation: 20th Stadler Genetics Symposium*. Springer US, Boston, MA, pp 87-107

Lightfoot DA, Meksem K (2002) Isolated polynucleotides and polypeptides relating to loci underlying resistance to soybean cyst nematode and soybean sudden death syndrome and methods employing same. U.S. Pat Appl Publ No. 2002144310

Linsell KJ, Rahman MS, Taylor JD, Davey RS, Gogel BJ, Wallwork H, Forrest KL, Hayden MJ, Taylor SP, Oldach KH (2014a) QTL for resistance to root lesion nematode (*Pratylenchus thornei*) from a synthetic hexaploid wheat source. *Theoretical and Applied Genetics* 127:1409-1421

Linsell KJ, Riley IT, Davies KA, Oldach KH (2014b) Characterization of resistance to *Pratylenchus thornei* (nematoda) in wheat (*Triticum aestivum*): attraction, penetration, motility, and reproduction. *Phytopathology* 104:174-187

Liu S, Kandoth PK, Warren SD, Yeckel G, Heinz R, Alden J, Yang C, Jamai A, El-Mellouki T, Juvalle PS, Hill J, Baum TJ, Cianzio S, Whitham SA, Korkin D, Mitchum MG, Meksem K (2012) A soybean cyst nematode resistance gene points to a new mechanism of plant resistance to pathogens. *Nature* 492:256-260

Liu T, Zhu S, Tang Q, Tang S (2015) Genome-wide transcriptomic profiling of ramie (*Boehmeria nivea* L. Gaud) in response to cadmium stress. *Gene* 558:131-137

Luc M, Sikora RA, Bridge J (2005) *Plant parasitic nematodes in subtropical and tropical agriculture*. CABI Publishing, Wallington, UK

McDonald AH, Nicol JM (2005) *Nematode parasites of cereals*. CABI Publishing, Wallingford, UK

Melillo MT, Leonetti P, Bongiovanni M, Castagnone-Sereno P, Bleve-Zacheo T (2006) Modulation of reactive oxygen species activities and H<sub>2</sub>O<sub>2</sub> accumulation during compatible and incompatible tomato–root-knot nematode interactions. *New Phytologist* 170:501-512

Milligan SB, Bodeau J, Yaghoobi J, Kaloshian I, Zabel P, Williamson VM (1998) The root knot nematode resistance gene *Mi* from tomato is a member of the leucine zipper, nucleotide binding, leucine-rich repeat family of plant genes. *Plant Cell* 10:1307-1319

Mohr H, Schopfer P (1995) Biosynthetic Metabolism. In: Mohr H, Schopfer P (eds) *Plant Physiology*. Springer Berlin Heidelberg, Berlin, Heidelberg, pp 275-284

- Mokrini F, Viaene N, Waeyenberge L, Dababat AA, Moens M (2019) Root-lesion nematodes in cereal fields: importance, distribution, identification, and management strategies. *Journal of Plant Diseases and Protection* 126:1-11
- Murray GM, Brennan JP (2010) Estimating disease losses to the Australian barley industry. *Australasian Plant Pathology* 39:85-96
- Murray SL, Ingle RA, Petersen LN, Denby KJ (2007) Basal resistance against *Pseudomonas syringae* in *Arabidopsis* involves WRKY53 and a protein with homology to a nematode resistance protein. *Molecular Plant-Microbe Interactions* 20:1431-1438
- Nicol JM, Davies KA, Hancock TW, Fisher JM (1999) Yield loss caused by *Pratylenchus thornei* on wheat in South Australia. *Journal of Nematology* 31:367-376
- Nombela G, Williamson VM, Muñiz M (2003) The root-knot nematode resistance gene *Mi-1.2* of tomato is responsible for resistance against the whitefly *Bemisia tabaci*. *Molecular Plant-Microbe Interactions* 16:645-649
- Ogbonnaya FC, Imtiaz M, Bariana HS, McLean M, Shankar MM, Hollaway GJ, Trethowan RM, Lagudah ES, van Ginkel M (2008) Mining synthetic hexaploids for multiple disease resistance to improve bread wheat. *Australian Journal of Agricultural Research* 59:421-431
- Owen KJ, Clewett TG, Bell KL, Thompson JP (2014) Wheat biomass and yield increased when populations of the root-lesion nematode (*Pratylenchus thornei*) were reduced through sequential rotation of partially resistant winter and summer crops. *Crop and Pasture Science* 65:227-241
- Paal J, Henselewski H, Muth J, Meksem K, Menéndez CM, Salamini F, Ballvora A, Gebhardt C (2004) Molecular cloning of the potato *Gro1-4* gene conferring resistance to pathotype Ro1 of the root cyst nematode *Globodera rostochiensis*, based on a candidate gene approach. *Plant Journal* 38:285-297
- Paulson RE, Webster JM (1972) Ultrastructure of the hypersensitive reaction in roots of tomato, *Lycopersicon esculentum* L., to infection by the root-knot nematode, *Meloidogyne incognita*. *Physiological Plant Pathology* 2:227-234
- Pudasaini MP, Viaene N, Moens M (2008) Hatching of the root-lesion nematode, *Pratylenchus penetrans*, under the influence of temperature and host. *Nematology* 10:47-54
- Rich JR, Keen NT, Thomason IJ (1977) Association of coumestans with the hypersensitivity of lima bean roots to *Pratylenchus scribneri*. *Physiological Plant Pathology* 10:105-116
- Ride JP (1978) The role of cell wall alterations in resistance to fungi. *Annals of Applied Biology* 89:302-306
- Roberts PA (2002) Concepts and consequences of resistance. In: Starr JL, Cook R, Bridge J (eds) *Plant resistance to parasitic nematodes*, CABI Publishing, New York, pp 23-41
- Rohde RA (1972) Expression of resistance in plants to nematodes. *Annual Review of Phytopathology* 10:233-252

Rossi M, Goggin FL, Milligan SB, Kaloshian I, Ullman DE, Williamson VM (1998) The nematode resistance gene *Mi* of tomato confers resistance against the potato aphid. *Proceedings of the National Academy of Sciences* 95:9750-9754

Seigler DS (1998) *Plant secondary metabolism*. Springer US, New York

Sharma S, Sharma S, Keil T, Laubach E, Jung C (2011) Screening of barley germplasm for resistance to root lesion nematodes. *Plant Genetic Resources: Characterization and Utilization* 9:236-239

Sheedy JG, Thompson JP, Kelly A (2012) Diploid and tetraploid progenitors of wheat are valuable sources of resistance to the root lesion nematode *Pratylenchus thornei*. *Euphytica* 186:377-391

Sheedy JG, Thompson JP (2009) Resistance to the root-lesion nematode *Pratylenchus thornei* of Iranian landrace wheat. *Australasian Plant Pathology* 38:478-489

Smant G, Stokkermans JPWG, Yan Y, de Boer JM, Baum TJ, Wang X, Hussey RS, Gommers FJ, Henrissat B, Davis EL, Helder J, Schots A, Bakker J (1998) Endogenous cellulases in animals: Isolation of  $\beta$ -1,4-endoglucanase genes from two species of plant-parasitic cyst nematodes. *Proceedings of the National Academy of Sciences* 95:4906-4911

Smiley RW (2009) Root-lesion nematodes reduce yield of intolerant wheat and barley. *Agronomy Journal* 101:1322-1335

Smiley RW, Gourlie JA, Yan G, Rhinhart KEL (2014) Resistance and tolerance of landrace wheat in fields infested with *Pratylenchus neglectus* and *P. thornei*. *Plant Disease* 98:797-805

Smiley RW, Nicol JM (2009) Nematodes which challenge global wheat production. In: Carver BF(ed) *Wheat Science and Trade*. Wiley-Blackwell, Ames, IA pp 171-187

Sobczak M, Avrova A, Jupowicz J, Phillips MS, Ernst K, Kumar A (2005) Characterization of susceptibility and resistance responses to potato cyst nematode (*Globodera* spp.) infection of tomato lines in the absence and presence of the broad-spectrum nematode resistance *Hero* gene. *Molecular Plant-Microbe Interactions* 18:158-168

Taylor SP, Evans M (1998) Vertical and horizontal distribution of and soil sampling for root lesion nematodes (*Pratylenchus neglectus* and *P. thornei*) in South Australia. *Australasian Plant Pathology* 27:90-96

Taylor SP, Vanstone VA, Ware AH, McKay AC, Szot D, Russ MH (1999) Measuring yield loss in cereals caused by root lesion nematodes (*Pratylenchus neglectus* and *P. thornei*) with and without nematicide. *Australian Journal of Agricultural Research* 50:617-622

Thompson JP (2008) Resistance to root-lesion nematodes (*Pratylenchus thornei* and *P. neglectus*) in synthetic hexaploid wheats and their durum and *Aegilops tauschii* parents. *Australian Journal of Agricultural Research* 59:432-446

Thompson JP, Clewett TG (1986) Research on root lesion nematode: occurrence and wheat varietal reaction. Queensland Wheat Research Institute Biennial Report for 1982-84. Queensland Department of Primary Industries, Toowoomba, pp 32-34

Thompson JP, Clewett TG, Sheedy JG, Reen RA, O'Reilly MM, Bell KL (2010) Occurrence of root-lesion nematodes (*Pratylenchus thornei* and *P. neglectus*) and stunt nematode (*Merlinius brevidens*) in the northern grain region of Australia. Australasian Plant Pathology 39:254-264

Thompson JP, Haak MI (1997) Resistance to root-lesion nematode (*Pratylenchus thornei*) in *Aegilops tauschii* Coss., the D-genome donor to wheat. Australian Journal of Agricultural Research 48:553-559

Thompson JP, Mackenzie J, Amos R (1995) Root-lesion nematode (*Pratylenchus thornei*) limits response of wheat but not barley to stored soil moisture in the Hermitage long-term tillage experiment. Australian Journal of Experimental Agriculture 35:1049-1055

Thompson JP, Owen KJ, Stirling GR, Bell MJ (2008) Root-lesion nematodes (*Pratylenchus thornei* and *P. neglectus*): a review of recent progress in managing a significant pest of grain crops in northern Australia. Australasian Plant Pathology 37:235-242

Thurau T, Kifle S, Jung C, Cai D (2003) The promoter of the nematode resistance gene *Hs1pro-1* activates a nematode-responsive and feeding site-specific gene expression in sugar beet (*Beta vulgaris* L.) and *Arabidopsis thaliana*. Plant Molecular Biology 52:643-660

Townshend JL (1963a) The pathogenicity of *Pratylenchus penetrans* to celery. Canadian Journal of Plant Science 43:70-74

Townshend JL (1963b) The pathogenicity of *Pratylenchus penetrans* to strawberry. Canadian Journal of Plant Science 43:75-78

Townshend JL (1978) Infectivity of *Pratylenchus penetrans* on alfalfa. Journal of Nematology 10:318-323

Townshend JL (1984) Inoculum densities of five plant parasitic nematodes in relation to alfalfa seedling growth. Canadian Journal of Plant Pathology 6:309-312

Townshend JL, Stobbs L (1981) Histopathology and histochemistry of lesions caused by *Pratylenchus penetrans* in roots of forage legumes. Canadian Journal of Plant Pathology 3:123-128

Townshend JL, Stobbs L, Carter R (1989) Ultrastructural pathology of cells affected by *Pratylenchus penetrans* in alfalfa roots. Journal of Nematology 21:530-539

Trudgill DL (1991) Resistance to and tolerance of plant parasitic nematodes in plants. Annual Review of Phytopathology 29:167-192

Valette C, Andary C, Geiger JP, Sarah JL, Nicole M (1998) Histochemical and cytochemical investigations of phenols in roots of banana infected by the burrowing nematode *Radopholus similis*. Phytopathology 88:1141-1148

Van der Vossen EAG, Van der Voort J, Kanyuka K, Bendahmane A, Sandbrink H, Baulcombe DC, Bakker J, Stiekema WJ, Klein-Lankhorst RM (2000) Homologues of a single resistance-gene cluster in potato confer resistance to distinct pathogens: a virus and a nematode. *Plant Journal* 23:567-576

Vance CP, Kirk TK, Sherwood RT (1980) Lignification as a mechanism of disease resistance. *Annual Review of Phytopathology* 18:259-288

VanEtten HD, Mansfield JW, Bailey JA, Farmer EE (1994) Two classes of plant antibiotics: phytoalexins versus "phytoanticipins". *The Plant Cell* 6:1191-1192

Vanstone VA, Hollaway GJ, Stirling GR (2008) Managing nematode pests in the southern and western regions of the Australian cereal industry: continuing progress in a challenging environment. *Australasian Plant Pathology* 37:220-234

Vanstone VA, Rathjen AJ, Ware AH, Wheeler RD (1998) Relationship between root lesion nematodes (*Pratylenchus neglectus* and *P. thornei*) and performance of wheat varieties. *Australian Journal of Experimental Agriculture* 38:181-188

Veech JA (1979) Histochemical-localization and nematotoxicity of terpenoid aldehydes in cotton. *Journal of Nematology* 11:240-246

Veech JA (1982) Phytoalexins and their role in the resistance of plants to nematodes. *Journal of Nematology* 14:2-9

Veech JA, McClure MA (1977) Terpenoid aldehydes in cotton roots susceptible and resistant to root-knot nematode, *Meloidogyne incognita*. *Journal of Nematology* 9:225-229

Vos P, Simons G, Jesse T, Wijbrandi J, Heinen L, Hogers R, Frijters A, Groenendijk J, Diergaarde P, Reijans M, Fierens-Onstenk J, Both Md, Peleman J, Liharska T, Hontelez J, ZabeauMarc (1998) The tomato *Mi-1* gene confers resistance to both root-knot nematodes and potato aphids. *Nature Biotechnology* 16:1365-1369

Waele DD, Elsen A (2002) Migratory endoparasites: *Pratylenchus* and *Radopholus* species. In: Starr JL, Cook R and Bridge J (eds) *Plant resistance to parasitic nematodes*, CABI publishing, Wallingford UK, pp 175-206

Wallace HR (1974) *Nematology ecology and plant disease*. Alden, London, Oxford

Wallace HR (1989) Environment and plant health: A nematological perception. *Annual Review of Phytopathology* 27:59-75

Whish JPM, Thompson JP, Clewett TG, Lawrence JL, Wood J (2014) *Pratylenchus thornei* populations reduce water uptake in intolerant wheat cultivars. *Field Crops Research* 161:1-10

Whitehead AG (1997) *Plant nematode control*. CAB International, Wallingford, UK

Williamson VM, Kumar A (2006) Nematode resistance in plants: the battle underground. *Trends in Genetics* 22:396-403

Wuyts N, Lognay G, Verscheure M, Marlier M, De Waele D, Swennen R (2007) Potential physical and chemical barriers to infection by the burrowing nematode *Radopholus similis* in roots of susceptible and resistant banana (*Musa* spp.). *Plant Pathology* 56:878-890

Wuyts N, Swennen R, De Waele D (2006) Effects of plant phenylpropanoid pathway products and selected terpenoids and alkaloids on the behaviour of the plant-parasitic nematodes *Radopholus similis*, *Pratylenchus penetrans* and *Meloidogyne incognita*. *Nematology* 8:89-101

Wyss U, Zunke U (1986) Observations on the behaviour of second stage juveniles of *Heterodera schachtii* inside host roots. *Revue de Nematologie* 9:153-165

Yoji M, Taketo U, Atsuhiko K (2001) PCR-based cloning of two  $\beta$ -1,4-endoglucanases from the root-lesion nematode *Pratylenchus penetrans*. *Nematology* 3:335-341

Zinov'eva SV, Vasyukova NI, Ozeretskovskaya OL (2004) Biochemical aspects of plant interactions with phytoparasitic nematodes: a review. *Applied Biochemistry and Microbiology* 40:111-119

Zunke U (1990) Observations on the invasion and endoparasitic behaviour of the root lesion nematode *Pratylenchus penetrans*. *Journal of Nematology* 22:309-320



### **Chapter 3**

**Fine mapping of root lesion nematode (*Pratylenchus thornei*)**

**resistance loci on chromosomes 6D and 2B of wheat**

## **Chapter 3**

### **Fine mapping of root lesion nematode (*Pratylenchus thornei*) resistance loci on chromosomes 6D and 2B of wheat**

#### **3.1 Statement of authorship**

## **Statement of Authorship**

Title of the paper	Fine mapping of root lesion nematode ( <i>Pratylenchus thornei</i> ) resistance loci on chromosomes 6D and 2B of wheat
Publication Status	Published
Publication details	Rahman MS, Linsell KJ, Taylor JD, Hayden MJ, Collins NC, Oldach KH (2019) Fine mapping of root lesion nematode ( <i>Pratylenchus thornei</i> ) resistance loci on chromosomes 6D and 2B of wheat. Theoretical and Applied Genetics. <a href="https://doi.org/10.1007/s00122-019-03495-x">https://doi.org/10.1007/s00122-019-03495-x</a>

#### **Principal Author**

Name of Principal Author (Candidate)	Muhammad Shefatur Rahman		
Contribution to the paper	Involved in designing the research project conception and development of overall research plan. Conducted hands-on experiments, data collection and analysis. Wrote the first draft of the manuscript and took primary responsibility for manuscript revision.		
Overall percentage (%)	70		
Certification	This paper reports on original research I conducted during the period of my Higher Degree by Research candidature and is not subject to any obligations or contractual agreements with a third party that would constrain its inclusion in this thesis. I am the primary author of this paper.		
Signature		Date	4.12.2019

#### **Co-Author Contributions**

By signing the Statement of Authorship, each author certifies that:

- I. the candidate's stated contribution to the publication is accurate (as detailed above);
- II. permission is granted for the candidate to include the publication in the thesis; and
- III. the sum of all co-author contributions is equal to 100% less the candidate's stated contribution.

Name of Co- Author	Katherine J. Linsell		
Contribution to the paper	Provided suggestions for the nematode assay, provided input for the manuscript.		
Signature		Date	5/12/19

Name of Co- Author	Julian D.Taylor		
Contribution to the paper	Performed the statistical data analysis		
Signature		Date	9/12/2019

Name of Co- Author	Matthew J. Hayden		
Contribution to the paper	Performed the 90K SNP array analysis of the DH lines and DNA bulks		
Signature		Date	09/12/2019

Name of Co- Author	Nicholas C. Collins		
Contribution to the paper	Helped in data analysis and writing the manuscript. Read the manuscript and suggested revisions.		
Signature		Date	9/12/19

Name of Co- Author	Klaus H. Oldach		
Contribution to the paper	Provided overall supervision of the research project and helped writing the manuscript		
Signature		Date	4. 12. 2019

### 3.2 Abstract

Two previously known resistance QTL for root lesion nematode (*Pratylenchus thornei*) in bread wheat (*Triticum aestivum*), *QRlnt.sk-6D* and *QRlnt.sk-2B*, were fine mapped using a Sokoll (moderately resistant) by Krichauff (susceptible) doubled haploid (DH) population and six newly developed recombinant inbred line populations. Bulk segregant analysis with the 90K Wheat SNP array identified linked SNPs which were subsequently converted to KASP assays for mapping in the DH and RIL populations. On chromosome 6D, 60 KASP and five SSR markers spanned a total genetic distance of 23.7 cM. *QRlnt.sk-6D* was delimited to a 3.5 cM interval, representing 1.77 Mbp in the bread wheat cv. Chinese Spring reference genome sequence and 2.29 Mbp in the *Ae. tauschii* genome sequence. These intervals contained 42 and 43 gene models in the respective annotated genome sequences. On chromosome 2B, 41 KASP and 5 SSR markers produced a map spanning 19.9 cM. *QRlnt.sk-2B* was delimited to 1.4 cM, corresponding 3.14 Mbp in the durum wheat cv. Svevo reference sequence and 2.19 Mbp in Chinese Spring. The interval in Chinese Spring contained 56 high confidence gene models. Intervals for both QTL contained genes with similarity to those previously reported to be involved in disease resistance, namely genes for phenylpropanoid-biosynthetic-pathway-related enzymes, NBS-LRR proteins and protein kinases. The potential roles of these candidate genes in *P. thornei* resistance are discussed. The KASP markers reported in this study could potentially be used for marker assisted breeding of *P. thornei* resistant wheat cultivars.

### 3.3 Keywords

QTL, fine mapping, wheat, nematode resistance, *Pratylenchus thornei*

### **3.4 Author contribution statement**

MSR and KHO designed the research (project conception and development of overall research plan. MSR conducted hands-on experiments and data collection. MSR, KL, NCC and KHO conducted data analysis. MSR, MH and JT performed statistical analysis. MSR, KL, NCC and KHO wrote the paper and have primary responsibility for the final content.

### **3.5 Key message**

Resistance QTL to root lesion nematode (*Pratylenchus thornei*) in wheat (*Triticum aestivum*), *QRlnt.sk-6D* and *QRlnt.sk-2B*, were mapped to intervals of 3.5 cM/1.77 Mbp on chromosome 6D and 1.4 cM/2.19 Mbp on chromosome 2B, respectively. Candidate resistance genes were identified in the QTL regions and molecular markers developed for marker-assisted breeding.

### 3.6 Introduction

Wheat (*Triticum aestivum* L.) is one of the most important grain crops for global food security. From 2013 to 2017, the world harvest averaged about 742 million tonnes per annum (<http://faostat.fao.org/>). However, current trends in wheat production increases appear to be insufficient for feeding the projected population by 2050 (Curtis and Halford 2014). Improvements in global wheat production will depend partly on how well the effects of various stresses (both biotic and abiotic) on wheat production can be mitigated (Shiferaw et al. 2013).

Root lesion nematodes of the genus *Pratylenchus* are one of the most important biotic stress factors in wheat production, particularly in dryland agriculture, as in the Australian wheatbelt (Vanstone et al. 2008), and the Pacific Northwest of the United States (Smiley et al. 2014). At least eight *Pratylenchus* species parasitise wheat, with *P. thornei* and *P. neglectus* being the most prevalent and associated with the greatest wheat yield loss (Smiley and Nicol 2009; Vanstone et al. 1998). It was estimated that *P. thornei* causes up to 62% wheat yield loss in the northern grain region of Australia (Owen et al. 2014).

As migratory endoparasites, root lesion nematodes penetrate the root using their stylet, and with the release of cell wall degrading enzymes they migrate intra-cellularly (Davis et al. 2011). They predominantly feed on the cortical tissues of the roots, causing significant damage (Castillo et al. 1998). Consequently, plants are unable to uptake nutrients and water from the soil properly, producing foliage symptoms resembling those of nutrient and water deficiencies. The current status of molecular research on root lesion nematodes including their life cycle, feeding behaviour and host-nematode interactions has recently been reviewed (Fosu-Nyarko and Jones 2016; Jones and Fosu-Nyarko 2014).

Cultural practices and application of nematicides for control root lesion nematodes are of doubtful sustainability, either environmentally or economically (Thompson et al. 2008). By contrast, growing resistant or tolerant cultivars is considered to be a more effective, economically viable and environmentally friendly method of control. A resistant cultivar can restrict nematode reproduction and nematode densities in the soil (Rohde 1972), while a tolerant cultivar can withstand nematode infection and yield well when grown in nematode infested soil, although will allow nematode reproduction, leaving nematodes within the soil to infest subsequent crops (Cook 1974; Robinson et al. 2019).

To improve resistance in wheat varieties by breeding, wheat germplasm has been screened for sources of resistance. Initially, the bread wheat line GS50a was identified as a source of partial resistance to *P. thornei* from a severely infested field of a susceptible wheat variety Gatcher (Thompson et al. 1999). Due to the partial nature of the resistance in GS50a, additional wheat germplasm was evaluated for resistance, for example, Middle Eastern land races, wild wheat progenitors, synthetic wheats and CIMMYT wheat accessions (Dababat et al. 2019; Ogonnaya et al. 2008; Sheedy et al. 2012; Sheedy and Thompson 2009).

Most screening for root lesion nematode resistance has been done by quantifying nematodes from soil and roots through extraction of live nematodes and direct counting down a microscope. However, high variation between replicates occurs with these traditional techniques due to variable nematode extraction efficiencies, taxonomic misidentification and sub-sampling errors (Hollaway et al. 2003; Taylor and Evans 1998). However, once identified, molecular markers closely linked to resistance loci can offer a much cheaper and more reliable strategy to select for resistance in breeding. To identify genomic locations of resistance and markers suitable for selection, genetic analyses have been conducted in mapping populations

segregating for resistance using large sets of molecular markers covering all chromosomes. Several quantitative trait loci (QTL) for *P. thornei* resistance have been mapped on wheat chromosomes (predominantly on 2B and 6D) (Table 2 in Linsell et al. 2014a; Table 2 in Mokrini et al. 2019), yet complete resistance has not been achieved (Dababat et al. 2019). One possible reason is the wide genetic distance (>10 centiMorgan) between the closest available markers and the resistance loci (Linsell et al. 2014a). Detailed fine mapping of the QTL is needed for the development of closely linked molecular markers for selection of the resistance alleles in breeding programs, as well as to facilitate the molecular identification of the *P. thornei* resistance genes, which is most likely necessary for the development of diagnostic markers. Further, molecular dissection of resistance loci will help to identify the underlying molecular/physiological basis for the plant's defences. Once identified, it may be possible to stack together QTL controlling different resistance mechanisms to achieve longer lasting resistance.

In a previous study, a doubled haploid (DH) wheat population of 150 lines, developed from a cross between a synthetic derived wheat cultivar Sokoll (*P. thornei* moderately resistant) and the cultivar Krichauff (susceptible) was investigated to identify quantitative trait loci (QTL) for resistance (Linsell et al. 2014a). Two highly significant QTL for *P. thornei* resistance were identified, on the distal ends of the short arms of chromosomes 6D (*QRlnt.sk-6D*) and 2B (*QRlnt.sk-2B*). The 6DS and 2BS QTL explained 43% (Likelihood Ratio Statistics, LRS = 82.9) and 24% (LRS = 39.9) of the total phenotypic variation, respectively. The peak of the QTL effects on 6DS and 2BS were estimated to be at positions 12.8 centiMorgans (cM) and 16.7 cM, respectively. Fine mapping of these QTL is required to deliver closely-linked molecular markers suitable for breeding and progress the positional cloning of the resistance genes. Opportunities for fine mapping have been enhanced by recent progress in wheat genome



sequencing and development of high throughput/density Single Nucleotide Polymorphism (SNP) based marker technologies in wheat.

SNPs are abundant in wheat and provide the basis for efficient new marker genotyping technologies (Rimbert et al. 2018). Several genome-wide SNP-based marker arrays have been developed in wheat such as the 9K (Cavanagh et al. 2013) and 90K (Wang et al. 2014) arrays. These wheat SNP arrays are based on BeadArray<sup>TM</sup> technology from Illumina (<http://www.illumina.com>) and are widely used in genetic studies including genome-wide association studies and QTL mapping. However, chip-based assays are expensive for large numbers of samples. For analysis of specific chromosome regions in a large number of samples, single-plex assays such as Kompetitive Allele Specific PCR (KASP<sup>TM</sup>, <http://www.lgcgroup.com>) are usually more affordable, and have been widely adopted (Allen et al. 2011).

With the advances in genome sequencing technologies, significant progress has been achieved in sequencing the genomes of wheat and its close relatives. Among those recently sequenced are hexaploid wheat (*Triticum aestivum*) cv. Chinese Spring [IWGSC Reference Sequence v1.0, <http://wheatgenome.org>, The International Wheat Genome Sequencing Consortium (IWGSC) 2014], wheat D-genome progenitor (*Aegilops tauschii*) accession AL8/78 (<http://aegilops.wheat.ucdavis.edu>, Luo et al. 2017), wild emmer wheat (*Triticum turgidum* subsp. *dicoccoides*) accession Zavitan (WEWSeq v1.0, <http://wewseq.wixsite.com/consortium>, Avni et al. 2017), durum wheat (*Triticum durum*) cv. Svevo (<https://www.interomics.eu/durum-wheat-genome>; Maccaferri et al. 2019) and an accession of the wheat A-genome progenitor *Triticum urartu* (Ling et al. 2018).

The current study was undertaken to more accurately map the *QRlnt.sk-6D* and *QRlnt.sk-2B* QTL for *P. thornei* resistance. To achieve this, both loci were further genetically mapped using the wheat 90K SNP array, KASP assays and large segregating populations. Furthermore, the physical locations of the QTL in the reference genome sequences were defined, allowing identification of candidates for the underlying *P. thornei* resistance genes.

## 3.7 Materials and methods

### 3.7.1 Plant Material

Initial work was undertaken using the Sokoll  $\times$  Krichauff  $F_1$ -derived DH population of 150 lines (Linsell et al. 2014a). Additionally, a high-resolution mapping population was used, comprising of 1,727 recombinant inbred lines (RILs) from six bi-parental crosses (Table 3.1). The six sub-populations were developed by crossing two *P. thornei* resistant Sokoll/Krichauff DH lines with three *P. thornei* susceptible wheat cultivars, Correll, Mace and Scout. Both DH lines (DH-139 and DH-67) carried resistance alleles from Sokoll at the 6DS and 2BS loci. Seeds of these populations were kindly provided by Dr Hugh Wallwork (South Australian Research and Development Institute, Crop pathology, South Australia). The 1,727 RIL lines ( $F_{2:5}$  individuals) were genotyped with two pairs of flanking markers for each QTL. A total of 108 RIL lines recombinant for the flanking markers (33, 34 and 41 from the crosses with Correll, Mace and Scout, respectively) were further analysed genotypically and phenotypically.

**Table 3.1** Six bi-parental recombinant inbred line (RIL) populations used for high resolution mapping of *Pratylenchus thornei* resistance loci in wheat

Population	Cross	Number of RILs
HW-1318	Correll × HW2-894*C12 (DH-139)	294
HW-1319	Mace × HW2-894*C12 (DH-139)	224
HW-1320	Scout × HW2-894*C12 (DH-139)	280
HW-1325	Correll × HW-894*C16 (DH-67)	324
HW-1326	Mace × HW-894*C16 (DH-67)	294
HW-1327	Scout × HW-894*C16 (DH-67)	311
Total number of lines		1,727

### 3.7.2 *P. thornei* resistance experimental design and assessment

The 108 recombinant RILs and seven parental lines were evaluated for *P. thornei* resistance in a controlled environmental room (CER) in trolleys (Fig. 3.1). Each of the trolleys contained two wire baskets each containing  $5 \times 5 = 25$  sand-filled pots of 150 g in which the plants (one per pot) were grown for eight weeks. A total of six trolleys were used for the experiment, giving 600 plants arranged in 20 rows and 30 columns. RIL lines and parents were replicated five times with inoculation, and parents were replicated 5 times without inoculation to provide negative controls. With these constraints, the experiment was designed as a randomized complete block design (RCBD) using the optimal design R package OD (Butler 2013) available in the R statistical computing environment. The model-based design functionality of the OD package allowed specification of row and column model terms to additionally ensure the RCBD was spatially optimal for the constraints of the experimental layout.

Seeds were surface sterilized with 70% ethanol for one minute, soaked in 0.5% sodium hypochlorite for one minute and rinsed three times with deionised water. Seeds were then germinated on moist filter paper in petri dishes for three days. Seedlings were transplanted into the pots filled with 150 g of steam-pasteurized sand quarried near Tailem Bend, South Australia (Sloans Sand Pty Ltd, Dry Creek, SA). Plants were grown in a growth chamber with 12 h light at 22°C, 12 h darkness at 15°C, and 70% (daily average) relative humidity. Seven days after transplantation, approximately 1,500 nematodes were applied to the base of each plant, then plants were not watered for the next three days (Linsell et al. 2014a). Two days after inoculation, a slow release fertilizer (Osmocote, Scotts Miracle-Gro, USA) was added to the surface of the sand (4 g/kg sand) and each pot was covered with plastic beads to reduce water evaporation. The baskets with the plants were then placed in a hydroponic system. Water was pumped upwards three times a week, to one third the height of the tubes, which was sufficient

to wet the sand yet gentle enough to prevent excessive removal of *P. thornei* from the sand and roots of the plants. Eight weeks after inoculation, the shoots were cut off and discarded, and the sand with roots submitted to the SARDI Root Disease Testing Service where the DNA was extracted and the amount of *P. thornei* assessed via DNA quantification using a real time TaqMan PCR system (Haling et al. 2011; Ophel-Keller et al. 2008; Riley et al. 2010).

Before analysing the nematode counts for the controlled environment RIL experiment, the *P. thornei* counts were log transformed to satisfy model assumption. The transformed nematode counts were then analysed using a linear mixed model (LMM) that appropriately partitioned genetic and non-genetic components of variation. Specifically, the LMM consisted of a fixed effect term to appropriately estimate means for each of the parental controls as well as estimate an overall mean for the RIL population. The random component of the LMM consisted of terms to capture potential differences in nematode variation between replicate blocks as well as potential variation differences between trolleys and between crates nested within trolleys. Importantly, the random component also contained a term to capture the genetic differences between the RIL lines. To ensure small scale spatial trends were appropriately modelled across the dimensions of the experimental layout, the residual error of the LMM was assumed to contain a separable autoregressive correlation structure in the row and column directions of the experiment. After fitting of the LMM, the best linear unbiased predictors (BLUPs) of the log transformed nematode counts were extracted for subsequent QTL analysis. Computationally, the LMM was fitted using the flexible LMM R package ASReml-R (Butler et al. 2009) available in the R statistical computing environment.

**Fig. 3.1** Recombinant inbred lines (RILs) were evaluated for resistance to *Pratylenchus thornei* in a growth room. Plants were grown in steam-pasteurized sand-filled plastic pots fitted into baskets, which were in turn placed in plastic tubs. Water was supplied periodically from reservoirs to the tubs



### **3.7.3 90K SNP genotyping**

Total genomic DNA for 90K genotyping was extracted using the DNeasy<sup>®</sup> Plant Minikit (Qiagen, Germany). 90K SNP genotyping was done at the Department of Primary Industries (Victorian Agri Biosciences Centre, Bundoora, VIC 3083, Australia).

### **3.7.4 KASP assays**

To extract wheat genomic DNA for KASP assays (LGC genomics, <http://www.lgcgroup.com>, Allen et al. 2011) a cetyltrimethylammonium bromide (CTAB) protocol was followed (Saghai-Marooft et al. 1984). KASP assays were performed in 5 µL reactions containing 50-100 ng genomic DNA, 0.2 µM of each allele-specific forward primer, 0.5 µM of reverse primer, and 2 µL of KASP master mix (LGC genomics, UK). KASP thermal cycling was carried out according to the manufacturer's protocol: 94°C for 15 min; 10 step-down cycles of 94°C for 20 s, and 61–55°C for 60 s (decreasing by 0.6°C each cycle); and 26 cycles of 94°C for 20 s, and 55°C for 60 s. The repliKator instrument (LGC genomics, UK) was used to dispense DNA samples. KASP master mix was dispensed using a Meridian dispenser. A FUSION laser sealer and KUBE heat sealer was used for sealing the polypropylene PCR plate. A HydroCycler16 was used for thermal cycling and a BMG PHERAstar fluorescent plate reader was used for KASP marker fluorescence detection. The software Kraken was used to manage the KASP genotyping project, including designing the primers and allele calling. Newly designed KASP assays were initially tested on parental DNA and artificial F<sub>1</sub> DNA (equal amount mix of parental line DNA) to ensure that genotypic classes could be differentiated.

### **3.7.5 Initial identification and mapping of linked SNPs using Sokoll/Krichauff DH lines**

Bulked segregant analysis (BSA) was initially conducted using the 90K wheat SNP array to identify SNPs linked to the QTL. The 90K SNP genotyping was performed on three bulk DNA



samples derived from Sokoll/Krichauff DH lines: lines carrying resistance alleles at one or the other locus (6DS or 2BS) or lines carrying susceptibility alleles at both loci. Resistance status of lines defined using the marker data was corroborated by previous *P. thornei* resistance data (Linsell et al. 2014a), namely *P. thornei* DNA concentrations of 3,381 to 12,162 pg/plant for the resistant lines (carrying 6DS or 2BS resistance alleles), and 15,851 to 27,466 pg/plant for the susceptible lines (carrying susceptibility alleles at 6DS and 2BS). DNA samples were combined in equal amounts to produce the respective DNA bulks; 39 lines for the 6DS resistant bulk, 23 lines for the 2BS resistant bulk and 20 lines for the susceptible bulk. Parental lines Sokoll and Krichauff were also analysed.

A subset of the 65 Sokoll/Krichauff DH lines were also analysed individually using the 90K wheat SNP array. These lines were chosen on the basis of marker data from the study of Linsell et al. (2014a): 38 were recombinant for the *QRlnt.sk-6D* flanking markers *cfld49* and *gdm36*, located 68.0 cM apart, 10 were recombinant for the *QRlnt.sk-2B* flanking markers *barc35* and *wmc661*, located 52.8 cM apart, 16 non-recombinants carried resistance alleles at both loci and one carried susceptibility alleles at both loci.

The 90K SNP marker scores for the 65 Sokoll/Krichauff DH lines were diagnostically assessed and used to construct genetic maps of each of the two chromosome regions, using the functionality of the QTL (Broman and Sen 2009) and ASMap (Taylor and Butler 2017) R packages available in the R statistical computing environment (R Core Team 2018). Markers were initially assessed for missing alleles and markers with more than 20% missing scores were discarded. Additionally, markers were removed that showed segregation distortion significantly greater than a Bonferroni p-value threshold of 0.05 corrected for multiple comparisons. The remaining markers in each chromosome were then optimally ordered using

the MSTmap (Wu et al. 2008) functionality available in ASMap. From these initial marker linkages, the marker diagnostics were profiled and markers exhibiting a large number of double recombination were removed. For each chromosome, the markers were then optimally ordered a final time and chromosome orientations assigned using the 90K consensus map positions. It should be noted that because the scored DH lines were pre-selected as having recombinants in the QTL intervals, the genetic distances in the resulting maps were expected to be over-estimates inside of the selected intervals and under-estimates (due to genetic interference) outside of the QTL intervals.

### **3.7.6 QTL re-analysis in Sokoll/Krichauff DH lines using revised genetic maps**

Linkage between the KASP markers was established using the Map Manager QTX program (Manly et al. 2001). The linkage groups were constructed based on strong linkage criterion ( $p = 10^{-5}$ ) between the markers and employing the Kosambi mapping function (Kosambi 1943). The ordering of the markers was done by using the software RECORD (Van Os et al. 2005) with the aim of minimizing apparent double crossovers. Markers with a large number of double crossovers were eliminated from the analysis. The map was illustrated using the software MapChart (Voorrips 2002). The Map Manager QTX software was also used for QTL analysis. The likelihood ratio statistics (LRS) was calculated using the interval mapping functions with  $p = 0.0001$ . Permutation analyses (1000 iterations) were carried out to determine whether a particular LRS value was highly significant (Churchill and Doerge 1994).

### **3.7.7 Reference genome sequence and gene annotation**

Physical genomic positions of the SNPs were determined by BLAST searching the sequence around each SNP (Wang et al. 2014) to the genome sequences of Chinese Spring (<http://www.wheatgenome.org/>), *Aegilops tauschii* (<http://aegilops.wheat.ucdavis.edu>, Luo et

al. 2017), wild emmer wheat (WEWSeq v1.0, <http://wewseq.wixsite.com/consortium>, Avni et al. 2017) and durum wheat (<https://www.interomics.eu/durum-wheat-genome>). Gene annotations in the Chinese Spring IWGSC RefSeq v1.0 (<https://wheat-urgi.versailles.inra.fr/Seq-Repository/Annotations>) and *Aegilops tauschii* (<http://aegilops.wheat.ucdavis.edu/ATGSP/annotation/>) were used to search for candidate *P. thornei* resistance genes. Expression data for the genes were obtained using the Wheat Expression Browser database ([wheat-expression.com](http://wheat-expression.com), Ramírez-González et al. 2018).

## 3.8 Results

### 3.8.1 Identification of SNPs

The 90K wheat SNP array (Wang et al. 2014) was used on Sokoll/Krichauff DH lines and DNA bulks to identify SNPs linked to the *P. thornei* resistance QTL, *QRlnt.sk-6D* and *QRlnt.sk-2B*. A total of 16,907 SNPs were identified as being polymorphic between Sokoll and Krichauff. On the basis of best BLASTn hits against the Chinese Spring chromosome survey sequence (Wang et al. 2014), 776 and 1,597 of these SNPs were located on chromosome 6D and 2B, respectively. Of these, the DNA bulks identified that 58 and 120 of these SNPs were genetically linked to *QRlnt.sk-6D* and *QRlnt.sk-2B*, respectively (Supplementary Table 3.1 and 3.2).

### 3.8.2 90K maps

Genotyping of the 65 DH lines with the 90K wheat SNP array enabled full-chromosome maps to be constructed. A total of 255 SNPs were mapped on chromosome 6D, spanning a genetic distance of 201.3 cM (Supplementary Table 3.3). For chromosome 2B, a total of 1,325 SNPs were mapped, spanning 290.1 cM (Supplementary Table 3.4).

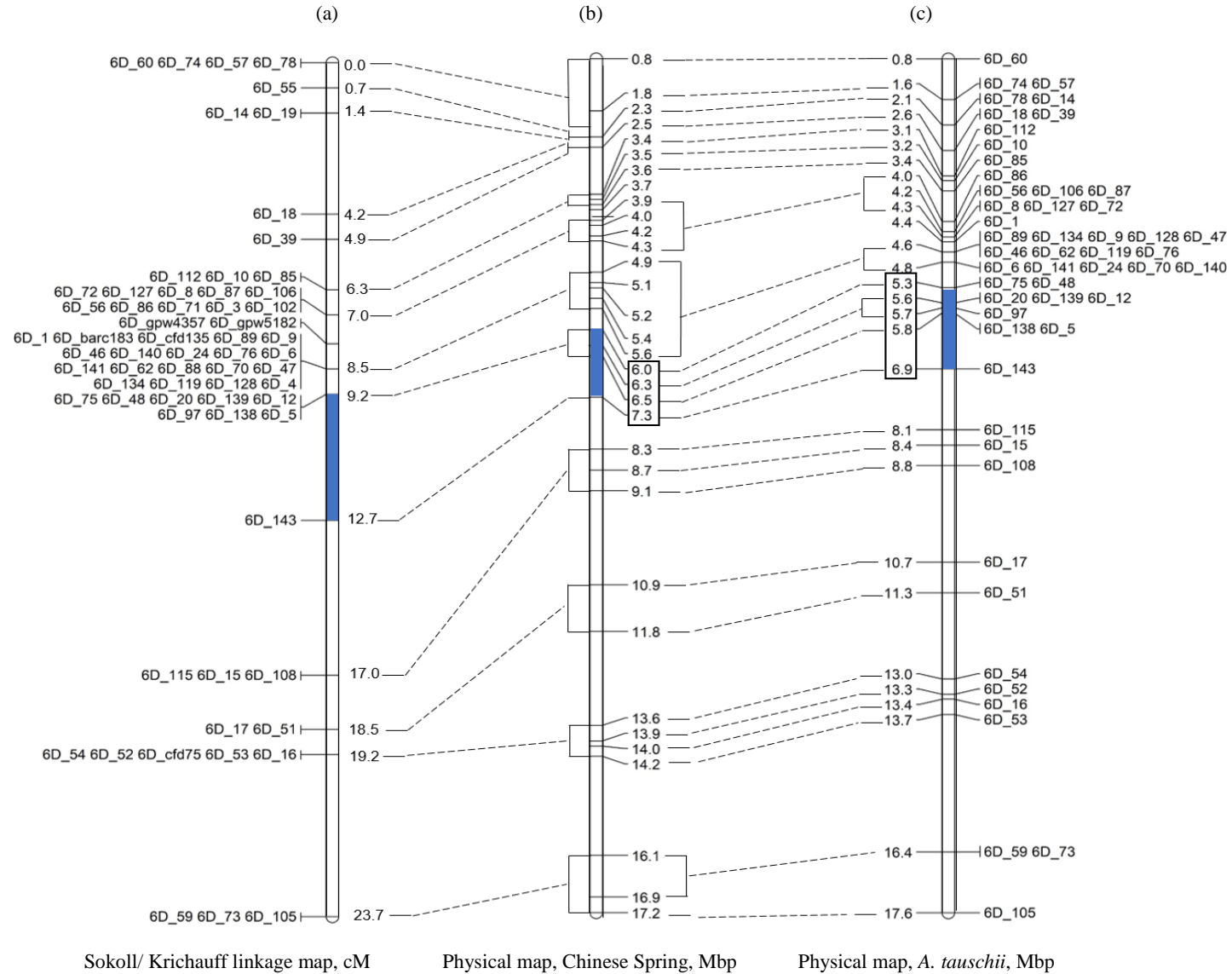
### 3.8.3 QTL re-mapping *QRlnt.sk-6D* using the whole DH population

KASP assays were designed for 143 SNPs mapped to the 6DS QTL interval (Supplementary Table 3.5). These markers were identified as being closely linked to the QTL, based on the BSA, 90K SNP map and cereal database (Allen et al. 2011) data. Of these, 60 KASP assays that gave clear allele calling were then chosen for mapping across the entire Sokoll/Krichauff DH population of 150 DH lines. In addition, five SSR markers that had been mapped close to *QRlnt.sk-6D* including the flanking markers (Linsell et al. 2014a) were integrated into the map. The markers were located in the Chinese Spring and *Ae. tauschii* genome sequences to obtain

the correct orientation. The map spanned a total genetic distance of 23.7 cM, representing 16.36 Mbp in Chinese Spring and 16.81 Mbp in *Ae. tauschii* (Fig. 3.2). The relative positions of the markers in the genetic map corresponded well with their positions in both physical maps (Fig. 3.2).

Available *P. thornei* resistance data for the DH lines (Linsell et al. 2014a) were used for a QTL analysis with the new linkage map. Simple interval mapping defined the QTL interval (LRS score of 92.0) as being located between the KASP markers 6D\_5 (and seven other co-segregating markers) and 6D\_143 (Fig. 3.2), with the QTL explaining 47% of the total phenotypic variation.

**Fig. 3.2** Genetic linkage map of part of the 6DS chromosome arm made using the Sokoll/Krichauff doubled haploid population (a) and its alignment to the physical map of Chinese spring (b) and *Aegilops tauschii* (c). The interval of the *Pratylenchus thornei* resistance QTL *QRInt.sk-6D* is shown as shaded bars and the physical locations of the markers defining the QTL interval are boxed



#### 3.8.4 Fine mapping of *QRInt.sk-6D* by graphical genotyping using DH and RIL recombinants

The DH lines clearly grouped according to their resistance phenotype (*P. thornei* DNA per plant), into those that had more or less than 10,000 pg/plant, representing those lines likely to carry the susceptibility or resistance allele at *QRInt.sk-6D*, respectively (Fig. 3.3a). This was consistent with *QRInt.sk-6D* being between the markers 6D\_4 and 6D\_143, located 4.2 cM apart. These flanking markers were at positions 5.57 Mbp to 7.34 Mbp, respectively, in the Chinese Spring chromosome 6D sequence. In *Ae. tauschii*, a BLAST search using the 6D\_4 sequence detected no match, so the marker 6D\_128, located a little further out in Chinese Spring, was considered as the flanking marker on that side. 6D\_128 and 6D\_143 were located at 4.64 Mbp and 6.93 Mbp in the *Ae. tauschii* chromosome 6D sequence. The co-segregating region for *QRInt.sk-6D* in the DH lines spanned markers 6D\_75 to 6D\_5 (Fig. 3.3a).

To validate the QTL and further fine map it, 108 RILs were used. These lines were selected from a larger set of lines (1,727 RILs from six bi-parental crosses) based on the presence of recombination between the markers flanking the QTL. Of the 65 KASP and SSR markers mapped in the DH lines, 32 were found to be polymorphic across all six bi-parental populations and these were scored in the 108 RILs.

Compared to the DHs, the RILs could not be as clearly allocated to two phenotype groups (in this case using BLUPs for nematode DNA quantity; Fig 3.3b), likely owing to the lower number of replications with the RILs (three plants were phenotyped per RIL in one experiment vs. five plants total per DH in each of two experiments). Consequently, the RILs (Fig 3.3b) suggested two alternative intervals for *QRInt.sk-6D*, depending on which threshold was chosen for defining the groups. A threshold of 0.5 gave the interval between markers 6D\_139 and

6D\_115, whereas a threshold of 1.0 gave the interval between 6D\_128 and 6D\_20. Both of these intervals were consistent with the (larger) interval defined using the DH recombinants. This interval defined by the DHs (between 6D\_4 and 6D\_143) was therefore regarded as the smallest interval to which *QRlnt.sk-6D* could be reliably ascribed.

Subsequent mapping of the *QRlnt.sk-2B* locus (following sections) identified which lines were likely to carry the resistance allele at this locus (Fig 3.3). Due to the much larger effect of the *QRlnt.sk-6D* locus, the *QRlnt.sk-2B* locus status of individual lines did not influence their categorization as resistant or susceptible for the purposes of mapping *QRlnt.sk-6D* (not shown).





### **3.8.5 Identification of candidate nematode resistance genes in the *QRlnt.sk-6D* interval**

In the annotation of the Chinese Spring reference genome (IWGSC RefSeq v1.0), the 1.77 Mbp interval of *QRlnt.sk-6D* contained 42 high confidence gene models (Supplementary Table 3.6). The corresponding 2.29 Mb interval in *Ae. tauschii* contained 43 high confidence gene models. Several of the functional classes to which these genes belong have members known to contribute to plant disease defence or resistance. Encoded products include protein kinases, nucleotide binding site leucine-rich repeat (NBS-LRR) proteins and enzymes involved in secondary metabolism. The gene models that are related to disease resistance are highlighted in Table 3.2. According to the Wheat Expression Browser database (Ramírez-González et al. 2018), the majority of these genes were found to be expressed in wheat roots. Details on the involvement of these gene classes in resistance are provided in the Discussion section.

**Table 3.2** Candidate nematode resistance genes in the *QRInt.sk-6D* QTL interval, in genomic sequence annotations of Chinese Spring IWGSC RefSeq v1.0 and *Aegilops tauschii*, Aet v4.0. Homologous genes between two species are aligned in the same line and homologous group of genes are segmented with the horizontal lines

Chinese spring					<i>Aegilops tauschii</i>			
Gene-ID	Start	end	Annotation	Root <sup>1</sup>	Gene ID	Start	End	Annotation
TraesCS6D01G013400.1	5477924	5481671	Receptor-like protein kinase, putative, expressed	<b>Y</b>	AET6Gv20022000	4632196	4719648	Disease resistance protein RPM1
TraesCS6D01G013600.1	5562123	5566425	Receptor-like protein kinase, putative, expressed	<b>Y</b>	AET6Gv20022200	4655806	4662191	putative disease resistance RPP13-like protein 3
					AET6Gv20023100	4773368	4785358	putative disease resistance RPP13-like protein 3
TraesCS6D01G013900.1	5844543	5845856	F-box family protein	N				
TraesCS6D01G015100.1	6314769	6316761	4,5-dioxygenase-like protein	<b>Y</b>				
					AET6Gv20024100	4980269	4982544	Tyrosine/DOPA decarboxylase 3
					AET6Gv20025500	5253288	5255652	Ribosome-inactivating protein 9
					AET6Gv20026500	5486946	5488469	tyrosine decarboxylase 1-like
TraesCS6D01G015000.1	6274077	6276905	Cytochrome P450	<b>Y</b>	AET6Gv20027000	5607974	5611243	cytochrome P450 709B2-like
TraesCS6D01G015200.1	6319338	6321386	Flavonoid 3'-hydroxylase	<b>Y</b>	AET6Gv20027200	5657247	5666250	flavonoid 3'-monooxygenase-like
TraesCS6D01G015300.1	6328264	6328920	Flavonoid 3'-hydroxylase	Y				
TraesCS6D01G015400.1	6342582	6344284	Isoflavone reductase-like protein	<b>Y</b>	AET6Gv20027300	5686821	5709253	Isoflavone reductase-IRL-like protein
TraesCS6D01G015500.1	6351577	6353794	LRR receptor-like protein kinase family protein	Y	AET6Gv20027400	5695258	5698881	LRR receptor-like serine/threonine-protein kinase
TraesCS6D01G015600.1	6354023	6354982	LRR receptor-like protein kinase family protein	Y	AET6Gv20027600	5756181	5759396	LRR receptor-like serine/threonine-protein kinase
TraesCS6D01G015700.1	6370264	6373164	LRR receptor-like protein kinase family protein	N	AET6Gv20027700	5772461	5775676	LRR receptor-like serine/threonine-protein kinase
TraesCS6D01G015800.1	6425195	6426922	LRR receptor-like protein kinase family protein	N	AET6Gv20027800	5805867	5809727	LRR receptor-like serine/threonine-protein kinase
TraesCS6D01G015900.1	6426980	6428089	LRR receptor-like protein kinase family protein	N	AET6Gv20028900	6236911	6239682	LRR receptor-like serine/threonine-protein kinase
TraesCS6D01G016000.1	6441826	6443688	LRR receptor-like protein kinase family protein	Y	AET6Gv20029000	6241694	6243240	probable glutathione S-transferase GSTF1
TraesCS6D01G016100.1	6496165	6501558	LRR receptor-like protein kinase family protein	Y	AET6Gv20029300	6296365	6299276	probable LRR receptor-like serine/threonine-protein kinase At1g34110
TraesCS6D01G016600.1	6977348	6980077	LRR receptor-like protein kinase family protein	Y	AET6Gv20029500	6349131	6352966	wall-associated receptor kinase-like 6
TraesCS6D01G016700.1	6982048	6983620	Glutathione S-transferase	<b>Y</b>				
TraesCS6D01G016800.1	7032180	7035207	LRR receptor-like protein kinase family protein	Y	AET6Gv20033100	6564371	6570298	disease resistance protein RPP13-like
TraesCS6D01G016900.1	7085603	7089322	Protein kinase family protein	Y	AET6Gv20034300	6696137	6700725	disease resistance protein RPM1-like
TraesCS6D01G017500.1	7280447	7285137	Disease resistance protein RPM1	Y	AET6Gv20034400	6702403	6707351	disease resistance protein RPM1-like
TraesCS6D01G017600.1	7290076	7293584	Disease resistance protein (NBS-LRR class)	<b>Y</b>				

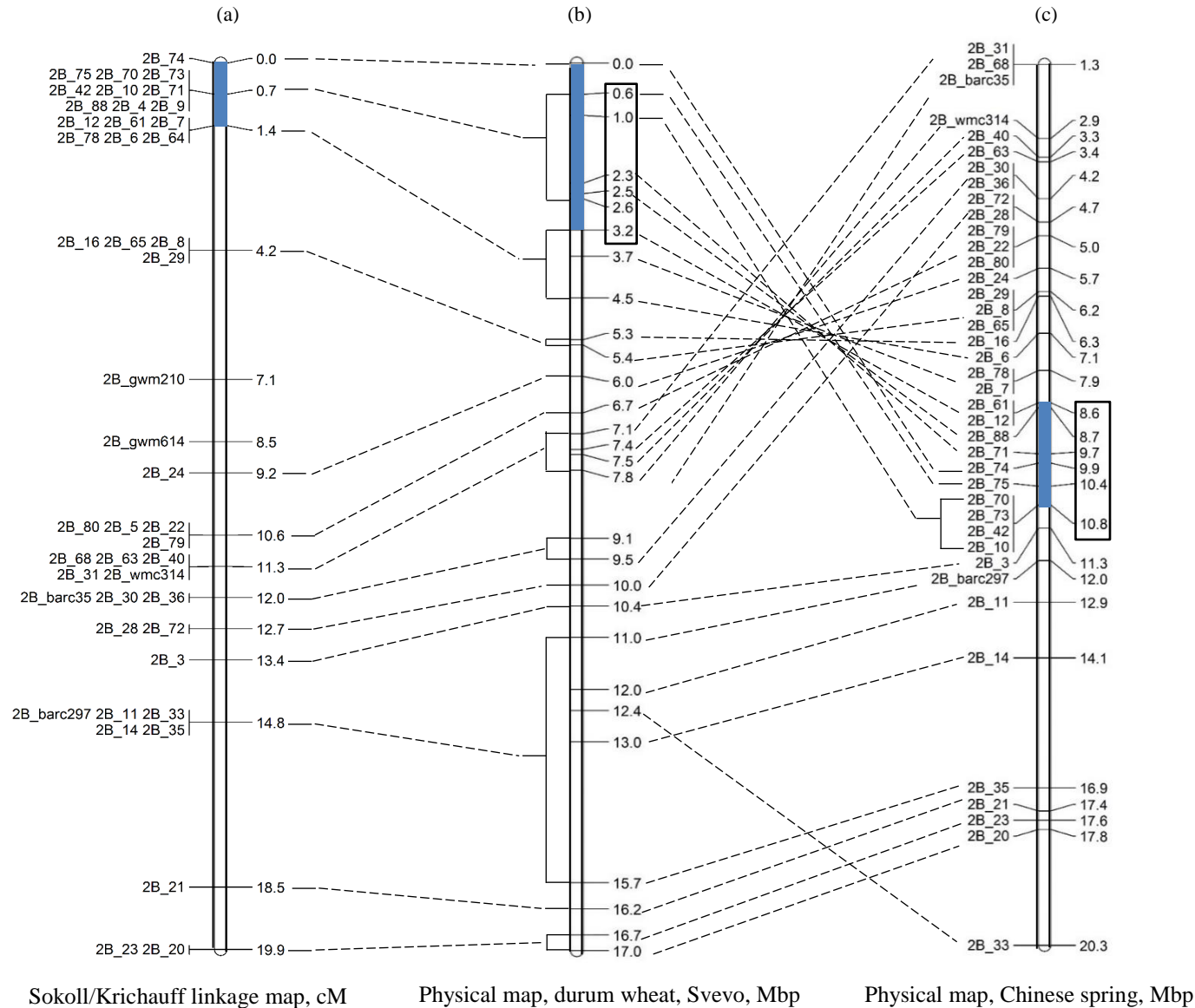
1: According to the Wheat Expression Browser, presence and absence of gene expression in root are referred as Y and N, respectively. Genes that are expressed at least 0.5 transcript per million (tpm) are shown as 'bold'

### 3.8.6 QTL re-mapping *QRlnt.sk-2B* using the whole DH population

KASP assays were designed on 92 SNPs (Supplementary Table 3.7), identified as being closely linked to the QTL, based on the BSA, 90K SNP map and cereal database (Allen et al. 2011) data. Of these, 41 were judged to be of high quality and were mapped across the entire population of 150 Sokoll/Krichauff DH lines. Together with five SSR markers previously mapped near the 2BS resistance locus, including the QTL flanking markers (Linsell et al. 2014a), the KASP markers were used to produce a map spanning 19.9 cM (Fig. 3.4). The genetic map corresponded to a 16.92 Mbp physical interval in the genome sequences of durum wheat cv. Svevo (Maccaferri et al. 2019) and a 19.08 Mbp interval in bread wheat (Chinese Spring). The order of the markers corresponded well with the physical maps, except that 36 of the markers were inverted in the bread wheat physical map relative to the durum wheat physical map and the bread wheat genetic map (Fig. 3.4).

Simple interval mapping analysis suggested a QTL interval of *QRlnt.sk-2B* between the markers 2B\_74 and 2B\_12 (and five other co-segregating markers; LRS score of 44.5) (Fig. 3.4), with the QTL explaining 25% of the total phenotypic variation.

**Fig. 3.4** Genetic linkage map of part of the 2BS chromosome arm made using the Sokoll/Krichauff DH population (a), aligned with the sequence in durum wheat (Svevo) (b) and Chinese Spring (c). The interval of the *QRlnt.sk-6D* *Pratylenchus thornei* resistance QTL is shown as shaded bars and the physical locations of the markers defining the QTL interval are boxed



### **3.8.7 Fine mapping of *QRlnt.sk-2B* by graphical genotyping using DH and RIL recombinants**

Graphical genotypes of the DH lines and RILs in the *QRlnt.sk-2B* QTL region are presented in Fig. 3.5 and Fig. 3.6, respectively. The DH lines were subdivided into two classes (Class ‘a’ and ‘b’) based on the presence of the Krichauff or Sokoll allele at the stronger *QRlnt.sk-6D* QTL (6D\_4 to 6D\_143 interval), respectively. A threshold level of *P. thornei* DNA for defining groups as resistant or susceptible at *QRlnt.sk-2B*, of 12,000 pg/plant in class ‘a’ and of 5,000 pg/plant in class ‘b’, was consistent with a position for *QRlnt.sk-2B* between the markers 2B\_74 and 2B\_12. The flanking markers were 1.4 cM apart and correspond to physical intervals of 0.04 to 3.18 Mbp in durum wheat cv. Svevo, and 8.59 to 10.78 Mbp in bread wheat cv. Chinese Spring (Fig. 3.5). The co-segregating region spanned markers 2B\_75 to 2B\_9.

The 108 RILs were genotyped for 21 KASP markers on chromosome 2B that were polymorphic across the six RIL populations. Again, lines were separated into two groups (‘a’ and ‘b’) based on the presence of the susceptible (Correll, Mace or Scout) or resistant (Sokoll) allele at *QRlnt.sk-6D*. If a threshold of nematode DNA quantity per plant (BLUPs) for declaring the presence of the resistance or susceptibility allele at *QRlnt.sk-2B* was set at 1.0 for group ‘a’ and at 0.4 for group ‘b’, the data were consistent with a location of *QRlnt.sk-2B* distal to the marker 2B\_78 (Fig. 3.6). This region covered the interval defined in the DHs (Fig 3.5), i.e., the *QRlnt.sk-2B* interval defined by the DHs (2B\_74 to 2B\_12) was smaller.

### **3.8.8 Identification of candidate nematode resistance genes in the *QRlnt.sk-2B* interval**

The *QRlnt.sk-2B* interval was contained entirely within the previously mentioned inversion difference between the maps, and hence this inversion difference didn’t interfere with defining the *QRlnt.sk-2B* interval in the Chinese Spring genomic sequence. In the Chinese Spring gene

annotations, there were 56 high confidence gene models in the *QRlnt.sk-2B* interval (Supplementary Table 3.8). Of these, 26 were related to plant disease resistance, including those with similarities to NBS-LRR disease resistance proteins and receptor-like protein kinases (Table 3.3). A total of 20 genes were reported to be expressed in wheat root (Ramírez-González et al. 2018).

**Fig. 3.5** Graphical genotypes of Sokoll/ Krichauff (S/K) doubled haploid (DH) lines in the *QRlnt.sk-2B* QTL region. The lines are grouped into two classes, ‘a’ and ‘b’ based on the presence of either the susceptibility (Krichauff) or resistance (Sokoll) allele at the stronger *QRlnt.sk-6D* QTL. Marker positions are shown as the genetic location (cM) in the S/K DH map, and the physical positions in the genome sequences of emmer wheat, bread wheat cv. Chinese Spring, and durum wheat cv. Svevo. Marker alleles from the resistant parent Sokoll are denoted by ‘A’ and alleles from the susceptible parent Krichauff are denoted by ‘B’

1: DH group are defined by marker score; 2: number of lines in respective groups; 3: average phenotypic values of the lines in each group; *P. thornei* DNA (pg/plant) are given as raw means across two experiments in the DH lines. Some markers that co-segregated with the asterisked markers (\*) are not shown, due to space limitations. The QTL co-segregating region is denoted by the vertical lines



**Fig. 3.6** Graphical genotypes of recombinant RILs derived from six crosses, for the *QRlnt.sk-2B* QTL region. The lines were grouped into two classes, ‘a’ and ‘b’ based on the presence of either the susceptible (Correll, Mace and Scout) or resistance (Sokoll) allele at the 6DS QTL. Marker positions are shown as the genetic location (cM) in the Sokoll/Krichauff DH map, and the physical positions in the genome sequences of emmer wheat, bread wheat cv. Chinese Spring, and durum wheat cv. Svevo. Alleles from Sokoll are denoted by ‘A’ and alleles from the susceptible parents are denoted by ‘B’

Marker	2B_74	2B_73	2B_42	2B_10	2B_71	2B_4	2B_9	2B_12	2B_78	2B_16	2B_65*	2B_22	2B_40	2B_41	2B_87	2B_3	2B_37	2B_11	2B_34	2B_33
Emmer Wheat (Mbp)	na	1.6	1.6	1.6	1.0	na	36.1	40.7	2.5	3.4	3.4	4.3	4.8	6.1	7.5	8.2	9.0	9.6	157.1	41.7
C. Spring (Mbp)	9.9	10.8	10.8	10.8	9.7	na	na	8.6	7.9	6.3	6.2	5.0	3.3	2.1	1.3	11.3	12.1	12.9	13.2	20.3
Durum Wheat (Mbp)	0.0	1.0	1.0	1.0	2.3	2.6	2.6	3.2	3.7	5.3	5.4	6.7	7.5	8.6	9.1	10.4	11.1	12.0	12.1	12.4
S/K map (cM)	0.0	0.7	0.7	0.7	0.7	0.7	0.7	1.4	1.4	4.2	4.2	10.6	11.3	na	na	13.4	na	14.8	na	14.8
<b>a</b>	<sup>1</sup> RIL Group	<sup>2</sup> n	<sup>3</sup> <i>P. thornei</i> DNA, BLUPs																	
	1	16	A A A A A A A A	A A A A A A A A	A A A A A A A A	A A A A A A A A	A A A A A A A A	A A A A A A A A	A A A A A A A A	A A A A A A A A	A A A A A A A A	A A A A A A A A	A A A A A A A A	A A A A A A A A	A A A A A A A A	A A A A A A A A	A A A A A A A A	A A A A A A A A	A A A A A A A A	0.17
	2	1	A A A A A A A A	A A A A A A A A	A A A A A A A A	A A A A A A A A	A A A A A A A A	A A A A A A A A	A A A A A A A A	A A A A A A A A	A A A A A A A A	B B B B B B B B	B B B B B B B B	B B B B B B B B	B B B B B B B B	B B B B B B B B	B B B B B B B B	B B B B B B B B	B B B B B B B B	0.11
	3	3	A A A A A A A A	A A A A A A A A	A A A A A A A A	A A A A A A A A	A A A A A A A A	A A A A A A A A	A A A A A A A A	A A A A A A A A	A A A A A A A A	B B B B B B B B	B B B B B B B B	B B B B B B B B	B B B B B B B B	B B B B B B B B	B B B B B B B B	B B B B B B B B	B B B B B B B B	0.35
	4	2	A A A A A A A A	A A A A A A A A	A A A A A A A A	A A A A A A A A	A A A A A A A A	A A A A A A A A	A A A A A A A A	A A A A A A A A	A A A A A A A A	B B B B B B B B	B B B B B B B B	B B B B B B B B	B B B B B B B B	B B B B B B B B	B B B B B B B B	B B B B B B B B	B B B B B B B B	0.88
	5	1	B B B B B B B B	B B B B B B B B	B B B B B B B B	B B B B B B B B	B B B B B B B B	B B B B B B B B	B B B B B B B B	B B B B B B B B	B B B B B B B B	A A A A A A A A	A A A A A A A A	A A A A A A A A	A A A A A A A A	A A A A A A A A	A A A A A A A A	A A A A A A A A	A A A A A A A A	1.64
	6	6	B B B B B B B B	B B B B B B B B	B B B B B B B B	B B B B B B B B	B B B B B B B B	B B B B B B B B	B B B B B B B B	B B B B B B B B	B B B B B B B B	A A A A A A A A	A A A A A A A A	A A A A A A A A	A A A A A A A A	A A A A A A A A	A A A A A A A A	A A A A A A A A	A A A A A A A A	1.31
	7	1	B B B B B B B B	B B B B B B B B	B B B B B B B B	B B B B B B B B	B B B B B B B B	B B B B B B B B	B B B B B B B B	B B B B B B B B	B B B B B B B B	A A A A A A A A	A A A A A A A A	A A A A A A A A	A A A A A A A A	A A A A A A A A	A A A A A A A A	A A A A A A A A	A A A A A A A A	1.19
	8	9	B B B B B B B B	B B B B B B B B	B B B B B B B B	B B B B B B B B	B B B B B B B B	B B B B B B B B	B B B B B B B B	B B B B B B B B	B B B B B B B B	B B B B B B B B	B B B B B B B B	B B B B B B B B	B B B B B B B B	B B B B B B B B	B B B B B B B B	B B B B B B B B	B B B B B B B B	1.52
<b>b</b>																				
	1	18	A A A A A A A A	A A A A A A A A	A A A A A A A A	A A A A A A A A	A A A A A A A A	A A A A A A A A	A A A A A A A A	A A A A A A A A	A A A A A A A A	A A A A A A A A	A A A A A A A A	A A A A A A A A	A A A A A A A A	A A A A A A A A	A A A A A A A A	A A A A A A A A	A A A A A A A A	-0.77
	2	1	A A A A A A A A	A A A A A A A A	A A A A A A A A	A A A A A A A A	A A A A A A A A	A A A A A A A A	A A A A A A A A	A A A A A A A A	A A A A A A A A	A A A A A A A A	A A A A A A A A	A A A A A A A A	A A A A A A A A	A A A A A A A A	A A A A A A A A	A A A A A A A A	A A A A A A A A	-0.95
	3	5	A A A A A A A A	A A A A A A A A	A A A A A A A A	A A A A A A A A	A A A A A A A A	A A A A A A A A	A A A A A A A A	A A A A A A A A	A A A A A A A A	B B B B B B B B	B B B B B B B B	B B B B B B B B	B B B B B B B B	B B B B B B B B	B B B B B B B B	B B B B B B B B	B B B B B B B B	-1.01
	4	1	A A A A A A A A	A A A A A A A A	A A A A A A A A	A A A A A A A A	A A A A A A A A	A A A A A A A A	A A A A A A A A	A A A A A A A A	A A A A A A A A	B B B B B B B B	B B B B B B B B	B B B B B B B B	B B B B B B B B	B B B B B B B B	B B B B B B B B	B B B B B B B B	B B B B B B B B	-0.48
	5	2	B B B B B B B B	B B B B B B B B	B B B B B B B B	B B B B B B B B	B B B B B B B B	B B B B B B B B	B B B B B B B B	B B B B B B B B	B B B B B B B B	A A A A A A A A	A A A A A A A A	A A A A A A A A	A A A A A A A A	A A A A A A A A	A A A A A A A A	A A A A A A A A	A A A A A A A A	-0.03
	6	1	B B B B B B B B	B B B B B B B B	B B B B B B B B	B B B B B B B B	B B B B B B B B	B B B B B B B B	B B B B B B B B	B B B B B B B B	B B B B B B B B	A A A A A A A A	A A A A A A A A	A A A A A A A A	A A A A A A A A	A A A A A A A A	A A A A A A A A	A A A A A A A A	A A A A A A A A	-0.29
	7	2	B B B B B B B B	B B B B B B B B	B B B B B B B B	B B B B B B B B	B B B B B B B B	B B B B B B B B	B B B B B B B B	B B B B B B B B	B B B B B B B B	B B B B B B B B	B B B B B B B B	B B B B B B B B	B B B B B B B B	B B B B B B B B	B B B B B B B B	B B B B B B B B	B B B B B B B B	-0.23
	8	22	B B B B B B B B	B B B B B B B B	B B B B B B B B	B B B B B B B B	B B B B B B B B	B B B B B B B B	B B B B B B B B	B B B B B B B B	B B B B B B B B	B B B B B B B B	B B B B B B B B	B B B B B B B B	B B B B B B B B	B B B B B B B B	B B B B B B B B	B B B B B B B B	B B B B B B B B	-0.13

1: RIL group are defined by marker score; 2: number of lines in respective group; 3: average *P. thornei* DNA (pg/plant) estimated as BLUPs of the lines from the respective group. Some markers that co-segregated with the asterisked markers (\*) are not shown, due to space limitations. The QTL co-segregating region is denoted by the vertical lines

**Table 3.3** Candidate resistance genes in the *QRInt.sk-2B* QTL interval on chromosome 2B, in the Chinese Spring IWGSC RefSeq v1.0 gene annotations

Gene-ID	Start	End	Root <sup>1</sup>	Annotation
TraesCS2B01G018500.1	8561501	8569381	<b>Y</b>	NBS-LRR disease resistance protein-like protein
TraesCS2B01G018600.1	8592551	8596822	<b>Y</b>	NBS-LRR disease resistance protein-like protein
TraesCS2B01G018700.1	8666351	8668189	<b>Y</b>	NBS-LRR disease resistance protein-like protein
TraesCS2B01G018800.1	8670792	8671418	<b>Y</b>	NBS-LRR-like resistance protein
TraesCS2B01G018900.1	8747772	8748197	Y	Cytochrome P450
TraesCS2B01G019000.1	8749777	8750544	N	Cytochrome P450
TraesCS2B01G019200.1	8941857	8943384	<b>Y</b>	Chalcone synthase
TraesCS2B01G019300.1	8994419	8997178	<b>Y</b>	NBS-LRR disease resistance protein-like protein
TraesCS2B01G019400.1	8997920	8998846	<b>Y</b>	Disease resistance protein (TIR-NBS-LRR class) family
TraesCS2B01G019500.1	9016257	9034173	<b>Y</b>	RING/U-box superfamily protein
TraesCS2B01G019600.1	9104917	9105804	N	Cytochrome P450 family protein, expressed
TraesCS2B01G019800.1	9122805	9127661	<b>Y</b>	NBS-LRR disease resistance protein-like protein
TraesCS2B01G019900.1	9143706	9146396	Y	Serine/threonine-protein kinase
TraesCS2B01G020000.1	9197533	9199065	N	Cytochrome P450 family protein, expressed
TraesCS2B01G020100.1	9281721	9284724	Y	Phenylalanine ammonia-lyase
TraesCS2B01G020200.1	9617719	9622480	Y	Disease resistance protein
TraesCS2B01G020300.1	9724163	9725705	<b>Y</b>	Zinc finger family protein
TraesCS2B01G020600.1	9887738	9891511	<b>Y</b>	Disease resistance protein
TraesCS2B01G020700.1	10071914	10072957	N	PP2A regulatory subunit TAP46
TraesCS2B01G021000.1	10088694	10089647	N	rRNA N-glycosidase
TraesCS2B01G021200.1	10187555	10188157	N	P-loop containing nucleoside triphosphate hydrolases superfamily protein
TraesCS2B01G021400.1	10218063	10219031	Y	Leucine-rich repeat receptor-like protein kinase
TraesCS2B01G021500.1	10355958	10359967	<b>Y</b>	Receptor-like protein kinase
TraesCS2B01G021700.1	10382823	10389006	<b>Y</b>	Disease resistance protein RPM1
TraesCS2B01G021800.1	10575914	10593462	<b>Y</b>	Receptor-like protein kinase
TraesCS2B01G021900.1	10595588	10599145	<b>Y</b>	receptor kinase 1

1: According to the Wheat Expression Browser, presence and absence of gene expression data in root are referred as Y and N, respectively. Genes that are expressed at least 0.5 tpm are shown as ‘bold’

### 3.9 Discussion

Development of resistant cultivars is considered the best option for sustainable and economical control of root lesion nematode in wheat (Mokrini et al. 2019). Although several resistance QTL have been identified, wheat cultivars (commercial) with complete resistance have not yet been developed, perhaps partly owing to a lack of markers that are very closely linked to the resistance loci. Fine mapping of *P. thornei* resistance QTL is therefore needed for the development of molecular markers suitable for effective resistance breeding. With the aid of the recently available wheat genome sequence information, fine mapping of QTL for other traits has allowed identification of candidate genes underlying the QTL (Alaux et al. 2018; Wu et al. 2018; Wu et al. 2019).

In a previous study, QTL for *P. thornei* resistance were mapped on the short arms of chromosome 6D and 2B, to intervals of 12.8 cM and 16.7 cM, respectively (Linsell et al. 2014a). In the current study, the intervals for these loci were significantly reduced, to 3.5 cM and 1.4 cM, respectively, and validated in other genetic backgrounds represented by the RIL populations. The intervals were delimited to 1.77 Mbp and 2.19 Mbp in the Chinese Spring reference genome, respectively.

The wheat 90K SNP array was utilised to fine map the QTL. The SNP array analysis of the DNA bulks made from resistant and susceptible lines identified SNPs that were linked with the QTL. Some of these were used to design KASP marker assays to provide markers suitable for further mapping in the DH and RIL populations.

The order of the markers within chromosomal segments in the present study was largely consistent with those found in published physical maps. On 6DS, markers were in the same

order in the Chinese Spring and *Ae. tauschii* genome sequences. On 2BS, the order of markers was the same in the genetic map and genome of durum wheat, but differed in the Chinese Spring genome by an inverted segment. A chromosomal rearrangement or pericentric inversion might be an explanation for the disagreement (Ma et al. 2014).

The wheat D-genome progenitor *Ae. tauschii* and durum wheat cv. Altar 84 were parents of the synthetic derived wheat cultivar Sokoll (Pastor/3/Altar84/*Aegilops squarrosa* (Taus)//Opata). The other parent Krichauff is bread wheat cultivar with the pedigree: Wariquam//Kloka/Pitic62/3/Warimek/Halberd/4/3Ag3Aroona. Thus, it was not surprising to see co-linearity for 6DS markers between Chinese Spring and *Ae. tauschii*, and for 2BS markers with durum wheat cv. Svevo. Consequently, in addition to the Chinese Spring assembly, the *Ae. tauschii* and durum wheat assemblies (not shown) were excellent resources for identifying genes in the resistance QTL intervals.

Markers that co-segregated with the resistance loci in the DH and RIL populations might be useful for selecting for *P. thornei* resistance in breeding populations. Markers co-segregating with *QRInt.sk-6D* were 6D\_75, 6D\_48, 6D\_20, 6D\_139, 6D\_12 and 6D\_5, while those co-segregating with *QRInt.sk-2B* were 2B\_73, 2B\_42, 2B-10, 2B\_71, 2B\_4 and 2B\_9. Markers further out could be used to rule out the possibility of marker-trait dissociation by recombination. The susceptible parents used in the mapping crosses (Krichauff, Correll, Mace and Scout) were all southern-Australian cultivars, suggesting that these resistance genes and markers should be useful at least in a southern-Australian breeding context.

### 3.9.1 Candidate genes for *P. thornei* resistance

The physical interval for *QRInt.sk-6D*, between the flanking markers 6D\_4 and 6D\_143, was 1.77 Mbp (5.57 Mbp to 7.34 Mbp in Chinese Spring) (Fig. 3.3). The physical interval for *QRInt.sk-2B*, between the flanking markers 2B\_74 and 2B\_12, was 3.14 Mbp (0.04 Mbp to 3.18 Mbp in durum wheat) (Fig. 3.5). Both QTL intervals contained genes with similarity to those previously reported to be involved in disease resistance (Table 3.2 and 3.3). In the following section some of the candidates for *P. thornei* resistance genes are discussed.

#### *Isoflavone reductase (IFR) and Flavonoid 3'-hydroxylases*

Isoflavone reductase (IR) [EC 1.3.1.45] and flavonoid 3'-hydroxylase (F3'H) are involved in isoflavonoid and flavonoid phytoalexin biosynthesis, respectively (Dixon et al. 2002; Naoumkina et al. 2010). IR accumulation in plants increases with greater resistance toward various plant pathogen infections. For instance, overexpression of soybean IR (*GmIFR*) enhanced resistance to *Phytophthora sojae* in transgenic soybean (Cheng et al. 2015). Moreover, a rice blast fungal elicitor induced an IR-like gene in rice (Kim et al. 2003). A few studies also discuss a role of IR in plant parasitic nematode resistance. For instance, the isoflavonoid phytoalexin synthesis pathway is inferred to be under the control of the soybean cyst nematode resistance gene *rhg1* (Afzal et al. 2009). IR is a key enzyme in biosynthesis of the phytoalexin medicarpin. In lucerne (*Medicago sativa*) genotypes with contrasting resistance to the root lesion nematode, *Pratylenchus penetrans*, resistance was positively associated with levels of root medicarpin. An *in vitro* study revealed that medicarpin inhibits motility of *P. penetrans* (Baldrige et al. 1998). Isoflavone reductase was also identified as a crucial enzyme involved in the biosynthesis of the phytoalexin glyceollin (Yu et al. 2003). Glyceollin has been shown to inhibit *Meloidogyne* and *Heterodera* motility in soybean (Boydston et al. 1983; Kaplan et al. 1980). Taken together, IR is an important enzyme in the biosynthesis of the phytoalexins

medicarpin and glyceollin. These phytoalexins were previously reported as inhibitors of nematode motility. Motility of *P. thornei* was found to be inhibited in Sokoll root extracts as compared to Krichauff root extracts (Linsell et al. 2014b). This seems consistent with the possibility that IR contributes to *P. thornei* resistance.

### ***Chalcone synthase***

Chalcone synthase (CHS, EC 2.3.1.74) is a key enzyme of the flavonoid/isoflavonoid biosynthesis pathway which is required for flavonoid and isoflavonoid phytoalexin synthesis. It is also involved in the salicylic acid defence pathway (Dao et al. 2011). Upon nematode (*Meloidogyne javanica*) infection of white clover, abundance of CHS transcripts increased (Hutangura et al. 1999).

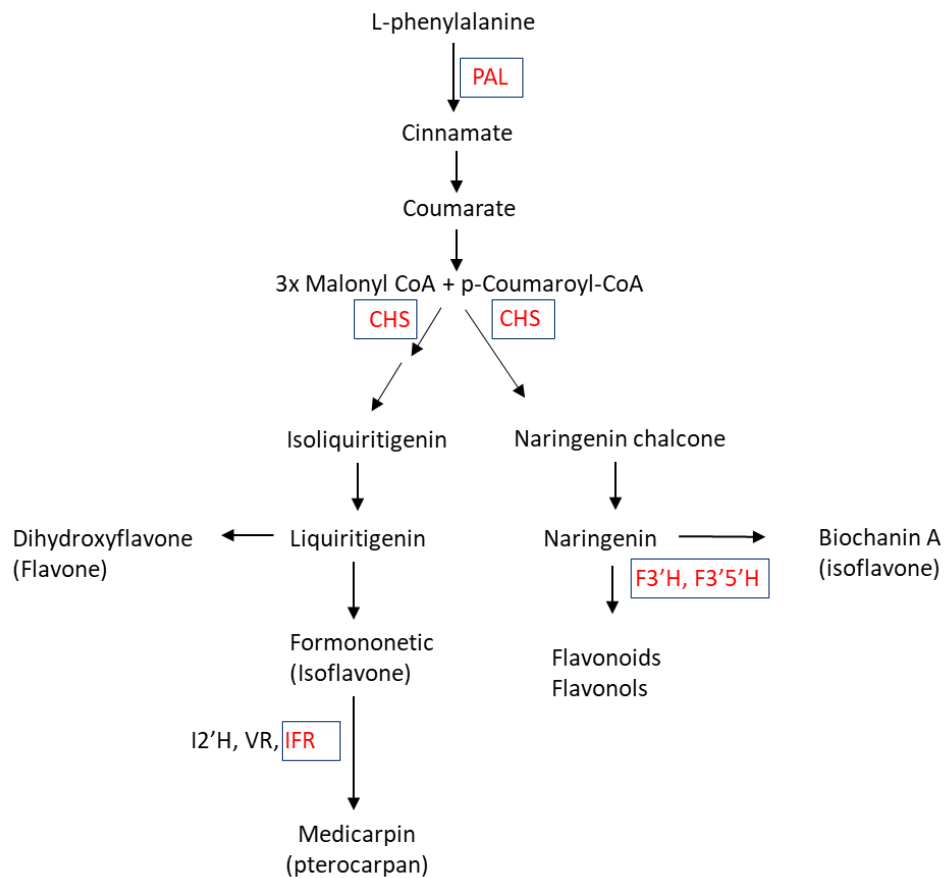
### ***Phenylalanine ammonia-lyases***

Phenylalanine ammonia-lyase (PAL) plays a crucial role in secondary phenylpropanoid metabolism (Kim and Hwang 2014). PAL is involved in the biosynthesis of salicylic acid (SA), an essential signal involved in plant systemic resistance (Nugroho et al. 2002).

The above mentioned IFR, F3'H, CHS and PAL enzymes are involved in biosynthesis of flavonoids and isoflavonoids. A simplified schematic diagram of the flavonoid and isoflavonoid biosynthetic pathways is presented in Fig. 3.7, where these 4 enzymes are highlighted. Phenylpropanoids including flavonoids and isoflavonoids are products derived from the amino acid L-phenylalanine via deamination by L-phenylalanine ammonia lyase (PAL) (Dixon et al. 2002). Their role in plant defence against pathogens is well documented (Reviewed in Dixon 2001; Dixon et al. 2002; Naoumkina et al. 2010). These products may be synthesized constitutively or in a pathogen-induced manner (VanEtten et al. 1994). Their action

can be through creating a toxic environment, or suppressing the development and reproduction of the pathogen, including nematodes. The identified candidate genes related to the phenylpropanoid pathway could contribute to *P. thornei* resistance, given that root exudates and roots of Sokoll and Sokoll-derived *P. thornei* resistant DH lines reduced nematode motility and migration relative to those of susceptible cultivar Krichauff, respectively (Linsell et al. 2014b). Moreover, phenylpropanoids are reported to be involved in a resistance mechanism against the migratory nematode *P. penetrans* (Baldrige et al. 1998) and *R. similis* (Hölscher et al. 2014; Valette et al. 1998; Wuyts et al. 2007; Wuyts et al. 2006). It will be worthwhile to characterise these genes and gene products to understand their role in *P. thornei* resistance in wheat.

**Fig. 3.7** The flavonoid and isoflavonoid biosynthetic pathway (Dixon et al. 2002, Naoumkina et al. 2010). The enzymes are as follows: PAL: L-phenylalanine ammonia-lyase; CHS: Chalcone synthase; IFR: Isoflavone reductase; F3'H: Flavonoid 3'-hydroxylase; I2'H: Isoflavone 2'-hydroxylase; VR: Vestitone reductase. The products of the candidate resistance genes for *QRlnt.sk-6D* and *QRlnt.sk-2B* QTL are boxed





### ***NBS-LRR proteins***

NBS-LRR genes are the most commonly reported type of resistance gene among cloned resistance genes, and relate to a wide range of plant-pathogen systems. Eight NBS-LRR genes against plant nematodes have been cloned so far (Fuller et al. 2008; Davies and Elling 2015).

NBS-LRR proteins are composed of a LRR domain involved in pathogen specificity, linked to an N-terminal NBS domain required for signal transduction (Takken and Govere 2012). NBS-LRR proteins directly or indirectly recognize an isolate-specific avirulence factor and trigger a resistance signalling cascade, which, in the majority of cases, includes localized cell death, termed the hypersensitive response.

All the NBS-LRR nematode resistance proteins cloned so far confer resistance against sedentary plant parasitic nematodes. No resistance gene to a migratory plant parasitic nematode has been cloned so far. Further study is required to find out whether NBS-LRR genes act against the migratory root lesion nematodes.

### ***Receptor-like protein kinases***

Receptor-like kinases (RLKs) are cell surface receptors, mediating cellular signal transduction (Shiu and Bleecker 2001). Leucine-rich repeat RLK proteins (LRR-RLK) constitute the largest group of plant RLKs. They contain three functional domains; an extracellular LRR domain that perceives signals, a transmembrane domain, and an intracellular kinase domain that transduces the signal (Gou et al. 2010). Some LRR-RLKs are involved in plant responses to pathogens, in which case they are classified as pattern recognition receptors (PRRs). For instance, the pathogen associated molecular pattern (PAMP) flagellin from bacteria is recognized by the Arabidopsis receptor kinase, FLAGELLIN SENSING 2 (FLS2), mediating plant resistance

against bacterial pathogens (Gómez-Gómez and Boller 2000). PRRs that can detect nematode PAMPs have not been conclusively identified. However, a candidate is a homologue of the *Arabidopsis* brassinosteroid-associated kinase 1 (BAK 1) in tomato, which, when silenced in tomato, significantly increased susceptibility against root knot nematode (*Meloidogyne* spp.) (Peng and Kaloshian 2014). Conserved molecules in nematodes, such as ascarosides, chitin, and cuticle are potential PAMPs, which may play a role in PRR-mediated defence mechanisms (Holbein et al. 2016).

### ***Ribosome-inactivating proteins***

Ribosome-inactivating proteins (RIPs) are toxic *N*-glycosidases that depurinate eukaryotic and prokaryotic rRNAs inhibiting protein synthesis during translation (de Virgilio et al. 2010). Several studies suggested that plant derived RIPs have bioactive properties, including antibacterial, antifungal and antiviral (Reviewed in Zhu et al. 2018). However, a role of RIPs against nematodes has not yet been investigated.

According to the Wheat Gene Expression database, the majority of the listed candidate genes were found to be expressed in wheat root (Ramírez-González et al. 2018). However, it could be worthwhile to investigate the gene expression profile of the wheat root in response to *P. thornei* challenge.

In summary, two significant QTL for *P. thornei* resistance were fine mapped on wheat chromosome arms 6DS and 2BS, respectively. SNPs tightly linked to the QTL were identified first in a DH population and then validated using other bi-parental populations. The SNPs were used to design KASP assays, which could be used in marker-assisted breeding for *P. thornei* resistance. Several genes in the QTL intervals were identified that represent plausible

candidates for *P. thornei* resistance genes. Products of these genes included phenylpropanoid-biosynthetic-pathway-related enzymes, NBS-LRR proteins and protein kinases. Further study is required to identify which, if any, of the candidates are responsible for the resistance QTL effects.

### **3.10 Acknowledgments**

The authors thank the staff at SARDI Crop Pathology and SARDI Nematology groups for providing the initial seeds of the RIL populations and support in setting up the nematode experiments, respectively. We would also like to thank SARDI Root Disease Testing Service for their help and constructive interaction throughout this project. The 90k marker work was done with the support of DAV00127, a joint project Agriculture Victoria Research (AVR), CSIRO Agriculture and GRDC. Our appreciation is extended to the Grains Research and Development Corporation for their financial assistance and the University of Adelaide for the postgraduate scholarship to SR. NCC was supported by the University of Adelaide, the GRDC and the Government of South Australia.

### **3.11 Conflict of interest**

The authors declare that they have no conflict of interest.

### 3.12 References

- Afzal AJ, Natarajan A, Saini N, Iqbal MJ, Geisler M, El Shemy HA, Mungur R, Willmitzer L, Lightfoot DA (2009) The nematode resistance allele at the *rhg1* locus alters the proteome and primary metabolism of soybean roots. *Plant Physiology* 151:1264-1280
- Alaux M, Rogers J, Letellier T, Flores R, Alfama F, Pommier C, Mohellibi N, Durand S, Kimmel E, Michotey C, Guerche C, Loaec M, Lainé M, Steinbach D, Choulet F, Rimbart H, Leroy P, Guilhot N, Salse J, Feuillet C, International Wheat Genome Sequencing C, Paux E, Eversole K, Adam-Blondon A-F, Quesneville H (2018) Linking the International Wheat Genome Sequencing Consortium bread wheat reference genome sequence to wheat genetic and phenomic data. *Genome Biology* 19:111
- Allen AM, Barker GLA, Berry ST, Coghill JA, Gwilliam R, Kirby S, Robinson P, Brenchley RC, D'Amore R, McKenzie N, Waite D, Hall A, Bevan M, Hall N, Edwards KJ (2011) Transcript-specific, single-nucleotide polymorphism discovery and linkage analysis in hexaploid bread wheat (*Triticum aestivum* L.). *Plant Biotechnology Journal* 9:1086-1099
- Avni R, Nave M, Barad O, Baruch K, Twardziok SO, Gundlach H, Hale I, Mascher M, Spannagl M, Wiebe K, Jordan KW, Golan G, Deek J, Ben-Zvi B, Ben-Zvi G, Himmelbach A, MacLachlan RP, Sharpe AG, Fritz A, Ben-David R, Budak H, Fahima T, Korol A, Faris JD, Hernandez A, Mikel MA, Levy AA, Steffenson B, Maccaferri M, Tuberosa R, Cattivelli L, Faccioli P, Ceriotti A, Kashkush K, Pourkheirandish M, Komatsuda T, Eilam T, Sela H, Sharon A, Ohad N, Chamovitz DA, Mayer KFX, Stein N, Ronen G, Peleg Z, Pozniak CJ, Akhunov ED, Distelfeld A (2017) Wild emmer genome architecture and diversity elucidate wheat evolution and domestication. *Science* 357:93-97
- Baldrige GD, O'Neill NR, Samac DA (1998) Alfalfa (*Medicago sativa* L.) resistance to the root-lesion nematode, *Pratylenchus penetrans*: defense-response gene mRNA and isoflavonoid phytoalexin levels in roots. *Plant Molecular Biology* 38:999-1010
- Boydston R, Paxton JD, Koeppe DE (1983) Glyceollin: A site-specific inhibitor of electron transport in isolated soybean mitochondria. *Plant Physiology* 72:151-155
- Broman KW, Sen S (2009) A guide to QTL mapping with R/qtl. Springer-Verlag, New York
- Butler DG (2013) On the optimal design of experiments under the linear mixed model. PhD Thesis. School of Mathematics and Physics, The University of Queensland, Australia
- Butler DG, Cullis BR, Gilmour AR, Gogel BJ (2009) ASReml-R reference manual version 3. Queensland Department of Primary Industries and Fisheries, Brisbane
- Castillo P, Vovlas N, Jiménez-Díaz RM (1998) Pathogenicity and histopathology of *Pratylenchus thornei* populations on selected chickpea genotypes. *Plant Pathology* 47:370-376
- Cavanagh CR, Chao S, Wang S, Huang BE, Stephen S, Kiani S, Forrest K, Saintenac C, Brown-Guedira GL, Akhunova A, See D, Bai G, Pumphrey M, Tomar L, Wong D, Kong S, Reynolds M, da Silva ML, Bockelman H, Talbert L, Anderson JA, Dreisigacker S, Baenziger S, Carter A, Korzun V, Morrell PL, Dubcovsky J, Morell MK, Sorrells ME, Hayden MJ, Akhunov E

(2013) Genome-wide comparative diversity uncovers multiple targets of selection for improvement in hexaploid wheat landraces and cultivars. *Proceedings of the National Academy of Sciences* 110:8057-8062

Cheng Q, Li N, Dong L, Zhang D, Fan S, Jiang L, Wang X, Xu P, Zhang S (2015) Overexpression of soybean isoflavone reductase (*GmIFR*) enhances resistance to *Phytophthora sojae* in soybean. *Frontiers in Plant Science* 6:1024. <https://doi.org/10.3389/fpls.2015.01024>

Churchill GA, Doerge RW (1994) Empirical threshold values for quantitative trait mapping. *Genetics* 138:963-971

Cook R (1974) Nature and inheritance of nematode resistance in cereals. *Journal of Nematology* 6:165-174

Curtis T, Halford NG (2014) Food security: the challenge of increasing wheat yield and the importance of not compromising food safety. *Annals of Applied Biology* 164:354-372

Dababat AA, Mokriani F, Laasli SE, Yildiz S, Erginbas-Orakci G, Duman N, İmren M (2019) Host suitability of different wheat lines to *Pratylenchus thornei* under naturally infested field conditions in Turkey. *Nematology* 21:557-571

Dao TTH, Linthorst HJM, Verpoorte R (2011) Chalcone synthase and its functions in plant resistance. *Phytochemistry Reviews* 10:397-412

Davies LJ, Elling AA (2015) Resistance genes against plant-parasitic nematodes: a durable control strategy? *Nematology* 17:249-263

Davis EL, Haegeman A, Kikuchi T (2011) Degradation of the plant cell wall by nematodes. In: Jones J, Gheysen G, Fenoll C (eds) *Genomics and molecular genetics of plant-nematode interactions*. Springer Netherlands, Dordrecht, pp 255-272

de Virgilio M, Lombardi A, Caliandro R, Fabbrini MS (2010) Ribosome-inactivating proteins: from plant defense to tumor attack. *Toxins* 2:2699-2737

Dixon RA (2001) Natural products and plant disease resistance. *Nature* 411:843-847

Dixon RA, Achnine L, Kota P, Liu CJ, Reddy MSS, Wang L (2002) The phenylpropanoid pathway and plant defence-a genomics perspective. *Molecular Plant Pathology* 3:371-390

Fosu-Nyarko J, Jones MGK (2016) Advances in understanding the molecular mechanisms of root lesion nematode host interactions. *Annual Review of Phytopathology* 54:253-278

Fuller VL, Lilley CJ, Urwin PE (2008) Nematode resistance. *New Phytologist* 180:27-44

Gómez-Gómez L, Boller T (2000) FLS2: An LRR receptor-like kinase involved in the perception of the bacterial elicitor flagellin in *Arabidopsis*. *Molecular Cell* 5:1003-1011

Gou X, He K, Yang H, Yuan T, Lin H, Clouse SD, Li J (2010) Genome-wide cloning and sequence analysis of leucine-rich repeat receptor-like protein kinase genes in *Arabidopsis thaliana*. BMC Genomics 11:19. <https://doi.org/10.1186/1471-2164-11-19>

Haling RE, Simpson RJ, McKay AC, Hartley D, Lambers H, Ophel-Keller K, Wiebkin S, Herdina, Riley IT, Richardson AE (2011) Direct measurement of roots in soil for single and mixed species using a quantitative DNA-based method. Plant and Soil 348:123-137

Holbein J, Grundler FMW, Siddique S (2016) Plant basal resistance to nematodes: an update. Journal of Experimental Botany 67:2049-2061

Hollaway GJ, Ophel-Keller KM, Taylor SP, Burns RA, McKay AC (2003) Effect of soil water content, sampling method and sample storage on the quantification of root lesion nematodes (*Pratylenchus* spp.) by different methods. Australasian Plant Pathology 32:73-79

Hölscher D, Dhakshinamoorthy S, Alexandrov T, Becker M, Bretschneider T, Buerkert A, Crecelius AC, De Waele D, Elsen A, Heckel DG, Heklau H, Hertweck C, Kai M, Knop K, Krafft C, Maddula RK, Matthäus C, Popp J, Schneider B, Schubert US, Sikora RA, Svatoš A, Swennen RL (2014) Phenalenone-type phytoalexins mediate resistance of banana plants (*Musa* spp.) to the burrowing nematode *Radopholus similis*. Proceedings of the National Academy of Sciences 111:105-110

Hutangura P, Mathesius U, Jones MGK, Rolfe BG (1999) Auxin induction is a trigger for root gall formation caused by root-knot nematodes in white clover and is associated with the activation of the flavonoid pathway. Functional Plant Biology 26:221-231

The International Wheat Genome Sequencing Consortium (IWGSC) (2014) A chromosome-based draft sequence of the hexaploid bread wheat (*Triticum aestivum*) genome. Science 345:1251788. <http://dx.doi.org/10.1126/science.1250092>

Jones MGK, Fosu-Nyarko J (2014) Molecular biology of root lesion nematodes (*Pratylenchus* spp.) and their interaction with host plants. Annals of Applied Biology 164:163-181

Kaplan DT, Keen NT, Thomason IJ (1980) Studies on the mode of action of glyceollin in soybean incompatibility to the root knot nematode, *Meloidogyne incognita*. Physiological Plant Pathology 16:319-325

Kim DS, Hwang BK (2014) An important role of the pepper phenylalanine ammonia-lyase gene (*PAL1*) in salicylic acid-dependent signalling of the defence response to microbial pathogens. Journal of Experimental Botany 65:2295-2306

Kim ST, Cho KS, Kim SG, Kang SY, Kang KY (2003) A Rice isoflavone reductase-like gene, *OsIRL*, is induced by rice blast fungal elicitor. Molecules and Cells 16:224-231

Kosambi DD (1943) The estimation of map distances from recombination values. Annals of Eugenics 12:172-175

Ling H-Q, Ma B, Shi X, Liu H, Dong L, Sun H, Cao Y, Gao Q, Zheng S, Li Y, Yu Y, Du H, Qi M, Li Y, Lu H, Yu H, Cui Y, Wang N, Chen C, Wu H, Zhao Y, Zhang J, Li Y, Zhou W, Zhang B, Hu W, van Eijk MJT, Tang J, Witsenboer HMA, Zhao S, Li Z, Zhang A, Wang D,

Liang C (2018) Genome sequence of the progenitor of wheat A subgenome *Triticum urartu*. *Nature* 557:424-428

Linsell KJ, Rahman MS, Taylor JD, Davey RS, Gogel BJ, Wallwork H, Forrest KL, Hayden MJ, Taylor SP, Oldach KH (2014a) QTL for resistance to root lesion nematode (*Pratylenchus thornei*) from a synthetic hexaploid wheat source. *Theoretical and Applied Genetics* 127:1409-1421

Linsell KJ, Riley IT, Davies KA, Oldach KH (2014b) Characterization of resistance to *Pratylenchus thornei* (Nematoda) in wheat (*Triticum aestivum*): attraction, penetration, motility, and reproduction. *Phytopathology* 104:174-187

Luo M-C, Gu YQ, Puiu D, Wang H, Twardziok SO, Deal KR, Huo N, Zhu T, Wang L, Wang Y, McGuire PE, Liu S, Long H, Ramasamy RK, Rodriguez JC, Van SL, Yuan L, Wang Z, Xia Z, Xiao L, Anderson OD, Ouyang S, Liang Y, Zimin AV, Pertea G, Qi P, Bennetzen JL, Dai X, Dawson MW, Müller H-G, Kugler K, Rivarola-Duarte L, Spannagl M, Mayer KFX, Lu F-H, Bevan MW, Leroy P, Li P, You FM, Sun Q, Liu Z, Lyons E, Wicker T, Salzberg SL, Devos KM, Dvořák J (2017) Genome sequence of the progenitor of the wheat D genome *Aegilops tauschii*. *Nature* 551:498-502

Ma J, Stiller J, Wei Y, Zheng Y-L, Devos KM, Doležal J, Liu C (2014) Extensive pericentric rearrangements in the bread wheat (*Triticum aestivum* L.) genotype “Chinese Spring” revealed from chromosome shotgun sequence data. *Genome Biology and Evolution* 6:3039-3048

Maccaferri M, Harris NS, Twardziok SO, Pasam RK, Gundlach H, Spannagl M, Ormanbekova D, Lux T, Prade VM, Milner SG, Himmelbach A, Mascher M, Bagnaresi P, Faccioli P, Cozzi P, Lauria M, Lazzari B, Stella A, Manconi A, Gnocchi M, Moscatelli M, Avni R, Deek J, Biyiklioglu S, Frascaroli E, Corneti S, Salvi S, Sonnante G, Desiderio F, Marè C, Crosatti C, Mica E, Özkan H, Kilian B, De Vita P, Marone D, Joukhadar R, Mazzucotelli E, Nigro D, Gadaleta A, Chao S, Faris JD, Melo ATO, Pumphrey M, Pecchioni N, Milanese L, Wiebe K, Ens J, MacLachlan RP, Clarke JM, Sharpe AG, Koh CS, Liang KYH, Taylor GJ, Knox R, Budak H, Mastrangelo AM, Xu SS, Stein N, Hale I, Distelfeld A, Hayden MJ, Tuberosa R, Walkowiak S, Mayer KFX, Ceriotti A, Pozniak CJ, Cattivelli L (2019) Durum wheat genome highlights past domestication signatures and future improvement targets. *Nature Genetics* 51: 885-895

Manly KF, Cudmore JRH, Meer JM (2001) Map Manager QTX, cross-platform software for genetic mapping. *Mammalian Genome* 12:930-932

Mokrini F, Viaene N, Waeyenberge L, Dababat AA, Moens M (2019) Root-lesion nematodes in cereal fields: importance, distribution, identification, and management strategies. *Journal of Plant Diseases and Protection* 126:1-11

Naoumkina MA, Zhao Q, Gallego-Giraldo L, Dai X, Zhao PX, Dixon RA (2010) Genome-wide analysis of phenylpropanoid defence pathways. *Molecular Plant Pathology* 11:829-846

Nugroho LH, Verberne MC, Verpoorte R (2002) Activities of enzymes involved in the phenylpropanoid pathway in constitutively salicylic acid-producing tobacco plants. *Plant Physiology and Biochemistry* 40:755-760

Ogbonnaya FC, Imtiaz M, Bariana HS, McLean M, Shankar MM, Hollaway GJ, Trethowan RM, Lagudah ES, van Ginkel M (2008) Mining synthetic hexaploids for multiple disease resistance to improve bread wheat. *Australian Journal of Agricultural Research* 59:421-431

Ophel-Keller K, McKay A, Hartley D, Herdina, Curran J (2008) Development of a routine DNA-based testing service for soilborne diseases in Australia. *Australasian Plant Pathology* 37:243-253

Owen KJ, Clewett TG, Bell KL, Thompson JP (2014) Wheat biomass and yield increased when populations of the root-lesion nematode (*Pratylenchus thornei*) were reduced through sequential rotation of partially resistant winter and summer crops. *Crop and Pasture Science* 65:227-241

Peng H-C, Kaloshian I (2014) The tomato leucine-rich repeat receptor-like kinases *SISERK3A* and *SISERK3B* have overlapping functions in bacterial and nematode innate immunity. *PLoS ONE* 9:e93302. <http://doi.org/10.1371/journal.pone.0093302>

R Core Team (2018) R: A language and environment for statistical computing. R Foundation for Statistical Computing, Vienna, Austria. Retrieved from <https://www.R-project.org/>

Ramírez-González RH, Borrill P, Lang D, Harrington SA, Brinton J, Venturini L, Davey M, Jacobs J, van Ex F, Pasha A, Khedikar Y, Robinson SJ, Cory AT, Florio T, Concia L, Juery C, Schoonbeek H, Steuernagel B, Xiang D, Ridout CJ, Chalhoub B, Mayer KFX, Benhamed M, Latrasse D, Bendahmane A, Wulff BBH, Appels R, Tiwari V, Datla R, Choulet F, Pozniak CJ, Provart NJ, Sharpe AG, Paux E, Spannagl M, Bräutigam A, Uauy C (2018) The transcriptional landscape of polyploid wheat. *Science* 361:662

Riley IT, Wiebkin S, Hartley D, McKay AC (2010) Quantification of roots and seeds in soil with real-time PCR. *Plant and Soil* 331:151-163

Rimbert H, Darrier B, Navarro J, Kitt J, Choulet F, Leveugle M, Duarte J, Rivière N, Eversole K, on behalf of The International Wheat Genome Sequencing Consortium, Le Gouis J, on behalf The Breed Wheat Consortium, Davassi A, Balfourier F, Le Paslier M-C, Berard A, Brunel D, Feuillet C, Poncet C, Sourdille P, Paux E (2018) High throughput SNP discovery and genotyping in hexaploid wheat. *PLoS ONE* 13:e0186329. <https://doi.org/10.1371/journal.pone.0186329>

Robinson NA, Sheedy JG, MacDonald BJ, Owen KJ, Thompson JP (2019) Tolerance of wheat cultivars to root-lesion nematode (*Pratylenchus thornei*) assessed by normalised difference vegetation index is predictive of grain yield. *Annals of Applied Biology* 174:388-401

Rohde RA (1972) Expression of resistance in plants to nematodes. *Annual Review of Phytopathology* 10:233-252

Saghai-Maroo MA, Soliman KM, Jorgensen RA, Allard RW (1984) Ribosomal DNA spacer-length polymorphisms in barley: mendelian inheritance, chromosomal location, and population dynamics. *Proceedings of the National Academy of Sciences* 81:8014-8018



Sheedy JG, Thompson JP, Kelly A (2012) Diploid and tetraploid progenitors of wheat are valuable sources of resistance to the root lesion nematode *Pratylenchus thornei*. *Euphytica* 186:377-391

Sheedy JG, Thompson JP (2009) Resistance to the root-lesion nematode *Pratylenchus thornei* of Iranian landrace wheat. *Australasian Plant Pathology* 38:478-489

Shiferaw B, Smale M, Braun H-J, Duveiller E, Reynolds M, Muricho G (2013) Crops that feed the world 10. Past successes and future challenges to the role played by wheat in global food security. *Food Security* 5:291-317

Shiu S-H, Bleecker AB (2001) Receptor-like kinases from *Arabidopsis* form a monophyletic gene family related to animal receptor kinases. *Proceedings of the National Academy of Sciences* 98:10763-10768

Smiley RW, Gourlie JA, Yan G, Rhinhart KEL (2014) Resistance and tolerance of landrace wheat in fields infested with *Pratylenchus neglectus* and *P. thornei*. *Plant Disease* 98:797-805

Smiley RW, Nicol JM (2009) Nematodes which challenge global wheat production. In: Carver BF(ed) *Wheat Science and Trade*. Wiley-Blackwell, Ames, IA pp 171-187

Takken FLW, Goverse A (2012) How to build a pathogen detector: structural basis of NB-LRR function. *Current Opinion in Plant Biology* 15:375-384

Taylor J, Butler D (2017) R Package ASMap: Efficient genetic linkage map construction and diagnosis. *Journal of Statistical Software* 79:1-29

Taylor SP, Evans ML (1998) Vertical and horizontal distribution of and soil sampling for root lesion nematodes (*Pratylenchus neglectus* and *P. thornei*) in South Australia. *Australasian Plant Pathology* 27:90-96

Team RC (2018) R: A language and environment for statistical computing. R Foundation for Statistical Computing, Vienna, Austria

Thompson JP, Brennan PS, Clewett TG, Sheedy JG, Seymour NP (1999) Progress in breeding wheat for tolerance and resistance to root-lesion nematode (*Pratylenchus thornei*). *Australasian Plant Pathology* 28:45-52

Thompson JP, Owen KJ, Stirling GR, Bell MJ (2008) Root-lesion nematodes (*Pratylenchus thornei* and *P. neglectus*): a review of recent progress in managing a significant pest of grain crops in northern Australia. *Australasian Plant Pathology* 37:235-242

Valette C, Andary C, Geiger JP, Sarah JL, Nicole M (1998) Histochemical and Cytochemical Investigations of Phenols in Roots of Banana Infected by the Burrowing Nematode *Radopholus similis*. *Phytopathology* 88:1141-1148

Van Os H, Stam P, Visser RGF, Van Eck HJ (2005) RECORD: a novel method for ordering loci on a genetic linkage map. *Theoretical and Applied Genetics* 112:30-40

VanEtten HD, Mansfield JW, Bailey JA, Farmer EE (1994) Two classes of plant antibiotics: Phytoalexins versus "Phytoanticipins". *The Plant Cell* 6:1191-1192

Vanstone VA, Hollaway GJ, Stirling GR (2008) Managing nematode pests in the southern and western regions of the Australian cereal industry: continuing progress in a challenging environment. *Australasian Plant Pathology* 37:220-234

Vanstone VA, Rathjen AJ, Ware AH, Wheeler RD (1998) Relationship between root lesion nematodes (*Pratylenchus neglectus* and *P. thornei*) and performance of wheat varieties. *Australian Journal of Experimental Agriculture* 38:181-188

Voorrips RE (2002) MapChart: software for the graphical presentation of linkage maps and QTLs. *Journal of Heredity* 93:77-78

Wang S, Wong D, Forrest K, Allen A, Chao S, Huang BE, Maccaferri M, Salvi S, Milner SG, Cattivelli L, Mastrangelo AM, Whan A, Stephen S, Barker G, Wieseke R, Plieske J, Lillemo M, Mather D, Appels R, Dolferus R, Brown-Guedira G, Korol A, Akhunova AR, Feuillet C, Salse J, Morgante M, Pozniak C, Luo MC, Dvorak J, Morell M, Dubcovsky J, Ganai M, Tuberosa R, Lawley C, Mikoulitch I, Cavanagh C, Edwards KJ, Hayden M, Akhunov E (2014) Characterization of polyploid wheat genomic diversity using a high-density 90 000 single nucleotide polymorphism array. *Plant Biotechnology Journal* 12:787-796

Wu J, Liu S, Wang Q, Zeng Q, Mu J, Huang S, Yu S, Han D, Kang Z (2018) Rapid identification of an adult plant stripe rust resistance gene in hexaploid wheat by high-throughput SNP array genotyping of pooled extremes. *Theoretical and Applied Genetics* 131:43-58

Wu P, Hu J, Zou J, Qiu D, Qu Y, Li Y, Li T, Zhang H, Yang L, Liu H, Zhou Y, Zhang Z, Li J, Liu Z, Li H (2019) Fine mapping of the wheat powdery mildew resistance gene *Pm52* using comparative genomics analysis and the Chinese Spring reference genomic sequence. *Theoretical and Applied Genetics* 132:1451-1461

Wu Y, Bhat P, Close TJ, Lonardi S (2008) Efficient and accurate construction of genetic linkage maps from the minimum spanning tree of a graph. *PLoS Genetics* 4:e1000212. <https://doi.org/10.1371/journal.pgen.1000212>

Wuyts N, Lognay G, Verscheure M, Marlier M, De Waele D, Swennen R (2007) Potential physical and chemical barriers to infection by the burrowing nematode *Radopholus similis* in roots of susceptible and resistant banana (*Musa* spp.). *Plant Pathology* 56:878-890

Wuyts N, Swennen R, De Waele D (2006) Effects of plant phenylpropanoid pathway products and selected terpenoids and alkaloids on the behaviour of the plant-parasitic nematodes *Radopholus similis*, *Pratylenchus penetrans* and *Meloidogyne incognita*. *Nematology* 8:89-101

Yu O, Shi J, Hession AO, Maxwell CA, McGonigle B, Odell JT (2003) Metabolic engineering to increase isoflavone biosynthesis in soybean seed. *Phytochemistry* 63:753-763

Zhu F, Zhou Y-K, Ji Z-L, Chen X-R (2018) The plant ribosome-inactivating proteins play important roles in defense against pathogens and insect pest attacks. *Frontiers in Plant Science* 9:146. <https://doi.org/10.3389/fpls.2018.00146>

## **Chapter 4**

**Detection and quantification of *Pratylenchus thornei* in wheat root  
using quantitative real-time PCR**

## **Chapter 4**

### **Detection and quantification of *Pratylenchus thornei* in wheat root using quantitative real-time PCR**

#### **4.1 Statement of authorship**

## **Statement of Authorship**

Title of the paper	Detection and quantification of <i>Pratylenchus thornei</i> in wheat root using quantitative real-time PCR
Publication Status	Unpublished and unsubmitted work written in manuscript style
Publication details	This chapter will be prepared as a manuscript for submission to a refereed journal

### **Principal Author**

Name of Principal Author (Candidate)	Muhammad Shefatur Rahman		
Contribution to the paper	Involved in designing the research project conception and development of overall research plan. Conducted hands-on experiments, data collection and analysis. Wrote the first draft of the manuscript and took primary responsibility for manuscript revision.		
Overall percentage (%)	70		
Certification	This paper reports on original research I conducted during the period of my Higher Degree by Research candidature and is not subject to any obligations or contractual agreements with a third party that would constrain its inclusion in this thesis. I am the primary author of this paper.		
Signature		Date	4.12.2019

### **Co-Author Contributions**

By signing the Statement of Authorship, each author certifies that:

- I. the candidate's stated contribution to the publication is accurate (as detailed above);
- II. permission is granted for the candidate to include the publication in the thesis; and
- III. the sum of all co-author contributions is equal to 100% less the candidate's stated contribution.

Name of Co- Author	Katherine J. Linsell		
Contribution to the paper	Provided suggestions for the research experiment, helped in conducting the experiment, provided input for the manuscript.		
Signature		Date	5/12/19

Name of Co- Author	Danuta Pounsett		
Contribution to the paper	Helped in conducting the nematode assay		
Signature		Date	11/12/2019

Name of Co- Author	Nicholas C. Collins		
Contribution to the paper	Helped in data analysis and writing the manuscript. Read the manuscript and suggested revisions.		
Signature		Signature	9/12/19

Name of Co- Author	Klaus H. Oldach		
Contribution to the paper	Provided overall supervision of the research project and helped writing the manuscript.		
Signature		Date	4.12.2019

## 4.2 Introduction

*Pratylenchus thornei* is an important plant parasitic nematode species affecting bread wheat throughout the world, particularly in dryland agricultural areas of Australia and the Pacific Northwest of the United States of America (USA) (Nicol and Ortiz-Monasterio 2004; Smiley et al. 2005; Thompson et al. 2010). They penetrate the roots of a host plant and migrate through the root tissues, causing considerable damage to crop plants. Due to the damage in the root tissue, plants cannot uptake water and nutrients properly from the soil, impairing growth and development, and resulting in significant yield loss (Smiley and Nicol 2009; Thompson et al. 2015).

Many of the commercially available wheat cultivars are either susceptible or only moderately tolerant to *P. thornei*. A completely resistant commercial wheat cultivar has not been developed yet. Genetic improvement through exploiting natural genetic variation could be the most sustainable way to improve *P. thornei* resistance in wheat cultivars. Research so far has identified sources of resistance in middle-eastern landraces (Sheedy and Thompson 2009), wheat progenitor species (Thompson and Haak 1997), and in synthetic wheat cultivars (Thompson 2008).

A susceptible wheat cultivar allows *P. thornei* multiplication in the roots and the nematode population to remain stable or grow in the soil. On the other hand, a resistant cultivar restricts nematode multiplication in the roots; consequently, a lower number of *P. thornei* nematodes will exist in the soil. Resistance to *P. thornei* can be evaluated by estimating the nematode multiplication rate in the roots and/or soil. Estimating the number of nematodes by counting them under the compound microscope is a very time-consuming process and requires specialized skill and knowledge. In comparison to the microscopic method, a real-time

polymerase chain reaction-based quantification method (qPCR) offers a much quicker method to objectively measure nematode populations in plants and soil.

In recent years, several articles have reported on the use of qPCR for the quantitative detection of plant pathogenic nematodes, including migratory (Berry et al. 2008; Mokrini et al. 2014; Yan et al. 2011; Yan et al. 2013) and sedentary (Lopez-Nicora et al. 2012; Madani et al. 2005; Toumi et al. 2015) nematodes. At SARDI (South Australia Research and Development Institute), *P. thornei* quantification is offered as fee-for-service using crop and soil samples. Details on the protocol are proprietary information and thus not available to other researchers. A real-time qPCR protocol has been reported by Yan et al. (2011) to quantify *P. thornei* in soil samples. The assay was based on quantification of *P. thornei* using species-specific primers and DNA extracted from soil. They used a commercial DNA extraction kit (PowerSoil® DNA Isolation Kit, MoBio, Carlsbad, CA) to extract *P. thornei* DNA from soil. Again, the composition of the commercial DNA extraction kit is proprietary. A freely available DNA extraction protocol based on common laboratory chemicals would be desirable to keep the expenses low and thus make the quantification method available to a breeding program where large numbers of samples need to be processed. However, extraction of *P. thornei* DNA from soil using common laboratory chemicals can be challenging due to the presence of phenolic, humic and other PCR-inhibitory substances in soil. Alternatively, plant pathogenic nematodes can also be quantified from pure root extract (Lopez-Nicora et al. 2012). The objective of this study was to develop a working protocol that enables a reliable and cost-effective protocol to extract and quantify nematode DNA from wheat root tissue.

## 4.3 Materials and methods

### 4.3.1 Nematode DNA extraction from pure culture

*P. thornei* was obtained from wheat at Nunjirkompita, South Australia and cultures were maintained on carrot callus, as described by Moody et al. (1973). Cultures were kept at 22°C and subcultured every 3 months. *P. thornei* was extracted from carrot callus by placing them in a funnel set in a mister chamber with an intermittent aqueous mist for 10 s every 10 min for a total of 96 h. The collected nematodes were counted under a compound microscope in 250 µL aliquots in three replicates and diluted with water to the required concentration (Linsell et al. 2014a). *P. thornei* genomic DNA was extracted following the protocol of Yan et al. (2008), with the following modifications. The lysis buffer used to extract genomic DNA consisted of 500 mM KCl, 100 mM Tris-Cl (pH 8.3), 15 mM MgCl<sub>2</sub>, 10 mM dithiothreitol (DTT), 4.5% Tween 20 and 0.1% gelatin. At first, mixed-stage nematodes were put into 100 µL sterilized nanopure water in a 2 mL centrifuge tube. Then, 205 µL lysis buffer and 4 µL proteinase K (20 mg/ml) were added to the nematode solution. The solution was incubated at 65°C for 1 hour in a water bath, followed by incubation at 95°C for 10 min in a thermal block. The nematode extraction mix was centrifuged at 15,000 rpm (21,200 x g) for 10 min. The supernatant (150 µL) was transferred into a new tube and stored at -20°C for subsequent use as DNA template.

### 4.3.2 Nematode DNA extraction from plant root

To generate a standard curve and quantify nematodes from unknown samples, total DNA from nematode infected wheat root was extracted from wheat root powder following a modified cetyl trimethylammonium bromide (CTAB) DNA extraction protocol (Rahman et al. 2010). The root tissue was obtained from 8-week-old wheat seedlings. This time point was taken because *P. thornei* can complete its life cycle in 3-8 weeks (Agrios 1988, Linsell et al. 2014b).



Roots were gently removed from soil, washed under running tap water and stored at -80°C. Root tissue was freeze-dried, ground to a fine powder using a mortar and pestle, and 30 mg of root powder was used for DNA extraction. For each sample, three replications of DNA extraction were performed. The DNA extraction protocol is as follows:

1. 30 mg Amberlite XAD-4 (Sigma Chemical Co.) was added to 30 mg of root powder in a 2 mL centrifuge tube.
2. A lysis buffer (1000 µL) containing 4% (w/v) CTAB, 100 mM Tris-HCl (pH 8.0), 1.4 M NaCl, 50 mM NaEDTA (pH 8.0) and 1% (w/v) dithioerythritol (DTE) was added to the root powder (Rahman et al. 2010). Then, 4 µL proteinase K (20 mg/mL) was added to each tube. The solution was mixed thoroughly using a vortex machine for 1 min.
3. The samples were incubated at 65°C for 1 h in a water bath followed by incubation at 95°C for 10 min in a thermal incubator.
4. The solution was centrifuged at 15,000 rpm (21,200 x g) at room temperature for 10 min. The supernatant (850 µL) was transferred into a new 2 mL centrifuge tube. An equal volume of phenol:chloroform:isoamylalcohol [25:24:1] was added, thoroughly mixed by vortexing, and centrifuged at 21,200 x g for 10 min. The upper aqueous phase (700 µL) was transferred into a new 2 mL centrifuge tube. An equal volume of chloroform:isoamylalcohol [24:1] was added and mixed before centrifugation for 10 min at 21,200 x g. The upper aqueous phase (600 µL) was transferred into a new 1.5 mL centrifuge tube.
5. An equal volume of ice-cold isopropanol was added and mixed prior to incubation at -80°C for 1 h. The sample was thawed without agitation prior to centrifugation at 21,200 x g for 10 min.

6. The supernatant was discarded while the pellet was washed twice with 1 mL of 70% (v/v) ethanol. After each washing step, the sample was centrifuged at 21,200 x *g* at room temperature for 3 min.
7. Finally, the pellet was air-dried and dissolved in 100 µL R40 (40 ug/mL RNase A in 1X TE). The DNA concentration and absorbance ratio ( $A_{260/280}$  and  $A_{260/230}$ ) were determined using a NanoDrop® ND-1000 spectrophotometer (Nanodrop Products, Wilmington, DE, USA). DNA was stored at -20°C prior to qPCR.

#### **4.3.3 Real-time PCR**

The primer pair, THOITS- F2 (5'-GTGTGTCGCTGAGCAGTTGTTGCC-3') and THO-ITS-R2 (5'-GTTGCTGGCGTCCCCAGTCAATG-3') were used in this study. Primer development, selection and specificity were described by Yan et al. (2011). All real-time PCR assays were performed on a CFX384 Touch™ Real-Time PCR detection system (Bio-Rad Laboratories, USA) using the SsoAdvance™ SBVRR Green Supermix (Bio-Rad Laboratories, USA) following the protocol described by Yan et al. (2013) with minor modifications. Each reaction mix consisted of 1 µL DNA extract, 5 µL of SsoAdvance™ SBVRR Green Supermix, 250 nM of each primer and 40 µg BSA in a total volume of 10 µL. The amplification program consisted of an initial denaturation cycle for 10 min at 95°C, followed by 40 cycles of 5 s at 95°C, 10 s at 70°C, and 10 s at 72°C, with fluorescence data collected after each annealing step. Melting curve profiles were generated by increasing the temperature from 65°C to 95°C in increments of 0.1 °C per 0.2 s. DNA from pure culture of *P. thornei* and sterile nanopure water were used as positive and negative controls, respectively. All samples in this study were amplified in triplicate. The resulting data were analyzed with the program Bio-Rad CFX manager (Version 3.1) using the arithmetic baseline adjustment and second derivative maximum analysis to generate amplification curves, standard curves, and melting curves.

#### 4.3.4 Generation of standard curves

To examine the potential presence of PCR inhibitors in the roots that were used for generation of the standard curve, nematode DNA was extracted from five thousand *P. thornei*. DNA was serially diluted with wheat root DNA or with water. Amplification efficiencies (E) were calculated from the slope of a plot of cycle threshold (Ct) (y-axis) and log picograms (log pg) of DNA (x-axis) using the equation  $E = 10^{(1/-m)} - 1$ , where m is the slope. Inhibitor activity was assessed by comparing E from DNA in root extracts to E from DNA in water.

To generate a standard curve, DNA was extracted following above mentioned protocol from root powder mixed with various known amounts of pure nematode. For this, *P. thornei* (25, 50, 100, 500, 1000, 2500, 5000, 7500, 10000) were added separately to 30 mg of root powder prior to DNA extraction. Standard curves were generated by plotting logarithmic values of number of nematodes per 30 mg root powder versus the corresponding cycle threshold (Ct) values.

#### 4.3.5 Quantification of *P. thornei* in root samples

*P. thornei* was quantified from Sokoll (*P. thornei* resistant), Krichauff (*P. thornei* susceptible) and fourteen recombinant inbred wheat lines. The levels of *P. thornei* resistance (genetic and phenotypic) were evaluated in the previous experiment where *P. thornei* was quantified using PreDicta B test in a commercial laboratory (SARDI) (described in Chapter 3). Genetic resistance and susceptibility of these wheat lines towards *P. thornei* were determined as presence and absence of resistance alleles in 2B and/or 6D loci (described in Chapter 3). The wheat lines were grown under controlled growth conditions (12-hour light at 22°C and 12-hour dark at 18°C) in 2014. Each individual plant of each line was grown in a plastic tube containing 150 g of sterilized silt-loam soil (Linsell et al. 2014b). Each pot with a single plant at the one-leaf stage was inoculated with 1500 *P. thornei* nematodes derived from a culture maintained

on carrot. After 8 weeks of incubation, plant tops were removed, and roots were collected. DNA was extracted from 30 mg of powdered root samples and nematode DNA quantified using real-time PCR and the root standard curve. For each sample, three replications of DNA extraction were performed.

## 4.4 Results

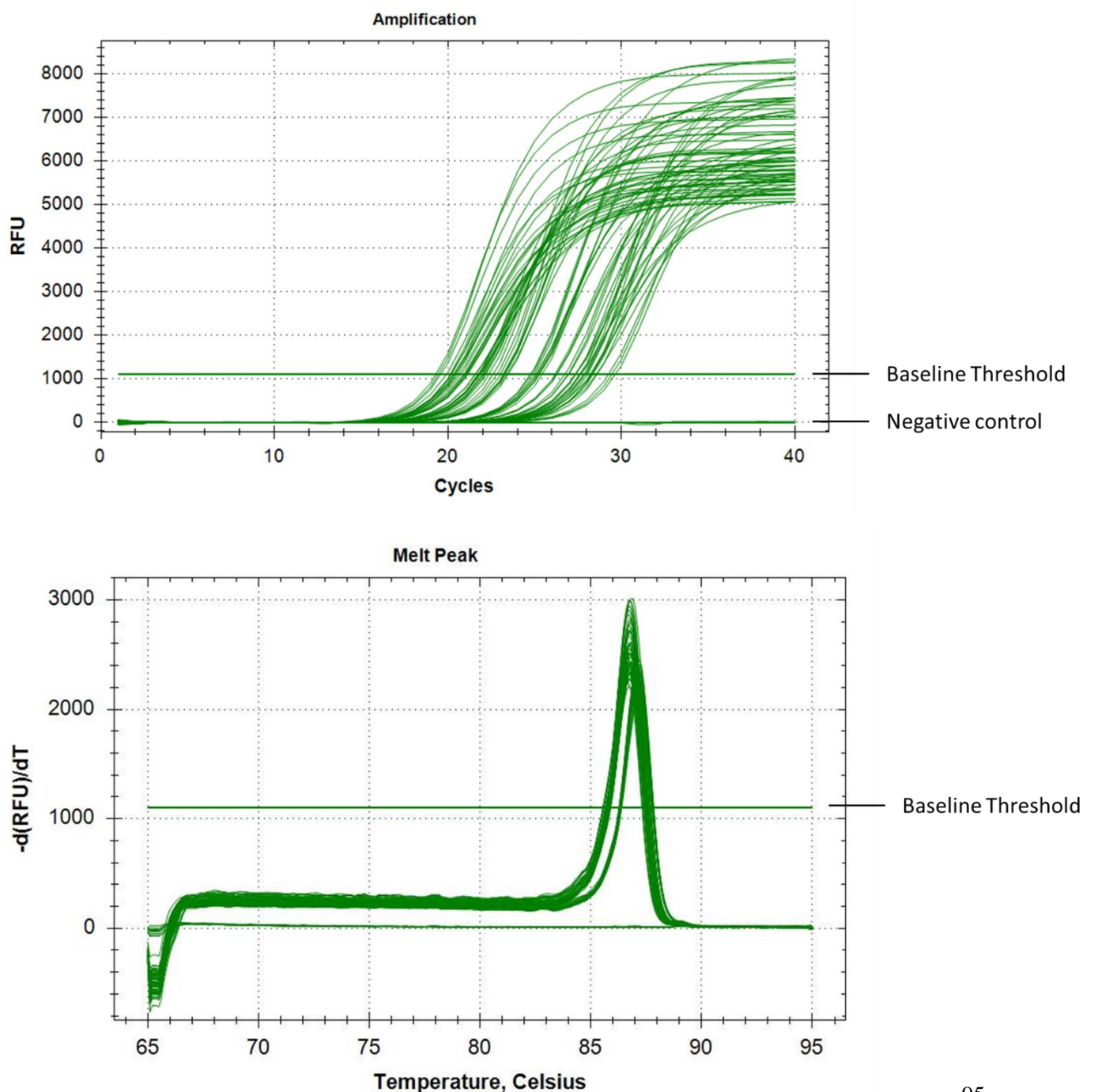
### 4.4.1 *P. thornei* DNA extraction from pure culture and wheat root

In the present experiment, *P. thornei* DNA was extracted from pure *P. thornei* culture and inoculated wheat root samples. The concentrations of DNA from pure culture and wheat root samples ranged from 145 ng/μL to 204 ng/μL and 653 ng/μL to 3595 ng/μL, respectively. The average  $A_{260}/A_{280}$  and  $A_{260}/A_{230}$  ratio was 1.84 and 2.01, respectively demonstrating a good degree of purity (Desjardins and Conklin 2010).

### 4.4.2 Real-time qPCR assay

The primer pair, THO-ITS-F2 and THO-ITS-R2 (Yan et al. 2011) amplified, a product from DNA of pure *P. thornei* culture and also from infected wheat root extracts. A single PCR product was generated with a size consistent with the expected one of 131 bp (Yan et al. 2011). The melting curve analysis revealed a single peak at 86.7°C (Fig. 4.1). Non-specific fluorescence due to primer-dimers or non-specific amplification products were not observed confirming absence of false positive results (Fig. 4.1). No amplification signals were observed in the negative control samples.

**Fig. 4.1** (A) Amplification curves of each quantitative real-time PCR reaction used in the development of the standard curve. Y-axis is the relative fluorescence unit (RFU), which rises in each cycle (x-axis). The baseline threshold is 1107 RFU which is auto calculated by the BioRad CFX manager software. Control reaction without *Pratylenchus thornei* DNA template did not produced any amplification. (B) Melting curve profiles of amplicons amplified by a *P. thornei*-specific primer pair, with melting temperature at 86.7°C. Y-axis is the changes in florescence level ( $-d(RFU)/dT$ ) with respect to per unit change (increase) in temperature (x-axis)



#### 4.4.3 Linear regression analysis from DNA of pure *P. thornei* culture and identification of PCR inhibitors

*Pratylenchus thornei* DNA extracted from pure culture was serially diluted (100 ng/μL to 100 pg/μL) with either nanopure water or DNA (100 ng/μL) extracted from uninoculated wheat root (Table 4.1). qPCR on these two sets of samples were compared to test for any inhibition of the qPCR by the root DNA. Plots from the respective qPCR data sets (Fig. 4.2) had log<sub>10</sub> values of *P. thornei* DNA concentrations (pg) in the x-axis and Ct values in the y-axis. The linear regressions generated from *P. thornei* DNA diluted with water and root DNA were  $y = -2.81x + 31.61$  ( $R^2 = 0.97$ ) and  $y = -3.28x + 33.32$  ( $R^2 = 0.99$ ), respectively (Table 4.1, Fig 4.2-A). The qPCR efficiency (E) for *P. thornei* DNA in water and root extracts was 126.7% and 102%, respectively (Table 4.1). Higher amplification efficiency (compared to the acceptable limit of 110%) from *P. thornei* DNA in water (126.7%) may result from higher DNA concentration in water. The efficiency can be improved by diluting the DNA concentration (Rogers-Broadway and Karteris 2015). There was a high correlation ( $y = 1.15x - 3.16$ ,  $R^2 = 0.99$ ) between the Ct values obtained in these two-dilution series, for the same corresponding amount of input nematode DNA (Fig. 4.2-B), indicating that there was little or no interference in the qPCR assay caused by the wheat genomic DNA.

**Table 4.1** Cycle threshold (Ct) values of quantitative real-time PCR reactions with a *Pratylenchus thornei* specific primer pair, using as template *Pratylenchus thornei* DNA serially diluted in either water or uninoculated root DNA extract

Dilution	Nematode concentration (pg/ $\mu$ L) <sup>1</sup>	DNA Ct values <sup>2</sup> using nematode DNA from pure culture in water	Ct values <sup>2</sup> using nematode DNA from pure culture diluted with root DNA <sup>3</sup>
1:0	100,000	18.34	17.21
1:1	50,000	18.43	18.13
1:4	20,000	18.95	19.16
1:9	10,000	20.28	19.84
1:49	2,000	21.59	21.89
1:99	1,000	22.99	23.62
1:499	200	25.26	25.56
1:999	100	26.55	27.29
E (Amplification efficiency)		126.7 %	102%
R <sup>2</sup>		0.97	0.99
		y= -2.81x + 31.61	y= -3.28x + 33.32

<sup>1</sup>Concentration of *P. thornei* DNA in the solution

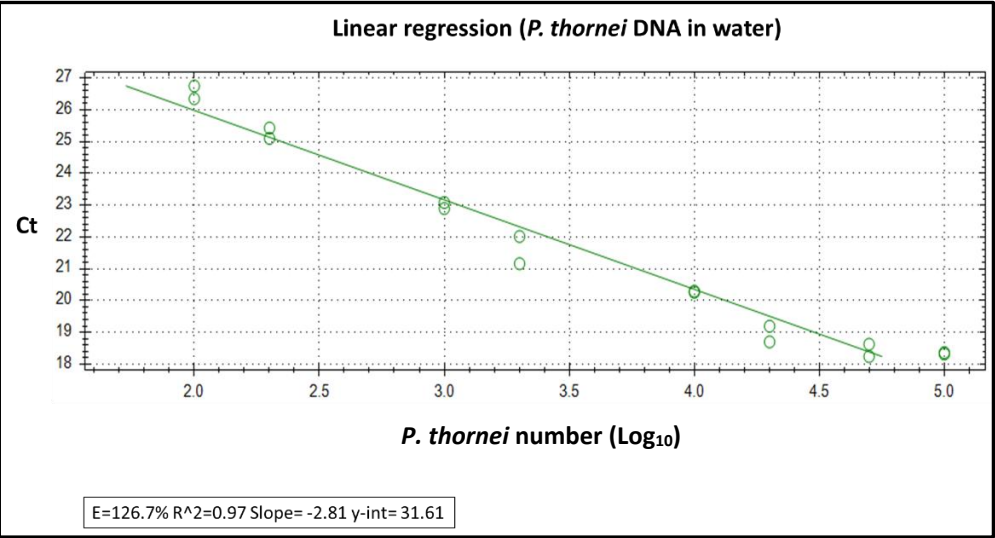
<sup>2</sup>Mean and standard deviation of Ct obtained from qPCR detection of DNA extraction from two replicated samples

<sup>3</sup>Root DNA = DNA extracted from uninoculated roots of a hexaploid wheat cultivar, Krichauff.

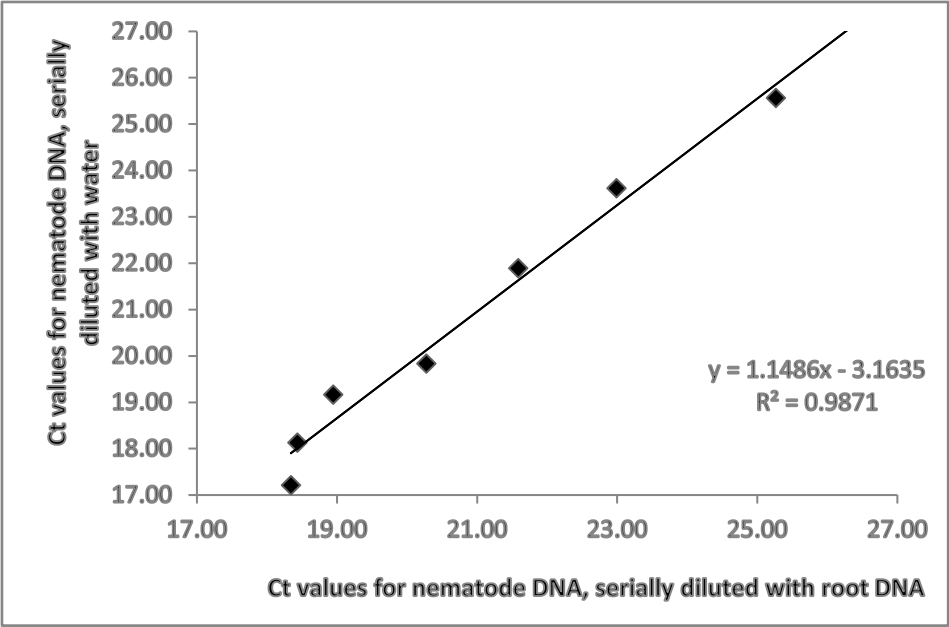
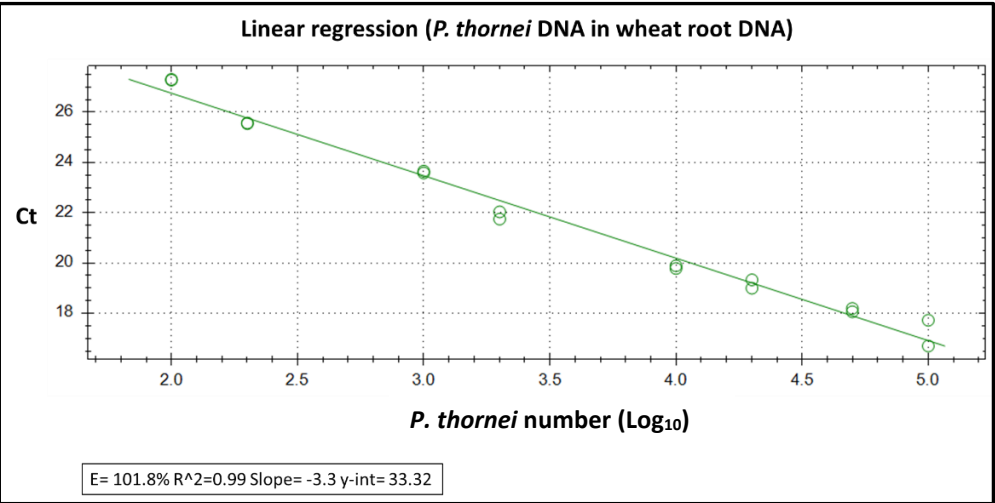


**Fig. 4.2** (A) Linear regressions created from qPCR assays of *Pratylenchus thornei* DNA diluted with nano pure water or (B) uninoculated wheat root DNA. (C) Plot showing correlation between the regression curves in terms of Ct values of these qPCR assays

A



B



#### **4.4.4 Generation of a Standard Regression using DNA extracted from mixtures of *P. thornei* and root powder**

A standard regression was generated using DNA extracted from a mixture of 30 mg uninoculated root powder to which various numbers of *P. thornei* were added, ranging from 25 to 10,000 nematodes (Fig. 4.3). All of the samples were replicated (biological) three times and each biological sample was replicated (technical) three times. The linear regression was described by the equation,  $y = -3.16x + 32.02$  ( $R^2 = 0.99$ ). The amplification efficiency (E) was 118.7% and average Ct values ranged from 19.23 to 27.76 (Table 4.2). No amplification was observed with control roots that were not inoculated with *P. thornei* (Fig. 4.1)

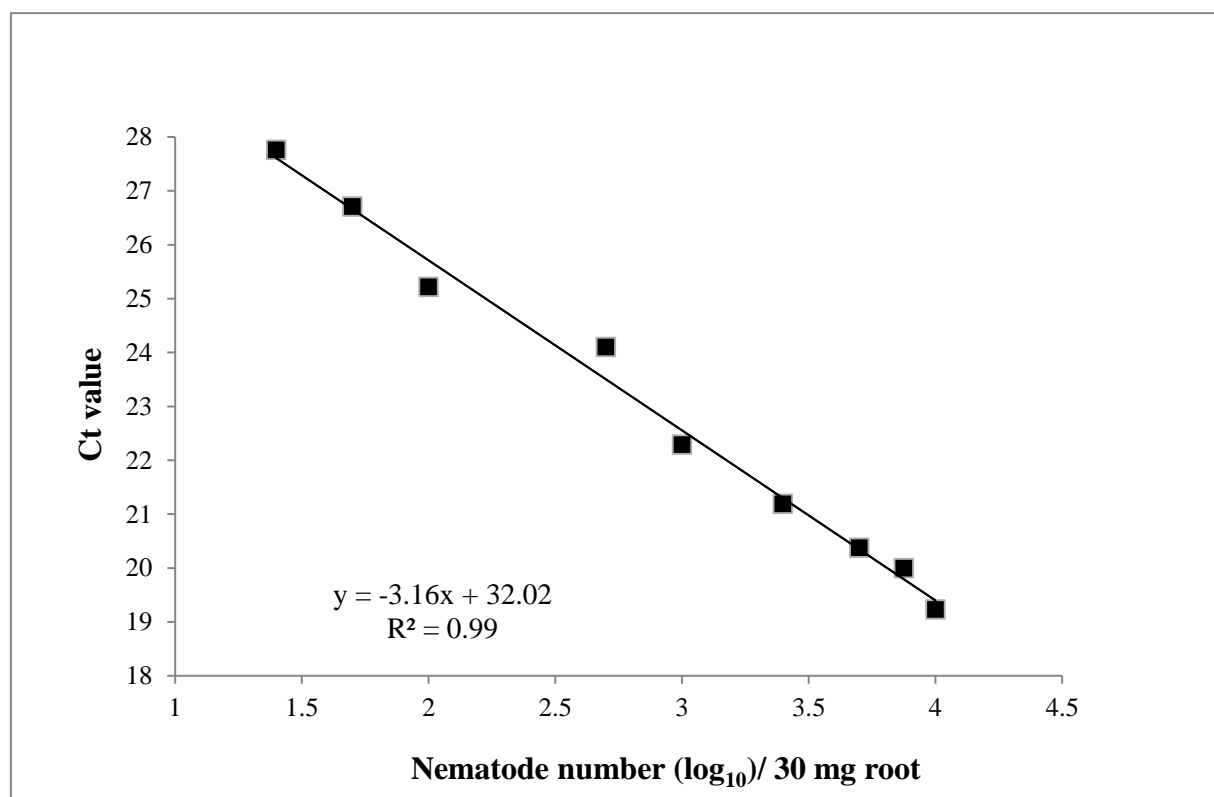
The Ct values obtained using this method of nematode quantification was compared to those obtained by combining separately extracted nematode and (uninoculated) root DNA (taken from Table 4.1 and Fig. 4.2-B).

The numbers of pure *P. thornei* added to root powder were highly correlated ( $R^2 = 0.93$ ) with the numbers of *P. thornei* determined by the real-time PCR assay using the above-mentioned standard curve (Fig. 4.4). The standard linear regression was described by the equation  $y = 0.76x - 228.46$ , where 'y' refers to the number of nematodes added to 30 mg root powder and 'x' refers to the number of nematodes determined by qPCR assay (Fig. 4.4).

**Table 4.2** Ct values of the individual data points used for the development of the standard curve using the *Pratylenchus thornei* DNA samples extracted from wheat root powder

Nematode numbers mixed with 30 mg root	Ct values	Standard deviation
25	27.76	0.64
50	26.71	0.07
100	25.22	0.13
500	24.10	0.23
1000	22.29	0.16
2500	21.19	0.27
5000	20.38	0.61
7500	20.00	0.52
10000	19.23	0.23
E (Amplification efficiency)	118.7%	
R <sup>2</sup>	0.99	
	$y = -3.1561x + 32.023$	

**Fig. 4.3** Standard regression based on *Pratylenchus thornei* DNA extracted from a series of *Pratylenchus thornei* (25 to 10,000 nematodes mixed with 30 mg root powder. Data also shown in Table 4.2





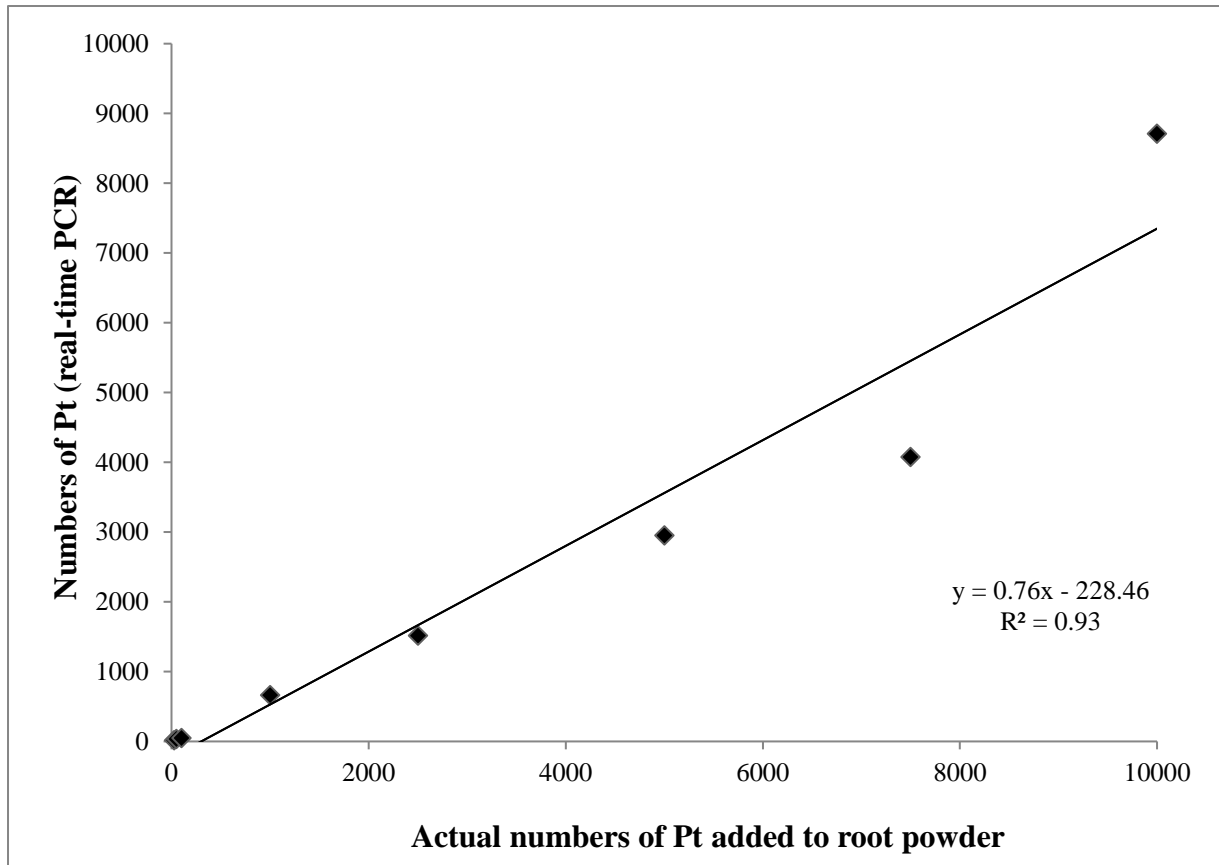






























**Fig. 4.4** Numbers of *Pratylenchus thornei* (Pt) determined by real-time PCR plotted against the numbers of *Pratylenchus thornei* added to the root powder. Pure *Pratylenchus thornei* (25, 50, 100, 500, 1000, 2500, 5000, 7500, 10000) were added to 30 mg of root powder



#### 4.4.5 Quantification of *P. thornei* grown on RIL lines of varying resistance levels

Using the standard regression in Fig 4.3 the qPCR-based *P. thornei* quantification assay was conducted on sixteen wheat lines (fourteen RILs and two parental) with known levels of resistance (Table 4.3). The number of *P. thornei* in Sokoll (resistant) and Krichauff (susceptible) were 4,792 and 33,241 per plant, respectively. The total number of *P. thornei*/plant among fourteen RILs were ranged from 1,939 to 53,120. Among the fourteen RILs, nine RILs were categorised as resistant, two RILs as moderately resistant and three RILs as susceptible lines. To categorise the level of resistance, fold- difference in *P. thornei* number/plant were estimated in comparison to the susceptible parent Krichauff. Fold differences of  $\leq 1.5$ , 1.6-2.0, 2.1-2.5 and  $\geq 2.6$  categorised susceptible (S), moderately susceptible (MS), moderately resistant (MR) and resistant (R) lines, respectively (Table 4.3). In the PreDicta B test assay, similar relative levels of resistance were estimated for these genotypes. In both the PreDicta B test and current qPCR based *P. thornei* quantification assay, ten lines (R\_55, R\_43, R\_68, R\_16, R\_12, R\_40, R\_18, R\_65 and R\_29) were categorised as resistant; two lines (R\_24 and R\_9) as moderately resistant and three lines (R\_10, R\_67 and R\_7) as susceptible (Table 4.3).

**Table 4.3** Quantification of *Pratylenchus thornei* in sixteen wheat lines (with various levels of *Pratylenchus thornei* resistance) using qPCR assay. The results (total nematode number and level of resistance) were compared with PreDicta B test conducted in a commercial laboratory (SARDI)

<i>P. thornei</i> quantified in commercial laboratory						<i>P. thornei</i> quantified by qPCR assay in present study						
Wheat lines	QTL <sup>1</sup>	<i>P. thornei</i> /plant (PreDicta B test)	Fold-change compared to Krichauff	Levels of resistance <sup>2</sup>		Ct values	<i>P. thornei</i> / 30 mg root	Total root weight, mg	<i>P. thornei</i> / Plant <sup>3</sup>	Fold-change compared to Krichauff	Levels of resistance <sup>2</sup>	
R_55	2B+6D		678	15.9	R	24.83	306	190		1,938	17.2	R
R_43	2B+6D		725	14.8	R	23.61	912	130		3,952	8.4	R
R_68	6D		810	13.3	R	25.50	259	380		3,281	10.1	R
R_16	6D		1,198	9.0	R	23.59	902	170		5,111	6.5	R
R_12	6D		1,370	7.9	R	24.20	707	280		6,599	5.0	R
Sokoll	2B+6D		1,534	7.0	R	23.43	958	150		4,790	6.9	R
R_40	2B+6D		1,592	6.8	R	25.40	235	560		4,387	7.6	R
R_18	6D		1,597	6.7	R	24.49	269	450		4,035	8.2	R
R_65	6D		2,320	4.6	R	24.25	573	460		8,786	3.8	R
R_29	6D		2,430	4.4	R	23.08	1181	140		5,511	6.0	R
R_24	2B		4,232	2.5	MR	22.82	1384	300		13,840	2.4	MR
R_9	2B		4,677	2.3	MR	22.62	1545	280		14,420	2.3	MR
R_10	None		7,526	1.4	S	20.27	9402	110		34,474	1.0	S
R_67	None		9,823	1.1	S	21.36	4326	230		33,166	1.0	S
Krichauff	None		10,759	1.0	S	20.32	7671	130		33,241	1.0	S
R_7	None		27,497	0.4	S	21.67	5141	310		53,124	0.6	S

<sup>1</sup>: Loci at which resistance allele was present; <sup>2</sup>: Levels of resistance = Fold differences of  $\leq 1.5$ , 1.6-2.0, 2.1-2.5 and  $\geq 2.6$  categorised susceptible (S), moderately susceptible (MS), moderately resistant (MR) and resistant (R) lines, respectively; <sup>3</sup>Total *P. thornei*/ plant = *P. thornei* in 30 mg root x Total processed root weight / 30

## 4.5 Discussion

The assay presented here represents the first study on evaluation of a SYBR Green real-time qPCR assay to detect and quantify *P. thornei* in infected wheat roots. Previously, a qPCR assay was developed to detect and quantify *P. thornei* (Yan et al. 2011) and *P. neglectus* (Yan et al. 2013) in DNA extracts of nematode-containing soil samples. In addition to soil samples, a plant pathogenic nematode quantification assay was also developed for DNA extracted from infected root. The authors describe detection and quantification of *H. glycine* from infected soybean roots using real-time qPCR (Lopez-Nicora et al. 2012). Plant pathogenic fungi and bacteria were also quantified from infected roots. For example, *Fusarium solani* from soybean roots (Gao et al. 2004; Li et al. 2008); *Rhizoctonia solani* from wheat roots (Okubara et al. 2008) and *Azospirillum brasilense* bacteria from wheat roots (Stets et al. 2015), were quantified.

In the current study, a modified CTAB DNA extraction protocol was developed to extract the nematode DNA from wheat root samples. The DNA extraction protocol was inexpensive as it works without costly commercial plant extraction kits. Moreover, the nematode quantification assay is less expensive compared to the commercial service provider (PreDicta B test at SARDI, PIRSA). For instance, the cost for *P. thornei* quantification using the current protocol is approximately 50 AUD/ sample. This includes laboratory consumables, chemicals, glasshouse facility and labour (Table 4.4). On the other hand, the cost for PreDicta B test at SARDI is 120 AUD/ sample (SARDI Molecular Diagnostic Group, Personal communication).



**Table 4.4** Estimated cost for QPCR based *Pratylenchus thornei* quantification from wheat root samples

Item	Estimated cost for 100 samples
Consumables and chemicals for nematode assay in the glasshouse, DNA extraction and QPCR assay	600 AUD
Access to glasshouse and laboratory facilities for 10 weeks	1000 AUD
Labour cost for a total 100 hours, 33 AUD/ hour	3300 AUD
Miscellaneous	100 AUD
Total cost for 100 samples	5000 AUD
Total cost per sample	50 AUD

The extraction protocol was able to produce DNA without noticeable inhibition of PCR reactions. For the precise quantification of the pathogen in infected roots, it is important to minimize the presence of any PCR inhibitor, such as humic acids, fulvic acids and polysaccharides which may lower the efficiency of qPCR (Demeke and Jenkins 2010; Gao et al. 2004). With the use of washed root samples in this study, PCR inhibitors from soil as observed by Yan et al. (2011) was minimized. Moreover, the presence of any PCR inhibitor was checked by comparing qPCR assays using DNA extracted from pure *P. thornei* vs. pure *P. thornei* DNA mixed with uninoculated wheat root DNA. Ct values for each of these experiments were well correlated, indicating little/no PCR inhibition by the wheat root DNA. Amberlite was added to the extraction buffer to minimize potential inhibition by wheat root or nematode compounds. Its beneficial effects on PCR performance had previously been reported by Okubara et al. (2008) who added acid-washed Amberlite XAD-4 for DNA extraction from *R. solani*-infected wheat roots.

The THOITS-F2 and THO-ITS-R2 primer pairs were designed from the internal transcribed spacer regions (ITS1) of the nuclear ribosomal RNA genes (Yan et al. 2011). The primers are highly specific to *P. thornei* and did not amplify DNA from 27 isolates of other *Pratylenchus* spp., other nematodes, and six fungal species. Moreover, in this study, the primer pairs did not amplify DNA from the wheat root samples.

Using the root standard curve developed in this study, qPCR based *P. thornei* quantification was performed on wheat lines with known levels of resistance. This experiment was conducted to compare the outcome of the quantification method with the PreDicta B test (SARDI). For both these assays, wheat lines were grown in the growth chamber under the similar growing conditions. *P. thornei* were also inoculated from the same sources and wheat samples (root and/or soil) samples were collected at the same time. Thus, sources of variation in *P. thornei* estimation from growing conditions and inoculation were avoided. However, in the PreDicta B test, a mixture of soil and plant root were used to extract *P. thornei* DNA. On the other hand, in the qPCR quantification assay, *P. thornei* DNA was extracted from root samples only. Approximately three fold higher total *P. thornei*/ plant were estimated from root samples (qPCR experiment) compared to the soil + root sample (PreDicta B test) (Table 4.3). Whether this difference occurred due to the type of the sample (soil + root vs root only), required further investigation. However, all the wheat lines were classified for resistance (resistant/moderately resistant/susceptible) the same in both assays. Thus, the present assay was able to accurately estimate *P. thornei* present in unknown wheat root samples.

The present study demonstrated that the real-time PCR assay can be used to detect and quantify *P. thornei* from infested roots. The method required DNA extraction from root samples washed clean of soil, but eliminated time consuming microscopic identification and nematode counting. The method required only basic laboratory chemicals and consumables, resulting in a more cost-effective method than that requiring a DNA extraction kit and commercial service provider. This assay forms the basis of a cost-effective tool for rapid and efficient detection and quantification of *P. thornei* for germplasm characterisation, genetic mapping studies and screening for breeding improved (*P. thornei* resistant) cultivars.

## 4.6 References

- Agrios GN (1988). Plant pathology. Academic press, San Diego, CA, USA, pp 313-314
- Berry SD, Fargette M, Spaul V, Morand S, Cadet P (2008) Detection and quantification of root-knot nematode (*Meloidogyne javanica*), lesion nematode (*Pratylenchus zeae*) and dagger nematode (*Xiphinema elongatum*) parasites of sugarcane using real-time PCR. Molecular and Cellular Probes 22:168-176
- Demeke T, Jenkins GR (2010) Influence of DNA extraction methods, PCR inhibitors and quantification methods on real-time PCR assay of biotechnology-derived traits. Analytical and Bioanalytical Chemistry 396:1977-1990
- Desjardins P, Conklin D (2010) NanoDrop microvolume quantitation of nucleic acids. Journal of Visualized Experiment 45:e2565. <https://doi.org/10.3791/2565>
- Gao X, Jackson TA, Lambert KN, Li S, Hartman GL, Niblack TL (2004) Detection and quantification of *Fusarium solani* f. sp. *glycines* in soybean roots with real-time quantitative polymerase chain reaction. Plant Disease 88:1372-1380
- Li S, Hartman GL, Domier LL, Boykin D (2008) Quantification of *Fusarium solani* f. sp. *glycines* isolates in soybean roots by colony-forming unit assays and real-time quantitative PCR. Theoretical and Applied Genetics 117:343-352
- Linsell KJ, Rahman MS, Taylor JD, Davey RS, Gogel BJ, Wallwork H, Forrest KL, Hayden MJ, Taylor SP, Oldach KH (2014a) QTL for resistance to root lesion nematode (*Pratylenchus thornei*) from a synthetic hexaploid wheat source. Theoretical and Applied Genetics 127:1409-1421
- Linsell KJ, Riley IT, Davies KA, Oldach KH (2014b) Characterization of resistance to *Pratylenchus thornei* (nematoda) in wheat (*Triticum aestivum*): attraction, penetration, motility, and reproduction. Phytopathology 104:174-187
- Lopez-Nicora HD, Craig JP, Gao X, Lambert KN, Niblack TL (2012) Evaluation of cultivar resistance to soybean cyst nematode with a quantitative polymerase chain reaction assay. Plant Disease 96:1556-1563
- Madani M, Subbotin SA, Moens M (2005) Quantitative detection of the potato cyst nematode, *Globodera pallida*, and the beet cyst nematode, *Heterodera schachtii*, using Real-Time PCR with SYBR green I dye. Molecular and Cellular Probes 19:81-86
- Mokrini F, Waeyenberge L, Viaene N, Andaloussi FA, Moens M (2014) The  $\beta$ - gene is suitable for the molecular quantification of the root-lesion nematode. Nematology 16:789-796
- Moody EH, Lownsbery BF, Ahmed JM (1973) Culture of the root-lesion nematode *Pratylenchus vulnus* on carrot disks. Journal of Nematology 5:225-226

Nicol JM, Ortiz-Monasterio I (2004) Effects of the root-lesion nematode, *Pratylenchus thornei*, on wheat yields in Mexico. *Nematology* 6:485-493

Okubara PA, Schroeder KL, Paulitz TC (2008) Identification and quantification of *Rhizoctonia solani* and *R. oryzae* using real-time polymerase chain reaction. *Phytopathology* 98:837-847

Rahman SA, Aisyafaznim S, Mohamed Z, Othman RY, Swennen R, Panis B, De Waele D, Remy S, Carpentier SC (2010) In planta PCR-based detection of early infection of plant-parasitic nematodes in the roots: a step towards the understanding of infection and plant defence. *European Journal of Plant Pathology* 128:343-351

Rogers-Broadway KR, Karteris E (2015) Amplification efficiency and thermal stability of qPCR instrumentation: current landscape and future perspectives. *Experimental and Therapeutic Medicine* 10:1261-1264

Sheedy JG, Thompson JP (2009) Resistance to the root-lesion nematode *Pratylenchus thornei* of Iranian landrace wheat. *Australasian Plant Pathology* 38:478-489

Smiley RW, Nicol JM (2009) Nematodes which challenge global wheat production. In: Carver BF(ed) *Wheat Science and Trade*. Wiley-Blackwell, Ames, IA pp 171-187

Smiley RW, Whittaker RG, Gourlie JA, Easley SA (2005) *Pratylenchus thornei* associated with reduced wheat yield in Oregon. *Journal of Nematology* 37:45-54

Stets MI, Alqueres SMC, Souza EM, Pedrosa FdO, Schmid M, Hartmann A, Cruz LM (2015) Quantification of *Azospirillum brasilense* FP2 bacteria in wheat Roots by strain-Specific quantitative PCR. *Applied and Environmental Microbiology* 81:6700-6709

Thompson JP, Clewett TG, Sheedy JG, Reen RA, O'Reilly MM, Bell KL (2010) Occurrence of root-lesion nematodes (*Pratylenchus thornei* and *P. neglectus*) and stunt nematode (*Merlinius brevidens*) in the northern grain region of Australia. *Australasian Plant Pathology* 39:254-264

Thompson JP (2008) Resistance to root-lesion nematodes (*Pratylenchus thornei* and *P. neglectus*) in synthetic hexaploid wheats and their durum and *Aegilops tauschii* parents. *Australian Journal of Agricultural Research* 59:432-446

Thompson JP, Clewett TG, O'Reilly MM (2015) Temperature response of root-lesion nematode (*Pratylenchus thornei*) reproduction on wheat cultivars has implications for resistance screening and wheat production. *Annals of Applied Biology* 167:1-10

Thompson JP, Haak MI (1997) Resistance to root-lesion nematode (*Pratylenchus thornei*) in *Aegilops tauschii* Coss., the D-genome donor to wheat. *Australian Journal of Agricultural Research* 48:553-559

Toumi F, Waeyenberge L, Viaene N, Dababat AA, Nicol JM, Ogonnaya FC, Moens M (2015) Development of qPCR assays for quantitative detection of *Heterodera avenae* and *H. latipons*. *European Journal of Plant Pathology* 143:305-316

Yan G, Smiley RW, Okubara PA (2011) Detection and quantification of *Pratylenchus thornei* in DNA extracted from soil using real-time PCR. *Phytopathology* 102:14-22

Yan G, Smiley RW, Okubara PA, Skantar A, Easley SA, Sheedy JG, Thompson AL (2008) Detection and discrimination of *Pratylenchus neglectus* and *P. thornei* in DNA extracts from soil. *Plant Disease* 92:1480-1487

Yan G, Smiley RW, Okubara PA, Skantar AM, Reardon CL (2013) Developing a Real-Time PCR assay for detection and quantification of *Pratylenchus neglectus* in soil. *Plant Disease* 97:757-764

## **Chapter 5**

**Metabolomic analysis of root tissues and root exudates from  
wheat lines contrasting for *Pratylenchus thornei* resistance**

## **Chapter 5**

### **Metabolomic analysis of root tissues and root exudates from wheat lines contrasting for *Pratylenchus thornei* resistance**

#### **5.1 Statement of authorship**

## **Statement of Authorship**

Title of the paper	Metabolomic analysis of root tissues and root exudates from wheat lines contrasting for <i>Pratylenchus thornei</i> resistance
Publication Status	Unpublished and unsubmitted work written in manuscript style
Publication details	This chapter will be prepared as a manuscript for submission to a refereed journal

### **Principal Author**

Name of Principal Author (Candidate)	Muhammad Shefatur Rahman		
Contribution to the paper	Involved in designing the research project conception and development of overall research plan. Prepared the root exudates and root tissue samples for metabolomics study, analysed and interpret the data provided by the Metabolomics, Australia. Wrote the first draft of the manuscript and took primary responsibility for manuscript revision.		
Overall percentage (%)	70		
Certification	This paper reports on original research I conducted during the period of my Higher Degree by Research candidature and is not subject to any obligations or contractual agreements with a third party that would constrain its inclusion in this thesis. I am the primary author of this paper.		
Signature		Date	4.12.2019.

### **Co-Author Contributions**

By signing the Statement of Authorship, each author certifies that:

- I. the candidate's stated contribution to the publication is accurate (as detailed above);
- II. permission is granted for the candidate to include the publication in the thesis; and
- III. the sum of all co-author contributions is equal to 100% less the candidate's stated contribution.

Name of Co- Author	Katherine J. Linsell		
Contribution to the paper	Provided suggestions for the research experiment, provided input for the manuscript.		
Signature		Date	5/12/19



Name of Co- Author	Ute Roessner		
Contribution to the paper	Supervised the GC-MS metabolomic assay at the Metabolomics Australia		
Signature		Date	10/12/19

Name of Co- Author	Nicholas C. Collins		
Contribution to the paper	Helped in data analysis and writing the manuscript. Read the manuscript and suggested revisions.		
Signature		Signature	9/12/19

Name of Co- Author	Klaus H. Oldach		
Contribution to the paper	Provided overall supervision of the research project and helped writing the manuscript.		
Signature		Date	4. 12. 2019

## 5.2 Introduction

The mode of root lesion nematode (*Pratylenchus thornei*) resistance in the Sokoll / Krichauff doubled haploid (DH) population was previously investigated by Linsell et al. (2014). The parental lines and six DH lines (three most resistant and three most susceptible) were examined to see whether resistance acts by affecting nematode attraction to roots, penetration of roots, nematode motility, maturation or reproduction within roots. Nematode motility was found to be suppressed in root exudates and crushed root suspensions from the resistant genotypes compared to the susceptible genotypes. Nematode migration was also found to be suppressed inside the roots of the resistant genotype. Maturation of the juvenile stage was suppressed in resistance genotypes. In addition, egg deposition and hatching of *P. thornei* was significantly reduced in resistant roots and their exudates (Linsell et al. 2014). These results suggested the presence of chemical compounds in resistant roots and root exudates acting on *P. thornei* by suppressing nematode motility, migration and reproduction.

Metabolomic analyses allow us to detect and, to some extent, identify compounds that are secreted by plants and the organisms interacting with them in the rhizosphere (reviewed in van Dam and Bouwmeester 2016). Metabolic profiling involves detection, quantification and identification of metabolites within an extract by employing chromatographic separation (gas chromatography or liquid chromatography) coupled with mass spectrometry (Allwood et al. 2008). Gas chromatography-mass spectrometry (GC-MS) based platforms allow analysis of volatile compounds and primary metabolites present in the root. For example, GC-MS analysis was employed to characterize the chemical composition of the root exudates of *Sedum alfredii* (Luo et al. 2017), sunflower (Bowsher et al. 2015), Arabidopsis (Schmidt et al. 2014) and rice (Suzuki et al. 2009). GC-MS based metabolic profiling has also been employed to reveal the metabolic changes occurring in plants due to pathogen infection, including by plant pathogenic

nematodes (Eloh et al. 2016; Hofmann et al. 2010; Machado et al. 2012), fungi (Aliferis et al. 2014; Kumar et al. 2015; Rosati et al. 2018; Scandiani et al. 2015) and bacteria (Camañes et al. 2015; López-Gresa et al. 2017).

Plant roots exude a diverse array of low-molecular weight primary and secondary metabolites (Dakora and Phillips 2002; Faure et al. 2009). Approximately 10% of the net photosynthetically fixed carbon is released by the soil-grown plant as root exudates into the rhizosphere (Jones et al. 2009), strongly influencing rhizosphere ecology (reviewd in Badri and Vivanco 2009; Bais et al. 2006; Bertin et al. 2003).

Root exudates have been shown attract or repel certain microbial species (Rudrappa et al. 2008). Several studies describe the allelopathic effects of root exudates on nematodes (Dutta et al. 2012; Hiltpold et al. 2015). Root exudates can affect egg hatching of plant parasitic nematodes (Gaur et al. 2000; Khokon et al. 2009; Oka and Mizukubo 2009; Perry and Clarke 2011; Pudasaini et al. 2008) and may also be involved in host identification by the nematodes. For example, plant parasitic nematodes respond to the signals originating from root exudates or sites of penetration (made by other nematodes) to locate their host (Prot 1980; Reynolds et al. 2011; Rolfe et al. 2000).

Yet root exudates can also protect roots against plant-parasitic nematodes. For instance, metabolites exuded from the root-cap cells of legumes and maize (*Zea mays*) slow down movement in plant-parasitic nematodes, sometimes resulting in a state of quiescence, reducing the ability of the nematodes to infect the plant (Zhao et al. 2000).

The current study involves a non-targeted metabolic profiling of root tissues and root exudates from wheat genotypes contrasting for *P. thornei* resistance. A GC-MS based platform was used to analyse the root samples. It was hypothesized that metabolic profiles of resistant and susceptible genotypes may differ, which could help to identify candidate metabolites that are important in understanding the wheat-root lesion nematode interaction.

## 5.3 Materials and methods

### 5.3.1 Plant Materials

The study investigated wheat lines from a DH mapping population which contrast in *P. thornei* resistance. Five wheat lines, Sokoll (*P. thornei* resistant parent), Krichauff (*P. thornei* susceptible parent) and three progenies, DH line-35, DH line-52 and DH line-114, were analysed. DH line-35 and DH line-52 carried the positive alleles for *P. thornei* resistance only at the 6DS and 2BS locus, respectively (described in Chapter 3). DH line-114 carried the susceptible alleles at both loci. For ease of reporting, these DH lines will be referred to as 6D-R, 2B-R and Null-S, respectively. The parental lines will be referred as Sk-R and Kr-S, respectively.

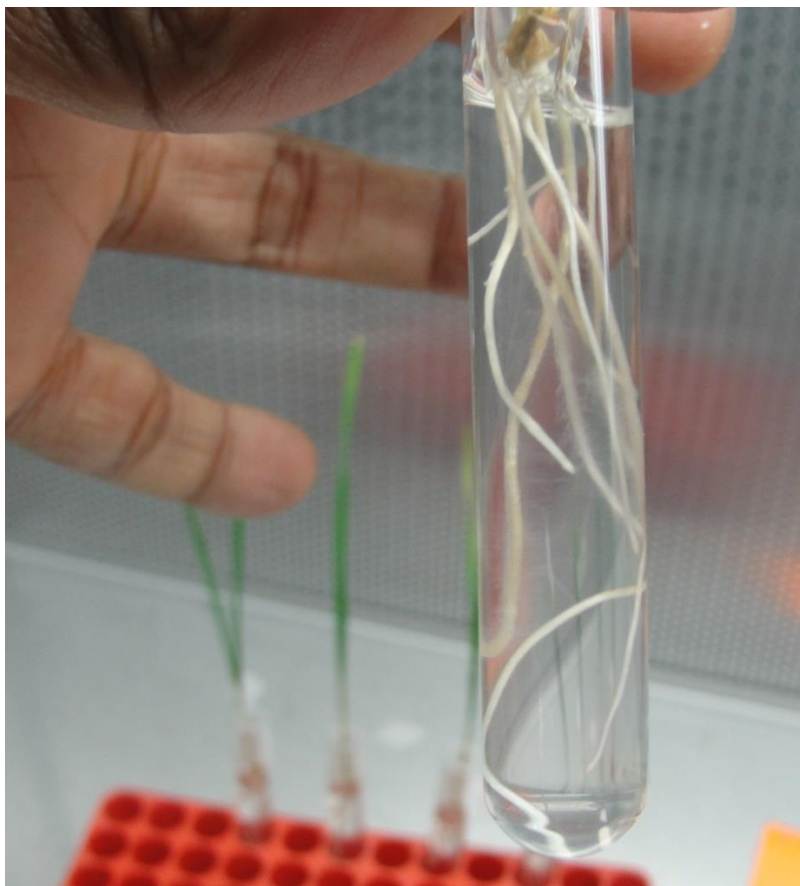
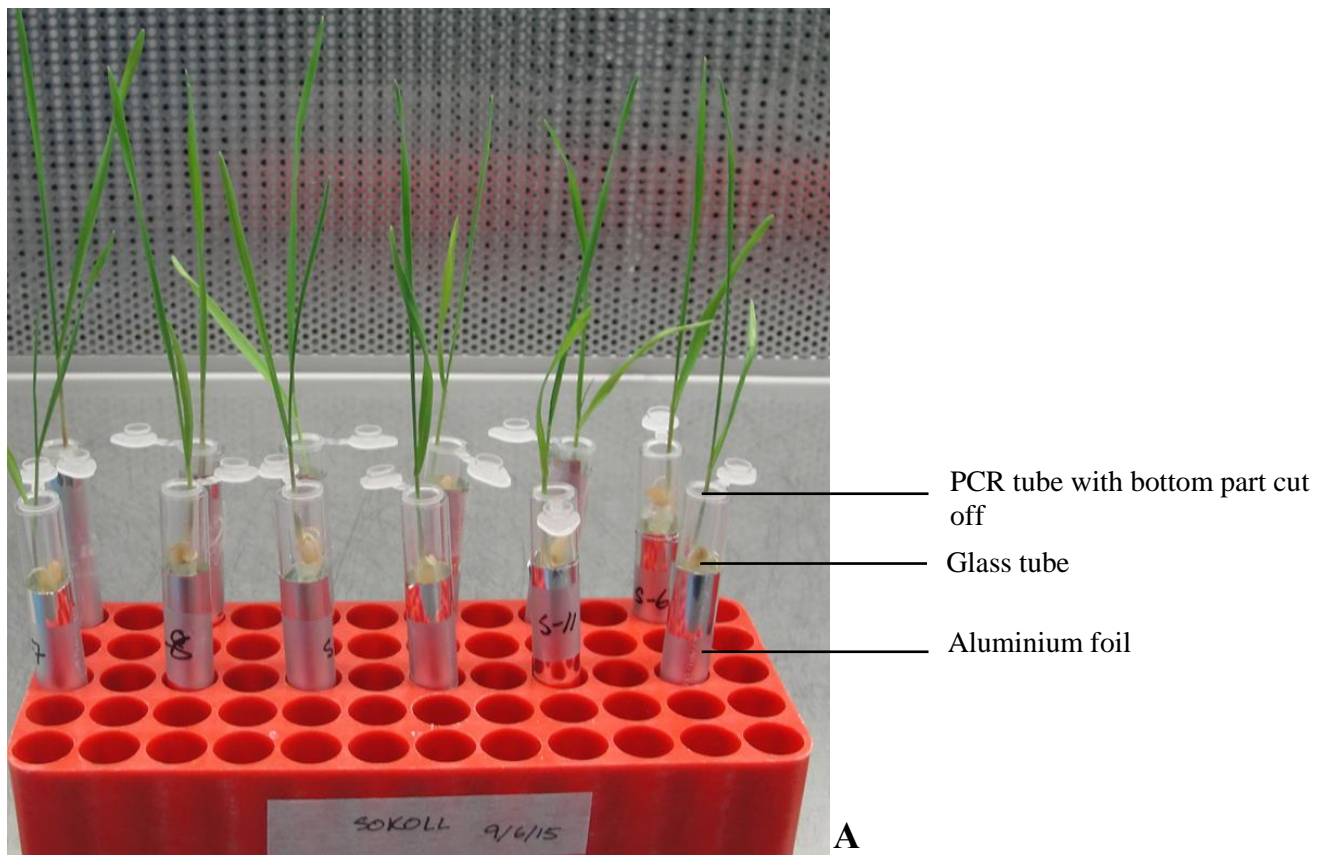
### 5.3.2 Collection of root exudates

- For root exudates, all five genotypes, Sk-R, Kr-S, 6D-R, 2B-R and Null-S were analysed.
- A total of 16 plants of each genotype were grown. Root exudates from four plants were bulked to produce each of four bulk samples for each genotype.
- At first, seeds were surface sterilised. Seeds were treated with 70% ethanol for one minute then rinsed with sterile reverse osmosis (RO) water (two times, five minutes each). Seeds were then treated with 0.5% sodium hypochlorite for one minute followed by a rinse with sterile RO water.
- After sterilisation, seeds were germinated on wet filter paper (Whatman) fitted in a Petri dish. When the root length of the seedlings reached approximately 2 cm, each seedling was transferred from the Petri dish to a 6.0 mL glass tube filled with 4.0 mL sterile milli-Q water. To prevent the seedling submerging completely, seeds were placed in a

0.2 mL PCR tube with the bottom part cut off, and the tube rested on the top of the glass tube. Each of the glass test tubes were wrapped with aluminium foil to prevent exposure of the roots to light. The seedlings were grown at room temperature for 14 days. Each day, the plants were monitored visually for any obvious microbial contamination, but no contamination was observed in the root exudate solution. Water was added when needed to keep the level at 4.0 mL. The experimental setup was shown in Fig. 5.1.

- After 14 days from transplantation, seedlings were removed from the tubes and 4.0 mL water containing root exudates were collected after passing through a 0.22  $\mu\text{m}$  syringe filter (Millex GV, Millipore). Filtration allowed removal of any potential microbial contaminants present in the root exudate solution. Moreover, root samples were collected, and fresh weights of the roots were measured.
- The concentration of the root exudate solution was adjusted per unit of root weight (mg). The root exudate solution was freeze dried for further analysis.

**Fig. 5.1** Collection of root exudates from wheat seedlings. A. Experimental setup B. Checking for contamination in root exudate solution



### 5.3.3 Sampling roots challenged with *P. thornei*

- Plants were grown in steam-pasteurized sand in plastic pots in a controlled environmental room (CER) (as described in Chapter 4). A total of 16 plants of each genotype were grown. Plants of each genotype were grown in separate crates.
- Two weeks after transplantation, approximately 5,000 *P. thornei* were inoculated near the root zone of each plant (as described in Chapter 4). The parental lines Sokoll and Krichauff were also grown without nematode inoculation as controls. For ease of reporting *P. thornei* challenged samples will be referred as Sk-R-I, Kr-S-I, 6D-R-I, 2B-R-I and Null-S and the uninoculated parental lines will be referred as Sk-R-C and Kr-S-C, respectively.
- Roots were harvested 6 weeks after inoculation. Root samples were freeze dried and ground in liquid nitrogen. For a given genotype, 0.5 g root powder from four plants were bulked to constitute 2.0 g of bulked sample. For each genotype four bulked samples were analysed.

### 5.3.4 Nematode samples

For GC-MS analysis and to inoculate wheat lines, *P. thornei* was collected from carrot callus and counted using a compound microscope (described in Chapter 4). Four replicated samples containing approximately 5,000 *P. thornei* were prepared in a 2.0 mL Eppendorf® tube. Nematode samples were freeze-dried and ground using an Eppendorf® micropestle.

### 5.3.5 Preparation of root exudates for metabolomic analysis

For metabolomics analyses, dried root exudate samples were further processed by Metabolomics, Australia (Victoria, Australia). Dried root exudate samples were re-constituted in 500 µL methanol containing the internal standards  $^{13}\text{C}_6$ -Sorbitol (0.005 mg/mL) and  $^{13}\text{C}_5$ -



$^{15}\text{N}$ -Valine (0.005 mg/mL) followed by a 30-sec sonication at room temperature. Samples were then vacuum-dried using a Rotational Vacuum Concentrator (RVC 2-33 CD plus, John Morris Scientific, Pty Ltd, Melbourne, Australia) set at room temperature. Dried samples were prepared by addition of 200  $\mu\text{L}$  methanol followed by a 10-min centrifugation at 15,000 rpm ( $21,200 \times g$ ). Aliquots of 120  $\mu\text{L}$  were transferred to clean glass inserts in Eppendorf tubes and vacuum dried as above.

### **5.3.6 Preparation of root tissues for metabolomic analysis**

Sub-samples (15 mg) of freeze-dried root material were transferred to Cryo-mill tubes and weights recorded. Methanol (MeOH, 600  $\mu\text{L}$ ), containing the internal standards  $^{13}\text{C}_6$ -Sorbitol (0.02 mg/mL) and  $^{13}\text{C}_5$ - $^{15}\text{N}$ -Valine (0.02 mg/mL), was added to the sample tubes. The samples were homogenized using a Cryo-mill (Bertin Technologies; program #2 (6800-3x30x30 at -10°C) and then incubated in a Thermomixer at 30°C with a mixing speed of 1,400 rpm for 15 minutes, followed by 5 minutes of centrifugation at 15,000 rpm ( $21,200 \times g$ ). The MeOH supernatant was transferred into a 2 mL Eppendorf tube and set aside. Water (600  $\mu\text{L}$ ) was added to the remaining sample pellet and vortexed before being centrifuged for 10 minutes at 15,000 rpm ( $21,200 \times g$ ). The supernatant was removed and combined with the MeOH supernatant. Aliquots of 50  $\mu\text{L}$  were transferred to clean glass inserts in Eppendorf tubes and vacuum dried as above.

### **5.3.7 Preparation of nematode samples for metabolomic analysis**

Sub-samples (15 mg) of ground freeze-dried nematodes were transferred to 2 mL Eppendorf tubes and accurate weights recorded. Methanol (MeOH, 600  $\mu\text{L}$ ) containing the internal standards  $^{13}\text{C}_6$ -Sorbitol (0.02 mg/mL) and  $^{13}\text{C}_5$ - $^{15}\text{N}$ -Valine (0.02 mg/mL) was added to the sample tubes. The samples were then incubated in a Thermomixer at 30°C with a mixing speed

of 1,400 rpm for 15 minutes, followed by a 5 minute centrifugation at 15,000 rpm (21,200 x g). The MeOH supernatant was transferred into a 2 mL Eppendorf tube and set aside. Water (600 µL) was added to the remaining sample pellet and vortexed before being centrifuged for 10 minutes at 15,000 rpm (21,200 x g). The supernatant was removed and combined with the MeOH supernatant. Aliquots of 50 µL were transferred to clean glass inserts in Eppendorf tubes and dried *in vacuo* using a Rotational Vacuum Concentrator (RVC 2-33 CD plus, John Morris Scientific, Pty Ltd, Melbourne, Australia) set at ambient temperature.

### 5.3.8 Sample derivatisation

Sample derivation was performed for the root and nematode samples to change the analyte properties for a better separation and for enhancing the method sensitivity. Dried root exudates were prepared by the addition of 10 µL of Methoxyamine Hydrochloride (30 mg/mL in Pyridine) followed by shaking at 37°C for 2h. The sample was then derivatised with 20 µL of *N*, *O*-bis (Trimethylsilyl) trifluoroacetamide with Trimethylchlorosilane (BSTFA with 1% TMCS, Thermo Scientific) for 30 minutes at 37°C. The sample was then left for 1 h before 1 µL was injected onto the GC column using a hot needle technique. Splitless injections were done for each sample.

Dried root exudates and nematode extracts were prepared by the addition of 10 µL of Methoxyamine Hydrochloride (30 mg/mL in Pyridine) followed by shaking at 37°C for 2h. The sample was then derivatised with 20 µL of *N*, *O*-bis (Trimethylsilyl) trifluoroacetamide with Trimethylchlorosilane (BSTFA with 1% TMCS, Thermo Scientific) for 30 minutes at 37°C. The sample was then left for 1 h before 1 µL was injected onto the GC column using a hot needle technique. Splitless injections were done for each sample.

### 5.3.9 GC-MS analysis

The GC-MS system used comprised of a Gerstel 2.5.2 autosampler, a 7890A Agilent gas chromatograph and a 5975C Agilent quadrupole mass spectrometer (Agilent, Santa Clara, USA). The mass spectrometer (MS) was tuned according to the manufacturer's recommendations using tris-(perfluorobutyl)-amine (CF43).

Gas chromatography was performed on a 30 m Agilent J & W VF-5MS column with 0.25  $\mu$ m film thickness and 0.25 mm internal diameter with a w/10 m Integra guard column. The injection temperature (Inlet) was set at 250°C, the MS transfer line at 280°C, the ion source adjusted to 230°C and the quadrupole at 150°C. Helium was used as the carrier gas at a flow rate of 1 mL/min.

The analysis of Trimethylsilyl (TMS) derivatized samples was performed under the following temperature program; start at injection 70°C, a hold for 1 minute, followed by a 7°C min<sup>-1</sup> oven temperature ramp to 325°C and a final 6 minute heating at 325°C. Mass spectra were recorded at 2.66 scans.s<sup>-1</sup> with an m/z 50-600 scanning range.

### 5.3.10 Data processing and statistical analysis

Data was processed using the Agilent MassHunter Quantitative Analysis software, version B.07.00. Mass spectra of eluting TMS compounds were identified using the commercial mass spectra library NIST (<http://www.nist.gov>), the public domain mass spectra library of Max-Planck-Institute for Plant Physiology, Golm, Germany (<http://csbdb.mpimp-golm.mpg.de/csbdb/dbma/msri.html>) and the in-house Metabolomics Australia mass spectral library. Resulting relative response ratios normalized per mg dry weight for each analysed metabolite were prepared as described in Roessner et al. (2001). Differences between sample

groups were tested for statistical significance using the Student's t-test ( $P$ -value < 0.05). Statistical analysis was performed using Excel (Microsoft, [www.microsoft.com](http://www.microsoft.com)) and metabolomic data was analysed using MetaboAnalyst 3.0 (Xia and Wishart 2002).

## 5.4 Results

In this section, the outcome of the two experiments, metabolomic analysis of root exudates and tissues will be described.

### 5.4.1 Metabolomic analysis of root exudates

Metabolomic profiles of root exudates from five wheat genotypes described 100 metabolites (Supplementary Table 5.1). These metabolites were categorized into classes: amino acids and amines (18), organic acids (14), sugars, sugar alcohols and sugar phosphates (17), miscellaneous (14) and unidentified (37). Significant differences in metabolite levels were observed between the *P. thornei* resistant (Sk-R, 6D-R and 2B-R) and susceptible (Kr-S and Null-S) genotypes.

#### 5.4.1.1 Metabolites in wheat root exudates associated with *P. thornei* resistance QTL

To identify the metabolites associated with the resistance QTL, levels of metabolites were compared between resistant (Sk-R, 6D-R and 2B-R) and susceptible (Kr-S, Null-S) wheat genotypes. The most important features from this comparison are shown in Table 5.3 and a more detailed analysis is presented in Supplementary Table 5.2.

#### *Exudate metabolites associated with both the 6D and 2B QTL (Table 5.1, section A)*

To identify metabolites in root exudates associated with both 6D and 2B loci, metabolites in Sk-R were compared with those in Kr-S and Null-S. Twenty-one metabolites were significantly higher ( $\geq 1.1$ -fold) in Sk-R than in Kr-S. These comprised six amino acids (alanine, beta alanine, methionine, proline, tyrosine and valine), eight organic acids (2-hydroxyglutaric acid, 4-hydroxy-benzoic acid, citric acid, glutaric acid, glyceric acid, malic acid, quinic acid and shikimic acid) and six sugars (arabitol, fructose, glucose, maltose, myo inositol and sucrose).

However, among these metabolites, only one (quinic acid) was also found to be significantly higher ( $\geq 1.1$ -fold) in Sk-R than in Null-S. Specifically, quinic acid was 3.84-fold and 3.46-fold higher in Sk-R as compared to Kr-S and Null-S, respectively. These metabolites might act in *P. thornei* resistance in Sokoll.

Eight metabolites (homoserine, fumaric acid, erythritol, galactitol, ribitol, threitol, uracil and uric acid) were found to be significantly lower ( $\leq 0.9$ -fold) in Sk-R than in Kr-S and Null-S. These metabolites may play a role in facilitating host-pathogen compatibility.

***Exudate metabolites associated only with the 6D QTL (Table 5.1, section B)***

To identify metabolites associated with the 6D QTL, metabolites in Sk-R and 6D-R were compared with those in Kr-S and Null-S.

None of the metabolites were found to be consistently higher in Sk-R and 6D-R ( $\geq 1.1$ -fold) as compared to Kr-S and Null-S. However, four metabolites (shikimic acid, malic acid, citric acid and alanine) were found to be significantly higher ( $\geq 2.0$ -fold) in both Sk-R and 6D-R as compared to Kr-S.

None of the metabolites were found to be consistently lower ( $\leq 0.9$ -fold) in Sk-R and 6D-R than in Kr-S and Null-S. However, uracil and ribitol were lower ( $\leq 0.9$ -fold) in Sk-R and 6D-R than in Kr-S, and threitol was lower in Sk-R and 6D-R than in Null-S.

***Exudate metabolites associated only with the 2B QTL (Table 5.1, section C)***

To identify metabolites associated with the 2B resistance QTL, metabolites in Sk-R and 2B-R were compared (fold-change) with those in Kr-S and Null-S. None of the metabolites were

found be consistently higher in Sk-R and 2B-R ( $\geq 1.1$ -fold) compared to Kr-S and Null-S. Ten metabolites were significantly higher ( $\geq 2.0$ -fold) in both the Sk-R and 2B-R lines relative to Krichauff. These metabolites were beta alanine, proline, 4-amino butyric acid, 2-hydroxyglutaric acid, glutaric acid, glyceric acid, shikimic acid, fructose and maltose. Uracil, erythritol and galactinol were significantly lower in Sk-R and 2B-R than in Kr-S. In addition, threitol was significantly lower in Sk-R and 2B-R than in Null-S.

**Table 5.1** Analysis of metabolites in root exudates associated with *Pratylenchus thornei* resistance. The level of metabolites (fold-difference) were compared between resistant (Sk-R, 6D-R and 2B-R) and susceptible (Kr-S and Null-S) lines to identify metabolites associated with 6D+2B (Section A), 6D (Section B) or 2B (Section C) resistance QTL. 1: Fold- differences were calculated based on average values from four replicates. 2: Highlights show compounds that were significantly (t-test,  $P < 0.05$ ) higher (green colour) or lower (blue colour) in resistant line compared to the susceptible line. AA, OA, S and M refers to amino acids, organic acids, sugars and miscellaneous biochemical groups, respectively

A. Differences in metabolites associated with 6D+2B QTL			B. Differences in metabolites associated with 6D QTL						C. Differences in metabolites associated with 2B QTL				
Fold-difference (Average) <sup>1</sup>		Metabolites <sup>2</sup>	Fold-difference (Average) <sup>1</sup>		Metabolites <sup>2</sup>				Fold-difference (Average) <sup>1</sup>		Metabolites <sup>2</sup>		
SK-R/ KR-S	Sk-R/ Null-S		SK-R/ KR-S	6D-R/ KR-S	Sk-R/ Null-S	6D-R/ Null-S		SK-R/ KR-S	2B-R/ KR-S	Sk-R/ Null-S	2B-R/ Null-S		
2.31	0.05	AA_4-amino butyric acid	2.31	204.87	0.05	3.74	AA_4-amino butyric acid	2.31	6.32	0.05	0.36	AA_4-amino butyric acid	
3.77	0.17	AA_beta alanine	3.77	14.17	0.17	1.21	AA_beta alanine	3.77	3.31	0.17	0.36	AA_beta alanine	
2.42	0.05	AA_Proline	2.42	30.35	0.05	2.47	AA_Proline	2.42	2.97	0.05	0.33	AA_Proline	
8.97	0.88	OA_2-hydroxyglutaric acid	8.97	24.10	0.88	2.13	OA_2-hydroxyglutaric acid	8.97	4.09	0.88	0.66	OA_2-hydroxyglutaric acid	
3.38	0.47	OA_4-hydroxy-benzoic acid	3.38	5.17	0.47	0.86	OA_4-hydroxy-benzoic acid	3.38	1.88	0.47	0.28	OA_4-hydroxy-benzoic acid	
2.19	0.31	OA_Glutaric acid	2.19	2.83	0.31	0.40	OA_Glutaric acid	2.19	2.90	0.31	0.96	OA_Glutaric acid	
1.97	0.28	OA_Glyceric acid	1.97	1.74	0.28	0.42	OA_Glyceric acid	1.97	1.60	0.28	0.83	OA_Glyceric acid	
13.87	1.01	S_Fructose	13.87	4.53	1.01	0.43	S_Fructose	13.87	5.61	1.01	0.12	S_Fructose	
4.90	0.14	S_Maltose	4.90	14.99	0.14	0.45	S_Maltose	4.90	9.61	0.14	0.28	S_Maltose	
3.72	0.26	OA_Shikimic acid	3.72	6.01	0.26	0.73	OA_Shikimic acid	3.72	5.85	0.26	0.16	OA_Shikimic acid	
2.10	0.44	AA_Alanine	2.10	5.12	0.44	2.40	AA_Alanine	2.10	1.41	0.44	0.41	AA_Alanine	
2.52	0.09	OA_Citric acid	2.52	9.19	0.09	1.95	OA_Citric acid	2.52	2.55	0.09	0.26	OA_Citric acid	
2.11	0.65	OA_Malic acid	2.11	3.69	0.65	3.25	OA_Malic acid	2.11	0.94	0.65	0.54	OA_Malic acid	
2.59	0.11	AA_Methionine	2.59	8.12	0.11	0.71	AA_Methionine	2.59	2.88	0.11	0.33	AA_Methionine	
2.74	0.17	AA_Tyrosine	2.74	37.85	0.17	6.09	AA_Tyrosine	2.74	1.65	0.17	0.45	AA_Tyrosine	
2.02	0.09	AA_Valine	2.02	21.19	0.09	3.80	AA_Valine	2.02	1.83	0.09	0.78	AA_Valine	
1.76	0.13	S_Arabitol	1.76	1.68	0.13	0.41	S_Arabitol	1.76	1.92	0.13	1.02	S_Arabitol	
4.82	0.24	S_Glucose	4.82	3.11	0.24	0.34	S_Glucose	4.82	3.42	0.24	0.94	S_Glucose	
3.35	0.27	S_myo inositol	3.35	1.62	0.27	0.40	S_myo inositol	3.35	1.47	0.27	0.19	S_myo inositol	
4.30	0.17	S_Sucrose	4.30	1.00	0.17	0.13	S_Sucrose	4.30	2.60	0.17	0.47	S_Sucrose	
3.84	3.46	OA_Quinic acid	3.84	0.55	3.46	0.60	OA_Quinic acid	3.84	0.75	3.46	0.47	OA_Quinic acid	
0.75	0.08	AA_Homoserine	0.75	3.05	0.08	0.52	AA_Homoserine	0.75	0.92	0.08	0.12	AA_Homoserine	
0.79	0.19	OA_Fumaric acid	0.79	1.18	0.19	1.27	OA_Fumaric acid	0.79	0.87	0.19	0.72	OA_Fumaric acid	
0.83	0.64	S_Erythritol	0.83	0.88	0.64	0.60	S_Erythritol	0.83	0.81	0.64	0.32	S_Erythritol	
0.87	0.20	S_Galactitol	0.87	0.81	0.20	0.84	S_Galactitol	0.87	0.69	0.20	0.67	S_Galactitol	
0.73	0.21	S_Threitol	0.73	1.05	0.21	0.68	S_Threitol	0.73	0.81	0.21	0.52	S_Threitol	
0.44	0.37	S_Ribitol	0.44	0.64	0.37	0.47	S_Ribitol	0.44	0.96	0.37	0.11	S_Ribitol	
0.51	0.39	V_Uracil	0.51	0.74	0.39	0.84	V_Uracil	0.51	0.73	0.39	0.83	V_Uracil	
0.44	0.79	V_Uric acid	0.44	0.89	0.79	2.43	V_Uric acid	0.44	0.51	0.79	1.39	V_Uric acid	



### 5.4.2 Metabolomic analysis of root tissues

Using the reference libraries, a total of 64 metabolites were identified in the metabolic profiles of root tissues from the five wheat genotypes (Supplementary Table 5.3). Metabolites were classified into the following biochemical classes; amino acids organic acids, sugars and a miscellaneous group.

#### 5.4.2.1 Principal Component Analysis (PCA)

To obtain a global view of the metabolic responses of the root tissues, a principal component analysis (PCA) was performed. Results of the PCA showed that first five components explained 81.3% of the overall variance of metabolic profiles (Fig. 5.2-A). The first two components, PC1 and PC2 explained half of the overall variance (50.8%) (Fig. 5.2-B). These two components clearly differentiated the metabolic profiles of *P. thornei* inoculated roots from those of uninoculated roots. Among the *P. thornei* inoculated root samples, the profiles also largely differentiated the genotypes.

The data were also used to construct a dendrogram of the sample replicates (Fig. 5.3). Again, the samples were differentiated on the basis of both treatment and genotype.

Differences in metabolite profiles were observed between the resistant and susceptible genotypes. In order to identify metabolites associated with *P. thornei* resistance, firstly, the metabolite profiles of the parental lines (control and *P. thornei* inoculated) were compared. Secondly, all the samples from nematode challenged roots were compared – both the double haploid lines and the parental lines (resistance vs susceptible).

**Fig. 5.2** Principal Component Analysis (PCA) of the root tissue metabolic profiles of Sokoll, Krichauff and three doubled haploid lines. *Pratylenchus thornei* resistance and susceptible lines are referred as R and S, respectively. *Pratylenchus thornei* inoculated and control samples are referred as I and C, respectively. The first and second principal components explained 51.1% of the variance

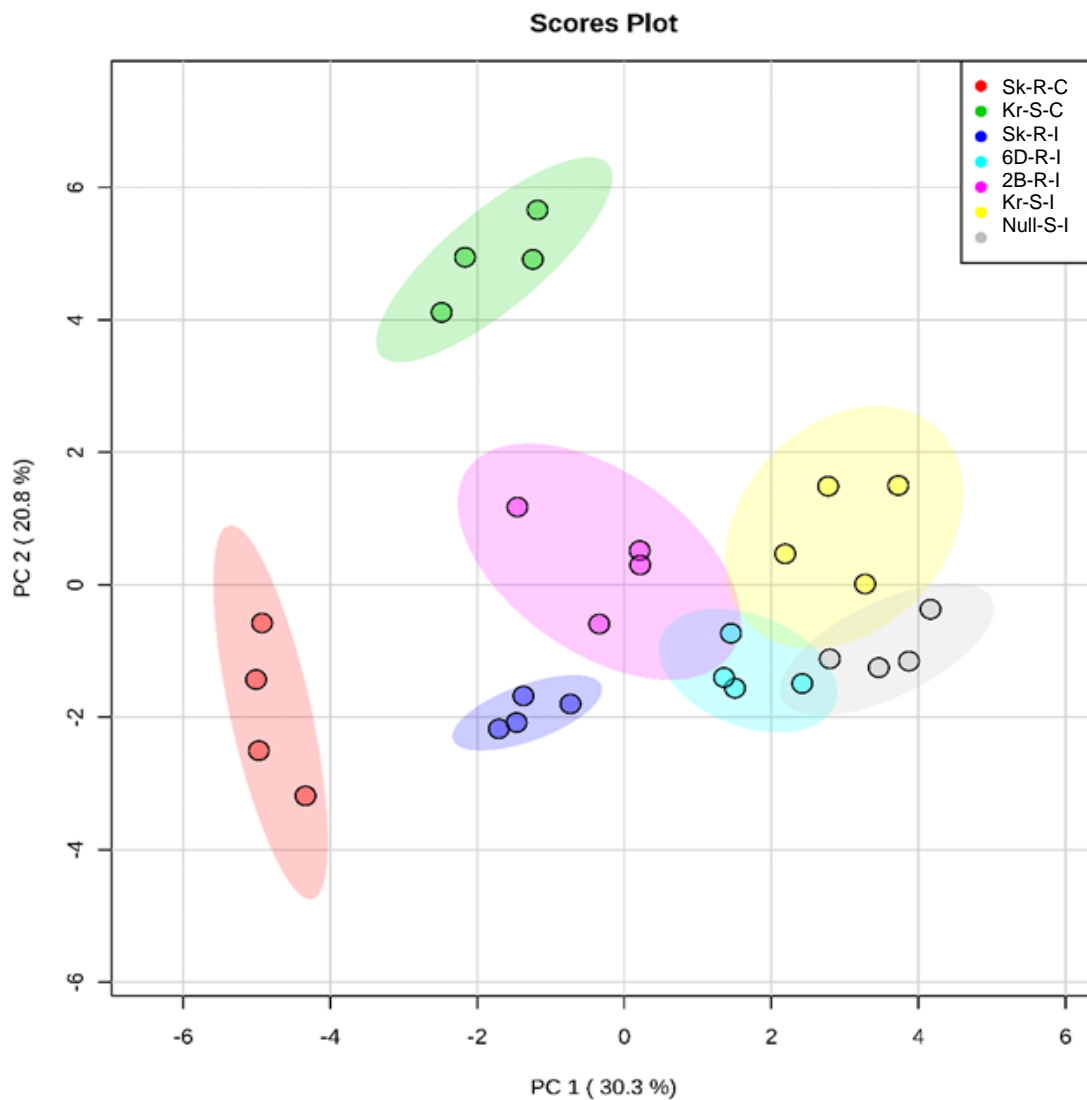
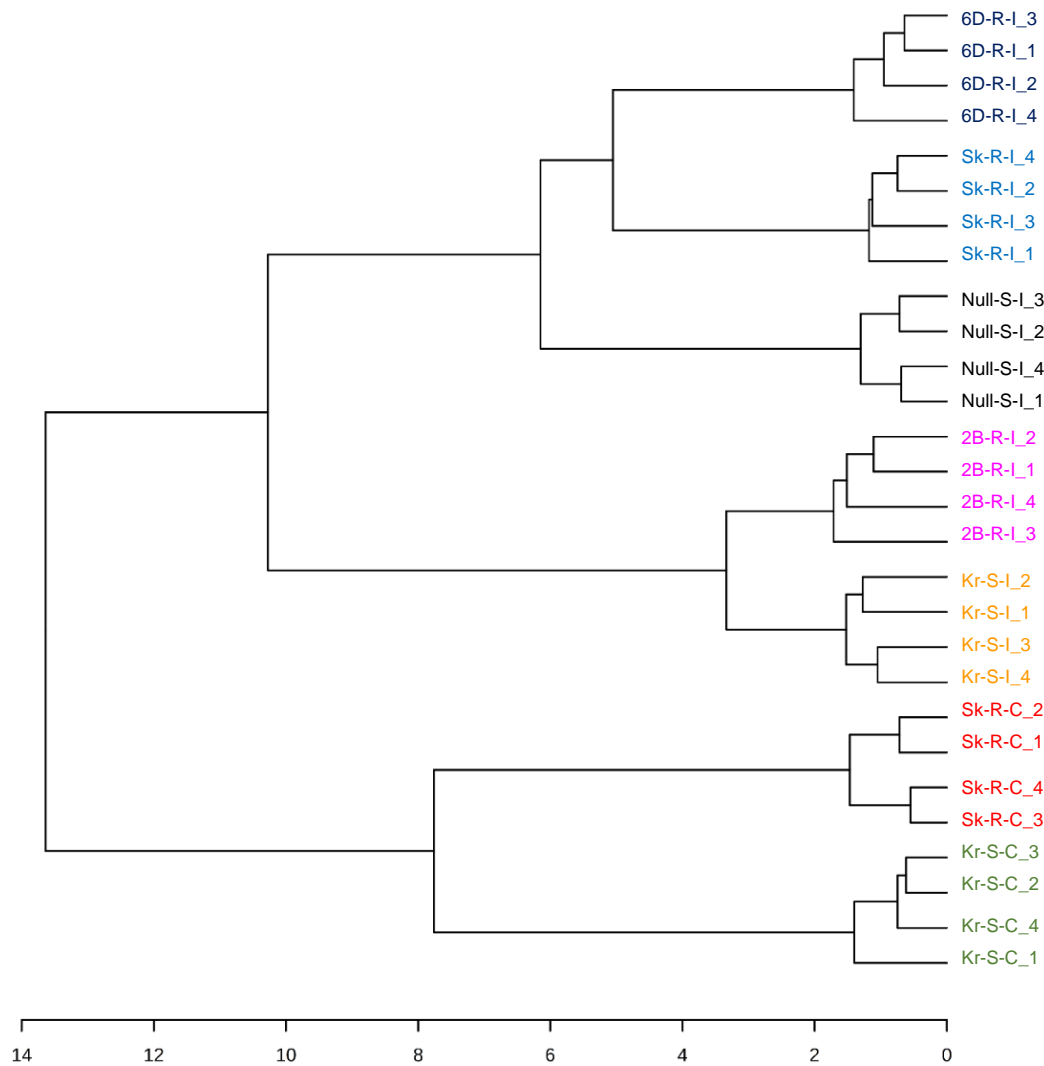


**Fig. 5.3** Dendrogram of root tissue metabolite samples (replicates of genotype treatment combinations) generated using the method of Ward as the algorithm method and the Spearman distance as the dissimilarity coefficient



#### **5.4.2.2 Root tissue metabolite differences between Sokoll and Krichauff**

##### ***Amino acids***

In the absence of nematode challenge, most of the amino acids (14 out of 16) were significantly more abundant in roots of Sk-R-C than in roots of Kr-S-C (Table 5.2). Sk-R-C contained considerably higher amounts of asparagine (21.1-fold), proline (16-fold) and tyrosine (8.4-fold) compared to Kr-S-C. In addition, ten amino acids (threonine, isoleucine, serine, phenylalanine, aspartic acid, beta alanine, pyroglutamic acid, valine, alanine and glycine) were 4.9 to 2.2 times more abundant in Sk-R-C than in Kr-S-C (Table 5.2).

With nematode challenge, levels of six amino acids were significantly different between Sk-R-I and Kr-S-I (Table 5.2). Among these, five amino acids were significantly higher in Sk-R-I than Kr-S-I; proline (2.5-fold), alanine, isoleucine, phenylalanine (1.7-fold) and valine (1.5-fold). The remaining amino acid, glycine, was significantly lower (0.8-fold) in Sk-R-I than in Kr-S-I (Table 5.2).

Within each cultivar, nematode challenge resulted in significant changes. In the susceptible cultivar Krichauff, 13 out of 16 amino acids were more abundant in Kr-S-I than in Kr-S-C (Table 5.2). The largest difference was for asparagine (37.2-fold increase). In the resistant cultivar Sokoll, five amino acids (glycine, beta alanine, 4-amino-butyric acid, pyroglutamic acid and ethanolamine) were significantly lower in Sk-R-I than in Sk-R-C (Table 5.2).

##### ***Organic acids***

In the absence of nematode challenge, levels of five organic acids were significantly higher in Sk-R-C than in Kr-S-C (Table 5.2). These were, gluconic acid (3.9-fold), pipercollic acid (3.0-fold), quinic acid (2.2-fold), benzoic acid (1.6-fold), and glyceric acid (1.5-fold). Citric acid,

threonic acid and malic acid were significantly lower ( $\leq 0.9$ -fold) in Sk-R-C than in Kr-S-C (Table 5.2). With *P. thornei* challenge, levels of four organic acids were significantly higher in Sk-R-I than in Kr-S-I (Table 5.1-B). These were, quinic acid (2.5-fold), malic acid (2.0-fold), shikimic acid (1.8-fold), and gluconic acid (1.6-fold). However, levels of six organic acids were significantly lower ( $\leq 0.8$ -fold) in Sk-R-I than Kr-S-I (Table 5.2). These were ferulic acid, 4-hydroxybenzoic acid, 4-hydroxy-3-methoxybenzoic acid, azelaic acid, 4-hydroxy-cinnamic acid and threonic acid.

Within each cultivar, nematode challenge resulted in significant changes. The level of five organic acids; citric acid, shikimic acid, malic acid, aconitic acid and ribonic acid were significantly higher (2.7-fold to 1.5-fold) in Sk-R-I than in Sk-R-C (Table 5.1-D), while levels of seven organic acids were significantly lower (0.4-fold to 0.7-fold) in Sk-R-I than in Sk-R-C (Table 5.2). In Krichauff, the level of pipercolic acid, ferulic acid and 4-hydroxy-cinnamic acid were significantly higher (2.1-fold to 1.3-fold), and level of malic acid was significantly lower (0.7-fold), in Kr-S-I as compared to Kr-S-C.

### ***Sugars***

In the absence of *P. thornei* challenge, higher level of mannitol (2.5-fold) and myo-inositol (1.6-fold) were observed in Sk-R-C than in Kr-S-C (Table 5.2). Levels of 1-kestose (0.1-fold) and melezitose (0.3-fold) were significantly lower in Sk-R-C than in Kr-S-C. With *P. thornei* challenge, glucose-6-phosphate (3.6-fold), fructose (1.8-fold) and erythritol (1.6-fold) were significantly higher in Sk-R-I than in Kr-S-I (Table 5.2).

With *P. thornei* challenge, 10 sugars differed significantly between Sk-R-I and Sk-R-C (Table 5.2). Among them, four were significantly higher (3.0-fold to 2.5-fold); 1-kestose, sucrose,

melezitose and galactinol, and six metabolites were significantly lower (0.4-fold to 0.7-fold), in Sk-R-I as compared to Sk-R-C (Table 5.2).

### *Miscellaneous*

In the absence of inoculation, Urea was significantly higher (11.3-fold) in Sk-R-C than in Kr-S-C (Table 5.2). Four other metabolites (guanosine, phosphoric acid, adenosine and glycerol) were also significantly higher (2.7-fold to 1.4-fold) in Sk-R-C than in Kr-S-C. After nematode infection, the level of octadecenoic acid was significantly lower in Sk-R-I (0.1-fold) than in Kr-S-I (Table 5.2).

In Krichauff, octadecenoic acid (38.4-fold) and urea (10.1-fold) were significantly higher in Kr-S-I than in Kr-S-C (Table 5.2). However, in Sokoll, the levels of five metabolites were significantly lower (0.4-fold to 0.6-fold) in Sk-R-I than in Sk-R-C (Table 5.2).

**Table 5.2** Fold- differences of metabolites between root samples of *Pratylenchus thornei* resistant (R) and susceptible (S) cultivars Sokoll (Sk) and Krichauff (Kr), respectively. Control (without nematode inoculation) and nematode inoculated are denoted by C and I, respectively. Values that are highlighted in *cyan* have a t-test value (fold- difference between the two samples in the heading of each column) significant at  $P < 0.05$  but not for the Bonferroni-corrected P value. Values that are highlighted in *green* also have a t-test value significant for the Bonferroni-corrected P value (0.05 divided by the number of metabolites)

Metabolites	Sk-R-C/ Kr-S-C	Sk-R-I/ Kr-S-I	Kr-S-I/ Kr-S-C	Sk-R-I/ Sk-R-C
<b>Amino acids</b>				
Alanine	2.4	1.7	1.1	0.8
Valine	2.9	1.5	2.6	1.3
Ethanolamine	1.5	1.0	1.0	0.6
Isoleucine	4.7	1.7	4.4	1.6
Proline	16.0	2.5	3.1	0.5
Glycine	2.2	0.8	2.3	0.8
Serine	4.7	1.3	3.4	0.9
Threonine	4.9	1.3	4.9	1.3
beta Alanine	3.5	1.1	2.3	0.7
Aspartic acid	4.5	0.9	4.9	1.0
Pyroglutamic acid	3.4	1.1	2.2	0.7
4-amino-Butyric acid	1.3	1.0	0.8	0.7
Glutamic acid	1.1	1.0	1.5	1.4
Phenylalanine	4.6	1.7	2.6	0.9
Asparagine	21.1	0.7	37.2	1.2
Tyrosine	8.4	1.9	4.7	1.1
<b>Organic acids</b>				
Glycolic acid	1.0	0.9	0.9	0.7
Benzoic acid	1.6	1.1	0.9	0.6
Succinic acid	0.8	0.9	1.1	1.2
Glyceric acid	1.5	1.0	0.8	0.5
Fumaric acid	0.9	1.1	1.0	1.2
Pipecolic acid	3.0	0.9	2.1	0.6
Threonic acid	0.8	0.8	0.9	1.0
2-hydroxyglutaric acid	1.3	1.1	1.2	1.0
4-hydroxy benzoic acid	1.1	0.5	1.3	0.6
Aconitic acid	0.8	1.4	1.0	1.6
2-ketao-L-gluconic acid	0.9	1.1	0.9	1.1
Ribonic acid	0.7	0.9	1.1	1.5
4-hydroxy-3-methoxybenzoic acid	1.1	0.6	1.3	0.6
Azelaic acid	1.2	0.6	0.9	0.4
Shikimic acid	1.2	1.8	1.2	1.9
Quinic acid	2.2	2.5	1.1	1.2
4-hydroxy-Cinnamic acid	1.1	0.7	1.3	0.8

Gluconic acid	3.9	1.6	1.0	0.4
Ferulic acid	1.3	0.5	1.7	0.7
Malic acid	0.9	2.0	0.7	1.6
Citric acid	0.5	1.2	1.1	2.7
<b>Sugars</b>				
Erythritol	1.5	1.6	0.7	0.7
Xylose	0.9	0.4	1.3	0.5
Xylitol	1.3	0.9	0.7	0.5
Rhamnose	0.9	0.8	0.8	0.7
Arabitol	1.4	1.0	0.8	0.6
Ribitol	0.8	1.2	0.4	0.6
Mannitol	2.5	1.2	0.7	0.4
myo-Inositol	1.6	1.0	1.0	0.6
Glucose-6- phosphate	1.7	3.6	0.3	0.5
Trehelose	1.0	1.2	0.7	0.9
beta-Gentibiose	0.7	1.5	0.4	0.8
Galactinol	0.7	1.4	1.2	2.5
1-Kestose	0.1	0.9	0.4	3.0
Melezitose	0.3	1.2	0.6	2.6
Fructose	1.0	1.8	0.4	0.8
Glucose	0.8	1.8	0.4	0.9
Sucrose	0.6	1.5	1.0	2.6
<b>Miscellaneous</b>				
Urea	11.3	0.7	10.1	0.7
Glycerol	1.4	0.8	1.2	0.6
Phosphoric acid	1.8	1.2	0.6	0.4
Putrescine	1.0	0.7	2.2	1.6
Glycerol-3-phosphate	1.7	1.1	0.7	0.4
Hexadecanoic acid	1.3	0.9	1.0	0.7
Octadecenoic acid	1.8	0.1	38.4	2.3
Eicosanoic acid	2.0	0.9	1.3	0.6
Adenosine	1.4	0.8	1.3	0.7
Guanosine	2.7	0.8	2.0	0.6



### 5.4.2.3 Differences in metabolites of *P. thornei* challenged roots associated with resistance QTL

To identify metabolites related to resistance QTL, metabolites in resistant lines (Sk-R-I, 6D-R-I and 2B-R-I) were compared with those of susceptible lines (Kr-S-I and Null-S-I). Important features are described in Table 5.3 and a more detailed analysis is presented in Supplementary Table 5.4.

Firstly, the levels of metabolites in Sk-R-I were compared to those in Kr-S-I and Null-S-I to identify the metabolites associated with both loci. Secondly, Sk-R-I and 6D-R-I were compared with Kr-S-I and Null-S-I to identify 6D-QTL associated metabolites. Likewise, Sk-R-I and 2B-R-I were compared with Kr-S-I and Null-S-I to identify 2B-QTL associated metabolites. A total of 15 metabolites were found to be higher ( $\geq 1.1$ -fold) in Sk-R-I than in Kr-S-I and Null-S-I (Table 5.3, section A). Nine of these metabolites were amino acids (alanine, beta alanine, isoleucine, phenylalanine, pyroglutamic acid, serine, threonine, tyrosine and valine), three were organic acids (2-hydroxyglutaric acid, aconitic acid and benzoic acid) two were sugars (galactinol and mannitol) and one was from the miscellaneous group (phosphoric acid). Apart from three metabolites (2-hydroxyglutaric acid, galactinol and mannitol), the remaining 12 metabolites were also found to be associated with the 6D-QTL ( $\geq 1.1$ -fold higher in Sk-R-I and 6D-R-I than in Kr-S-I and Null-S-I) (Table 5.3, section B). Benzoic acid was the only metabolites found to be associated with 2B-QTL ( $\geq 1.1$ -fold higher in Sk-R-I and 2B-R-I than in Kr-S-I and Null-S-I) (Table 5.3, section C).

A total of 13 metabolites were also found to be lower ( $\leq 0.9$ -fold) in Sk-R-I than in Kr-R-I and Null-S-I (Table 5.3, section A). These comprised one amino acid (asparagine), five organic acids (4-hydroxy benzoic acid, ferulic acid, glycolic acid, pipecolic acid and threonic acid),

three sugars (1-kestose, rhamnose and xylose) and four from the miscellaneous group (eicosanoic acid, glycerol, hexadecenoic acid and octadecenoic acid). Of the 13 metabolites, six metabolites (asparagine, pipecolic acid, threonic acid, 1-kestose, rhamnose and octadecenoic acid) were found to be associated with the 2B-QTL ( $\leq 0.9$ -fold lower in Sk-R-I and 2B-R-I than in Kr-S-I and Null-S-I) (Table 5.3, section C). Likewise, four metabolites (rhamnose, octadecenoic acid, xylose and glycerol) were found to be associated with the 6D-QTL ( $\leq 0.9$ -fold lower in Sk-R-I and 6D-R-I than in Kr-S-I and Null-S-I) (Table 5.3, section B).

#### **5.4.2.4 Metabolic analysis of nematode samples**

A total of 50 metabolites were identified by GC-MS in the *P. thornei* samples (Supplementary Table 5.5). These compounds included eight amino acids, eight organic acids, six sugars, 14 miscellaneous metabolites and 14 unknown metabolites.

**Table 5.3** Analysis of metabolites in root tissues associated with *Pratylenchus thornei* resistance. The level of metabolites (fold-difference) were compared between resistant (Sk-R-I, 6D-R-I and 2B-R-I) and susceptible (Kr-S-I and Null-S-I) lines to identify metabolites associated with 6D+2B (Section A), 6D (Section B) or 2B (Section C) QTL. 1: Fold-differences were calculated based on average values from four replicates. 2: Highlights shows where compounds were significantly (t-test,  $P < 0.05$ ) higher (green colour) or lower (blue colour) in resistant line compared to the susceptible line. AA, OA, S and M refers to amino acids, organic acids, sugars and miscellaneous biochemical groups

A. Differences in metabolites associated with 6D+2B QTL			B. Differences in metabolites associated with 6D QTL					C. Differences in metabolites associated with 2B QTL				
Fold-difference (Average) <sup>1</sup>		Metabolites <sup>2</sup>	Fold-difference (Average) <sup>1</sup>		Metabolites <sup>2</sup>			Fold-difference (Average) <sup>1</sup>		Metabolites <sup>2</sup>		
Sk-R-I/ Kr-S-I	Sk-R-I/ Null-S-I		Sk-R-I/ KR-S-I	6D-R-I /KR-S-I	Sk-R-I/ Null-S-I	6D-R-I/ Null-R-I		Sk-R-I/ Kr-S-I	2B-R-I/ KR-S-I	Sk-R-I/ Null-S-I	2B-R-I/ Null-S-I	
1.7	1.1	AA_Alanine	1.7	1.9	1.1	1.2	AA_Alanine	1.7	0.7	1.1	0.5	AA_Alanine
1.1	3.5	AA_beta Alanine	1.1	1.3	3.5	4.2	AA_beta Alanine	1.1	0.4	3.5	1.4	AA_beta Alanine
1.7	1.3	AA_Isoleucine	1.7	1.7	1.3	1.3	AA_Isoleucine	1.7	0.7	1.3	0.5	AA_Isoleucine
1.7	1.2	AA_Phenylalanine	1.7	2.1	1.2	1.5	AA_Phenylalanine	1.7	0.9	1.2	0.6	AA_Phenylalanine
1.1	1.2	AA_Pyroglutamic acid	1.1	1.8	1.2	2.0	AA_Pyroglutamic acid	1.1	0.6	1.2	0.6	AA_Pyroglutamic acid
1.3	1.4	AA_Serine	1.3	1.5	1.4	1.6	AA_Serine	1.3	0.5	1.4	0.5	AA_Serine
1.3	1.6	AA_Threonine	1.3	1.5	1.6	1.8	AA_Threonine	1.3	0.6	1.6	0.7	AA_Threonine
1.9	2.0	AA_Tyrosine	1.9	2.7	2.0	2.9	AA_Tyrosine	1.9	0.7	2.0	0.8	AA_Tyrosine
1.5	1.5	AA_Valine	1.5	1.5	1.5	1.4	AA_Valine	1.5	0.7	1.5	0.7	AA_Valine
1.1	1.3	OA_2-hydroxyglutaric acid	1.1	1.0	1.3	1.2	OA_2-hydroxyglutaric acid	1.1	0.9	1.3	1.1	OA_2-hydroxyglutaric acid
1.4	1.2	OA_Aconitic acid	1.4	1.7	1.2	1.6	OA_Aconitic acid	1.4	1.1	1.2	1.0	OA_Aconitic acid
1.1	1.4	OA_Benzoic acid	1.1	1.2	1.4	1.4	OA_Benzoic acid	1.1	1.1	1.4	1.3	OA_Benzoic acid
1.4	1.3	S_Galactinol	1.4	0.9	1.3	0.8	S_Galactinol	1.4	1.1	1.3	1.0	S_Galactinol
1.2	1.6	S_Mannitol	1.2	1.0	1.6	1.2	S_Mannitol	1.2	0.8	1.6	1.0	S_Mannitol
1.2	1.4	M_Phosphoric acid	1.2	1.2	1.4	1.4	M_Phosphoric acid	1.2	0.9	1.4	1.0	M_Phosphoric acid
0.7	0.6	AA_Asparagine	0.7	2.2	0.6	2.2	AA_Asparagine	0.7	0.4	0.6	0.4	AA_Asparagine
0.5	0.8	OA_4-hydroxy benzoic acid	0.5	0.7	0.8	1.2	OA_4-hydroxy benzoic acid	0.5	0.7	0.8	1.2	OA_4-hydroxy benzoic acid
0.5	0.9	OA_Ferulic acid	0.5	0.8	0.9	1.3	OA_Ferulic acid	0.5	0.7	0.9	1.2	OA_Ferulic acid
0.9	0.9	OA_Glycolic acid	0.9	1.0	0.9	1.0	OA_Glycolic acid	0.9	0.9	0.9	0.9	OA_Glycolic acid
0.9	0.3	OA_Pipecolic acid	0.9	2.8	0.3	1.1	OA_Pipecolic acid	0.9	0.8	0.3	0.3	OA_Pipecolic acid
0.8	0.5	OA_Threonic acid	0.8	1.0	0.5	0.6	OA_Threonic acid	0.8	0.8	0.5	0.5	OA_Threonic acid
0.9	0.2	S_1-Kestose	0.9	1.4	0.2	0.3	S_1-Kestose	0.9	0.8	0.2	0.2	S_1-Kestose
0.8	0.8	S_Rhamnose	0.8	0.7	0.8	0.6	S_Rhamnose	0.8	0.9	0.8	0.8	S_Rhamnose
0.4	0.9	S_Xylose	0.4	0.3	0.9	0.8	S_Xylose	0.4	0.5	0.9	1.2	S_Xylose
0.9	0.7	M_Eicosanoic acid	0.9	1.1	0.7	0.8	M_Eicosanoic acid	0.9	1.1	0.7	0.8	M_Eicosanoic acid
0.8	0.8	M_Glycerol	0.8	0.9	0.8	0.9	M_Glycerol	0.8	0.9	0.8	1.0	M_Glycerol
0.9	0.8	M_Hexadecanoic acid	0.9	1.0	0.8	0.9	M_Hexadecanoic acid	0.9	1.0	0.8	0.9	M_Hexadecanoic acid
0.1	0.2	M_Octadecenoic acid	0.1	0.3	0.2	0.4	M_Octadecenoic acid	0.1	0.4	0.2	0.5	M_Octadecenoic acid

## 5.5 Discussion

Root exudates and root tissues from wheat cultivar Sk-R showed nematotoxic properties against *P. thornei* (Linsell et al. 2014). To reveal the biochemical basis of this resistance, metabolic profiles of root exudates and root tissues from Sk-R and related resistant wheat lines 6D-R and 2B-R were compared with those of the susceptible lines Kr-S and Null-S. In the following sections the outcome of these two experiments are discussed.

### 5.5.1 Analysis of root exudates

Growth and development of *P. thornei* was previously reported to be affected by root exudates, more so in the exudates from Sokoll (Sk-R) than those from Krichauff (Kr-S). Sokoll root exudates inhibited egg hatching, suppressed mobility and induced a state of quiescence in *P. thornei* as compared to Krichauff (Linsell et al. 2014). To understand the biochemical basis of this resistance, the present experiment was undertaken to compare the metabolic profiles of root exudates from Sk-R and Kr-S using the GC-MS platform. In addition, metabolic profiles of doubled haploid lines representing 6D, 2B and Null QTLs were also compared to identify candidate metabolites associated with the resistance loci.

Non-targeted GC-MS based metabolic analysis identified a total of 100 root exudate metabolites from diverse biochemical groups including amino acids, organic acids, sugars and miscellaneous compounds. These profiles are generally consistent with those seen in other studies of root exudates in wheat (Fan et al. 2001; Warren 2015). Significant differences were observed between resistant (Sk-R, 6D-R and 2B-R) and susceptible genotypes (Kr-S and Null-S) for certain metabolites. This supports the hypothesis that differences in root exudate composition of genotypes can influence the outcome of host-nematode interactions in the rhizosphere (Bais et al. 2006; Li et al. 2013). In an incompatible host-nematode relationship,

compounds in root exudates might restrict the nematodes by (i) paralysing (nematostatic compounds), (ii) killing (nematicide compounds), (iii) repelling the nematodes from the host (repelling compounds), or (iv) inhibiting egg hatching (egg hatching inhibiting compounds) (Huang et al. 2014; Rocha et al. 2017). On the other hand, in a compatible host-nematode relationship, compounds in root exudates might act as chemoattractant that allow the nematodes to locate their hosts (Curtis 2008; Fleming et al. 2017).

In the present experiment, 21 metabolites were found to be significantly higher in root exudates of Sk-R than in those of Kr-S and were therefore potentially associated with both 6D and 2B QTL. Of these, four were also found to be higher in 6D-R than in Kr-S, indicating a possible association with the 6D-QTL. Likewise, ten metabolites were found to be higher in 2B-R than in Kr-S and were therefore potentially associated with the 2B QTL. However, these metabolites were not found to be consistently higher in 6D-R and 2B-R as compared to Null-S. Further study is required to identify whether this variation resulted from the null-S line itself. Nevertheless, the above mentioned 21 metabolites were found to be higher in one or more of the resistance genotypes (Sk-R, 6D-R and 2B-R) as compared to the susceptible genotype Kr-S, indicating their possible role in resistance.

The 21 aforementioned resistance-associated metabolites comprised seven amino acids, eight organic acids and six sugars. Their possible roles in an incompatible wheat-*P. thornei* relationship is unknown. However, some of these compounds have been shown to possess nematotoxic (nematostatic and nematicidal) and egg hatching inhibition properties by *in-vitro* bioassays in which nematode behaviour (eg. motility, mortality, attraction, egg hatching) was studied in response to exogenous application of commercially sourced chemical compounds (eg. Čepulytė et al. 2018; Dutta et al. 2012; Linsell et al. 2014).

### ***Amino acids***

According to the present study, seven amino acids in root exudates (4-amino butyric acid, alanine, beta-alanine, methionine, proline, tyrosine and valine) were identified as potentially contributing to *P. thornei* resistance. Previous studies reported activity of these amino acids against plant parasitic nematodes. For instance, in *in vitro* bioassays alanine, proline and valine inhibited *M. incognita* egg hatching (Tanda et al. 1989). Methionine inhibited *M. incognita* egg hatching *in vitro* ( Reddy et al. 1975). Valine and proline were also found to be nematotoxic against *M. incognita* second-stage juveniles (J2) (Reddy et al. 1975). Valine was also reported to be toxic for *Caenorhabditis elegans* (Perelman and Lu 2000).

### ***Organic acids***

In the present study, the level of eight organic acids were higher in root exudates of the resistant genotypes than in those of the susceptible genotypes. These were 2-hydroxy glutaric acid, 4-hydroxy-benzoic acid, citric acid, glutaric acid, glyceric acid, malic acid, quinic acid and shikimic acid. These organic acids may possess nematotoxic activity against *P. thornei*. Previously, organic acids were reported to be toxic against plant parasitic nematodes. For example:

- 4-hydroxybenzoic acid caused strong mortality of *M. incognita* second-stage juveniles (J2) larvae in an *in vitro* bioassay. Nearly 100% of *M. incognita* J2 larvae died after 72 h of contact with 4-hydroxybenzoic acid at the highest tested concentration (400 µg mL<sup>-1</sup>) (Bogner et al. 2017). Hydroxybenzoic acids were also found to be act as repellents against *Radopholus similis* in an *in vitro* bioassay (Nathalie et al. 2006).
- Exposure of the plant parasitic nematode *M. incognita* to citric acid *in vitro* decreased egg hatching by 94% and completely immobilized second-stage juveniles after 4-6 days of exposure (Shemshura et al. 2016).

- Chemotactic responses of *M. incognita* and *G. pallida* to selected phytochemicals were investigated. Quinic was identified as a repellent of *M. incognita* and *G. pallida* relative to the negative control (Fleming et al. 2017).
- Malic acid and citric acid at concentration of 0.5 µg/µL demonstrated a nematostatic activity, paralyzing 90% *M. incognita* J2 after 48 h exposure (Rocha et al. 2017).

### **Sugars**

The root exudate sugar compounds that have potential to act against *P. thornei* nematodes were arabinol, fructose, glucose, maltose, myo inositol and sucrose. Previously, glucose was identified as nematotoxic against *M. incognita* J2. Treating *M. incognita* J2 for 48 h at 0.26 µg/µL paralyzed the majority of the nematodes. Moreover, glucose at higher concentration (0.5 µg/µL) exhibited a nematicidal effect, killing more than 90% of J2 after 48h exposure (Rocha et al. 2017). In another study, *G. pallida* infective stage juveniles were repelled by glucose (50 mM) relative to negative control (Warnock et al. 2016).

Molecules in root exudates also act as chemo-attractants that cause nematodes to migrate towards the roots (Fleming et al. 2017; Liu and Park 2018). Studies have illustrated that monosaccharide sugars, amino acids can act as chemo-attractants for plant parasitic nematodes (Warnock et al. 2016). In the present experiment, levels of four sugar compounds, erythritol, galactinol, ribitol and threitol were significantly lower in resistant genotypes relative to the susceptible genotypes. Further studies are required to see whether these compounds act as chemo-attractants for *P. thornei* and related root lesion nematode species.

GC-MS based metabolic analysis of wheat root exudates identified several metabolites that could potentially act against *P. thornei* nematodes. To test their effect against *P. thornei*, these

compounds require further investigation. Commercially sourced compounds can be applied to nematodes to see their effect on egg hatching, motility and migration. Whether synthesis of these nematotoxic compounds are induced by nematode infection also requires further investigation. Production and release of root-derived compounds are commonly constitutive, but may be induced by biotic stress (Badri and Vivanco 2009). For instance, nematodes change the metabolite level in root exudates of tomato and *Plantago* (Escudero et al. 2014; Wurst et al. 2010).

### **5.5.2 Metabolic profiling of wheat roots challenged by *P. thornei***

#### **5.5.2.1 Constitutively synthesized metabolites**

At first, metabolic profiles of root tissues from Sk-C-R and Kr-C-S were compared. In the absence of nematode challenge, 26 metabolites from diverse biochemical groups were found to be significantly higher in Sk-C-R compared to Kr-C-S. It will be worthwhile to investigate whether these constitutively synthesized metabolites are involved in *P. thornei* resistance in wheat.

Amino acids might play a significant role in *P. thornei* resistance. A total of 14 amino acids were synthesized constitutively at higher level in Sk-C-R than in Kr-C-S. Among these amino acids, levels of asparagine and proline were considerably higher (21.1-fold and 16-fold, respectively) in Sk-C-R than Kr-C-R. It is unknown whether higher level of root asparagine and proline contribute any resistance against plant parasitic nematodes. However, roles of asparagine and proline in plant defence against microbial pathogens have been described. For example, in pepper (*Capsicum annum*), increased level of asparagine synthetase (major enzyme for asparagine biosynthesis) was associated with resistance to *Pseudomonas syringae* and



*Hyaloperonospora arabidopsidis* (Hwang et al. 2011). Likewise, synthesis of pyrroline-5-carboxylate (an intermediate product of proline biosynthesis) has a role in resistance against *Pseudomonas syringae* in tobacco and Arabidopsis (Qamar et al. 2015). Whether wheat asparagine synthetase and pyrroline-5-carboxylate involves in *P. thornei* resistance, is yet to be investigated.

#### **5.5.2.2 Changes in wheat metabolites after *P. thornei* challenge**

Under *P. thornei* challenge, several metabolites were found to be more abundant in resistant wheat genotypes as compared to the susceptible genotypes. Fifteen metabolites were higher in 6D and /or 2B resistance QTL lines as compared to the lines lacking these resistance alleles. These comprised nine amino acids, three organic acids, two sugars and one from the miscellaneous group. Likewise, thirteen metabolites were lower in the 6D and /or 2B lines as compared to the lines lacking these resistance alleles. There were four organic acids, three sugars, one amino acid and four from the miscellaneous group.

#### ***Amino acids***

Previous studies indicated that total amino acid concentration in plant roots changed upon nematode infection (Hofmann et al. 2010; Shukla et al. 2018). In the present study, levels of nine amino acids were higher in resistant lines compared to susceptible lines. All these amino acids were found to be associated with the 6D-QTL. Among these amino acids, alanine, beta alanine and threonine have been shown to act against plant parasitic nematodes. For instance, higher root alanine content (relative to control) were found in *M. graminicola* resistance rice cultivars (Jena and Seshagiri Rao 1977). Up-regulation of alanine and beta-alanine was also found to be associated with *M. incognita* resistance in tomato (Eloh et al. 2016). In another

study, when threonine was added to the nutrient medium in Arabidopsis culture, the number of female *M. incognita* were significantly reduced in the host plant (Blümel et al. 2018).

### ***Organic acids***

In *P. thornei* challenged roots, three organic acids (benzoic acid, aconitic acid and 2-hydroxyglutaric acid) were higher in resistant wheat lines than in the susceptible lines. Among these, benzoic acid was associated with both the 6D and 2B QTL and aconitic acid was associated only with the 6D QTL. Benzoic acid is the immediate precursor of salicylic acid (SA) (Chen et al. 2009). In tomato, resistance against *M. incognita* was found to be associated with increased SA content in plant tissue (Zinovieva et al. 2011). SA might act as signalling component towards this resistance. SA is an important component of the signalling that leads to root-knot nematode resistance and the associated hypersensitive response in tomato (Branch et al. 2004). In another study, aconitic acid was found to possess nematotoxic properties against *M. incognita* (Rocha et al. 2017). These studies suggest that benzoic acid and aconitic might contribute in *P. thornei* resistance in wheat.

### ***Sugars***

Galactinol and mannitol were found to be higher in Sk-R-I than Kr-S-I and Null-S-I and might act in *P. thornei* resistance at both 6D and 2B loci. Galactinol was previously been reported as a nematotoxic compound. For instance, exogenous application of galactinol to Arabidopsis resulted a significant decrease in numbers of *H. schachtii* compared to the control. The nematotoxic effect of galactinol on *H. schachtii* was also observed *in vitro* and it might be involved in resistance signalling and act as osmoprotectant for this resistance (Siddique et al. 2014).

In *P. thornei* challenged roots, 13 metabolites were lower in Sk-R-I than in Kr-R-I and Null-S-I, suggesting a possible contribution of these compounds to compatible host-nematode interactions. For instance, the level of three sugar molecules were significantly lower in resistant lines as compared to susceptible lines. 1-kestose was found to be lower in Sk-R-I and 2B-R-I compared to Kr-S-I and Null-S-I. In a previous study, *H. schachtii* infection was shown to increase levels of 1-kestose in Arabidopsis roots. In a compatible host-nematode interaction, 1-kestose was proposed to play an essential role in the nematode diet as a carbohydrate source (Hofmann et al. 2010). Up-regulation of certain metabolites in Krichauff might promote *P. thornei* infection by providing source of nutrients for nematodes, assisting in host cell degradation processes and interrupting host resistance mechanisms (Qiao et al. 2019).

Metabolic profiling of samples collected at a single time point (six weeks after nematode infection) was one of the limitations of the current investigation. Metabolites in plants change throughout the various stages of nematode or fungal infection (Afzal et al. 2009; Hofmann et al. 2010; Scandiani et al. 2015). Future studies should consider sampling from various nematode infection stages, such as early, mid and late.

## 5.6 References

- Afzal AJ, Natarajan A, Saini N, Iqbal MJ, Geisler M, El Shemy HA, Mungur R, Willmitzer L, Lightfoot DA (2009) The nematode resistance allele at the *rhg1* locus alters the proteome and primary metabolism of soybean roots. *Plant Physiology* 151:1264-1280
- Aliferis KA, Faubert D, Jabaji S (2014) A metabolic profiling strategy for the dissection of plant defense against fungal pathogens. *PLOS ONE* 9:e111930. <https://doi.org/10.1371/journal.pone.0111930>
- Allwood JW, Ellis DI, Goodacre R (2008) Metabolomic technologies and their application to the study of plants and plant–host interactions. *Physiologia Plantarum* 132:117-135
- Badri DV, Vivanco JM (2009) Regulation and function of root exudates. *Plant, Cell and Environment* 32:666-681
- Bais HP, Weir TL, Perry LG, Gilroy S, Vivanco JM (2006) The role of root exudates in rhizosphere interactions with plants and other organisms. *Annual Review of Plant Biology* 57:233-266
- Bertin C, Yang X, Weston LA (2003) The role of root exudates and allelochemicals in the rhizosphere. *Plant and Soil* 256:67-83
- Bogner CW, Kamdem RST, Sichtermann G, Matthäus C, Hölscher D, Popp J, Proksch P, Grundler FMW, Schouten A (2017) Bioactive secondary metabolites with multiple activities from a fungal endophyte. *Microbial Biotechnology* 10:175-188
- Bowsher AW, Ali R, Harding SA, Tsai C-J, Donovan LA (2015) Analysis of wild sunflower (*Helianthus annuus* L.) root exudates using gas chromatography-mass spectrometry. *Journal of Plant Nutrition and Soil Science* 178:776-786
- Branch C, Hwang C-F, Navarre DA, Williamson VM (2004) Salicylic acid is part of the *Mi-1*-mediated defense response to root-knot nematode in tomato. *Molecular Plant-Microbe Interactions* 17:351-356
- Camañes G, Scalschi L, Vicedo B, González-Bosch C, García-Agustín P (2015) An untargeted global metabolomic analysis reveals the biochemical changes underlying basal resistance and priming in *Solanum lycopersicum*, and identifies 1-methyltryptophan as a metabolite involved in plant responses to *Botrytis cinerea* and *Pseudomonas syringae*. *The Plant Journal* 84:125-139
- Čepulytė R, Danquah WB, Bruening G, Williamson VM (2018) Potent attractant for root-knot nematodes in exudates from seedling root tips of two host species. *Scientific Reports* 8:10847. <https://doi.org/10.1038/s41598-018-29165-4>
- Chen Z, Zheng Z, Huang J, Lai Z, Fan B (2009) Biosynthesis of salicylic acid in plants. *Plant Signal Behav* 4:493-496

Curtis RH (2008) Plant-nematode interactions: environmental signals detected by the nematode's chemosensory organs control changes in the surface cuticle and behaviour. *Parasite* 15:310-316

Dakora FD, Phillips DA (2002) Root exudates as mediators of mineral acquisition in low-nutrient environments. *Plant and Soil* 245:35-47

Dutta TK, Powers SJ, Gaur HS, Birkett M, Curtis RHC (2012) Effect of small lipophilic molecules in tomato and rice root exudates on the behaviour of and *Nematology* 14:309-320

Eloh K, Sasanelli N, Maxia A, Caboni P (2016) Untargeted metabolomics of tomato plants after root-knot nematode infestation. *Journal of Agricultural and Food Chemistry* 64:5963-5968

Escudero N, Marhuenda-Egea FC, Ibanco-Cañete R, Zavala-Gonzalez EA, Lopez-Llorca LV (2014) A metabolomic approach to study the rhizodeposition in the tritrophic interaction: tomato, *Pochonia chlamydosporia* and *Meloidogyne javanica*. *Metabolomics* 10:788-804

Fan TWM, Lane AN, Shenker M, Bartley JP, Crowley D, Higashi RM (2001) Comprehensive chemical profiling of gramineous plant root exudates using high-resolution NMR and MS. *Phytochemistry* 57:209-221

Faure D, Vereecke D, Leveau JHJ (2009) Molecular communication in the rhizosphere. *Plant and Soil* 321:279-303

Fleming TR, Maule AG, Fleming CC (2017) Chemosensory responses of plant parasitic nematodes to selected phytochemicals reveal long-term habituation traits. *Journal of nematology* 49:462-471

Gaur H, Beane J, Perry R (2000) The influence of root diffusate, host age and water regimes on hatching of the root-knot nematode, *Meloidogyne triticroyzae*. *Nematology* 2:191-199

Hiltbold I, Jaffuel G, Turlings TCJ (2015) The dual effects of root-cap exudates on nematodes: from quiescence in plant-parasitic nematodes to frenzy in entomopathogenic nematodes. *Journal of Experimental Botany* 66:603-611

Hofmann J, El Ashry AEN, Anwar S, Erban A, Kopka J, Grundler F (2010) Metabolic profiling reveals local and systemic responses of host plants to nematode parasitism. *The Plant Journal* 62:1058-1071

Huang X-F, Chaparro JM, Reardon KF, Zhang R, Shen Q, Vivanco JM (2014) Rhizosphere interactions: root exudates, microbes, and microbial communities. *Botany* 92:267-275

Hwang IS, An SH, Hwang BK (2011) Pepper *asparagine synthetase 1* (*CaASI*) is required for plant nitrogen assimilation and defense responses to microbial pathogens. *The Plant Journal* 67:749-762

Jena RN, Seshagiri Rao Y (1977) Nature of resistance in rice (*Oryza sativa* L.) to the root-knot nematode (*Meloidogyne graminicola* Golden and birchheld). II. Mechanisms of resistance. *Proceedings of the Indian Academy of Sciences - Section B* 86:33-38

Jones DL, Nguyen C, Finlay RD (2009) Carbon flow in the rhizosphere: carbon trading at the soil–root interface. *Plant and Soil* 321:5-33

Khokon MAR, Okuma E, Rahman T, Wesemael WML, Murata Y, Moens M (2009) Quantitative analysis of the effects of diffusates from plant roots on the hatching of *Meloidogyne chitwoodi* from young and senescing host plants. *Bioscience, Biotechnology, and Biochemistry* 73:2345-2347

Kumar Y, Dholakia BB, Panigrahi P, Kadoo NY, Giri AP, Gupta VS (2015) Metabolic profiling of chickpea-Fusarium interaction identifies differential modulation of disease resistance pathways. *Phytochemistry* 116:120-129

Li X-g, Zhang T-l, Wang X-x, Hua K, Zhao L, Han Z-m (2013) The composition of root exudates from two different resistant peanut cultivars and their effects on the growth of soil-borne pathogen. *International Journal of Biological Sciences* 9:164-173

Linsell KJ, Riley IT, Davies KA, Oldach KH (2014) Characterization of resistance to *Pratylenchus thornei* (nematoda) in wheat (*Triticum aestivum*): attraction, penetration, motility, and reproduction. *Phytopathology* 104:174-187

Liu W, Park S-W (2018) Underground mystery: Interactions between plant roots and parasitic nematodes. *Current Plant Biology* 15:25-29

López-Gresa MP, Lisón P, Campos L, Rodrigo I, Rambla JL, Granell A, Conejero V, Bellés JM (2017) A non-targeted metabolomics approach unravels the vocs associated with the tomato immune response against *Pseudomonas syringae*. *Frontiers in Plant Science* 8:1188. <https://doi.org/10.3389/fpls.2017.01188>

Luo Q, Wang S, Sun L-n, Wang H (2017) Metabolic profiling of root exudates from two ecotypes of *Sedum alfredii* treated with Pb based on GC-MS. *Scientific Reports* 7:39878. <https://doi.org/10.1038/srep39878>

Machado ART, Campos VAC, da Silva WJR, Campos VP, Zeri ACdM, Oliveira DF (2012) Metabolic profiling in the roots of coffee plants exposed to the coffee root-knot nematode, *Meloidogyne exigua*. *European Journal of Plant Pathology* 134:431-441

Nathalie W, Rony S, Dirk De W (2006) Effects of plant phenylpropanoid pathway products and selected terpenoids and alkaloids on the behaviour of the plant-parasitic nematodes *Radopholus similis*, *Pratylenchus penetrans* and *Meloidogyne incognita*. *Nematology* 8:89-101

Oka Y, Mizukubo T (2009) Tomato culture filtrate stimulates hatching and activity of *Meloidogyne incognita* juveniles. *Nematology* 11:51-61

Reddy PR, Govindu HC, Shetty KGH (1975) Studies on the effect of amino acids on the root-knot nematode *Meloidogyne incognita* infecting tomato. *Indian Journal of Nematology* 5:36-41

Perelman D, Lu N (2000) Requirements for branched chain amino acids and their interactions in the nematode *Caenorhabditis elegans*. *Nematology* 2:501-506

- Perry RN, Clarke AJ (2011) Hatching mechanisms of nematodes. *Parasitology* 139:435-449
- Prot JC (1980) Migration of plant-parasitic nematodes towards plant roots. *Revue de Nematologie* 3:305-318
- Pudasaini M, Viaene N, Moens M (2008) Hatching of the root-lesion nematode, *Pratylenchus penetrans*, under the influence of temperature and host. *Nematology* 10:47-54
- Qamar A, Mysore K, Senthil-Kumar M (2015) Role of proline and pyrroline-5-carboxylate metabolism in plant defense against invading pathogens. *Frontiers in Plant Science* 6:503. <https://doi.org/10.3389/fpls.2015.00503>
- Qiao F, Kong L-A, Peng H, Huang W-K, Wu D-Q, Liu S-M, Clarke JL, Qiu D-W, Peng D-L (2019) Transcriptional profiling of wheat (*Triticum aestivum* L.) during a compatible interaction with the cereal cyst nematode *Heterodera avenae*. *Scientific Reports* 9:2184. <https://doi.org/10.1038/s41598-018-37824-9>
- Reynolds AM, Dutta TK, Curtis RHC, Powers SJ, Gaur HS, Kerry BR (2011) Chemotaxis can take plant-parasitic nematodes to the source of a chemo-attractant via the shortest possible routes. *Journal of The Royal Society Interface* 8:568-577
- Rocha TL, Soll CB, Boughton BA, Silva TS, Oldach K, Firmino AAP, Callahan DL, Sheedy J, Silveira ER, Carneiro RMDG, Silva LP, Polez VLP, Pelegrini PB, Bacic A, Grossi-de-Sa MF, Roessner U (2017) Prospection and identification of nematotoxic compounds from *Canavalia ensiformis* seeds effective in the control of the root knot nematode *Meloidogyne incognita*. *Biotechnology Research and Innovation* 1:87-100
- Roessner U, Luedemann A, Brust D, Fiehn O, Linke T, Willmitzer L, Fernie AR (2001) Metabolic profiling allows comprehensive phenotyping of genetically or environmentally modified plant systems. *The Plant Cell* 13:11-29
- Rolfe R, Barrett J, Perry R (2000) Analysis of chemosensory responses of second stage juveniles of *Globodera rostochiensis* using electrophysiological techniques. *Nematology* 2:523-533
- Blümel RC, Daniel F, Fischer, Grundler FMW (2018) Effects of exogenous amino acid applications on the plant-parasitic nematode *Heterodera schachtii*. *Nematology* 20:713-727
- Rosati RG, Lario LD, Hourcade ME, Cervigni GDL, Luque AG, Scandiani MM, Spampinato CP (2018) Primary metabolism changes triggered in soybean leaves by *Fusarium tucumaniae* infection. *Plant Science* 274:91-100
- Rudrappa T, Czymmek KJ, Paré PW, Bais HP (2008) Root-secreted malic acid recruits beneficial soil bacteria. *Plant Physiology* 148:1547-1556
- Scandiani MM, Luque AG, Razori MV, Ciano Casalini L, Aoki T, O'Donnell K, Cervigni GDL, Spampinato CP (2015) Metabolic profiles of soybean roots during early stages of *Fusarium tucumaniae* infection. *Journal of Experimental Botany* 66:391-402

Schmidt H, Günther C, Weber M, Spörlein C, Loscher S, Böttcher C, Schobert R, Clemens S (2014) Metabolome analysis of *Arabidopsis thaliana* roots identifies a key metabolic pathway for iron acquisition. PLOS ONE 9:e102444. <https://doi.org/10.1371/journal.pone.0102444>

Shemshura ON, Bekmakhanova NE, Mazunina MN, Meyer SLF, Rice CP, Masler EP (2016) Isolation and identification of nematode-antagonistic compounds from the fungus *Aspergillus candidus*. FEMS Microbiology Letters 363:fnw026. <https://doi.org/10.1093/femsle/fnw026>

Shukla N, Yadav R, Kaur P, Rasmussen S, Goel S, Agarwal M, Jagannath A, Gupta R, Kumar A (2018) Transcriptome analysis of root-knot nematode (*Meloidogyne incognita*)-infected tomato (*Solanum lycopersicum*) roots reveals complex gene expression profiles and metabolic networks of both host and nematode during susceptible and resistance responses. Molecular Plant Pathology 19:615-633

Siddique S, Endres S, Sobczak M, Radakovic ZS, Fragner L, Grundler FMW, Weckwerth W, Tenhaken R, Bohlmann H (2014) Myo-inositol oxygenase is important for the removal of excess myo-inositol from syncytia induced by *Heterodera schachtii* in Arabidopsis roots. New Phytologist 201:476-485

Suzuki K, Okazaki K, Tawaraya K, Osaki M, Shinano T (2009) Gas chromatography–mass spectrometry associated global analysis of rice root exudates under aseptical conditions. Soil Science & Plant Nutrition 55:505-513

Tanda AS, Atwal AS, Bajaj YPS (1989) *In vitro* inhibition of root-knot nematode *Meloidogyne incognita* by sesame root exudate and its amino acids. Nematologica 35:115-124

van Dam NM, Bouwmeester HJ (2016) Metabolomics in the rhizosphere: Tapping into belowground chemical communication. Trends in Plant Science 21:256-265

Warnock ND, Wilson L, Canet-Perez JV, Fleming T, Fleming CC, Maule AG, Dalzell JJ (2016) Exogenous RNA interference exposes contrasting roles for sugar exudation in host-finding by plant pathogens. International Journal for Parasitology 46:473-477

Warren CR (2015) Wheat roots efflux a diverse array of organic N compounds and are highly proficient at their recapture. Plant and Soil 397:147-162

Wurst S, Wagenaar R, Biere A, van der Putten WH (2010) Microorganisms and nematodes increase levels of secondary metabolites in roots and root exudates of *Plantago lanceolata*. Plant and Soil 329:117-126

Xia J, Wishart DS (2002) Using metaboanalyst 3.0 for comprehensive metabolomics data analysis. Current Protocols in Bioinformatics 55: 14.10.1-14.10.91. <https://doi.org/10.1002/cpbi.11>

Zhao X, Schmitt M, Hawes MC (2000) Species-dependent effects of border cell and root tip exudates on nematode behavior. Phytopathology 90:1239-1245

Zinovieva SV, Vasyukova NI, Udalova ZV, Gerasimova NG, Ozeretskovskaya OL (2011) Involvement of salicylic acid in induction of nematode resistance in plants. Biology Bulletin 38:453. <https://doi.org/10.1134/S1062359011050177>



## **Chapter 6**

**Histochemical and histopathological responses of wheat roots  
infected by *Pratylenchus thornei***

## **Chapter 6**

### **Histochemical and histopathological responses of wheat roots infected by *Pratylenchus thornei***

#### **6.1 Statement of authorship**

## Statement of Authorship

Title of the paper	Histochemical and histopathological responses of wheat roots infected by <i>Pratylenchus thornei</i>
Publication Status	Unpublished and unsubmitted work written in manuscript style
Publication details	This chapter will be prepared as a manuscript for submission to a refereed journal

### Principal Author

Name of Principal Author (Candidate)	Muhammad Shefatur Rahman		
Contribution to the paper	Involved in designing the research project conception and development of overall research plan. Conducted the hands-on experiment, data collection and analysis. Wrote the first draft of the manuscript and took primary responsibility for manuscript revision.		
Overall percentage (%)	70		
Certification	This paper reports on original research I conducted during the period of my Higher Degree by Research candidature and is not subject to any obligations or contractual agreements with a third party that would constrain its inclusion in this thesis. I am the primary author of this paper.		
Signature		Date	4.12.2019

### Co-Author Contributions

By signing the Statement of Authorship, each author certifies that:

- I. the candidate's stated contribution to the publication is accurate (as detailed above);
- II. permission is granted for the candidate to include the publication in the thesis; and
- III. the sum of all co-author contributions is equal to 100% less the candidate's stated contribution.

Name of Co- Author	Katherine J. Linsell		
Contribution to the paper	Provided suggestions for the research experiment, provided input for the manuscript.		
Signature		Date	5/12/19

Name of Co- Author	Nicholas C. Collins		
Contribution to the paper	Read the manuscript and suggested revisions.		
Signature		Signature	9/12/19

Name of Co- Author	Klaus H. Oldach		
Contribution to the paper	Provided overall supervision of the research project and helped writing the manuscript.		
Signature		Date	4.12.2019

## 6.2 Introduction

In a previous study, resistance to *Pratylenchus thornei* in wheat was found to be associated with restricted nematode migration within the root (Linsell et al. 2014). By staining the roots in acid fuchsin, it was found that *P. thornei* could only migrate 10 mm through the root cortex from the point of inoculation in the resistant genotype Sokoll, compared to 70 mm in the roots of the susceptible genotype Krichauff. A number of physical and chemical barriers might contribute to this resistance in Sokoll (reviewed in Chapter 1). It is expected that the plant cell wall is the primary barrier for the nematodes migrating within host tissue (Wieczorek 2015). Plant parasitic nematodes use their stylet and cell wall degrading enzymes to break the host cell wall (Davis et al. 2011). In reply, host plants trigger plant cell wall-mediated resistance mechanisms to resist nematodes (reviewd in Holbein et al. 2016; Wieczorek 2015). For instance, the presence of higher levels of lignin and suberin in endodermal cells of resistant banana roots (compared to the susceptible banana root) was thought to be associated with *Radopholus similis* resistance (Valette et al. 1998; Wuyts et al. 2007). Hence, cell wall thickening with callose, suberin, lignin or lignin-like structures might play an important role in restricting nematode migration in plant tissue (Wieczorek 2015).

Callose is a polysaccharide in the form of  $\beta$ -1,3-glucan with some  $\beta$ -1,6-branches and it exists in the cell walls of a wide variety of higher plants (Piršelová and Matušíková 2013). It is deposited at the interface between the plasma membrane and cell wall, and this process is a hallmark of the pathogen triggered immune (PTI) response (Ellinger and Voigt 2014; Luna et al. 2010). For instance, a common response of plants to fungal attack is the deposition of callose in the form of cell wall thickenings called papillae, at sites of attempted wall penetration (Luna et al. 2010; Voigt 2014).

Lignin is a natural phenolic polymer and one of the main components of certain kinds of plant cell walls (Liu et al. 2018). In plants, changes in lignin content and composition occur in response to pathogen attack, and this has been suggested as a defence mechanism (Moura et al. 2010). Accumulation of lignin or lignin-like phenolic compounds was shown to occur in a variety of plant-microbe interactions (Vance et al. 1980). Deposition of lignin in infected cells may prevent the spread of toxins and enzymes from the pathogen into the host, as well as prevent the transfer of water and nutrients from the host cells to the pathogen (Smith et al. 2007).

A number of histological staining techniques have been developed to visualise differences in cell wall components between various plant-pathogen interactions (Mori and Bellani 1996; Soukup 2014). Many of the synthetic dyes used for staining plant tissues are highly fluorescent, allowing the selective staining of cell wall components (Ursache et al. 2018). For instance, calcofluor white and aniline blue have been used to observe cellulose and callose, respectively, with fluorescent microscopy (Pradhan and Loqué 2014).

Sample preparation for histological staining can be a difficult and time-consuming process. At first, plant tissues need to be fixed with a fixation agent (such as an aldehyde), followed by embedding in resin, and finally by cutting the tissues into thin layers using a microtome (Hawes 2000). On the other hand, there are relatively easy protocols for cutting and fluorescence staining of fresh samples (Zelko et al. 2012). High quality images can be obtained from thick sections using laser scanning confocal microscopy (Atkinson and Wells 2017; Truernit and Palauqui 2009). Confocal microscopy also allows observation of living nematodes in the host tissue. For example, the PKH26 stain binds to lipid droplets in the nematode without any

observable effect on the nematode viability (Dinh et al. 2013). Observation of living nematodes during the infection process could help us understand their behaviour in planta.

The present study was done to test for the presence of cell wall thickening with cellulose, callose, lignin and suberin, in response to *P. thornei* infection, using a confocal microscope. The broader aim was to gain more of an understanding of the histopathological responses of wheat roots to challenge by *P. thornei*.

## 6.3 Materials and methods

### 6.3.1 PKH26 labelling of nematodes

*P. thornei* was collected from carrot callus and counted using a compound microscope (described in Chapter 4). Nematodes were labelled fluorescently with PKH26 using a MINI26 PKH26 Red Fluorescent Cell Linker Kit (Sigma-Aldrich, St. Louis, MO) and following the protocol described by Dinh et al. (2013). In short, approximately 50,000 nematodes were collected in a 1.5 mL microcentrifuge tube and resuspended in 1 mL of sterile water. Then, 1  $\mu$ L of PKH26 (stock solution  $1 \times 10^{-3}$  M) was added into the nematode solution and the tube incubated in the dark at room temperature for 15 min. After centrifuging the nematode solution at  $375 \times g$  for three min, the supernatant was discarded. Then the nematodes were resuspended in 50 mL sterile water. This washing process was done three times. Stained nematodes were immediately used for inoculation.

### 6.3.2 Plant materials and nematode inoculation

Wheat cultivars Sokoll (*P. thornei* resistant) and Krichauff (*P. thornei* susceptible) were used for this experiment. Seeds were surface sterilised using ethanol and sodium hypochlorite followed by two rinses in sterile water (described in Chapter 3). Seeds were then germinated on moist filter paper for three days. Seedlings were transplanted into petri dishes containing 0.5% phyto agar (Sigma-Aldrich, St Louis, MO). Two days after transplantation, approximately 500 nematodes were applied onto the roots of each plant. Root samples were collected 1, 3 and 5 days after inoculation for microscopy. In order to study infected roots beyond this time, a different subset of five-day old seedlings was grown in plastic pots filled with steam-pasteurized sand in a controlled environment room (CER) (as described in Chapter 3). These seedlings were inoculated with 1,500 nematodes seven days after transplantation. After nematode inoculation, plants were maintained (fertilized and watered) following the

protocol described in Chapter 3. Root samples were collected after seven and ten days and six weeks from inoculation for microscopy.

### **6.3.3 Root sample embedding and sectioning**

Confocal microscopy was conducted on fresh (without fixation) root samples using previously reported protocols for sample embedding and sectioning (Atkinson and Wells 2017; Truernit and Palauqui 2009; Zelko et al. 2012). Firstly, roots were observed under a compound microscope to locate the site of infection (where nematodes had aggregated). Then, nematode infected root samples were cut into segments (approximately 1 cm length) using a fresh double edge razor blade (Wilkinson Sword, United Kingdom) and these were embedded in 5% agarose. A vibrating blade microtome [Leica Microsystems (United Kingdom) Ltd] was used to produce sections of between 100 and 250  $\mu\text{m}$  thickness.

### **6.3.4 Staining**

For Calcofluor White staining, 0.1% Calcofluor White (Sigma-Aldrich, St. Louis, MO) was prepared and the root sections were stained for 30 min. To image Calcofluor White fluorescence, a wavelength of 405-nm was used for excitation and 425–475 nm used for emission (Ursache et al. 2018).

For aniline blue staining, 0.1% Aniline blue (Biosupplies Australia Pty Ltd, Victoria, Aus) was prepared and the root sections were stained for 30 min at room temperature. Next, the root samples were washed in sterile water for 30 min. Aniline blue interaction with  $\beta$ -1,3-glucan induces a yellow-green fluorescence under UV light (Wood and Fulcher 1984). For aniline blue fluorescence observation, a wavelength of 405 nm was used for excitation and 420-550 nm wavelength was used for emission (Zavaliev and Epel 2015).



The lignin found in plant cell walls can be stained with phloroglucinol in the presence of alcohol and HCl (Liljegren 2010; Pradhan and Loqué 2014). To test for lignin, sections were soaked in 10% (w/v) phloroglucinol solution in 95% (v/v) ethanol for 3 min, then the solution was decanted off and placed in a drop of 37% HCl on a slide, covered with a cover-slip and observed under the confocal microscope.

To visualise cell walls, sections were stained with propidium iodide (Merck KGaA, Darmstadt, Germany). Root sections were stained with propidium iodide solution (1%) for 30 min. For confocal microscopy the excitation and emission wavelength were 482 nm and 608 nm, respectively.

### **6.3.5 Whole-mount confocal imaging**

In order to observe live nematodes (PKH26 stained) in root tissue, whole-mount sections was prepared following the protocol of Truernit and Palauqui (2009). In short, nematode infected root samples (without fixation or agarose embedding) were cut into segments approximately 3 cm in length and put immediately in sterile water. The root sections were placed in a glass slide and mounted in water. The root sections were observed using a confocal microscope.

### **6.3.6 Confocal microscopy**

Image acquisition was performed using a Nikon A1R laser scanning confocal microscope (Nikon Instruments; Tokyo, Japan). The confocal microscope was equipped with three solid state lasers (405 nm, 561 nm and 640 nm) and a multiline Argon gas laser (457 nm, 488 nm and 514 nm). During scanning, all available wavelengths were used so that no data were missed. For each preparation, the most appropriate objectives were chosen to match the size of

the sample in the section. Images were analysed using the software NIS-Element (Nikon Instruments).

## 6.4 Results

### 6.4.1 Histological responses of wheat roots to *P. thornei* inoculation

After being labelled with PKH26, all vermiform life stages of *P. thornei* were shown to be fluorescent in the lip region, oesophagus and intestine (Fig. 6.1). Strong staining was observed, particularly in the lipid droplets of the intestine of *P. thornei*. PKH26 did not have any obvious effects on the viability of *P. thornei*.

The lesions in the wheat root were difficult to locate with the naked eye but were observable under the compound microscope. Nematodes were also observed under the compound microscope outside of the root accumulating at sites of infection already created by previous nematodes. Except the root cap, nematodes were observed throughout the entire root, hence there was no preferred zone of infection in the root for *P. thornei*.

Confocal microscopy enabled observation of *P. thornei* behaviour throughout the infection process, including intracellular migration, feeding, coiling and resting inside wheat root cells (Fig. 6.2 and 6.3). In addition, morphological features such as the stylet, intestine and metacarpus were visible in PKH26 labelled nematodes located inside the roots (Fig. 6.2). Nematodes were stretched out or coiled, occupying a single cell or multiple cell layers (Fig. 6.2 and 6.3). Nematodes were always seen in cortical cells, and never seen inside the endodermis or stele. They used their stylet at the corner of the cell to move on to the next cell (Movie clip 6.1 and Fig. 6.2). While striking with the stylet, the median bulb pulsated, and a globular secretion was seen from the stylet tip into the cell (Movie clip 6.1). Cortical cells penetrated and fed upon by the nematode were generally devoid of cytoplasm. Four weeks after nematode inoculation, extensive damage was observed in Krichauff root tissues (Fig. 6.3).

Empty cortical layers were observed in the passage of nematodes and egg masses were seen in the cavity of the cortical layer (Fig. 6.3). The passage of the nematode through the cortex was observed to be intracellular. A movie clip was captured with the confocal microscope showing the nematode was located inside the root cell. The nematode was trying to break the cell wall to move to the next cell. It was searching for a suitable site to thrust along the cell wall, and ultimately stylet thrusting was observed at the corner of the cell (Movie clip 6.1).

**Fig. 6.1** Confocal imaging of *Pratylenchus thornei* outside of plant roots. *Pratylenchus thornei* was stained with PKH26 for 24 h and stored at 4°C until imaging. A. Intense fluorescence of intestinal lipids (arrow). B. An entire PKH26 labelled *Pratylenchus thornei*. Morphological features such as the lip region (L) was visible in the labelled nematode. The anterior and posterior regions of *Pratylenchus thornei* are labelled AR and PR, respectively. Scale bars= 50  $\mu$ m

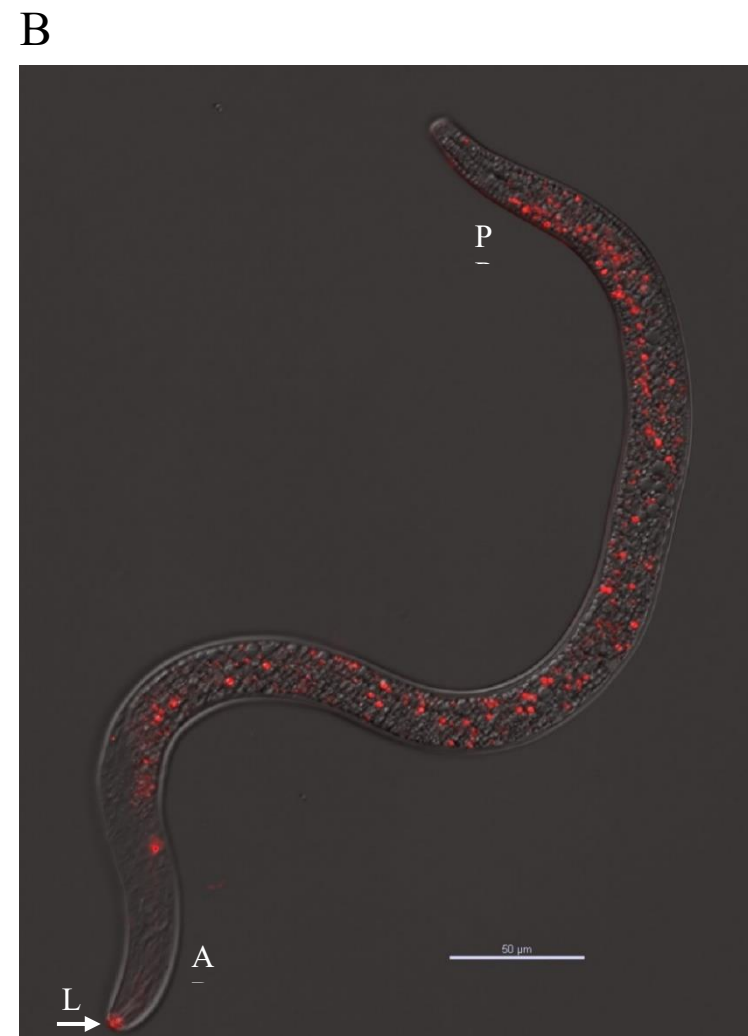
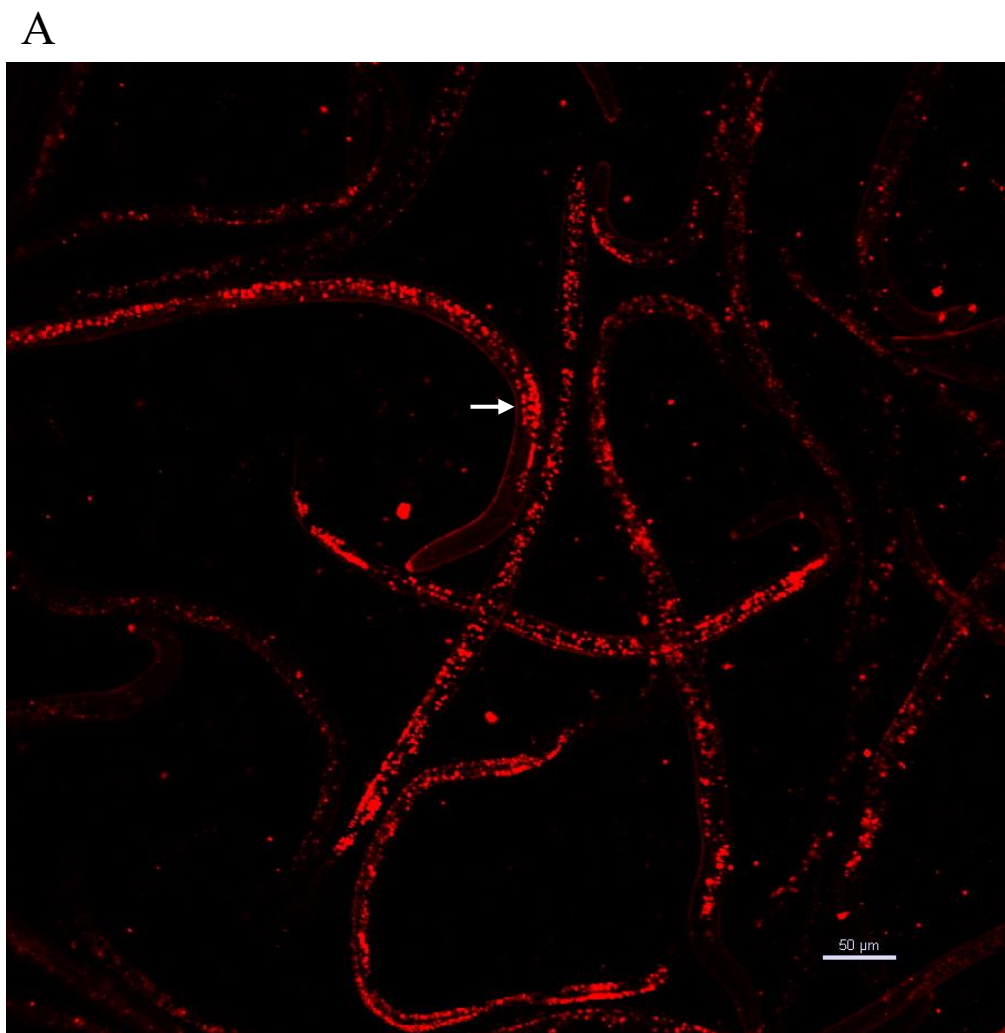


**Fig. 6.2** PKH26 labelled *Pratylenchus thornei* inside Sokoll root tissues. Images were taken 10 days after inoculation. Still images were taken of live nematodes inside root tissue using a confocal microscope. A. Nematode searching for suitable place to thrust at the cell wall. B and C. *Pratylenchus thornei* stylet thrusting (arrow) at the corner of the cell. I, Intestine; M, metacarpus; S, stylet. Scale bars= 50  $\mu$ m

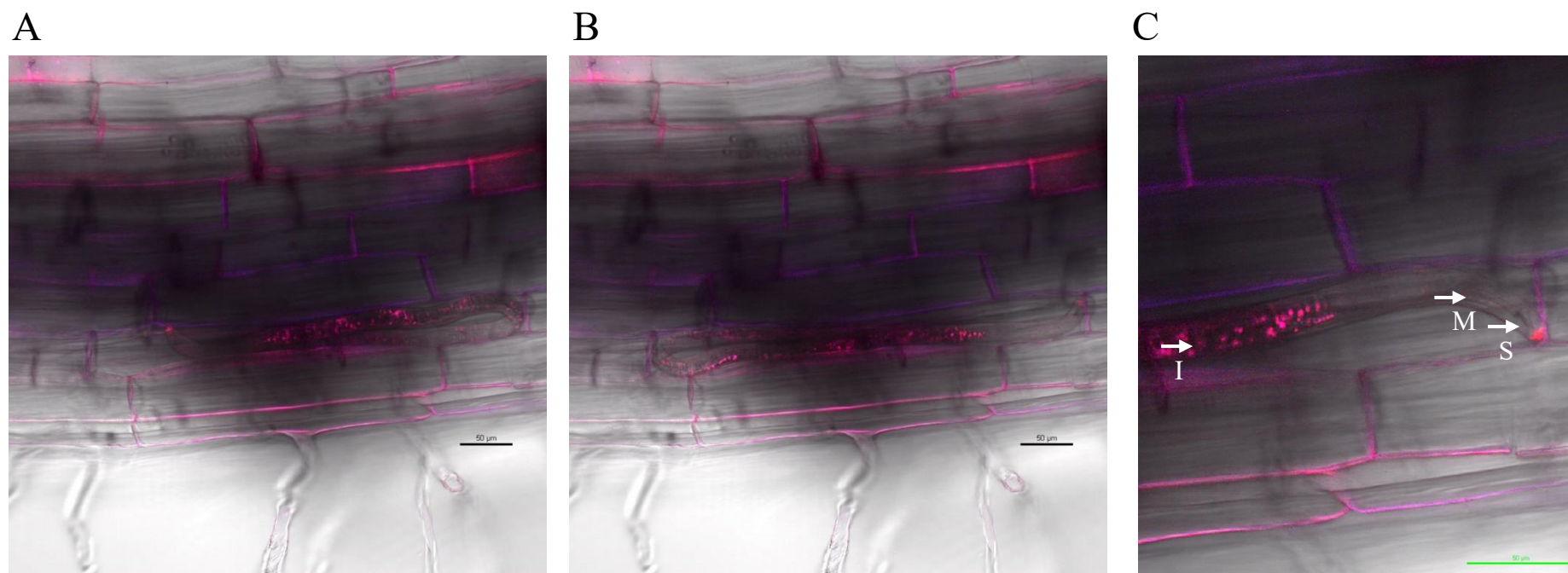
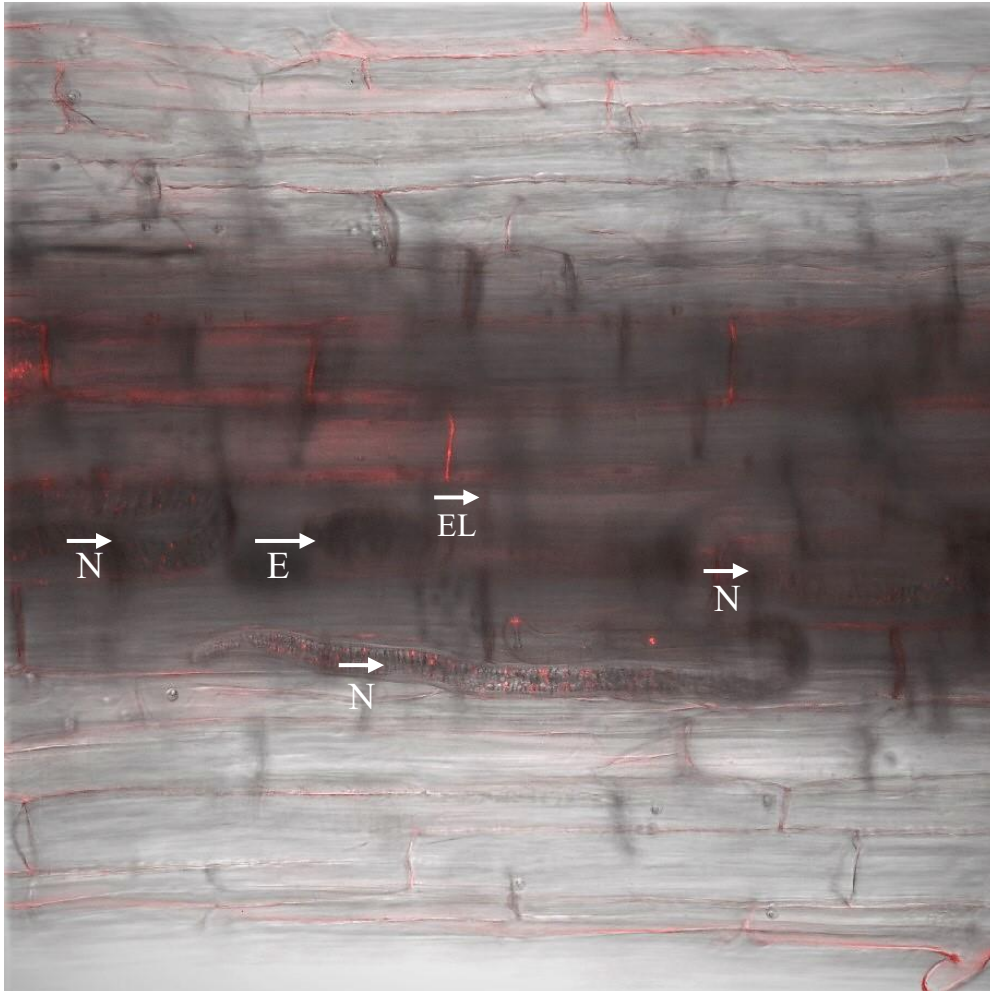


**Fig. 6.3** PKH26 labelled *Pratylenchus thornei* inside Krichauff root tissues. Images were captured four weeks after inoculation. Nematodes (N) occupied multiple cells by breaking the cell walls, resulting in an empty layer (EL) in the cortical tissues. Deposition of eggs (E) in empty layers were also observed



**Movie clip 6.1** *Pratylenchus thornei* in Sokoll root (10 days after inoculation). *Pratylenchus thornei* was labelled with PKH26. The movie of the live nematode was recorded using a Nikon A1 confocal microscope. Movie speed is 10x faster than real time

The movie clip is supplied as an electronic file



### 6.4.2 Histochemical staining

Calcofluor white (CW) treated Sokoll root sections (three DAI) showed blue fluorescence (excitation 404 nm and emission 450, blue channel) from the cell walls of the cortical tissues (Fig. 6.4-B). This was a distinct difference compared to the control root section (nematode uninfected) (Fig. 6.4-A). Blue fluorescence was also not observed in CW treated Krichauff root sections (either control or nematode infected) (Fig. 6.5). CW binds to the cell wall components cellulose or other  $\beta$ -1,4-linked carbohydrates (Albani and Plancke 1999; Herrera-Ubaldo and de Folter 2018; Ursache et al. 2018). Thus, blue fluorescence in CW treated Sokoll root tissue may have resulted from additional cellulose deposition in response to *P. thornei* infection. The intensity of blue fluorescence increased at a later stage (10 DAI) (Fig. 6.6), at a time the cortical cell layer was found to be damaged significantly by the nematodes.

To visualise callose ( $\beta$ -1,3-glucan) or callose-like substances (polysaccharides or glycoprotein) in the cell wall, *P. thornei* resistant Sokoll root tissues were stained with aniline blue. Callose deposition was observed in nematode infected Sokoll root tissues (Fig. 6.6). Due to the wide range of emission wavelengths of aniline blue (420 to 550 nm) (Zavaliev and Epel 2015), callose specific signals might be obtained from blue (450 nm), green (525 nm) or red (595 nm) channels. However, strong fluorescence was observed from green and red channels (Fig. 6.7).

*P. thornei* infected Sokoll root tissues were treated with phloroglucinol to stain lignin. Strong fluorescence was obtained at excitation 561 nm and emission 595 nm (red) (Fig. 6.8 and 6.9). Fluorescence was also obtained at other wavelengths (excitation 488 nm and emission 525 nm, green channel). This might be due to lignin autofluorescence (Decou et al. 2017; Mast et al. 2009). Lignin autofluorescence was observed from non-stained root sections (result not shown). In a different phloroglucinol treated Sokoll root section, nematode infected tissue was

found to be darker (Fig. 6.9). Red fluorescence observed surrounding this necrotic tissue, suggesting lignin or lignin like substances might be deposited surrounding the necrotic root tissues.

**Fig. 6.4** Comparative anatomies of *Pratylenchus thornei* uninfected (A) and infected (B) Sokoll root. Calcofluor-white and propidium iodide stained (simultaneous) transverse sections. Sequential excitation at 404, 488 and 561 nm with corresponding emission at 450 (blue), 525 (green) and 595 (red) nm resulted the confocal image a, b and c, respectively. The blue channel might show the presence of cellulose and other  $\beta$ -1,4-linked carbohydrates. The red channel shows the propidium iodide stained cell wall. The composite image of blue, red and green channels is shown in d. Co, cortical cells; Xy, Xylem; En, endodermis; Ep, epidermis; Ph, Phloem

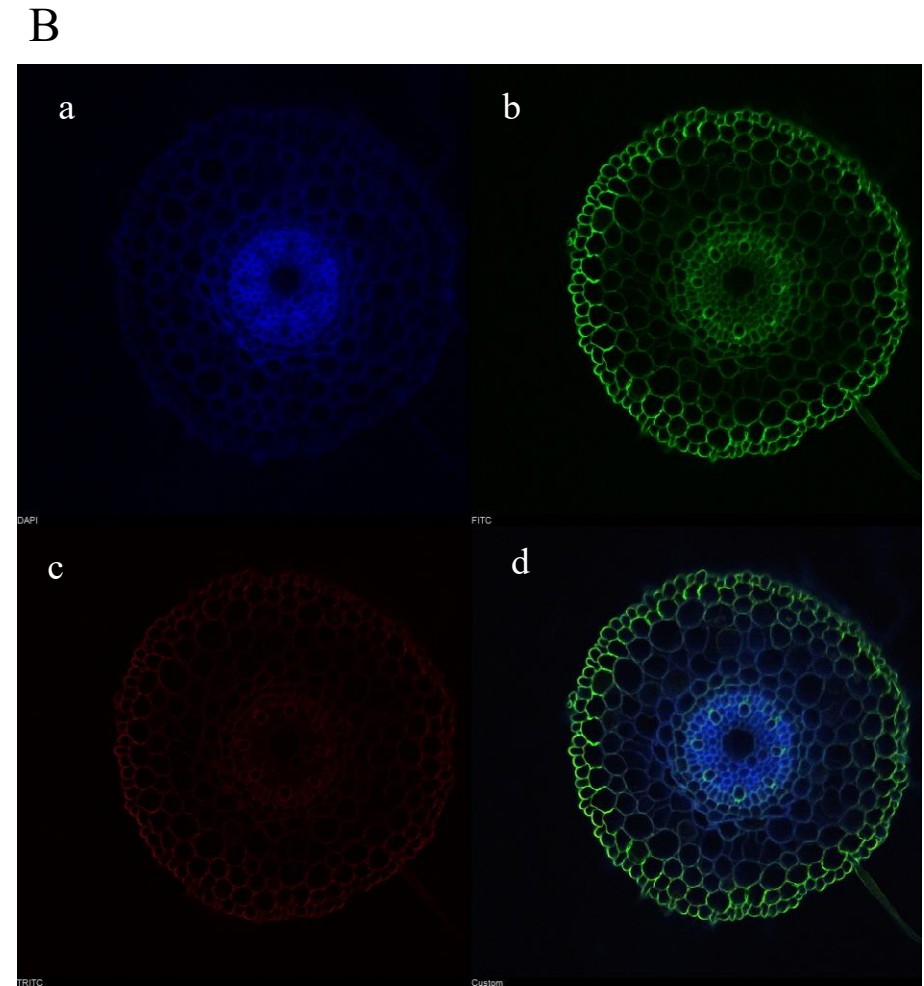
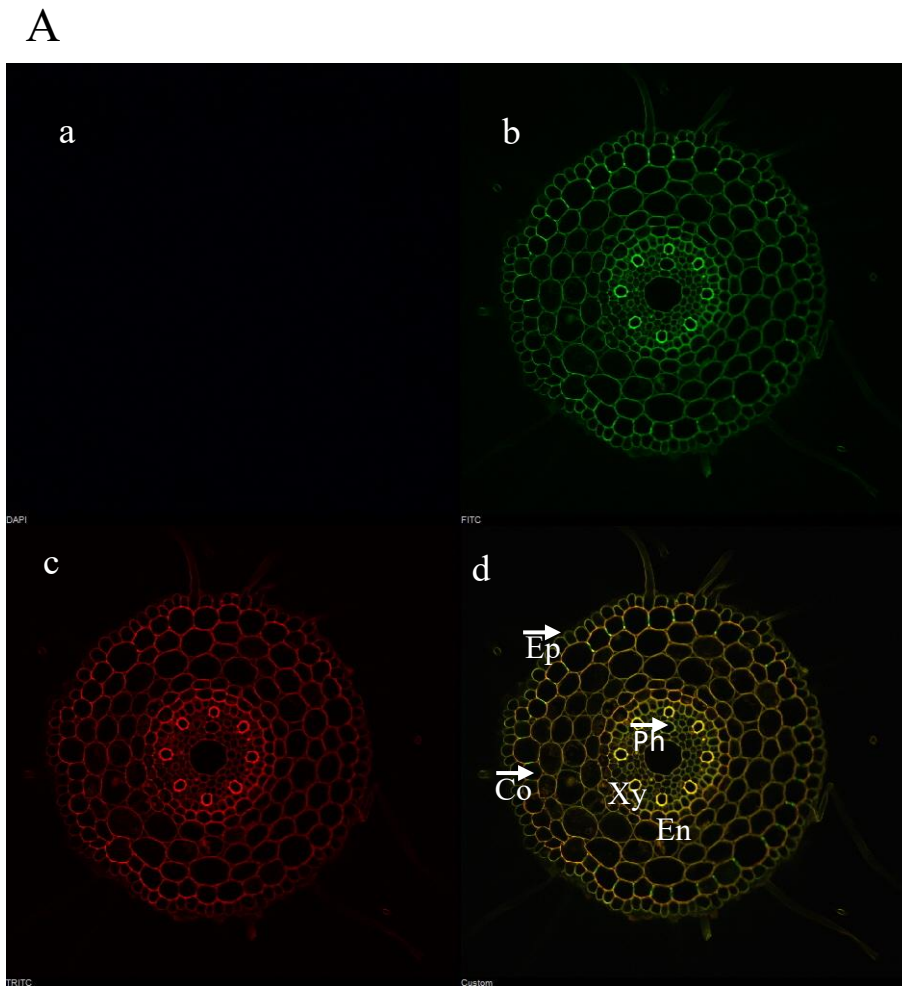


**Fig. 6.5** Comparative anatomies of *Pratylenchus thornei* uninfected (A) and infected (B) Krichauff root. Calcofluor-white and propidium iodide stained transverse sections. Sequential excitation at 404, 488 and 561 nm with corresponding emission at 450 (blue), 525 (green) and 595 (red) nm resulted the confocal image a, b and c, respectively. The blue channel might show the presence of cellulose and other  $\beta$ -1,4-linked carbohydrates. The red channel shows the propidium iodide stained cell wall. The composite image of blue, red and green channels is represented in image d

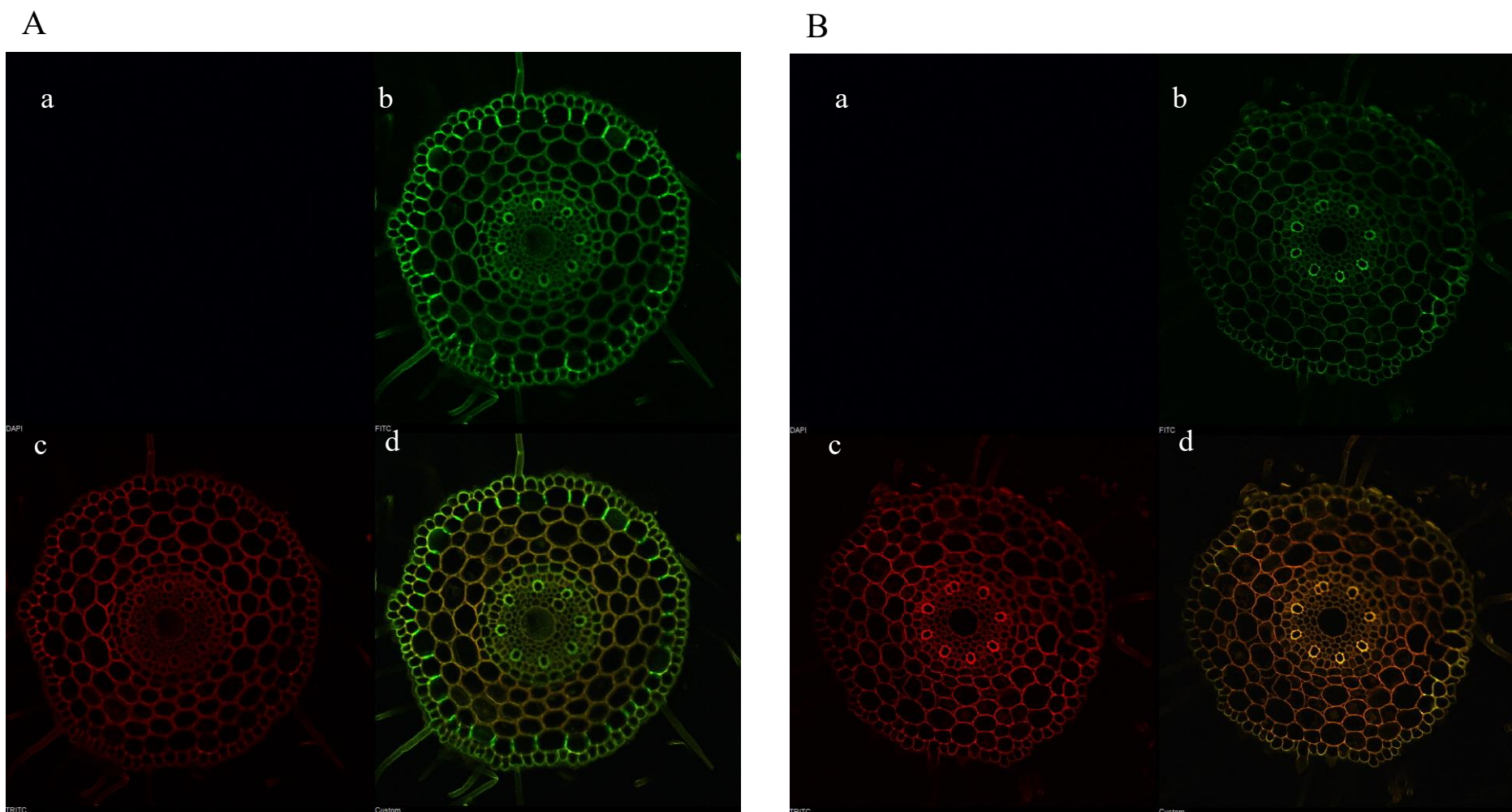


**Fig. 6.6** Transverse section of calcofluor-white stained Sokoll root. Confocal images were taken 10 days after *Pratylenchus thornei* infection. Sequential excitation at 404 and 561 nm with corresponding emission at 450 (blue) and 595 (red) nm resulted the confocal image a and b, respectively. The composite image of blue and red channels is represented by image c. PKH26 stained *Pratylenchus thornei* (N) was observed damaging the cortical cell layer. Scale bars represent 50  $\mu$ m

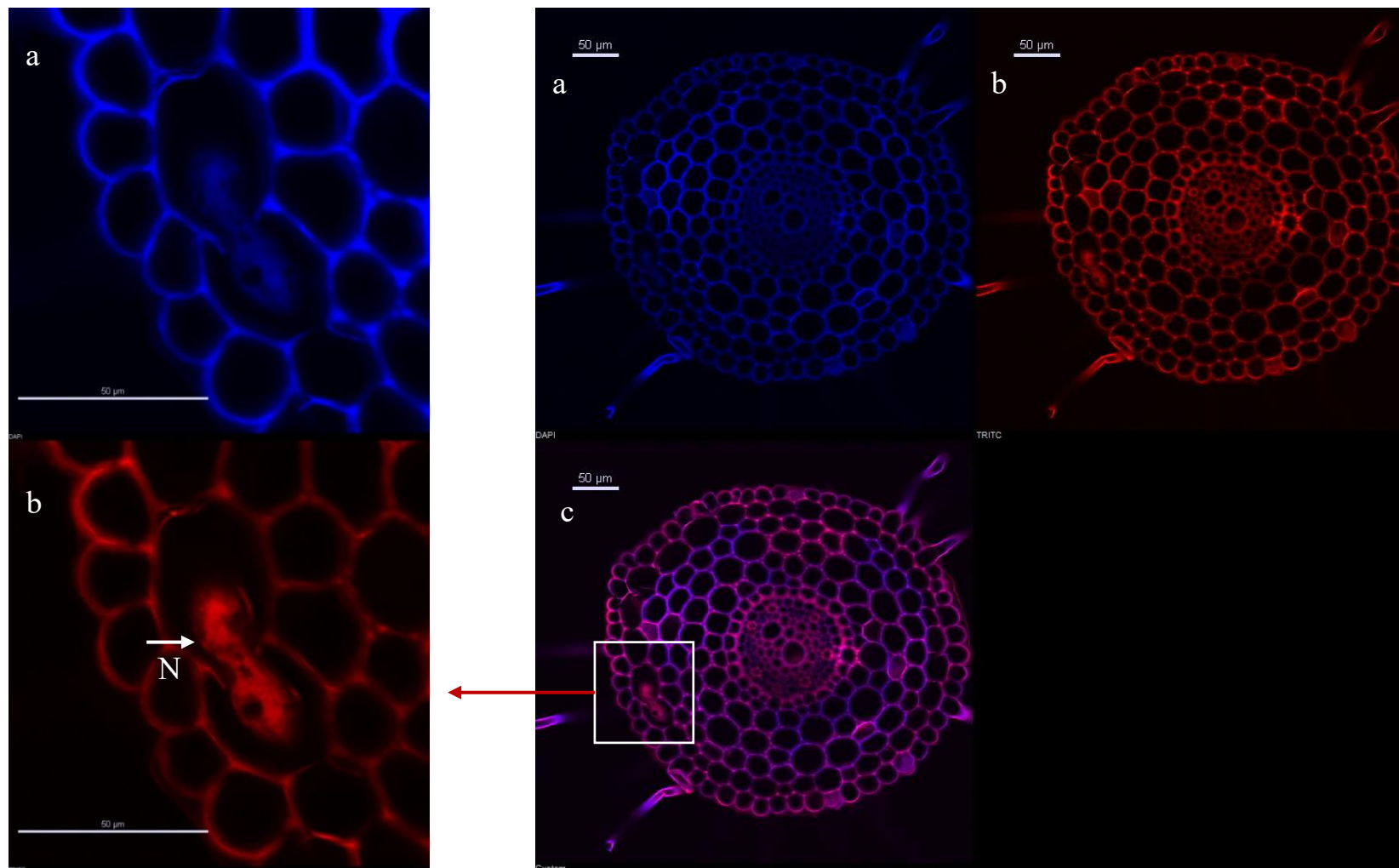




**Fig. 6.7** Deposition of callose or callose-like substances in *Pratylenchus thornei* infected (10 days after inoculation) Sokoll root section. Root tissues were treated with aniline blue and images were taken using a confocal microscope. Sequential excitation at 404, 488 and 561 nm with corresponding emission at 450 (blue), 525 (green) and 595 (red) nm resulted the confocal image a, b and c, respectively. The composite image of blue, red and green channels is represented by image d. Both green and red color shows the presence of callose and callose-like substances. N, nematode

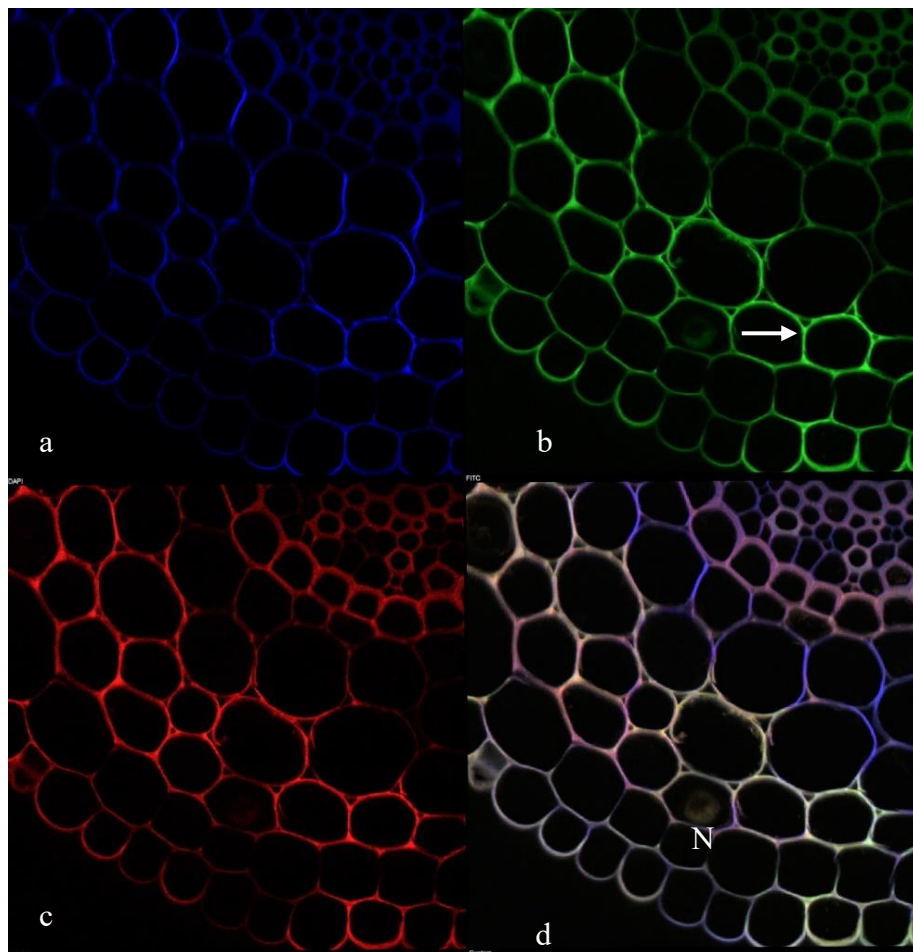


**Fig. 6.8** Observation of lignin or lignin-like substances in *Pratylenchus thornei* infected (10 days after inoculation) Sokoll root section. Root tissues were treated with phloroglucinol and images were taken using confocal microscope. Sequential excitation at 404, 488 and 561 nm with corresponding emission at 450 (blue), 525 (green) and 595 (red) nm resulted the confocal image a, b and c, respectively. Lignin was shown in red and green channel. The composite image of blue, red and green channels represented by image d. Cell layer damaged due to *Pratylenchus thornei* infection (arrow). N, nematode. Scale bars represent 50µm

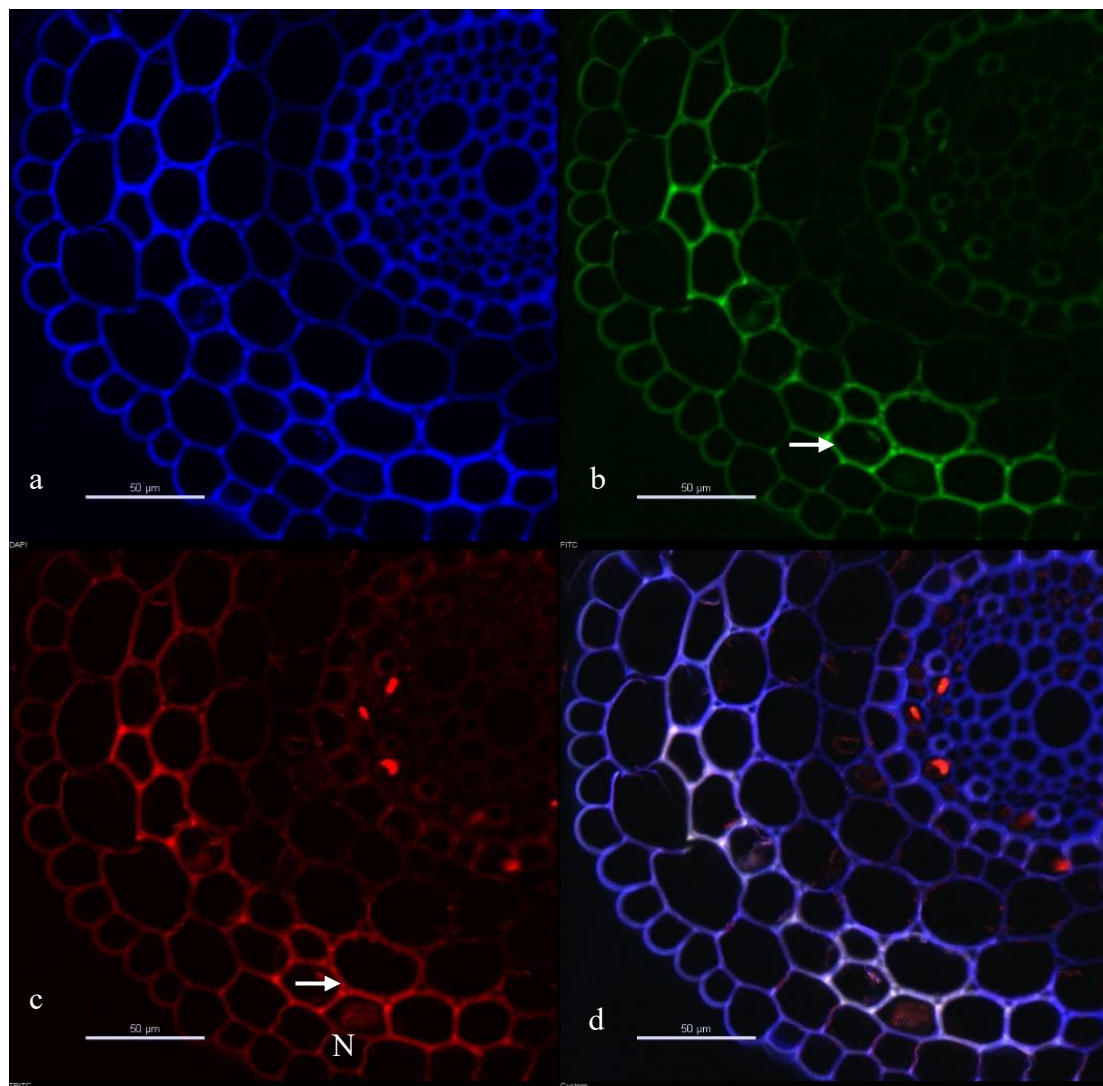
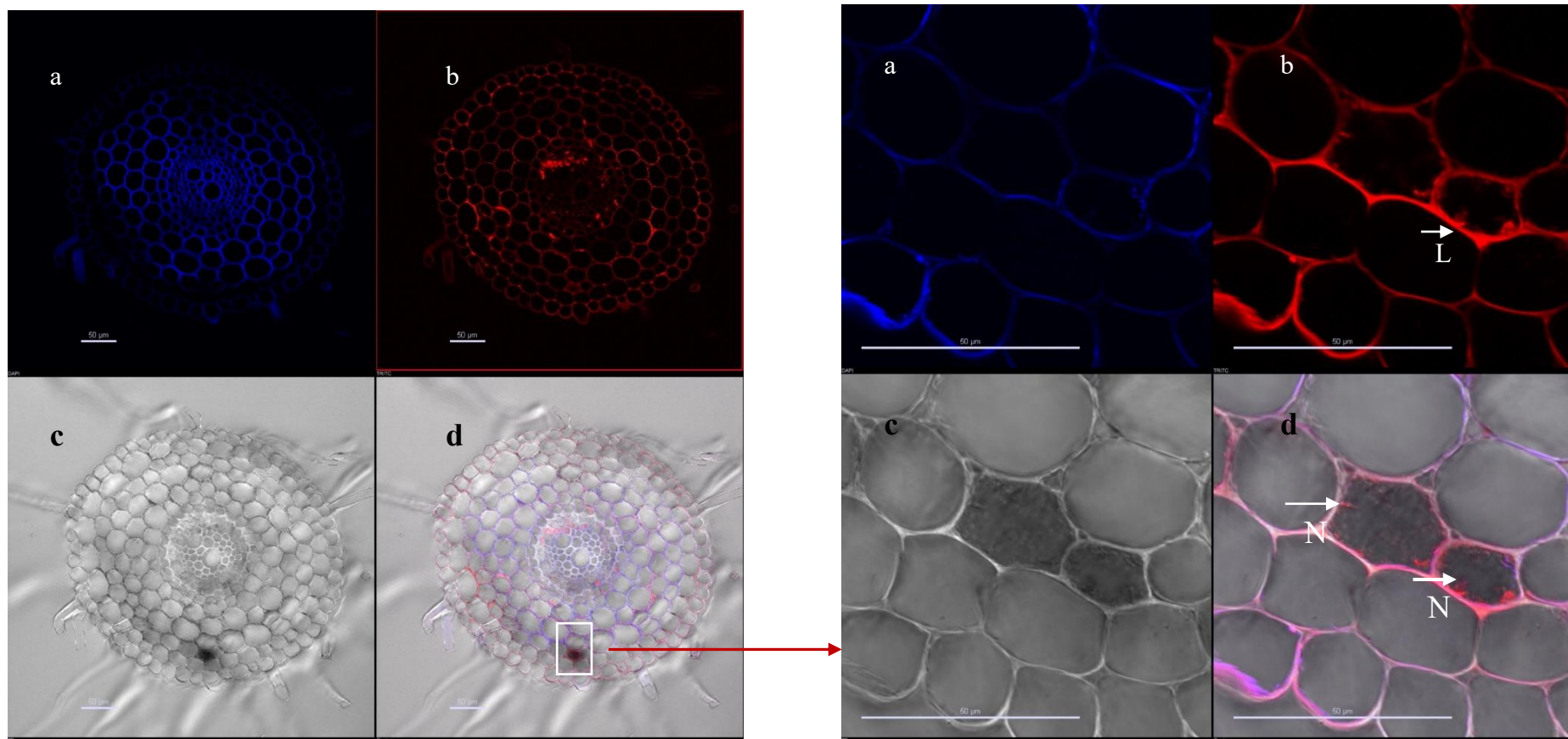


**Fig. 6.9** *Pratylenchus thornei* infected (10 days after inoculation) Sokoll root section, treated with calcofluor white and phloroglucinol. Images were taken using confocal microscope. Sequential excitation at 404 and 561 nm with corresponding emission at 450 (blue) and 595 (red) nm resulted the confocal image a and b, respectively. Confocal image from transmitted light channel shown in image c and a combination of blue, red and transmitted light channel shown in image d. Necrosis occurred in the cell due to *P. thornei* infection (Nc). Strong fluorescence observed in proximity to nematode infected cell indicating lignin or lignin-like substances deposition (L). N, nematode. Scale bars represent 50  $\mu$ m





## 6.5 Discussion

In present study, live *P. thornei* was able to be visualised inside wheat root tissue. This was possible due to the use of the fluorescent dye PKH26 (for *P. thornei* labelling) and confocal microscopy. In a previous study, labelling plant parasitic nematodes (*Pratylenchus penetrans*, *Heterodera schachtii*, and *Meloidogyne chitwoodi*) with PKH26 did not kill the nematodes (Dinh et al. 2013). Moreover, fluorescence was stable at all life stages of these nematodes. In the present study PKH26 also did not prevent *P. thornei* from infecting the root and they were able to be observed at late stages of their life (4 weeks after inoculation) inside the wheat root. Due to this stability in fluorescence, PKH26 was an excellent choice of fluorescent dye to study plant-nematode interactions.

Capturing images of living *P. thornei* inside wheat roots enabled us to observe the endoparasitic behaviour of *P. thornei*. In a previous study, endoparasitic behaviour of *P. penetrans* was described using video-enhanced contrast microscopy (Zunke 1990a). However, confocal microscopy offered higher resolution visualisation of fluorescent tagged molecules in both fixed and living cells (Cardinale 2014; Hardham 2012).

In the present study, the behavioural patterns of *P. thornei* observed inside wheat root were largely similar to those reported for other root lesion nematode species observed in various hosts. These include *P. thornei* in chickpea root (Castillo et al. 1998), *P. penetrans* in Arabidopsis, pea, strawberry and alfalfa root (Dinh et al. 2013; Kurppa and Vrain 1985; Oyekan et al. 1972; Townshend 1963; Townshend et al. 1989; Zunke 1990a, b) and *P. scribneri* in soybean, snap bean and lima bean root (Acosta and Malek 1981; Thomason et al. 1976). Initially, *P. thornei* was seen to be searching for a suitable site to penetrate the wheat root. Where the damage occurred, other nematodes aggregated and followed the same path. Damage

sites in wheat roots might produce molecules that attract other *P. thornei*. After entering the epidermal layer, *P. thornei* moved through the cortical layer parallel to the stele. They moved from one cell to another by breaking the cell wall using their stylet. *P. thornei* passage through the cortical layer seemed to be intracellular. Video images of *P. thornei* clearly showed stylet thrusting at the corners of the cells (Movie clip 1). This was followed by searches for suitable places to break in through other areas of the cell wall. The corner of the cell might be easier to penetrate than other parts of the cell wall. During stylet thrusting, strong fluorescence was observed at the lip region of PKH treated *P. thornei*. This might be the autofluorescence from the mixture of enzymes released by the nematodes (eg. cellulase, pectinase etc.) (Haegeman et al. 2012) or might be partially digested cell wall components. Like most of the plant parasitic nematodes, *P. thornei* was often observed to either be outstretched or coiled through several wheat root cell layers. *P. thornei* were also found to be confined within the epidermal and cortical layer of the wheat tissue. Nematodes were not observed feeding on the endodermis or the central stele. However, in a previous study, damage to the endodermal cells adjacent to nematode feeding sites was occasionally observed (Castillo et al. 1998). In the present study, such damage was not observed in the *P. thornei* susceptible wheat cultivar, Krichauff.

In the present study, distinct histopathological differences that correlated with resistance were not observed. The observable feeding behaviour, such as stylet probing, stylet insertion and feeding on root cortical tissues are the common features in root tissues. Perhaps additional root tissues need to be observed and over a longer period to identify any such differences, i.e., from root penetration until the end of lifecycle inside the root (eight weeks after inoculation). For instance, significant differences in *P. thornei* attraction, penetration, motility and reproduction were observed between Sokoll and Krichauff root tissues (Linsell et al. 2013b).

It is apparent that *P. thornei* uses its stylet to break the cell wall while migrating through the wheat root tissues. It may be possible to restrict this migration by strengthening root cell layers. In fact, in response to nematode attack, modification of cell wall, such as deposition of cellulose, callose, lignin and suberin have been reported in various plant-nematode interactions (reviewed in Holbein et al. 2016). Likewise, in the present study, cell wall thickening was observed in the *P. thornei* resistant cultivar, Sokoll.

Staining Sokoll root section with the fluorescent dye calcofluor white resulted in blue fluorescence. Calcofluor white exhibits selective binding to cellulose and has widely been used as a fluorescent dye to study host-pathogen relation (Pradhan and Loqué 2014; Zhou et al. 2009). Cellulose occurs naturally in all cell walls but deposition of additional cellulose might occur in response to nematode infection (Marques et al. 2018).

In the present study, aniline blue was used for callose staining. Imaging callose at plasmodesmata using aniline blue and confocal microscopy has previously been reported (Zavaliev and Epel 2015). Callose production is one of the earliest defence responses of plants against invading plant parasitic nematodes (Grundler et al. 1997). There is evidence that callose deposition is elicited in response to nematode infection (Holbein et al. 2016). For example, callose accumulates between the plasma membrane and cell wall around the nematode stylet (Hussey et al. 1992). Moreover, in transgenic *Arabidopsis* roots, overexpression of the transcription factor RAP2.6 lead to enhanced callose deposition in syncytia resulting in enhanced resistance against the beet cyst nematode *H. schachtii* (Ali et al. 2013). Callose deposition might interfere with nutrient import into syncytia. In response to *M. graminicola* infection, Callose deposition were enhanced in the resistant cultivar compared to the susceptible one (Kumari et al. 2016).

The contribution of lignin to plant defence against plant parasitic nematodes has been well documented. For instance, resistance to migratory nematodes correlates with increased lignin content in the cell walls of resistance banana plants (Suganthagunthalam et al. 2014; Wuyts et al. 2007). Similarly, changes in the lignin composition strongly influenced plants' susceptibility to the root-knot nematode *M. incognita* (Wuyts et al. 2006). Fujimoto et al. (2014) found that sclareol, an antimicrobial molecule, enhanced *Arabidopsis thaliana* root-knot nematode resistance by mediating ethylene-dependent lignin accumulation in the roots. Following nematode infection, resistance to rice stem nematode (*D. angustus*) was found to be associated with higher lignin content in a resistant rice cultivar, Manikpukha compared to a susceptible rice cultivar (Khanam et al. 2018). In the present study, the *P. thornei* resistant wheat cultivar Sokoll appeared to accumulate lignin upon nematode infection, which might strengthen the plant cell walls and inhibit nematode migration. However, further studies are required to confirm this result. Particularly, additional root samples from the susceptible cultivar need to be compared with the resistant cultivar.

In this study, histochemical staining suggested that due to *P. thornei* infection, cellulose, callose and lignin was deposited in the cell wall of the *P. thornei* resistant wheat cultivar Sokoll. Deposition of cellulose, callose, lignin or lignin might result in physical reinforcement of the cell walls. Consequently, penetration of the cell wall by stylet thrusting may become more challenging for the nematodes. However, further studies are required to confirm this results. Particularly, the root tissues of susceptible wheat cultivar, Krichauff requires further investigation.

## **Acknowledgement**

The authors thank Adelaide Microscopy (AM) and Microscopy Australia, The University of Adelaide for microscopy facilities. The author also thanks Dr. Gwen Mayo of Adelaide Microscopy, Waite Facility, for her consistent support in operating the microscope.

## 6.6 References

- Acosta N, Malek RB (1981) Symptomatology and histopathology of soybean roots infected by *Pratylenchus scribneri* and *P. alleni*. *Journal of Nematology* 13:6-12
- Albani JR, Plancke YD (1999) Interaction between calcofluor white and carbohydrates of  $\alpha$ 1-acid glycoprotein. *Carbohydrate Research* 318:194-200
- Ali MA, Abbas A, Kreil DP, Bohlmann H (2013) Overexpression of the transcription factor RAP2.6 leads to enhanced callose deposition in syncytia and enhanced resistance against the beet cyst nematode *Heterodera schachtii* Arabidopsis roots. *BMC Plant Biology* 13:47. <https://doi.org/10.1186/1471-2229-13-47>
- Atkinson JA, Wells DM (2017) An updated protocol for high throughput plant tissue sectioning. *Frontiers in Plant Science* 8: 1721. <https://doi.org/10.3389/fpls.2017.01721>
- Pradhan MP, Loqué D (2014) Histochemical staining of *Arabidopsis thaliana* secondary cell wall elements. *Journal of Visualized Experiments*:e51381. <https://doi.org/10.3791/51381>
- Cardinale M (2014) Scanning a microhabitat: plant-microbe interactions revealed by confocal laser microscopy. *Frontiers in Microbiology* 5: 94. <https://doi.org/10.3389/fmicb.2014.00094>
- Castillo P, Vovlas N, Jiménez-Díaz RM (1998) Pathogenicity and histopathology of *Pratylenchus thornei* populations on selected chickpea genotypes. *Plant Pathology* 47:370-376
- Davis EL, Haegeman A, Kikuchi T (2011) Degradation of the plant cell wall by nematodes. In: Jones J, Gheysen G, Fenoll C (eds) *Genomics and Molecular Genetics of Plant-Nematode Interactions*. Springer Netherlands, Dordrecht, pp 255-272
- Decou R, Serk H, Ménard D, Pesquet E (2017) Analysis of lignin composition and distribution using fluorescence laser confocal microspectroscopy. In: de Lucas M, Etchells JP (eds) *Xylem: Methods and Protocols*. Springer New York, NY, pp 233-247
- Dinh PTY, Knoblauch M, Elling AA (2013) Nondestructive imaging of plant-parasitic nematode development and host response to nematode pathogenesis. *Phytopathology* 104:497-506
- Ellinger D, Voigt CA (2014) Callose biosynthesis in Arabidopsis with a focus on pathogen response: what we have learned within the last decade. *Annals of Botany* 114:1349-1358
- Fujimoto T, Mizukubo T, Abe H, Seo S (2014) Sclareol induces plant resistance to root-knot nematode partially through ethylene-dependent enhancement of lignin accumulation. *Molecular Plant-Microbe Interactions* 28:398-407
- Grundler FMW, Sobczak M, Lange S (1997) Defence responses of *Arabidopsis thaliana* during invasion and feeding site induction by the plant-parasitic nematode *Heterodera glycines*. *Physiological and Molecular Plant Pathology* 50:419-429

- Haegeman A, Mantelin S, Jones JT, Gheysen G (2012) Functional roles of effectors of plant-parasitic nematodes. *Gene* 492:19-31
- Hardham AR (2012) Confocal microscopy in plant–pathogen interactions. In: Bolton MD, Thomma BPHJ (eds) *Plant Fungal Pathogens: Methods and Protocols*. Humana Press, Totowa, NJ, pp 295-309
- Hawes C (2000) Plant microtechnique and microscopy. *Journal of Microscopy* 197:320-321
- Herrera-Ubaldo H, de Folter S (2018) Exploring cell wall composition and modifications during the development of the gynoecium medial domain in *Arabidopsis*. *Frontiers in Plant Science* 9: 454. <https://doi.org/10.3389/fpls.2018.00454>
- Holbein J, Grundler F, Siddique S (2016) Plant basal resistance to nematodes: An update. *Journal of Experimental Botany* 67: 2049-2061
- Hussey RS, Mims CW, Westcott SW (1992) Immunocytochemical localization of callose in root cortical cells parasitized by the ring nematode *Criconebella xenoplax*. *Protoplasma* 171:1-6
- Khanam S, Bauters L, Singh RR, Verbeek R, Haeck A, Sultan SMD, Demeestere K, Kyndt T, Gheysen G (2018) Mechanisms of resistance in the rice cultivar Manikpukha to the rice stem nematode *Ditylenchus angustus*. *Molecular Plant Pathology* 19:1391-1402
- Kumari C, Dutta TK, Banakar P, Rao U (2016) Comparing the defence-related gene expression changes upon root-knot nematode attack in susceptible versus resistant cultivars of rice. *Scientific Reports* 6:22846-22846
- Kurppa S, Vrain TC (1985) Penetration and feeding behaviour of *Pratylenchus penetrans* in strawberry roots. *Revue de Nématologie* 8:273-276
- Liljegren S (2010) Phloroglucinol stain for lignin. *Cold Spring Harbor Protocols*. <https://doi.org/10.1101/pdb.prot4954>
- Linsell KJ, Riley IT, Davies KA, Oldach KH (2014) Characterization of resistance to *Pratylenchus thornei* (nematoda) in wheat (*Triticum aestivum*): attraction, penetration, motility, and reproduction. *Phytopathology* 104:174-187
- Liu Q, Luo L, Zheng L (2018) Lignins: biosynthesis and biological functions in plants. *International Journal of Molecular Sciences* 19:335. <https://doi.org/10.3390/ijms19020335>
- Luna E, Pastor V, Robert J, Flors V, Mauch-Mani B, Ton J (2010) Callose deposition: a multifaceted plant defense response. *Molecular Plant-Microbe Interactions* 24:183-193
- Marques JPR, Hoy JW, Appezzato-da-Glória B, Viveros AFG, Vieira MLC, Baisakh N (2018) Sugarcane cell wall-associated defense responses to infection by *Sporisorium scitamineum*. *Frontiers in Plant Science* 9: 698. <https://doi.org/10.3389/fpls.2018.00698>

- Mast SW, Donaldson L, Torr K, Phillips L, Flint H, West M, Strabala TJ, Wagner A (2009) Exploring the ultrastructural localization and biosynthesis of  $\beta(1,4)$ -galactan in *Pinus radiata* compression wood. *Plant Physiology* 150:573-583
- Mori B, Bellani LM (1996) Differential staining for cellulosic and modified plant cell walls. *Biotechnic and Histochemistry* 71:71-72
- Moura JCMS, Bonine CAV, De Oliveira Fernandes Viana J, Dornelas MC, Mazzafera P (2010) Abiotic and biotic stresses and changes in the lignin content and composition in plants. *Journal of Integrative Plant Biology* 52:360-376
- Oyekan PO, Blake CD, Mitchell JE (1972) Histopathology of pea roots axenically infected by *Pratylenchus penetrans*. *Journal of Nematology* 4:32-35
- Piršelová B, Matušíková I (2013) Callose: the plant cell wall polysaccharide with multiple biological functions. *Acta Physiologiae Plantarum* 35:635-644
- Pradhan MP, Loqué D (2014) Histochemical staining of *Arabidopsis thaliana* secondary cell wall elements. *Journal of Visualized Experiments* 87:e51381. <https://doi.org/10.3791/51381>
- Smith AH, Gill WM, Pinkard EA, Mohammed CL (2007) Anatomical and histochemical defence responses induced in juvenile leaves of *Eucalyptus globulus* and *Eucalyptus nitens* by *Mycosphaerella* infection. *Forest Pathology* 37:361-373
- Soukup A (2014) Selected simple methods of plant cell wall histochemistry and staining for light microscopy. In: Žárský V, Cvrčková F (eds) *Plant Cell Morphogenesis: Methods and Protocols*. Humana Press, Totowa, NJ, pp 25-40
- Suganthagunthalam D, Kahpui M, Annemie E, Dirk De W (2014) Phenols and lignin are involved in the defence response of banana (*Musa* Spp.) plants to *Radopholus similis* infection. *Nematology* 16:565-576
- Thomason IJ, Rich JR, O'Melia FC (1976) Pathology and histopathology of *Pratylenchus scribneri* infecting snap bean and lima bean. *Journal of Nematology* 8:347-352
- Townshend JL (1963) The pathogenicity of *Pratylenchus penetrans* to strawberry. *Canadian Journal of Plant Science* 43:75-78
- Townshend JL, Stobbs L, Carter R (1989) Ultrastructural pathology of cells affected by *Pratylenchus penetrans* in alfalfa roots. *Journal of Nematology* 21:530-539
- Truernit E, Palauqui JC (2009) Looking deeper: whole-mount confocal imaging of plant tissue for the accurate study of inner tissue layers. *Plant Signal and Behavior* 4:151-152
- Ursache R, Andersen TG, Marhavý P, Geldner N (2018) A protocol for combining fluorescent proteins with histological stains for diverse cell wall components. *The Plant Journal* 93:399-412



Valette C, Andary C, Geiger JP, Sarah JL, Nicole M (1998) Histochemical and cytochemical investigations of phenols in roots of banana infected by the burrowing nematode *Radopholus similis*. *Phytopathology* 88:1141-1148

Vance CP, Kirk TK, Sherwood RT (1980) Lignification as a mechanism of disease resistance. *Annual Review of Phytopathology* 18:259-288

Voigt CA (2014) Callose-mediated resistance to pathogenic intruders in plant defense-related papillae. *Frontiers in Plant Science* 5:168. <https://doi.org/10.3389/fpls.2014.00168>

Wieczorek K (2015) Chapter Three - cell wall alterations in nematode-infected roots. In: Escobar C, Fenoll C (eds) *Advances in Botanical Research*. Academic Press, pp 61-90

Wood PJ, Fulcher RG (1984) Specific interaction of aniline blue with (1→3)-β-d-glucan. *Carbohydrate Polymers* 4:49-72

Wuyts N, Lognay G, Swennen R, De Waele D (2006) Nematode infection and reproduction in transgenic and mutant *Arabidopsis* and tobacco with an altered phenylpropanoid metabolism. *Journal of Experimental Botany* 57:2825-2835

Wuyts N, Lognay G, Verscheure M, Marlier M, De Waele D, Swennen R (2007) Potential physical and chemical barriers to infection by the burrowing nematode *Radopholus similis* in roots of susceptible and resistant banana (*Musa* spp.). *Plant Pathology* 56:878-890

Zavaliev R, Epel BL (2015) Imaging callose at plasmodesmata using aniline blue: Quantitative confocal microscopy. In: Heinlein M (ed) *Plasmodesmata: Methods and Protocols*. Springer New York, New York, NY, pp 105-119

Zelko I, Lux A, Sterckeman T, Martinka M, Kollárová K, Lisková D (2012) An easy method for cutting and fluorescent staining of thin roots. *Annals of Botany* 110:475-478

Zhou J, Lee C, Zhong R, Ye Z-H (2009) MYB58 and MYB63 are transcriptional activators of the lignin biosynthetic pathway during secondary cell wall formation in *Arabidopsis*. *Plant Cell* 21:248-266

Zunke U (1990a) Ectoparasitic feeding behaviour of the root lesion nematode, *Pratylenchus penetrans*, on root hairs of different host plants. *Revue de Nématologie* 13:331-337

Zunke U (1990b) Observations on the invasion and endoparasitic behavior of the root lesion nematode *Pratylenchus penetrans*. *Journal of nematology* 22:309-320

## **Chapter 7**

**General discussion, contribution to the knowledge and future  
research direction**

## **Chapter 7**

### **General discussion, contribution to the knowledge and future research direction**

#### **7.1 Introduction**

In a previous study, a doubled haploid (DH) wheat population of 150 lines, developed from a cross between a synthetic derived wheat cultivar Sokoll (*Pratylenchus thornei* resistant) and the cultivar Krichauff (*P. thornei* susceptible) was investigated to identify quantitative trait loci (QTL) for resistance (Linsell et al. 2014a). Two highly significant QTL for *P. thornei* resistance were identified, on the short arms of chromosomes 6D (*QRInt.sk-6D*) and 2B (*QRInt.sk-2B*). The root and root exudates of the resistant lines also restricted nematode migration, development and reproduction (Linsell et al. 2014b). The present study aimed to investigate the genetic and biological basis of resistance of these *P. thornei* resistance loci in wheat. To achieve this aim, fine mapping was conducted for the root lesion resistant loci (Chapter 3), a cost-effective nematode quantification protocol was developed (Chapter 4), the metabolic profiles of the root exudates and root tissues from resistant and susceptible wheat lines were investigated (Chapter 5) and the histochemical and histological responses of *P. thornei* infected wheat roots were examined (Chapter 6). In the following section, the major findings of these studies, limitations and potential areas of future research are discussed.

## 7.2 Fine mapping of root lesion nematode (*Pratylenchus thornei*) resistance loci on chromosomes 6D and 2B of wheat

In order to refine the genetic intervals of the QTL, it was necessary to add more markers to the existing genetic linkage maps. For this purpose, in addition to the Sokoll/Krichauff DH population, a high-resolution mapping population was used, comprising of 1,727 RILs (Table 3.1). Of these, 108 RILs were identified as recombinant between the markers flanking the QTL, and these were further analysed genotypically and phenotypically. The *P. thornei* resistance data for the DH lines were available from a previous study (Linsell et al. 2014a), whereas the 108 RILs were analysed in the present study (Fig. 3.1).

The 90K SNP array was an excellent resource identifying single nucleotide polymorphic (SNP) markers in the wheat genome (Wang et al. 2014). The assay was performed using Sokoll/Krichauff DH lines and DNA bulks to identify SNPs linked to the QTL. A total of 16,907 SNPs were identified as being polymorphic between Sokoll and Krichauff. Of these, 776 and 1,597 SNPs were located on chromosome 6D and 2B, respectively. Of these, 143 and 92 SNPs were identified as being closely linked to the QTL, and subsequently converted to KASP assay, a single-plex genotyping platform (Supplementary Table 3.5 and 3.7). Among these KASP assays, 60 and 41 markers (Supplementary Table 3.5 and 3.7) gave clear allele calling, and together with previously identified SSR markers flanking the QTL, the 6DS and 2BS genetic linkage maps were re-constructed.

On chromosome 6DS, 60 KASP and five SSR markers spanned a total genetic distance of 23.7 cM, representing 16.36 Mbp in Chinese Spring and 16.81 Mbp in the *Ae. tauschii* reference genome (Fig. 3.2). With the use of previously available *P. thornei* resistance data for the DH lines (Linsell et al. 2014a), the *QRlnt.sk-6D* was mapped between the markers 6D\_5 (and seven

other co-segregating markers) and 6D\_143, explaining 47% of the total phenotypic variation (Fig. 3.2). The association between marker and phenotype was represented graphically, where the DH and RIL lines grouped according to their resistance phenotype (*P. thornei* DNA/plant). *QRlnt.sk-6D* was delimited to a 3.5 cM interval, representing 1.77 Mbp in the bread wheat cv. Chinese Spring reference genome sequence and 2.29 Mbp in the *Ae. tauschii* genome sequence (Fig. 3.3). These intervals contained 42 and 43 gene models in the respective annotated genome sequences (Supplementary Table 3.6).

The genetic linkage map of chromosome 2BS constituted 41 KASP and five SSR markers, spanning a total genetic distance of 19.9 M (Fig. 3.4). The genetic map corresponded to a 16.92 Mbp physical interval in the genome sequences of durum wheat cv. Svevo (Maccaferri et al. 2019) and a 19.08 Mbp interval in bread wheat (Chinese Spring). The QTL was mapped between the markers 2B\_74 and 2B\_12 (and five other co-segregating markers; LRS score of 44.5), and the closest markers explained 25% of the total phenotypic variation (Fig. 3.4). Fine mapping of *QRlnt.sk-2B* was performed using graphical genotyping, and the *QRlnt.sk-2B* interval was delimited to 1.4 cM, corresponding to 3.14 Mbp in the durum wheat cv. Svevo reference sequence and 2.19 Mbp in Chinese Spring (Fig. 3.5 and 3.6). The interval in Chinese Spring contained 56 high confidence gene models (Supplementary Table 3.8).

Markers that co-segregated with the resistance loci in the DH and RIL populations might be useful for marker assisted breeding. Markers co-segregating with *QRlnt.sk-6D* were 6D\_75, 6D\_48, 6D\_20, 6D\_139, 6D\_12 and 6D\_5, while those co-segregating with *QRlnt.sk-2B* were 2B\_73, 2B\_42, 2B-10, 2B\_71, 2B\_4 and 2B\_9. Details of these markers (SNP and primer sequence) are available in Supplementary Tables 3.5 and 3.7, respectively.

The *QRlnt.sk-6D* and *QRlnt.sk-2B* intervals contained genes with similarity to those previously reported to be involved in disease resistance, namely genes for phenylpropanoid-biosynthetic-pathway-related enzymes, NBS-LRR proteins and protein kinases (Table 3.2 and 3.3). Among these candidate genes, isoflavone reductase (IFR), flavonoid 3'-hydroxylases (F3'H), Chalcone synthase (CHS), phenylalanine ammonia-lyase (PAL) are involved in biosynthesis of flavonoids and isoflavonoids (Fig. 3.7). They might involve in *P. thornei* resistance by creating a toxic environment or suppressing the development and reproduction. It will be worthwhile to characterise these genes and gene products to understand their role in *P. thornei* resistance in wheat. Among the other candidate genes, NBS-LRR, receptor like protein kinase and ribosome-inactive proteins also need to be investigated to identify which, if any, of the candidates are responsible for the resistance QTL effect.

### **7.3 Detection and quantification of *P. thornei* in wheat root using quantitative real-time PCR**

For fine mapping (Chapter 3), *P. thornei* resistance assays on the wheat lines were conducted by the SARDI Root Disease Testing Service, where the DNA was extracted and the amount of *P. thornei* assessed using a real time TaqMan PCR system (Haling et al. 2011; Ophel-Keller et al. 2008; Riley et al. 2010). At SARDI, *P. thornei* quantification is offered as fee-for-service using crop and soil samples. Details of the protocol are proprietary information, and thus not available to other researchers. However, a real-time qPCR protocol has been reported by Yan et al. (2011) to quantify *P. thornei* in soil samples. They used a commercial DNA extraction kit (PowerSoil® DNA Isolation Kit, MoBio, Carlsbad, CA) to extract *P. thornei* DNA from soil. Again, the composition of the commercial DNA extraction kit is proprietary. A freely available DNA extraction protocol based on common laboratory chemicals would be desirable to keep the expenses low, and thus make the quantification method available to a breeding

program where large numbers of samples need to be processed. Consequently, this study was aimed to develop a protocol to allow reliable and cost-effective extraction and quantification of nematode DNA from wheat root tissue.

To amplify the *P. thornei* DNA, primer pairs THO-ITS-F2 and THO-ITS-R2 were used in the assay. The development and species specificity of the primer pairs were explained by Yan et al. (2011). In the present study, the primer pairs amplified *P. thornei* DNA with the expected amplification profile (Fig. 4.1). Moreover, the primer pairs did not amplify from wheat DNA alone.

In the present study, a modified CTAB DNA extraction protocol was developed to extract the DNA from nematode infected wheat root samples. The details of the protocol are available in section 4.3.2 of Chapter 4. The protocol was able to produce good quality DNA, where the concentration ranged from 653 ng/μL to 3595 ng/μL, and the average  $A_{260}/A_{280}$  and  $A_{260}/A_{230}$  ratio was 1.84 and 2.01. The extraction protocol was able to produce DNA without noticeable inhibition of PCR reactions (Table 4.1 and Fig. 4.2). With the use of washed root samples in this study, PCR inhibition from soil as observed by Yan et al. (2011), was minimized.

A standard regression was generated using DNA extracted from a mixture of 30 mg uninoculated root powder to which various numbers of *P. thornei* were added, ranging from 25 to 10,000 nematodes (Fig. 4.3). The numbers of pure *P. thornei* added to root powder were highly correlated ( $R^2 = 0.93$ ) with the numbers of *P. thornei* determined by the real-time PCR assay using the above-mentioned standard curve (Fig. 4.4). Moreover, the standard regression was used to quantify *P. thornei* from sixteen wheat lines with known levels of resistance. All the wheat lines were classified for resistance (resistance/moderately resistance/susceptible)

similar to the PreDicta B test (Table 4.3). Moreover, the present assay was able to distinguish the resistant and susceptible lines more clearly (2.0-fold difference) compared to the PreDicta B test (1.6-fold difference). Thus, the present assay able to accurately estimate *P. thornei* from wheat root samples.

Another important factor of the present study was the cost effectiveness of the experiment compared to the commercial service provider. To quantify *P. thornei* from wheat samples, the estimated cost was 50 AUD/ sample, whereas, the cost for PreDicta B test at SARDI is 120 AUD/ sample (Table 4.4). The DNA extraction protocol was less expensive as it works without costly commercial plant extraction kits. Thus, the assay provides the basis of a cost-effective tool for rapid and efficient detection and quantification of *P. thornei* in wheat.

#### **7.4 Metabolomic analysis of root tissues and root exudates from wheat lines contrasting for *Pratylenchus thornei* resistance**

In a previous study, *P. thornei* resistant wheat roots and root exudates were found to suppress nematode motility, migration and reproduction (Linsell et al. 2014b). Chemical compounds in root and root exudates of the resistant wheat lines might act on *P. thornei*. In order to investigate such compounds, the present study employed a non-targeted GC-MS based metabolic profiling of root tissue and root exudates from wheat genotypes contrasting for *P. thornei* resistance.

A root exudate collection protocol was described in section 5.3.2 (Fig. 5.1). Passing the root exudate solution through the 0.22 µm syringe filter (Millex GV, Millipore) allowed removal of any potential microbial contaminants present in the solution.



The GC-MS based metabolic profiling of root exudates and root tissues from five wheat genotypes described 100 and 64 metabolites, respectively (Supplementary Table 5.1 and 5.3). These metabolites were categorised into major biochemical classes; amino acids and amines, organic acids, sugars, sugar alcohol and sugar phosphates. In addition, metabolic profiling of *P. thornei* samples identified 50 metabolites (Supplementary Table 5.5).

To identify root exudate metabolites associated with resistance QTL, metabolic profiles of resistant lines (SK-R, 6D-R and 2B-R) were compared with those of susceptible lines (Kr-S and Null-S). A total of 21 metabolites were found to be associated with the resistance QTL, of which four and ten metabolites were associated with 6D and 2B QTL, respectively (Table 5.1, Supplementary Table 5.2). These 21 metabolites comprised six amino acids (alanine, beta alanine, methionine, proline, tyrosine and valine), eight organic acids (2-hydroxyglutaric acid, 4-hydroxy-benzoic acid, citric acid, glutaric acid, glyceric acid, malic acid, quinic acid and shikimic acid) and six sugar compounds (arabitol, fructose, glucose, maltose, myo inositol and sucrose). Their possible roles against *P. thornei* is unknown, but some of these compounds have been shown to possess nematotoxic (nematostatic and nematocidal) and egg hatching inhibition properties in *in-vitro* bioassays in which nematode behaviour (eg. motility, mortality, attraction, egg hatching) were studied in response to exogenous application of commercially sourced chemical compounds (eg. Čepulytė et al. 2018; Dutta et al. 2012; Linsell et al. 2014b).

In the present experiment, levels of four sugar compounds, erythritol, galactinol, ribitol and threitol were significantly lower in root exudates of the resistant genotypes relative to those of the susceptible genotypes. Further studies are required to see whether these compounds act as chemo-attractants towards *P. thornei* and related root lesion nematode species.

To identify root tissue metabolites associated with resistance QTL, metabolites in resistant lines (Sk-R-I, 6D-R-I and 2B-R-I) were compared with those of susceptible lines (Kr-S-I and Null-S-I) (Table 5.3, Supplementary Table 5.4). Fifteen metabolites were higher in 6D and /or 2B resistant QTL lines as compared to the lines lacking the resistance alleles. Nine of these metabolites were amino acids (alanine, beta alanine, isoleucine, phenylalanine, pyroglutamic acid, serine, threonine, tyrosine and valine), three were organic acids (2-hydroxyglutaric acid, aconitic acid and benzoic acid), two were sugars (galactinol and mannitol) and one was from the miscellaneous group (phosphoric acid). Their role against *P. thornei* is unknown. However, in previous studies, these compounds were shown to act against plant parasitic nematodes (discussed in section 5.5.2 of Chapter 5).

In *P. thornei* challenged roots, 13 metabolites were lower in Sk-R-I than in Kr-R-I and Null-S-I (Table 5.3), suggesting a possible contribution of these compounds towards compatible host-nematode interactions. These metabolites might promote *P. thornei* infection by providing sources of nutrients for nematodes, assisting in host cell degradation processes or interrupting host resistance mechanisms (Qiao et al. 2019). Further studies are required to investigate their roles in the wheat-*P. thornei* relationship.

## **7.5 Histochemical and histopathological responses of wheat roots infected by *P. thornei***

Resistance to *P. thornei* in wheat was found to be associated with restricted nematode migration within the root (Linsell et al. 2014b). The present study was conducted to gain more of an understanding of the histochemical and histopathological responses of wheat roots to challenge by *P. thornei*.

In the present study, the use of fluorescent dye PKH26 (for *P. thornei* labelling) and confocal microscopy enabled visualisation of live *P. thornei* both out and inside wheat root tissue (Fig. 6.1, 6.2, 6.3). The PKH26 dye did not prevent *P. thornei* from infecting the root and nematodes were observed at late stages of their life (four weeks after inoculation) inside the wheat root (Fig 6.3). Due to this stability in fluorescence, PKH26 can be use studying wheat-*P. thornei* interaction.

Capturing images of living *P. thornei* inside wheat roots enabled the endoparasitic behaviour of *P. thornei* to be observed (Fig. 6.2, 6.3, Movie clip 6.1). The resolution of the images are better than the previous study reported by Zunke (1990), where the author used video-enhanced contrast microscopy. Some of the important findings from the histopathological study were as follows:

- *P. thornei* was seen to be searching for a suitable site to penetrate the wheat root, and once damage occurred, other *P. thornei* aggregated and followed the same path.
- *P. thornei* moved from one cell to another by breaking the cell wall using their stylet.
- Video images of *P. thornei* clearly showed stylet thrusting at the corner of the cells, followed by searches for suitable places to break in through other areas of the cell wall (Movie clip 1).
- *P. thornei* were found to be confined within the epidermal and cortical layer of wheat tissue, and they were not observed feeding on the endodermis or central stele.

The above mentioned endoparasitic behaviour of *P. thornei* in wheat roots was largely like those reported for other root lesion nematode species in various hosts (discussed in section 6.5 of Chapter 6). Additional study is required to test for differences between Sokoll and Krichauff.

Root tissues would need to be observed over a long period of time, from root penetration until the end of lifecycle inside the root (eight weeks after inoculation).

In response to *P. thornei* infection, secondary cell wall thickening (deposition of cellulose, callose, lignin and suberin) was observed in the *P. thornei* resistant cultivar, Sokoll (Fig 6.4 to Fig. 6.9). Some of the important findings were as follows:

- Calcofluor white staining Sokoll root sections resulted blue fluorescence confirming deposition of cellulose (Fig. 6.4). Although cellulose occurs in all cell walls, deposition of additional cellulose might occur in response to nematode infection (Marques et al. 2018).
- With aniline blue staining, callose (or callose-like substances) deposition was observed in nematode infected Sokoll root tissue (Fig. 6.6, 6.7).
- Phloroglucinol stained Sokoll root tissues showed accumulation of lignin upon nematode infection, which might strengthen the plant cell walls and inhibit nematode migration (Fig. 6.8 and 6.9).

Deposition of cellulose, callose and lignin might result in physical reinforcement of the cell walls in Sokoll. Therefore, penetration of the cell wall by stylet thrusting may become more challenging for the nematodes.

## **7.6 Wheat *P. thornei* resistance genes may contribute to biochemical and physical resistance at the metabolic and cellular level**

In the present study, several genes in the *QRlnt.sk-6D* and *QRlnt.sk-2B* intervals were identified as plausible candidates for *P. thornei* resistance genes (Chapter 3). These genes might be related to the metabolic changes observed in wheat roots (Chapter 5) or the identified histochemical changes in root cells at nematode infection sites (Chapter 6).

Several phenylpropanoid pathway related genes have been identified underlying *QRlnt.sk-6D* and *QRlnt.sk-2B QTL* (Table 3.2 and 3.3 in Chapter 3). The genes encoding isoflavone reductase (IFR), flavonoid 3'-hydroxylases (F3'H), chalcone synthase (CHS) and phenylalanine ammonia-lyase (PAL). These enzymes are involved in biosynthesis of the phenylpropanoids, flavonoids and isoflavonoids (Fig. 3.7, Chapter 3). It is well documented that the phenylpropanoid compounds play important roles in resistance to pathogen attack (Reviewed in Dixon et al. 2002; Naoumkina et al. 2010). The resistance loci-associated metabolites found in this study (Table 5.1, 5.2 and 5.3 in Chapter 5) were searched in the Kyoto Encyclopedia of Genes and Genomes (KEGG) pathway database (<https://www.genome.jp/kegg/pathway.html>) to identify phenylpropanoid pathway metabolites. As a result, several organic acids were found to be involved in the phenylpropanoid pathway; namely, 4-hydroxy-benzoic acid, malic acid, quinic acid, shikimic acid, aconitic acid and benzoic acid. Besides, the amino acids; alanine and phenylalanine were also found to be associated with phenylpropanoid biosynthetic pathway. Moreover, in response to *P. thornei* infection, lignin deposition was observed in the Sokoll root section (Fig. 6.8 and 6.9, Chapter 6). Lignin is a product of phenylpropanoid biosynthetic pathway (Fraser and Chapple 2011) that may provide physical resistance to nematode infection. These results suggest that phenylpropanoids might be excellent candidates for compounds acting against *P. thornei* in wheat. It will be worth doing further work to validate these potential resistance mechanisms against *P. thornei* in wheat. The outcomes of the present study suggest further research directions. In the following section, limitations of the present study and some potential areas of future research are discussed.

## 7.7 Limitations and future research directions

Firstly, the candidate genes identified in present study require further characterisation. It will be worthwhile to investigate whether the resistance genes to *P. thornei* infection are differentially expressed in resistant and susceptible lines. Their expression profiles can be analysed by RT-PCR (eg. Hu et al. 2019). The use of near isogenic lines (NILs) contrasting for the presence of the QTL could be a valuable tool in studying the relative expression pattern for these candidate genes. NILs can be generated by crossing a donor line carrying the gene of interest to a recurrent parent and then backcrossing to the recurrent parent for five to six generations, followed by self-pollination (Zhou et al. 2005). The flanking markers identified in this study (Chapter 3) can be used for marker assisted selection strategies to accelerate this NIL development process (Xu et al. 2017).

The present study has provided the foundation for further cloning of the resistance genes. Molecular cloning of the resistance QTL will be required to achieve a detailed understanding of the molecular mechanisms of resistance, and to develop perfect markers for marker assisted breeding. Again, the NILs can be valuable materials to clone the resistance genes. Map-based cloning techniques can be used for this purpose (Krattinger et al. 2009). Alternatively, recently developed rapid cloning techniques can be used to clone the nematode resistance genes (Reviewed in Bettgenhaeuser and Krattinger 2019). Some of these techniques are Mutagenesis Resistance gene enrichment and Sequencing (MutRenSeq) (Steuernagel et al. 2016) and Targeted Chromosome-based Cloning via long-range Assembly (TACCA) (Thind et al. 2017).

GC-MS based metabolic analysis is limited to volatile and thermally stable molecules (Balmer et al. 2013; Hill et al. 2016). However, most plant metabolites are not volatile, and may not be detectable by GC-MS. For example, flavonoids are an important class of defence metabolites

that cannot be detected by GC-MS. In such context, other metabolic technology, such as liquid chromatography-mass spectrometry (LC-MS) or nuclear magnetic resonance spectroscopy (NMR) can be considered. Compounds with higher molecular weight and lower thermostability are amenable for analysis via LC-MS (Allwood et al. 2008; Balmer et al. 2013). As a result, a much wider range of metabolites (compared to the GC-MS) can be analysed by LC-MS analysis. In fact, LC-MS metabolic analysis has already been conducted for the samples used in present study. Due to the time constraints, these large data set has not been analysed yet. It is very important to analyse these data to identify additional plant metabolites potentially acting against *P. thornei*.

In present study, root tissue was collected from a single time point (six weeks after nematode infection) for metabolic profiling. This is one of the limitations in the root tissue metabolic analysis, as previous studies showed that metabolites in plants change throughout the various stages of nematode or fungal infection (Afzal et al. 2009; Hofmann et al. 2010; Scandiani et al. 2015). Future studies should consider sampling from multiple nematode infection stages, such as early, mid and late.

In relation to the root exudate study, metabolic analysis was performed only for the samples without nematode infection. Future work should consider exudates from roots challenged by *P. thornei*. Metabolic analysis of root exudates (in response to nematode infection) might provide an insight into biotic stress induced metabolites that are exuded from the roots.

In present study, several nematode resistant metabolites were identified using GC-MS based metabolic analysis of the root exudates and root tissues of the wheat lines contrasting for *P. thornei* resistance (Table 5.1, Table 5.2 and Table 5.3; Chapter 5). Their possible roles in an

incompatible wheat-*P. thornei* relationship is unknown. They may possess nematotoxic (nematostatic and nematocidal) and egg hatching inhibition properties against *P. thornei*. To test their effect against *P. thornei*, these compounds require further investigation. Commercially sourced chemical compounds can be applied to *P. thornei* to investigate their effect on motility, migration and egg hatching (eg. Čepulytė et al. 2018; Dutta et al. 2012; Rocha et al. 2017).

The microscopic study investigated histopathological responses of *P. thornei* resistant and susceptible wheat roots infected by *P. thornei* (Chapter 6). The behavioural patterns of *P. thornei* observed inside wheat roots were largely similar to those reported for other root lesion nematode species observed in various hosts. However, distinct histopathological differences that correlated with resistance were not observed in this study. Additional root tissue from *P. thornei* resistant and susceptible wheat lines needs to be investigated microscopically over a longer period to identify any such differences, i.e., from root penetration until the end of lifecycle inside the root (eight weeks after inoculation). In present study, the fluorescent dye PKH26 (for *P. thornei* labelling) and confocal microscopy offered a non-destructive method of histopathological investigation of live nematodes inside root tissue. For further investigation, in addition to confocal microscopy, transmission electron microscopy could be considered for observing ultra-structural changes in the host cells.

The histochemical staining suggested that due to *P. thornei* infection, cellulose, callose and lignin was deposited in the cell wall of the *P. thornei* resistant wheat cultivar, Sokoll (Chapter 6). They may contribute to physical reinforcement of the cell walls, restricting *P. thornei* movement inside the root tissue. Whether cell wall modifications act against *P. thornei*, requires further investigation. For instance, nanoscale fluorescence microscopy can be



considered to decipher cell wall modifications during nematode resistance. Specifically, fluorescence resonance energy transfer (FRET) microscopy can be used to visualise protein-protein interaction within living tissue, complementing other information on plant resistance pathways and putative host-pathogen interactions (Ellinger and Voigt 2014). Moreover, future study should consider histochemical observation of additional nematode resistance compounds. For example, flavonoids can be visualised in wheat root tissue using DPBA staining (Ferrara and Thompson 2019; Kawanishi et al. 2015). It will be worthwhile to investigate presence/absence or semi-quantitative differences in phenylpropanoid deposition between resistant and susceptible wheat lines, and to see if any such differences are correlated with resistance.

## 7.8 Conclusion

*P. thornei* resistance mechanisms in wheat were investigated from genetic, metabolomic and histopathological points of view. The *P. thornei* resistance QTL, *QRInt.sk-6D* and *QRInt.sk-2B* were fine mapped on wheat chromosome 6DS and 2BS, respectively. Several genes in these QTL intervals were identified representing plausible candidates for *P. thornei* resistance genes. Products of these genes included phenylpropanoid-biosynthetic-related enzymes, NBS-LRR proteins and protein kinases. The GC-MS based metabolic analysis of the wheat lines contrasting in *P. thornei* resistance revealed several nematode resistant metabolites, including the phenylpropanoid-biosynthetic-related compounds. The phenylpropanoid, lignin was also observed to be deposited in the cell wall of the *P. thornei* resistant wheat line. It will be worthwhile to further characterise the candidate genes and to investigate whether the identified compounds possess nematotoxic properties against *P. thornei* in wheat. Additionally, the cost-effective *P. thornei* quantification method reported in this study, and the molecular markers

linked to the two resistance QTL could be used for selection of *P. thornei* resistant wheat cultivars.

## 7.9 References

- Afzal AJ, Natarajan A, Saini N, Iqbal MJ, Geisler M, El Shemy HA, Mungur R, Willmitzer L, Lightfoot DA (2009) The nematode resistance allele at the *rhg1* locus alters the proteome and primary metabolism of soybean roots. *Plant Physiology* 151:1264
- Allwood JW, Ellis DI, Goodacre R (2008) Metabolomic technologies and their application to the study of plants and plant–host interactions. *Physiologia Plantarum* 132:117-135
- Balmer D, Flors V, Glauser G, Mauch-Mani B (2013) Metabolomics of cereals under biotic stress: current knowledge and techniques. *Frontiers in Plant Science* 4:82. <https://doi.org/10.3389/fpls.2013.00082>
- Bettgenhaeuser J, Krattinger SG (2019) Rapid gene cloning in cereals. *Theoretical and Applied Genetics* 132:699-711
- Čepulytė R, Danquah WB, Bruening G, Williamson VM (2018) Potent attractant for root-knot nematodes in exudates from seedling root tips of two host species. *Scientific Reports* 8:10847. <https://doi.org/10.1038/s41598-018-29165-4>
- Dixon RA, Achnine L, Kota P, Liu CJ, Reddy MSS, Wang L (2002) The phenylpropanoid pathway and plant defence—a genomics perspective. *Molecular Plant Pathology* 3:371-390
- Dutta TK, Powers SJ, Gaur HS, Birkett M, Curtis RHC (2012) Effect of small lipophilic molecules in tomato and rice root exudates on the behaviour of *Meloidogyne incognita* and *M. graminicola*. *Nematology* 14:309-320
- Ellinger D, Voigt CA (2014) The use of nanoscale fluorescence microscopic to decipher cell wall modifications during fungal penetration. *Frontiers in Plant Science* 5:270. <https://doi.org/10.3389/fpls.2014.00270>
- Ferrara BT, Thompson EP (2019) A method for visualizing fluorescence of flavonoid therapeutics in vivo in the model eukaryote *Dictyostelium discoideum*. *BioTechniques* 66:65-71
- Fraser CM, Chapple C (2011) The phenylpropanoid pathway in Arabidopsis. *Arabidopsis Book* 9:e0152. <https://doi.org/10.1199/tab.0152>
- Haling RE, Simpson RJ, McKay AC, Hartley D, Lambers H, Ophel-Keller K, Wiebkin S, Herdina, Riley IT, Richardson AE (2011) Direct measurement of roots in soil for single and mixed species using a quantitative DNA-based method. *Plant and Soil* 348:123-137
- Hill CB, Dias DA, Roessner U (2016) Current and emerging applications of metabolomics in the field of agricultural biotechnology. In: Ravishankar RV (ed) *Advances in food biotechnology*, John Wiley & Sons, Ltd., pp 13-26
- Hofmann J, El Ashry AEN, Anwar S, Erban A, Kopka J, Grundler F (2010) Metabolic profiling reveals local and systemic responses of host plants to nematode parasitism. *The Plant Journal* 62:1058-1071

Hu X, Rocheleau H, McCartney C, Biselli C, Bagnaresi P, Balcerzak M, Fedak G, Yan Z, Valè G, Khanizadeh S, Ouellet T (2019) Identification and mapping of expressed genes associated with the 2DL QTL for fusarium head blight resistance in the wheat line Wuhan 1. *BMC Genetics* 20:47. <https://doi.org/10.1186/s12863-019-0748-6>

Kawanishi Y, Bito N, Nakada R, Imai T (2015) Visualization of the distribution of flavonoids in *Larix kaempferi* wood by fluorescence microscopy. *Mokuzai Gakkaishi* 61:297-307

Krattinger S, Wicker T, Keller B (2009) Map-Based Cloning of Genes in Triticeae (Wheat and Barley). In: Muehlbauer GJ, Feuillet C (eds) *Genetics and Genomics of the Triticeae*. Springer US, New York, NY, pp 337-357

Linsell KJ, Rahman MS, Taylor JD, Davey RS, Gogel BJ, Wallwork H, Forrest KL, Hayden MJ, Taylor SP, Oldach KH (2014a) QTL for resistance to root lesion nematode (*Pratylenchus thornei*) from a synthetic hexaploid wheat source. *Theoretical and Applied Genetics* 127:1409-1421

Linsell KJ, Riley IT, Davies KA, Oldach KH (2014b) Characterization of Resistance to *Pratylenchus thornei* (Nematoda) in Wheat (*Triticum aestivum*): attraction, Penetration, Motility, and Reproduction. *Phytopathology* 104:174-187

Maccaferri M, Harris NS, Twardziok SO, Pasam RK, Gundlach H, Spannagl M, Ormanbekova D, Lux T, Prade VM, Milner SG, Himmelbach A, Mascher M, Bagnaresi P, Faccioli P, Cozzi P, Lauria M, Lazzari B, Stella A, Manconi A, Gnocchi M, Moscatelli M, Avni R, Deek J, Biyiklioglu S, Frascaroli E, Corneti S, Salvi S, Sonnante G, Desiderio F, Marè C, Crosatti C, Mica E, Özkan H, Kilian B, De Vita P, Marone D, Joukhadar R, Mazzucotelli E, Nigro D, Gadaleta A, Chao S, Faris JD, Melo ATO, Pumphrey M, Pecchioni N, Milanese L, Wiebe K, Ens J, MacLachlan RP, Clarke JM, Sharpe AG, Koh CS, Liang KYH, Taylor GJ, Knox R, Budak H, Mastrangelo AM, Xu SS, Stein N, Hale I, Distelfeld A, Hayden MJ, Tuberosa R, Walkowiak S, Mayer KFX, Ceriotti A, Pozniak CJ, Cattivelli L (2019) Durum wheat genome highlights past domestication signatures and future improvement targets. *Nature Genetics* 51:885-895

Marques JPR, Hoy JW, Appezzato-da-Glória B, Viveros AFG, Vieira MLC, Baisakh N (2018) Sugarcane cell wall-associated defense responses to infection by *Sporisorium scitamineum*. *Frontiers in Plant Science* 9:696. <https://doi.org/10.3389/fpls.2018.00698>

Naoumkina M, A., Zhao Q, Gallego-Giraldo L, Dai X, Zhao Patrick X, Dixon Richard A (2010) Genome-wide analysis of phenylpropanoid defence pathways. *Molecular Plant Pathology* 11:829-846

Ophel-Keller K, McKay A, Hartley D, Herdina, Curran J (2008) Development of a routine DNA-based testing service for soilborne diseases in Australia. *Australasian Plant Pathology* 37:243-253

Qiao F, Kong L-A, Peng H, Huang W-K, Wu D-Q, Liu S-M, Clarke JL, Qiu D-W, Peng D-L (2019) Transcriptional profiling of wheat (*Triticum aestivum* L.) during a compatible interaction with the cereal cyst nematode *Heterodera avenae*. *Scientific Reports* 9:2184. <https://doi.org/10.1038/s41598-018-37824-9>

Riley IT, Wiebkin S, Hartley D, McKay AC (2010) Quantification of roots and seeds in soil with real-time PCR. *Plant and Soil* 331:151-163

Rocha TL, Soll CB, Boughton BA, Silva TS, Oldach K, Firmino AAP, Callahan DL, Sheedy J, Silveira ER, Carneiro RMDG, Silva LP, Polez VLP, Pelegrini PB, Bacic A, Grossi-de-Sa MF, Roessner U (2017) Prospection and identification of nematotoxic compounds from *Canavalia ensiformis* seeds effective in the control of the root knot nematode *Meloidogyne incognita*. *Biotechnology Research and Innovation* 1:87-100

Scandiani MM, Luque AG, Razori MV, Ciancio Casalini L, Aoki T, O'Donnell K, Cervigni GDL, Spampinato CP (2015) Metabolic profiles of soybean roots during early stages of *Fusarium tucumaniae* infection. *Journal of Experimental Botany* 66:391-402

Steuernagel B, Periyannan SK, Hernández-Pinzón I, Witek K, Rouse MN, Yu G, Hatta A, Ayliffe M, Bariana H, Jones JDG, Lagudah ES, Wulff BBH (2016) Rapid cloning of disease-resistance genes in plants using mutagenesis and sequence capture. *Nature Biotechnology* 34:652-655

Thind AK, Wicker T, Šimková H, Fossati D, Moullet O, Brabant C, Vrána J, Doležel J, Krattinger SG (2017) Rapid cloning of genes in hexaploid wheat using cultivar-specific long-range chromosome assembly. *Nature Biotechnology* 35:793-796

Wang S, Wong D, Forrest K, Allen A, Chao S, Huang Bevan E, Maccaferri M, Salvi S, Milner Sara G, Cattivelli L, Mastrangelo Anna M, Whan A, Stephen S, Barker G, Wieseke R, Plieske J, Lillemo M, Mather D, Appels R, Dolferus R, Brown-Guedira G, Korol A, Akhunova Alina R, Feuillet C, Salse J, Morgante M, Pozniak C, Luo MC, Dvorak J, Morell M, Dubcovsky J, Ganai M, Tuberosa R, Lawley C, Mikoulitch I, Cavanagh C, Edwards Keith J, Hayden M, Akhunov E (2014) Characterization of polyploid wheat genomic diversity using a high-density 90,000 single nucleotide polymorphism array. *Plant Biotechnology Journal* 12:787-796

Xu H, Cao Y, Xu Y, Ma P, Ma F, Song L, Li L, An D (2017) Marker-assisted development and evaluation of near-isogenic lines for broad-spectrum powdery mildew resistance gene pm2b introgressed into different genetic backgrounds of wheat. *Frontiers in Plant Science* 8: 1322, <https://doi.org/10.3389/fpls.2017.01322>

Yan G, Smiley RW, Okubara PA (2011) Detection and quantification of *Pratylenchus thornei* in DNA extracted from soil using real-time PCR. *Phytopathology* 102:14-22

Zhou R, Zhu Z, Kong X, Huo N, Tian Q, Li P, Jin C, Dong Y, Jia J (2005) Development of wheat near-isogenic lines for powdery mildew resistance. *Theoretical and Applied Genetics* 110:640-648

Zunke U (1990) Observations on the invasion and endoparasitic behavior of the root lesion nematode *Pratylenchus penetrans*. *Journal of Nematology* 22:309-320

## **Appendix**

## **Appendix 1**

### **Supplementary tables of chapter 3**

The following supplementary tables of chapter 3 was provided as an electronic file (Microsoft Excel spreadsheets).

Supplementary Table 3.1	Details of SNPs from the 90 K wheat SNP array that were shown using bulked segregation analysis to be linked to the <i>QRlnt.sk-6D</i> nematode resistance locus. Details of these SNPs were derived from Wang et al. (2014)
Supplementary Table 3.2	Details of SNPs from the 90 K wheat SNP array that were shown using bulked segregation analysis to be linked to the <i>QRlnt.sk-2B</i> nematode resistance locus. Details of these SNPs were derived from Wang et al. (2014)
Supplementary Table 3.3	Genetic linkage map of chromosome 6D of Sokoll /Krichauff double haploid population (65 lines) obtained using the 90K wheat SNP chip assay
Supplementary Table 3.4	Genetic linkage map of chromosome 2B of Sokoll /Krichauff double haploid population (65 lines) obtained using the 90K wheat SNP chip assay
Supplementary Table 3.5	Details of KASP markers used for constructing the genetic linkage map of chromosome 6DS. 1: 'A' refers to 90K wheat SNP chip array (Wang et al. 2014) and 'B' refers to cereal database, University of Bristol (Allen et al. 2011)
Supplementary Table 3.6	List of gene models between the markers flanking <i>QRlnt.sk-6D</i> QTL. Gene annotation based in Chinese spring IWGSC RefSeq v1.0

Supplementary Table 3.7	Details of KASP markers used for constructing the genetic linkage map of chromosome 2BS. 1: Source of SNPs, 1 refers to 90 K wheat SNP chip array (Wang et al. 2014) and 2 refers to cereal database, University of Bristol (Allen et al. 2011)
Supplementary Table 3.8	List of gene modes located between markers flanking <i>QRInt.sk-2B</i> QTL. Gene annotation based in Chinese spring IWGSC RefSeq v1.0



## **Appendix 2**

### **Supplementary tables of chapter 5**

The following supplementary tables of chapter 5 was provided as an electronic file (Microsoft Excel spreadsheets).

Supplementary Table 5.1	Entire data set for metabolite profile from root exudates of <i>Pratylenchus thornei</i> resistance (R) and susceptible (S) wheat cultivars, Sokoll (Sk), Krichauff (Kr), 6D-QTL representative doubled haploid (DH) line 35 (6D-R), 2B-QTL DH line 52 (2B-R) and Null QTL DH line 114 (Null-S)
Supplementary Table 5.2	Analysis of metabolites in root exudates associated with <i>Pratylenchus thornei</i> resistance. The level of metabolites (fold-change) were compared between resistant (Sk-R, 6D-R and 2B-R) and susceptible (Kr-S and Null-S) lines to identify metabolites linked to 6D+2B (Section A), 6D (Section B) and 2B (Section C) QTL. 1: Fold-change differences were calculated based on average values from four replicates. 2: Highlighted values refers to the significantly ( $P < 0.05$ ) higher (green colour) and lower (blue colour) level of metabolites (fold-change) in resistance line compared to the susceptible line. AA, OA, S, M refers to Amino Acids, Organic Acids, Sugars and Miscellaneous biochemical groups
Supplementary Table 5.3	Entire data set for metabolite profile from root tissues of <i>Pratylenchus thornei</i> resistance (R) and susceptible (S) wheat cultivars, Sokoll (Sk), Krichauff (Kr), 6D-QTL representative doubled haploid (DH) line 35 (6D-R), 2B-QTL DH line 52 (2B-R) and Null QTL DH line 114 (Null-S)

Supplementary  
Table 5.4

Analysis of metabolites association with *Pratylenchus thornei* resistance QTL. The level of metabolites (fold-change) were compared between resistant (Sk-R-I, 6D-R-I and 2B-R-I) and susceptible (Kr-S-I and Null-S-I) lines to analyse metabolites linked to 6D+2B (Section A), 6D (Section B) and 2B (Section C) QTL. 1: Fold-change difference were calculated based on average values from four replicates. 2: Green and blue coloured metabolites refer to higher and lower level of metabolites in resistance line compared to susceptible lines. AA, OA, S, M refers to Amino Acids, Organic Acids, Sugars and Miscellaneous biochemical groups

Supplementary  
Table 5.5

List of metabolites present in *Pratylenchus thornei* sample